THE UNIVERSITY *of* EDINBURGH

The role of innate immune cells in neurogenesis after spinal cord injury in zebrafish larvae

Louisa K. Drake

Doctor of Philosophy

University of Edinburgh

2022

Statement of original contribution

Unless stated otherwise, the work in this thesis has been performed by the candidate, Louisa K. Drake.

Neither this dissertation nor part thereof has been submitted for academic merit at another educational institution. Data and information within this thesis have been submitted for the following publications:

Drake, L. K., Keatinge, M., Tsarouchas, T. M., Becker, C. G., Lyons, D. A. & Becker, T. (2023) Rapid Testing of Gene Function in Axonal Regeneration After Spinal Cord Injury Using Larval Zebrafish. *Methods Mol Biol*, 2636, 263-277.

Cavone, L.*, McCann, T.*, **Drake, L**.*, Aguzzi, E., Oprişoreanu, A., & Pedersen, E. et al. (2021). A unique macrophage subpopulation signals directly to progenitor cells to promote regenerative neurogenesis in the zebrafish spinal cord. *Developmental Cell*, 56(11), 1617-1630.e6.

*: Joint first authors

Abstract

Unlike mammals, zebrafish can undergo complete functional recovery after spinal cord injury. One likely mechanism contributing to this regeneration is the proliferation and differentiation of ependymo-radial glial cells into new neurons. It is possible that some immune pathways are involved in re-initiating neurogenesis, as immune cells immediately infiltrate the site of spinal cord injury. Previously, global pharmacological manipulations of inflammation has shown that reducing inflammation results in lower levels of neurogenesis after central nervous system injury. However, the exact cell types and signals involved were still unknown. This project aimed to characterise the populations of immune cells and progenitor cells in the lesioned zebrafish and to identify potential pro-neurogenic signalling signals between the cell types.

To identify any immune-derived signals at the lesion site, I performed single cell sequencing experiment on *mpeg1*+ progeny from both naïve and lesioned fish (24 hours post injury). Using marker genes, I identified the main subtypes of innate immune cells present at the lesion site including macrophages, microglia and neutrophils. Comparisons of the populations isolated from the naïve and lesioned fish revealed injury induced changes in these populations. I observed a notable expansion of the microglia cells in the lesioned fish compared to the unlesioned fish. Furthermore, I use changes in gene expression in the macrophages and microglia to deduce the injury induced changes undergone by these cells. Macrophages adopt an activated and secretory programme in the lesioned spinal cord.

Similarly, single cell sequencing was performed on FAC sorted h*er4.3*+ ependymo-radial glial cells and their progeny in the same injury conditions. Following unsupervised clustering, identities of the derived neuronal and glial clusters were assigned based on marker gene expression. Comparisons of these cell types before and after injury showed an expansion of a rare neuronal population with a putative neurosecretory function in the lesioned fish. Injury induced gene expression changes in our dataset were also compared to gene expression changes following injury in mice, to identify conserved and unique pathways across species. The transcription factor *irf9* was upregulated in all mice progenitor populations after injury as well as our zebrafish dataset, indicating a conserved role in the injured spinal cord.

Finally, the datasets were considered together in order to identify pathways of innate immune cell signalling to neuronal progenitor cells which may initiate promote neurogenesis. Receptor-ligand pairs were identified in which the ligands are up-regulated in the immune cells after injury and the corresponding receptors are present in the

ependymo-radial glial cells. This identified some candidates for immune derived neurogenic pathways including Tnf signalling. Manipulating genes in the Tnf signalling cascade using CRISPR/Cas9 confirmed a pro-neurogenic function for immune-derived Tnf via its receptor on ependymo-radial glial cells.

Overall, this research characterises the main immune and progenitor cell types involved in regenerative neurogenesis after spinal cord injury in zebrafish larvae. Comparing the cell populations before and after injury provides insight into the role of the immune system in promoting neurogenesis.

Lay summary

Spinal cord injuries in humans and most other mammals often result in permanent and severe disabilities including paralysis. Some animals, including fish and amphibians, have the ability to regenerate their spinal cord after injury, and can recover normal movement. To understand how fish can achieve spinal cord regeneration we use the zebrafish as a model organism. This project aimed to understand more about how fish undergo spinal cord regeneration, with the hope that one day these findings may help human spinal cord injury patients.

Following a spinal cord injury, one process which occurs in fish is the creation of new neurons from their parent cells, called neuronal progenitor cells. In this project, I analysed the neuronal progenitor cells in healthy zebrafish larvae and compared them to the neuronal progenitor cells in injured zebrafish larvae of the same age, to see what changes these cells undergo when the nearby spinal cord has been damaged. One thing I found was that a different subtype of cells exist in the injured zebrafish which are not found in very large numbers in the uninjured zebrafish larvae. This cell type expresses a unique set of genes and have not been fully characterised before. These cells may play an essential role in the successful regeneration of zebrafish larvae.

We know that inflammation is important in some of the processes of spinal cord regeneration in zebrafish. I also wanted to find out if immune cells involved in the inflammation can communicate to the neuronal progenitor cells and encourage them to generate new neurons. To do this, I compared the immune cells from a healthy zebrafish spinal cord to that of a zebrafish larvae spinal cord which had been injured. One interesting thing which was different in the injured fish was that one of the types of immune cells known as macrophages expressed a different combination of molecules. This combination of molecules suggests that macrophages become more secretory after injury.

Therefore, I looked at specific signals released from immune cells which were likely to be involved in communicating to the neuronal progenitor cells. For this to be possible, the corresponding receptor for the signal must be present on the neuronal progenitor cells. One of the most interesting pairs of molecules I found was Tnf released from the immune cells, and the Tnf receptor on the neuronal progenitor cells. Tnf is an immune molecule which is also present in humans and other animals. It is best known for its role in promoting inflammation. I investigated how important these signals were for spinal cord regeneration by using genetic tools to reduce the levels of the Tnf receptor. These

experiments found that inflammation of the injured spinal cord leads to new neurons being made.

Overall, this research has helped to further our understanding about what is happening in the injured zebrafish spinal cord, and in particular about how inflammation is involved in encouraging the generation of new neurons. This research may lead the way to future therapeutic tools involving the human immune system to support regeneration of the human spinal cord.

Acknowledgements

I would like to thank my supervisors, Professors Thomas and Catherina Becker for their guidance and support over the past four years, and the opportunity to be part of their lab. Additionally, I would like to thank EastBio for the funding to pursue this PhD.

Past and present members of the Becker lab have been invaluable throughout my PhD. Special mention goes to Leo Cavone whose work led to this project's conception, and whose help and relentless expertise in the first year of my PhD allowed the single cell sequencing experiments to go ahead. To Tahimina and Leslie who made my first year so enjoyable, I forgive you not extending your stay in the lab. Thanks to the other Becker lab PhDs: Lizi, Tom, Claire and Rachel, thanks for keeping me sane, grounded and caffeinated, and for being a sounding board for science chats and troubleshooting. To Zoë, I am thankful for our extended coffee breaks, for reminding me of life outside of the lab, and never failing to make me laugh! Finally, thank you to the post-docs who have endless patience and helped to keep the lab ticking over during my time in the Becker lab – Themis, Leo, Helena, Nicola, Ana-Maria and François.

The zebrafish are at the core of this research, and so I'd like to thank the staff at the QMRI for their expert fish care and help. In particular, thank you to Nicola for always going above and beyond for us and the fish!

Thanks to everyone in Chancellor's building who have kept me safe, trained and informed over the past four years, and to my colleagues in other labs who are always willing to share resources and knowledge. In particular I am grateful to Marcus Keatinge for sharing some of your CRISPR/Cas9 expertise with me.

Last but not least, thank you to my family and friends for being supportive and understanding especially during these last months of my PhD, to Gracie for always lifting my spirits, and especially to Rob for encouraging me along with your optimistic outlook and unrelenting support.

Table of Contents

Chapter 1: General Introduction

1.1 The nervous system

The nervous system is a complex network of neuronal and glial cells which sense, integrate, and respond to signals from an organism's external environment. The neurons provide a substrate for electrical signals to travel through an organism's body. These electrical signals form the basis for all movement, behaviour, learning, and interactions of an organism. Whilst the complexity and cellular composition varies between species, the basic nature of the nervous system is preserved throughout vertebrate phylogeny. Thus, a complete understanding of the composition and biology of the nervous system is fundamental for our understanding of complex life itself.

Most organisms have both a central nervous system (CNS), comprising of the brain and spinal cord, and a peripheral nervous system (PNS) which consists of the nerves and neurons originating from the spinal cord which innervate the organs and muscles. Interestingly, the PNS has the ability to regenerate itself in response even to severe injury. This proceeds in the stereotypical fashion of Wallerian degeneration, involving axonal breakdown, increased production of neurotrophic factors and regrowth of severed axons.

1.2 Regeneration in the CNS

In contrast to the universal regenerative ability of the PNS, the regenerative capacity of the CNS varies between species, developmental states, and cell type. Most adult mammals lack significant regenerative ability, demonstrated by the permanence of traumatic brain and spinal cord injuries and irreversibility of degenerative diseases such as Alzheimer's and Parkinson's disease in humans. However, the CNS of some non-mammalian adult vertebrates including fish and salamanders undergo fast and functional regeneration in a timeframe of only weeks (Becker et al, 1997b; Bernstein, 1964; Butler & Ward, 1967). Further animals, including amphibians, some marsupials (opossum) and birds (chickens) demonstrate successful CNS regeneration only at early developmental stages (Beattie et al, 1990; Hasan et al, 1991; Terman et al, 1996). It has recently been reported that neo-natal mice can also demonstrate growth of long projecting axons through the injury site (Li et al, 2020). Remarkably, limited regeneration of the spinal cord has been demonstrated in an adult mammal, the spiny mouse (Nogueira-Rodrigues et al, 2021). Furthering our understanding of the molecular and cellular pathways behind successful regeneration in regeneration-capable species may allow us to encourage CNS regeneration in other non-regenerating species.

1.3 Types of CNS injury

Like the rest of the body, the CNS is susceptible to different forms of injury or illness resulting in loss of function. In some cases, these injuries may be caused solely by extrinsic contributors. These include traumatic brain injuries (TBI) or spinal cord injuries (SCI). SCIs can be further subcategorised by the type of damage undergone, for example partial transections, complete transection, crush, or dislocation (Cheriyan et al, 2014). Similarly, TBIs can be classified as either closed head injury or penetrating brain injury, and further as mild or severe (Petersen et al, 2021). Such injuries can be induced experimentally in the lab using physical apparatus.

Other forms of CNS injury are not caused solely by physical events and instead can occur without external forces. One example of this is an ischaemic attack which leads to cell death in a particular location of the brain due to the absence of oxygen supply. Furthermore, neurodegenerative diseases result in the selective death of particular neuronal subtypes. For example, Parkinson's disease and Spinal Muscular Atrophy (SMA) in humans lead to degeneration of dopaminergic neurons or motor neurons respectively. These diseases result in progressive and irreversible damage to neurons. Understanding the underlying molecular mechanisms of neurodegenerative diseases relies on the use of animal models of the specific disease of interest. CNS damage as a result of ischaemic attack and neurodegenerative diseases are outside the scope of this thesis, but comprehensively reviewed in (Amantea et al, 2009; Dugger & Dickson, 2017)

1.3.1 Spinal cord injury in humans

Spinal cord injuries are a life-limiting injury affecting an estimated 250,000 - 500,000 people annually (WHO, 2013). Patients suffering from these injuries experience high rates of premature death (Lidal et al, 2007), unemployment (E. Young & Murphy, 2009) and lower levels of life satisfaction (Post & van Leeuwen, 2012).

The severity of spinal cord injuries can vary based on the severity of the original injury - whether the injury is a partial crush or full transection. Additionally, the vertebral level primarily effected by the injury will determine the physical extent of functional impairment (McDonald & Sadowsky, 2002).

The clinical consequences of spinal cord injury are threefold. Firstly, the patient will experience loss of sensory function corresponding to the level of neurological injury. Secondly, motor function below the level of injury is also lost. Finally, in many cases the sympathetic innervation to the patient's organs is disrupted. This leads to a variety of systemic manifestations of the SCI including bradycardia, hypotension and even immunodeficiency (Guha & Tator, 1988; Schwab et al, 2014). Loss of bladder control and

sexual function are also implicated and can contribute to a poorer quality of life (Hagen et al, 2011; Reitz et al, 2004). Together, these contribute to the reduced mortality experienced by SCI patients.

Currently, spinal cord injury is incurable in humans and treatment is based on maximising residual function and minimising secondary injury (Ramer et al, 2014). Regeneration of the spinal cord in humans (and most mammals) is prevented by lack of intrinsic neuronal growth ability along with the presence of extrinsic growth inhibitors. Furthermore, there is a lack of injury-induced neurogenesis and endogenous stem cell populations in the spinal cord overwhelmingly generate new astrocytes and oligodendrocytes instead of new neurons which may contribute to functional recovery. Whilst there have been some promising breakthroughs in promoting spinal cord regeneration in humans in recent years, as yet these approaches are irreproducible or not clinically useful (reviewed in (Sofroniew, 2018) and (Fawcett, 2020)).

1.4 Zebrafish as a model organism for spinal cord regeneration

In comparison to this irreversible loss of function in mammals after spinal cord injury, anamniotes such as urodele amphibians and fishes demonstrate complete regeneration of their spinal cord in a timeframe of only weeks after injury. Consequently, studying the regeneration of these successful organisms may lead to insight and therapeutic approaches towards promoting regeneration after spinal cord injuries in humans.

Zebrafish have many advantages for use in spinal cord research over the other regenerating species. Firstly, they are a cost-effective animal for research due to their high fecundity and tolerance to a large range of conditions. As they have been used in the wider scientific community for a few decades now, many genetic tools are available which allow observation and manipulation of the zebrafish's underlying biology. For example, it is possible to produce reporter lines which express fluorescent proteins under the control of cell or tissue-specific promoters. In terms of spinal cord regeneration, reporter lines allowing visualisation of neurons, glial cells and immune cells are commonly used. Furthermore, the accessibility of a zebrafish's genome and the abundance of genetic tools allows fast gene knockout. Traditionally this has been done with morpholinos or TALENs, but within the last decade CRISPR/Cas9 technology has allowed more efficient gene knockouts (Varshney et al, 2015). More advanced CRISPR/Cas9 based tools also offer the chance for tissue specific or induced knockouts of genes, controllable by drug application or even light (Liu et al, 2019; Reade et al, 2017; Sun et al, 2019).

There are also disadvantages of using zebrafish for studying CNS regeneration. In some cases, it may be preferable to use model organisms which are as similar to humans as

possible. Inevitably, mammals share more anatomical and physiological features with humans and consequently model organisms such as *Mus musculus* and *Rattus norvegicus* are popular in many fields of biological research including CNS regeneration. (Cheriyan et al, 2014). The use of nonhuman primates is also used in some studies for an even better approximate of human SCI than rodents (Iwanami et al, 2005). In addition, other regenerating species offer a different and sometimes preferable set of characteristics making them well suited for specific research questions. For example, anuran amphibians transition from a regeneration-competent state before metamorphosis to a regeneration-incompetent state following metamorphosis (Phipps et al, 2020). Hence, anuran amphibians provide a unique opportunity to assess the mechanisms which result in regenerative success and failure within the same species (Lee-Liu et al, 2014).

Recently, the larval zebrafish, rather than adult zebrafish, has been established as a model for spinal cord regeneration research. It has been shown that 3-day-old larvae only need 48 hours to functionally regenerate their spinal cord (Wehner et al, 2017b). In comparison, adult zebrafish require 4-6 weeks for functional regeneration (Becker et al, 1997a; van Raamsdonk et al, 1998). Consequently, larval zebrafish can be a time-efficient model for answering experimental questions. The transparency of the larvae is a powerful characteristic, as the use of transgenic reporter lines allows observation of cell types of interest in a live animal.

The replacement of adult zebrafish with larval zebrafish is also favourable when considering the 3Rs of humane animal research (reduction, replacement and refinement) (Tannenbaum & Bennett, 2015). However, the disadvantages of the larval model must also be discussed. Importantly, the use of an organism which is still undergoing major developmental changes can complicate any experimental findings. In the case of regeneration, it can be difficult to disentangle the changes associated with development from those specific to regeneration. Interestingly, drug screening results for the same drug can differ between adults and larvae, likely due to the difference in developmental stage and therefore physiology (Cho et al, 2020). Furthermore, the smaller size of zebrafish larvae makes experimental manipulations technically challenging and the larvae can be more susceptible to minor environmental changes than adult zebrafish. Hence, adult zebrafish remain a popular choice for many situations.

1.5 Spinal cord development in zebrafish

Due to some of the advantages discussed earlier of zebrafish larvae, including their *ex vivo* development and optical accessibility, the early development of the spinal cord in zebrafish has been extensively studied. The timeline of spinal cord development from

neural induction to fully functional spinal cord as it is currently understood is outlined below.

Zebrafish embryos progress from the blastula to gastrula stage at approximately 6 hpf (Kimmel et al, 1995), which consists of three germinal layers of cells: ectoderm, mesoderm, and endoderm. Neural identity is induced in the ectodermal epithelium on the dorsal side of the embryo, henceforth referred to as the neural plate. Cell organisers, including the Spemann organiser, are primarily responsible for this neural induction by secreting bone morphogenetic protein (BMP) antagonists such as Noggin and Chordin (Appel, 2000). Since BMPs block neural induction in favour of an epidermal fate, the antagonism of BMP signalling results in neural induction. In addition, other secreted molecules such as fibroblast growth factors (FGFs) are necessary to induce neural fate (Schmidt et al, 2013). This repertoire of secreted signals works in concordance with intrinsic transcription factor programs including members of the SoxB1 family (Schmidt et al, 2013).

Signalling molecules are also utilised to induce anterior-posterior patterning. The anterior CNS region, the forebrain, is the default fate in the embryonic neural plate. Signals are required to posteriorize the neural plate and specify more posterior CNS regions, including the spinal cord. These signals include FGF and Wnt proteins, which first suppress anterior gene expression in the posterior neural plate, and then later, in an retinoic acid (RA) dependent manner, activate the posterior patterning genes (Schier & Talbot, 2005). This anterior-posterior patterning may begin even before gastrulation (Kudoh et al, 2002).

Patterning also occurs along the dorso-ventral axis, controlled by hedgehog (Hh), Wnt and BMP signal gradients (Le Dréau & Martí, 2012). Based on the exposure of the cells to the combination of these signals, specific domains of progenitor cells have specific transcriptional programs active and hence give rise to distinct population of neural cells (Xiong et al, 2013).

Between 10-18 hours post fertilisation (hpf) (and concomitantly with dorsal-ventral and anterior-posterior patterning), morphogenesis shapes the neural plate into a neural keel, which in turn becomes a neural rod (Araya et al, 2016). By 18 hpf, the neural rod becomes a hollow neural tube with a lumen. This lumen is the precursor to the ventricles and central canal in the brain and spinal cord respectively (Schmitz et al, 1993).

Occurring alongside neural tube closure is the specification of proneural clusters and subsequent neurogenesis. The first proneural clusters in the neural plate can be identified by approximately 11 hpf by expression of neuronal genes such as *neurog1* and *ascl1a* (Allende & Weinberg, 1994; Blader et al, 1997). This first wave of neurogenesis generates

neurons only (in contrast to secondary neurogenesis which can also generate oligodendrocytes), the first of which can be traced as early as 18 hpf (Wilson et al, 1990). This primary neurogenesis is vital for the establishment of a functional neuronal network allowing stereotyped movements such as escape responses as early as 2 days post fertilisation) (O'Malley et al, 1996)

Neurogenesis taking place at late embryonic and larval stages is referred to as secondary neurogenesis and is responsible for increasing the number of neurons generated, along with the generation of glial cells. This period establishes the neural networks responsible for generating higher order circuits including sensory and motor systems (Budick & O'Malley, 2000). Another essential distinction between primary and secondary neurogenesis is the cell type which is responsible for the generation of neurons/glia. During primary neurogenesis, neuroepithelial cells are converted to neurons. Some of these neuroepithelial cells later adopt a new phenotype which is characterised by radial processes and expression of astroglial markers e.g GFAP (Bernardos & Raymond, 2006). It is these ependymo-radial glial cells which are responsible for neurons and glial cells generated during secondary neurogenesis.

As discussed above, temporal exposure to specific concentrations of morphogens is responsible for determining the domains of neuronal progenitor cells, and their subsequent neurons. Subpopulations of these progenitor cells are fate-restricted by 3 dpf. In the case of the pMN domain, a specific domain can sequentially generate different cell types. These progenitors produce the majority of spinal cord motor neurons by 25 hpf (Myers et al, 1986) and most spinal cord oligodendrocyte precursor cells between approximately 28 and 42 hpf (Ravanelli & Appel, 2015). These quickly mature into oligodendrocytes, which begin myelinating axon tracts by 2.5 (Kirby et al, 2006; Park et al, 2002). Overall, the identity and position of differentiated neuronal subtypes is largely established by 3 dpf (Andrzejczuk et al, 2018; Reimer et al, 2013) and by 4 dpf these neurons are assembled into functional circuits required for mature swimming patterns and foraging behavior (Borla et al, 2002; Kroll et al, 2021).

1.6 Spinal cord injury model

This project investigates the mechanisms of regeneration after complete spinal cord transection injuries in the successfully regenerating zebrafish larvae. There are two main processes undergone by neuronal cells following injury: axon regeneration and neurogenesis. Many cellular, molecular and physical factors contribute to both axon regeneration and neurogenesis, including remodelling of the extracellular environment, angiogenesis, and infiltration of immune cells (Becker & Becker, 2020; Cigliola et al, 2020;

Vasudevan et al, 2021). Below, the current understanding of axon regeneration and neurogenesis in zebrafish after spinal cord injury is outlined.

1.6.1 Axonal regeneration

Axonal regeneration refers to the ability of transected axons to regrow across the injury site and re-innervate appropriate targets. The necessity of axonal regeneration has been demonstrated both experimentally and observationally using species which have capacity for successful CNS regeneration and recovery of function. For example,in zebrafish larvae, individuals which failed to regrow axonal bridges demonstrated impaired functional recovery as measured by touch-evoked swim distance (Wehner et al, 2017a). Similarly, Interfering with axonal regrowth experimentally using a physical block in the injury site in zebrafish spinal cord abolished any functional recovery observed (Becker et al, 2004).

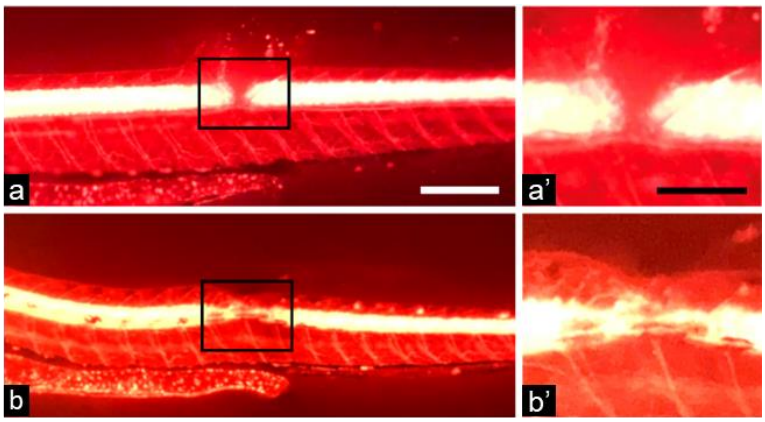

Figure 1.1: Spinal cord of lesioned XIaTubb:DsRed transgenic zebrafish larvae, in which axons are fluorescing red. A, A': This larvae is imaged directly after injury (at 3 days post fertilisation). The injury site is shown close-up in a'. **B, B'**: This larvae is imaged 24 hours post injury, and shows axon regeneration across the lesion site (boxed). A close-up of the bridging axons is shown in b'. Scale bar in a is 300 µm and applies to a and b. Scale bar in a' is 100 µm and applies to a' and b'. In all images, rostal is on the left and dorsal is up. Figure adapted from (Drake et al, 2023)

The molecular and cellular mechanisms leading to successful axonal regeneration have been extensively studied in zebrafish. Many extrinsic factors and non-neuronal cell types have been shown to be necessary for repair. Immediately following injury, macrophages infiltrate the injury site and temporally control the release of signalling cytokines Tnf and Il1b. This tight control of inflammation promotes axonal regrowth (Tsarouchas et al, 2018). Macrophages provide further support by phagocytosing cell debris (Becker & Becker, 2001; Hui et al, 2010; Tsarouchas et al, 2018). Pdgfrb expressing fibroblasts are also involved in the axon regrowth by deposition of Collagen XII. Collagen XII immuno-positive fibrils have been shown to act as a scaffold for the regenerating axons and this is required

for regeneration (Wehner et al, 2017a). Supporting glial cells are also likely to provide structural support for axons traversing the injury site (Goldshmit et al, 2012; Mokalled et al, 2016), although this does not appear to be necessary for regeneration (Briona et al, 2015; Dervan & Roberts, 2003; Wehner et al, 2017a).

The axons themselves also undergo intrinsic changes priming them for successful axonal regeneration. There is evidence for major changes to transcriptional programs in regenerating CNS axons. A study using regenerating retinal ganglia cells in the adult zebrafish revealed sequential activation of pathways regulated by a temporally controlled set of transcription factors (Dhara et al, 2019). While there is so far no similar comprehensive study in regenerating spinal cord axons, individual transcriptional regulators have been shown to be involved. High mobility group box 1 (HMGB1) is an architectural chromatin protein which could alter transcriptionally accessibility of other genes (Bustin, 1999; Fang et al, 2014), and its expression is tightly regulated following spinal cord injury in zebrafish. Four hours following injury there is a two-fold increase in *hmgb1* mRNA expression followed by a significant decrease at 12 hours post injury. Inhibiting HMGB1 levels using antisense morpholinos lead to a 34% reduction in axonal regrowth (Fang et al, 2014). The involvement of other transcription factors in spinal cord injury also supports the idea that axons undergo widespread changes to the expression of entire programs of genes. For example, both activating transcription factor 3 (ATF3) and activating transcription 6 (ATF6) have also been shown to promote axonal regeneration in adult zebrafish (Ji et al, 2021; Wang et al, 2017a).

As well as these broad transcriptional changes which neurons with regrowing axons undergo, the involvement of some individual specific genes in neurons with regrowing axons has been reported. The upregulation of recognition molecules on the cell surface helps the regrowing axons to navigate the lesion environment and eventually re-innervate targets. An early example of such a molecule is L1.1, which is upregulated in regenerating axons. Morpholino based knockdown of L1.1 resulted in poorer regeneration (Becker et al, 2004), whereas pharmacologically increasing expression of L1.1 resulted in faster regeneration (Li et al, 2018). Similarly, other recognition molecules including Syntenin-a (Yu & Schachner, 2013) and Sema4d (Peng et al, 2017) have been implicated in successful axon regrowth.

1.6.2 Neurogenesis

Spinal cord injuries inevitably result in neuronal cell death. Some of these neurons die due to the original impact of the injury, whilst others are lost due to the secondary effects of the injury. Damage to vasculature, exposure to inflammatory and cytotoxic signals are all

examples of secondary effects after spinal cord injury which may lead to apoptotic cell death. The peak of apoptotic cell death after spinal cord injury occurs at 24 hpi in adult zebrafish (Hui et al, 2010), suggesting that these secondary effects are responsible for the majority of cell loss. It is logical that these lost neurons need to be replaced in the regenerating system. In the zebrafish spinal cord, the major source of these new neurons are ependymo-radial glial cells (ERGs) (Reimer et al, 2008).

ERGs are named as such because they have much in common with mammalian radial glial cells whilst also having clear ependymal features. Their radial morphology and expression of astrocyte markers such as glial fibrillary acidic protein (GFAP) suggest a radial glial identity, but they also contribute to the ependyma and possess motile cilia (Hui et al, 2015; Kishimoto et al, 2011). Their contribution to the ependyma along with their contact with the pial surface means that these ERG cells span the entire width of the brain or spinal cord (Reimer et al, 2008). As well as in the zebrafish CNS, these cells have also been identified in salamander (Fei et al, 2014; Holder et al, 1990) and *Xenopus* (Muñoz et al, 2015; Tao et al, 2015).

A defining feature of ERGs is their ability to generate multiple glial and neuronal cell types. It has been demonstrated that after neuronal loss, these cells generate motor neurons and multiple subtypes of interneurons (Caldwell et al, 2019; Hui et al, 2010; Kuscha et al, 2012b). This is true both for cells lost by injury, and by ablation (Ohnmacht et al, 2016). In response to this neuronal loss, ERGs increase their proliferation rate and a subset of their progeny begin to express differentiation markers (Briona et al, 2015; Reimer et al, 2008). Interestingly, the eventual identity of these progeny is determined by the domain of the original ERG cell and the combination of transcription factors they express (Figure 1.2). ERG cells residing in the most ventral domain give rise to serotonergic neurons. Adjacent to these is the pMN domain (identified by its expression of *olig2*), followed by most ventrally the V2 neurons (expressing *vsx1*) (Kuscha et al, 2012a; Kuscha et al, 2012b; Reimer et al, 2008) This organisation is depicted in Figure 1.2.

The motor neuron progenitor domain is particularly interesting, as cells of this domain have been reported to switch transcriptional programmes following spinal cord injury. Cells of this domain, which co-express *olig2*, *pax6* and *nkx6.1*, generate motor neurons primarily during early development (0-48 hpf) and produce oligodendrocytes in later development (48+ hpf) (Ohnmacht et al, 2016; Ravanelli & Appel, 2015). Following an injury, these cells revert to motor neuron generation. In larval fish, this motor neuron generation even comes at the expense of the developmentally appropriate ongoing

oligodendrogliogenesis which would otherwise be ongoing in larval animals (Ohnmacht et al, 2016).

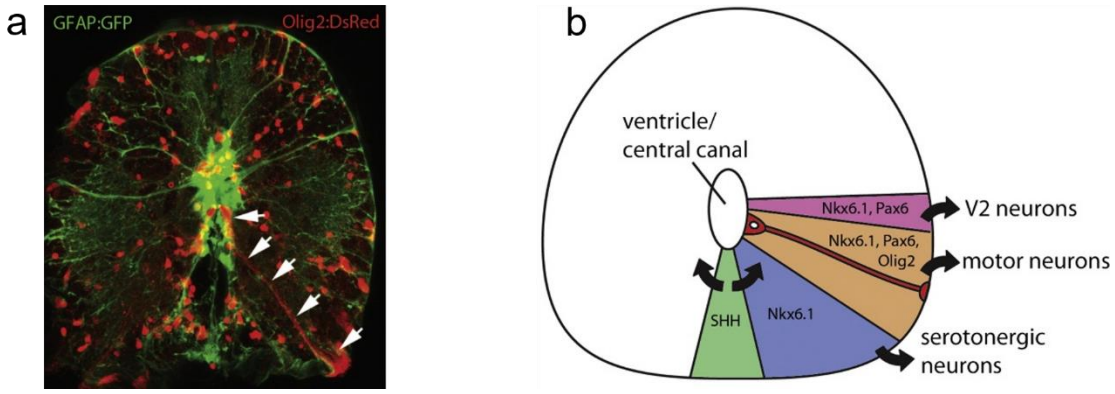

Figure 1.2: ERG domains in a cross section of the zebrafish spinal cord. A: *olig2* expressing ERG cells in adult spinal cord are depicted by arrows**. B:** The domains are schematically depicted with their transcription factor identity. Figure from (Becker & Becker, 2015)

In the last decade, much progress has been made into understanding what signals stimulate ERGs to proliferate and differentiate in order to generate new neurons in the zebrafish spinal cord after injury. It is clear that there is a large scale reactivation of developmental signalling systems in the successfully regenerating spinal cord. Wnt, BMP, Hh, Notch, RA and FGF pathways as well as some neurotransmitters have been shown to regulate developmental neurogenesis and also regenerative neurogenesis (reviewed in (Becker & Becker, 2015).

Delta-Notch signalling is one example of a pathway which is utilised both in normal development of the zebrafish spinal cord and is redeployed during regeneration. Notch signalling is important in juxtracrine cell-cell communication and via lateral inhibition can regulate neural progenitor cell fate during unperturbed development. Expressing a dominant negative form of Delta in zebrafish embryos causes an increase in the number of early specified motor neurons in zebrafish which later results in a depletion of progenitors in the motor neuron progenitor domain (Appel & Eisen, 1998; Appel et al, 2001). Likewise, delta-notch lateral inhibition is involved in regeneration, as the transgenic conditional over-activation of Notch signalling in ERG cells after injury reduces proliferation of ERGs and the number of new motor neurons generated. Conversely, the same study showed that pharmacological inhibition of Notch increased the generation of motor neurons following injury (Dias et al, 2012).

Along with their renowned role in transmitting neuronal information, neurotransmitters also have a function in development and regeneration of the CNS. Descending dopaminergic

projections from the brain influence the proportions of different types of neuron generation in the developing zebrafish spinal cord (Reimer et al, 2013). The same role for dopamine appears to be involved in regeneration, as ablating dopaminergic axons with 6-OHDA reduced the number of newly generated motor neurons rostral to the lesion site. In both development and regeneration, dopamine acts by the activation of the hedgehog pathway via the D4a receptor in ERG cells (Reimer et al, 2013).

Alongside the recapitulation of developmental neurogenic signals, there is some recently emerging evidence suggesting that the immune system may be a source of regeneration specific neurogenic factors in zebrafish. Whilst the presence of an immune response to CNS injury in zebrafish is well known (Becker & Becker, 2001), until the last decade the possibility of signals from the immune system acting on progenitor cells to stimulate the generation of new neurons was not investigated. The earliest direct evidence of the role of inflammation in zebrafish neurogenesis was provided by Kyritsis et al., who showed that inflammation is required and sufficient for neurogenesis from radial glial cells in the zebrafish telencephalon after injury (Kyritsis et al, 2012). This role was specifically linked to leukotriene C4 signalling, as injecting leukotriene C4 into unlesioned zebrafish brains showed elevated levels of radial glial proliferation. Following this, the role of the immune system in zebrafish spinal cord regeneration has been demonstrated broadly in two studies which showed that neurogenesis is drastically reduced when the fish are treated with the immunosuppressant dexamethasone in both larval (Ohnmacht et al, 2016) and adult (Caldwell et al, 2019) zebrafish.

The above studies use either global suppression or activation of the immune system and therefore do not reveal specific mechanistic details about the immune signalling pathways involved. In the larval system, it can be assumed that the immune signals are derived from the innate immune system, since the adaptive immune system is not fully functional until 4-6 weeks post fertilisation in zebrafish (Danilova & Steiner, 2002; Lam et al, 2004; Willett et al, 1999). Since the phenomenon has been observed in both larval and adult zebrafish, it is possible that the signals even in adult zebrafish are derived from innate immune system. The unique advantages of the zebrafish larvae, discussed above, provide a powerful model to study the neurogenic signals derived from the innate immune system independently to the adaptive immune system.

1.7 Spinal cord regeneration in other regeneration-competent animals

The dual processes of axon regeneration and neurogenesis are also present in other regeneration-competent vertebrates. For example, axon guidance associated genes such as semaphorins *sema4b* and *sema3f* are highly expressed after SCI in regeneration-

competent stages of *Xenopus laevis* development but not after SCI inflicted during the latter regeneration-incompetent stages (Lee-Liu et al, 2014). Similarly, there is also evidence for the role of neurogenesis after injury as pro-neural genes including *neurod4* and *ascl1* are shown to be upregulated after injury in regeneration-competent *Xenopus laevis* larvae but not the regeneration-incompetent post-metamorphosis juveniles or adults (Lee-Liu et al, 2014). Whether these changes in gene expression are due to the differing developmental stages or directly implicated in regenerative success requires further experimental investigation. More direct evidence for the involvement of a specific transcription factor in *Xenopus* regeneration was reported by (Pelzer et al, 2021), in which *foxm1* is shown to affect neural progenitor fate after division in injured *Xenopus tropicalis.* Furthermore, the necessity of the proliferation of these neural stem/progenitor cells was implied by the lack of functional recovery seen in *Xenopus laevis* in which these neural stem/progenitor cells were ablated (Edwards-Faret et al, 2021).

Other regeneration-competent animals, including spiny mice, neo-natal mice, embryonic chick and opossum also demonstrate successful and scar-free axon regeneration after spinal cord injury (Fry et al, 2003; Hasan et al, 1991; Li et al, 2020; Nogueira-Rodrigues et al, 2021). In both neo-natal mice and spiny mice, a role for a permissive extracellular matrix (ECM) has been identified as crucial for axon regeneration (Li et al, 2020; Nogueira-Rodrigues et al, 2021). The role of neurogenesis in these systems has yet to be experimentally investigated. However, there is some evidence for the upregulation of signalling pathways and molecules associated with neurogenesis in spiny mice after SCI (Streeter et al, 2020). In neo-natal and embryonic models, developmental neurogenesis is ongoing so may contribute to the functional recovery and decoupling these processes may prove challenging.

1.8 Zebrafish innate immune system

It is hypothesised that the innate immune response may be the source of pro-regenerative signals following SCI in regenerating species, including zebrafish. The zebrafish innate immune response during development is described henceforth.

The innate immune system is the first stage of defence to infiltrating pathogens. It is characterised by a fast and non-specific response to infections. The timeline of development, main cell types, and functions are all largely conserved across veterbrates (Renshaw & Trede, 2012).

The main cell types and systems in the zebrafish innate immune system are shared with the innate immune system of other vertebrates. At early developmental timepoints (<5 dpf), the zebrafish innate immune system consists mainly of macrophages, microglia and

neutrophils. Additionally, mast cells and hematopoietic stem cells (HSCs) are reported to be present at this time (Butko et al, 2015; Dobson et al, 2008). The presence of some other innate immune cells, specifically natural killer cells, dendritic cells and eosinophils, have been reported in adult zebrafish (Balla et al, 2010; Lugo-Villarino et al, 2010; Muire et al, 2016) but so far their presence in larval zebrafish has not been comprehensively investigated.

The immune cells in zebrafish arise from three separate waves of hematopoiesis. Each wave gives rise to a specific subset of immune cells and occurs during limited developmental windows, in restricted tissues. These waves of hematopoiesis are highly conserved in all vertebrates, although the timeframes differ between species (Galloway & Zon, 2003). These waves of hematopoeisis in zebrafish larvae are displayed in Figure 1.3a, and the location of each hematopoietic organ is highlighted in Figure 1.3b. Notably, whilst macrophages, microglia and neutrophils occur during the first primitive wave of hematopoiesis, cells of the adaptive immune system (T lymphocytes and B lymphocytes) do not arise until halfway through the definitive wave of hematopoiesis (and are not functionally mature until 4-6 wpf). Innate immune cells arise independently during each wave of hematopoiesis, and share a progenitor cell type during each wave. Whilst the primitive and intermediate waves of hematopoiesis do give rise to functional innate immune cells, cells which arise from the definitive wave are the longest lasting. Indeed, cells can be continuously generated from HSCs when necessary, in response to immunological threat or physical wounding (Galloway & Zon, 2003).

Each cell has distinct characteristics, roles, and response to pathophysiological conditions. Below is a discussion of each immune cell type in the zebrafish larvae (up to 5 dpf), with a focus on their response to SCI.

1.8.1 Neutrophils

Neutrophils are reliably observed in zebrafish trunk and tail from 48 hpf onwards (Lieschke et al, 2001; Willett et al, 1999). Early in development (2-14 dpf), neutrophils have multiple sites of origin, but from 4 dpf the main site of hematopoeisis is the kidney (Bennett et al, 2001; Brownlie & Zon, 1999). While some neutrophils are found in circulation, the majority are located within tissues and migrate through the interstitial fluid (Deng et al, 2011).

Neutrophils are easily identified by their unique morphology, which is generally conserved between mammalian and teleost neutrophils. They are recognised by their pale cytoplasm with a multilobulated segmented nucleus (Lieschke et al, 2001). They also express high

levels of the enzyme myeloperoxidase, which can be used as a marker for neutrophils in both mammalian and zebrafish neutrophils.

The primary role of neutrophils is understood to be in host defence against infiltrating pathogens. Neutrophils are consistently the first cell type to be recruited to different injury sites in many varied models of injury in zebrafish larvae, including spinal cord (Tsarouchas et al, 2018), heart (Lai et al, 2017) and tail fin (Li et al, 2012a). In order to perform this protective role, neutrophils respond to injury and infiltrating pathogens in a plethora of ways. They undergo degranulation, in which they release toxic intracellular granules and reactive oxygen species to sterilise the wound (Isles et al, 2021). They also produce extracellular traps (NETs) made of extracellular DNA which can trap bacteria (Palić et al, 2007). Neutrophils also play an important role in the recruitment of other phagocytic innate immune cells, particularly macrophages. Neutrophils are themselves involved in phagocytosis of infiltrating bacteria and debris, however it has been demonstrated that the role of phagocytosis by neutrophils in larval zebrafish is limited (Le Guyader et al, 2008).

As well as their involvement in infection control, neutrophils have also been shown to be involved in wound repair and regeneration after injury. Their contribution towards regeneration is complex and varies based upon the site of injury and/or the organism of interest. For example, in mice, neutrophils appear to have a detrimental effect in wound closure (Dovi et al, 2003) but a neuroprotective role after spinal cord injury (Stirling et al, 2009). In zebrafish there is currently a lack of tools allowing neutrophil-specific knockdown, so the contribution of neutrophils (separately from other leukocytes) has not yet been determined. However, due to the fast recruitment of neutrophils to the site of injury, and the fact that this recruitment occurs even after sterile laser injury (Kaveh et al, 2020) points to their involvement in regeneration. Due to the known crosstalk between neutrophils and monocytes (Loynes et al, 2018; Tauzin et al, 2014), as well as the earlier recruitment of neutrophils to the injury site, it is likely that neutrophils at least have a role in regeneration by triggering the recruitment and potentially the clearance of macrophages, which have an established pro-regenerative role in zebrafish (Sanz-Morejón et al, 2019; Tsarouchas et al, 2018). Since neutrophils have secretory roles, it is possible that they have a more direct contribution to regeneration by way of secreted molecules which may be recognised by regenerating cell types.

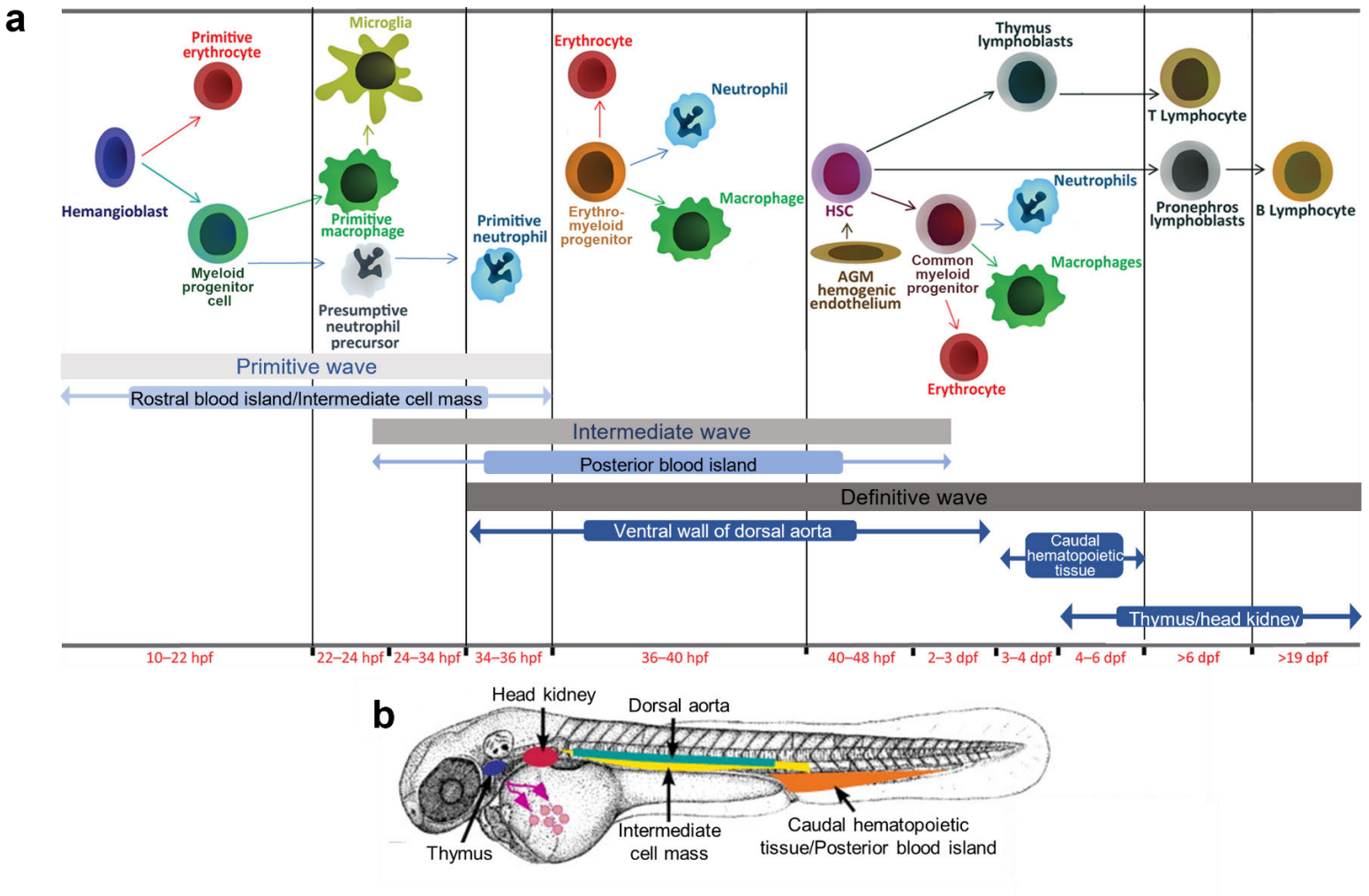

Figure 1.3: Immune cell development in zebrafish larvae. A: Zebrafish immune cells arise in three waves of development: primitive, intermediate and definitive. Adapted from (Masud et al, 2017) **B:** An illustration of the main sites of immune cell origin. Pink arrows signify the migration of primitive macrophages into the yolk ball. Adapted from (Stachura & Traver, 2011)

Resolution of inflammation is implicated in the successful regeneration of both zebrafish and mice. Despite the longstanding school of thought which suggests neutrophil are cleared by apoptosis (as occurs in mice (Dockrell & Whyte, 2006)), there is evidence that clearance by retrograde chemotaxis is the primary method of neutrophil resolution in zebrafish (Mathias et al, 2006).

1.8.2 Macrophages

Macrophages arise in a series of successive waves of haematopoiesis during zebrafish embryogenesis. The earliest macrophages, primitive macrophages, appear as early as 12-16 hpf from the rostral blood island (Herbomel et al, 1999; Herbomel et al, 2001) (Figure 1.3). By 72 hpf, macrophages are found in major peripheral tissues such as the brain and heart, and others reside in the caudal hematopoietic tissue (Bohaud et al, 2021; Herbomel et al, 2001).

In zebrafish, macrophages are large cells with the ability to change their morphology depending on pathology. Within developmental settings they are amoeboid, but they shift to an elongated morphology during migration through tissue. They also extend long pseudopods which function in migration, and undertake cell signalling roles (Mathias et al, 2009).

Macrophages are most notable for their highly phagocytic activity. Zebrafish blood circulation begins around 25 hpf, and as early as 30 hpf macrophages can phagocytose circulating bacteria (Herbomel et al, 1999). By 2 dpf there are enough functional circulating macrophages that injected carbon particles are wholly cleared within an hour (Lieschke et al, 2001). Whilst they are slower to be recruited to a site of injury than neutrophils, they are retained longer (Mathias et al, 2009).

Along with their phagocytic activity, macrophages have a variety of other roles in zebrafish host defence. They are a key component of the granuloma, a structure to contain infiltrating bacteria (Davis et al, 2002). Macrophages also produce and secrete cytokines in response to infection (Nguyen-Chi et al, 2015; Rougeot et al, 2019), which act in a temporal manner to control the infection by recruiting further immune cells (Bernut et al, 2016; Nguyen-Chi et al, 2014) and later promoting resolution of infection (Nguyen-Chi et al, 2015).

In addition to their role in infection control, macrophages have been demonstrated to have roles in tissue regeneration after injury in zebrafish larvae. Some of their pro-regenerative roles have been elucidated in heart (Kaveh et al, 2020), fin (Kawakami

et al, 2004; Nguyen-Chi et al, 2017), hair cell (Carrillo et al, 2016; Hirose et al, 2017; Zhang et al, 2020b) and spinal cord regeneration (Tsarouchas et al, 2018). In the spinal cord, they are recruited to an injury site within hours of initial impact, and their absence leads to reduced regenerative success (Tsarouchas et al, 2018). One way in which macrophages contribute to successful regeneration after spinal cord injury is via secretion of cytokines Tnf and Il1b; the precise temporal dynamics of these promotes axonal regeneration across the injury site (Tsarouchas et al, 2018). It has been speculated that macrophages can also act promote spinal cord regeneration in zebrafish by promoting neurogenesis from endogenous stem cells, however this had not been investigated before this project.

1.8.3 Microglia

Microglia are the CNS resident macrophages. Early in development, they are derived from primitive macrophages which colonise the CNS from 48 hpf, and then rapidly differentiate into early microglia over the following 24 hours (Herbomel et al, 2001).

They differ from macrophages both due to their location, and their molecular identity. Microglia show stronger expression of *apoE* and *p2ry12* than macrophages (Haynes et al, 2006; Herbomel et al, 2001; Mazzolini et al, 2020; Sieger et al, 2012). The morphology of microglia transforms from ramified in their resting state to amoeboid in their activated state (Herbomel et al, 2001; Kettenmann et al, 2011; Mojzesz et al, 2021; Wu et al, 2020).

Microglial activation in zebrafish is most commonly studied in the context of developmental and regeneration processes. However, they have been shown to also be activated by viral and bacterial infections in the brain and appear to play a role in containing these assaults. Similarly to macrophages, they can phagocytose bacteria (Peri & Nüsslein-Volhard, 2008; Wu et al, 2020), form granuloma-like structures (Chen et al, 2018; van Leeuwen et al, 2014), and secrete pro- and anti-inflammatory cytokines (Chen et al, 2018; Wu et al, 2020).

Microglia also play an essential role in zebrafish brain development and homeostasis. They can clear apoptotic neurons by phagocytosis after programmed cell death in the developing fish (Herbomel et al, 2001; Mazaheri et al, 2014; Peri & Nüsslein-Volhard, 2008), and physically interact with highly active neurons to decrease spontaneous firing (Li et al, 2012b). A subset of microglia with a distinct

transcriptome are enriched in synaptic regions and engulf neuronal synaptic proteins in the midbrain and hindbrain (Silva et al, 2021). Microglia also prune excess myelin sheaths during zebrafish development (Hughes & Appel, 2020). Despite these myriad functions of microglia, there is an absence of overt neuropathology in *csf1r* mutant zebrafish, which have severely reduced microglia numbers (Oosterhof et al, 2018). It has yet to be ascertained whether this is due to the remaining microglia performing these functions sufficiently, or compensation of other cell types to help perform these functions in the absence of microglia.

Microglia are involved in the response to disease and injury in the zebrafish brain. Laser ablations in the living brain leads to polarization of microglial cellular branching followed by migration towards the lesion (Sieger et al, 2012). They have also been reported to locally increase their numbers by self-renewal in the neurodegenerative zebrafish brain (Oosterhof et al, 2017). Unusual microglial behaviour and activation have been associated with zebrafish models of Alzheimer's disease (Bhattarai et al, 2017) and Parkinson's disease (Sanderson et al, 2021). In our lab, we recently discovered that mechanical forces applied by microglia to ERG cells are essential for wound closure after CNS injury (El-Daher, Drake et al., manuscript submitted). Intriguingly, a recent pre-print reports that microglia are essential for telencephalic regeneration and that their ablation inhibited injury-induced neurogenesis and regeneration (Kanagaraj et al, 2022).

There are a few studies which provide insight into the role of microglial cells after spinal cord injuries in the zebrafish. In the spinal cord lesion site of larval zebrafish, Ohnmacht et al. observed a 369% increase in microglial cells compared to unlesioned spinal cord (Ohnmacht et al, 2016). The number of both macrophages and microglia cells at the lesion site is highest at 48 hpi, but the migration of microglial cells is less immediate than macrophages (Tsarouchas et al, 2018). A similar increase in microglia numbers was observed following chemico-genetic neuron ablation, demonstrating that it is neuronal loss, not physical damage to the tissue, that leads to this increase in microglia number (Ohnmacht et al, 2016). This confirms previous work which showed that microglia migrate to the site of neuronal ablation and phagocytose the debris and degrading neurons (Caldwell et al, 2019; Morsch et al, 2015). Dampening the immune response with dexamethasone lead to a reduction in both axon regrowth and number of newly generated new neurons (Caldwell et al, 2019; Ohnmacht et al, 2016). Finer manipulations to demonstrate

whether this reduction in number of newly generated neurons is due to macrophage or microglial loss have not yet been performed. Intriguingly, while there is direct evidence for the role of microglia in neurogenesis in the zebrafish telencephalon (Kanagaraj et al, 2022), so far no direct role for microglia in axon regrowth has been reported. Indeed, when *csf1ra*/*b* knockouts (which lack microglia) were analysed there was no effect on axon regrowth (Tsarouchas et al, 2018).

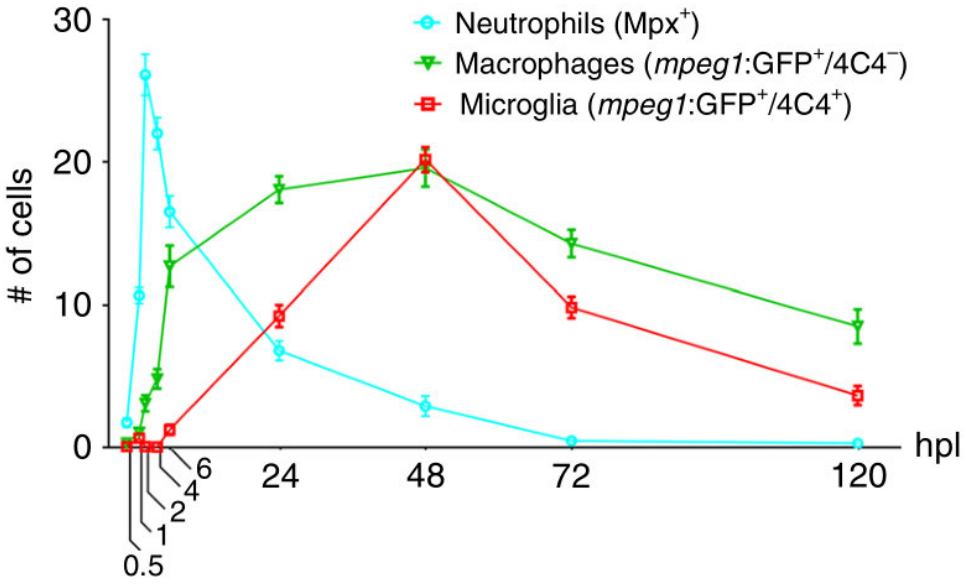

Figure 1.4: Time-course of immune cell infiltration to lesion site in larval zebrafish. Spinal cord injury was performed on zebrafish at the protruding mouth stage (72 hours post fertilisation) and number of immune cells were measured at intervals from this timepoint to 5 days post lesion. From (Tsarouchas et al, 2018)

1.8.4 Other innate immune cells

Other immune cells present in zebrafish larvae are mast cells and hematopoietic stem cells. Mast cells are proposed to arise from a common granulocyte/monocyte progenitor and primarily reside in the gastrointestinal submucosa and gills of zebrafish (Dobson et al, 2008). They act as early effector cells in response to noxious or infectious environmental stimuli and undergo degranulation in response to immunological threats. In zebrafish, this response is partly mediated by high affinity immunoglobulin E-like receptor (FcεRI) and likely also involves activation of toll-like receptors (Da'as et al, 2011).

The role of mast cells in zebrafish outside of pathogen response has not been well studied. In mammalian systems, they are known to release a plethora of cytokines

including TGF, TNF and IL8 (Grimbaldeston et al, 2006). Furthermore, other major constituents of mast cells include heparin and ECM-degrading enzymes tryptase and matrix metalloproteinases (Norrby, 2002). Hence, it is possible that these molecules signal to regenerating systems and influence the regenerative outcome, perhaps by direct signalling to regenerating axons or neuronal progenitor cells, or alternatively by remodelling the extracellular environment to provide a permissive substrate. For similar reasons, it is speculated that mast cells contribute to angiogenesis in mammals, specifically in the context of tumorigenesis (Norrby, 2002). Whether matrix play a secretory and/or matrix remodelling role in CNS regeneration is currently unclear.

HSCs are also present in the larval zebrafish (Butko et al, 2015). Their role is as a progenitor of blood cells, including immune cells, during the definitive wave of hematopoiesis (see Figure 1.3a). In mammals, HSCs have been shown to respond to external inflammatory factors and thus contribute to specific immune subtypes in order to facilitate the immune response (Zheng et al, 2011). However, more direct roles of HSCs such as secretion or phagocytosis are not reported, hence it is unlikely these cell types directly contribute to CNS regeneration.

1.9 The innate immune system in other regenerating species

Zebrafish are not the only species in which the immune system is implicated in successful regeneration of the CNS and other tissues. Indeed, in many other successfully regenerating species, immune cells have either been observed to correlate with the timing of injury or to directly contribute to CNS or tissue regeneration. The conservation of an innate immune response to injury across an array of regenerating species may suggest that the innate immune system is a vital contributor to successful regeneration.

1.9.1 *Ambystoma*

In axolotl *(Ambystoma mexicanum)*, recruitment of macrophages to the lesion site occurs within 24 hours and persists until 2 weeks post spinal cord injury (Zammit et al, 1993). More recently, a microarray analysis of axolotl spinal cord regeneration revealed that Il-1β cytokine is up-regulated at 24 hours post injury (Sabin et al, 2015). More direct involvement of the immune system in tissue regeneration (although not CNS regeneration) in axolotl was shown by Godwin et al., in which peritoneal injection of clodronate (a macrophage inhibitor) impaired limb

regeneration and replenishing macrophages later restored regenerative ability (Godwin et al, 2013).

1.9.2 *Xenopus*

After tail injury in *Xenopus laevis*, a high density of macrophages has been reported, and these have been observed in the role of granulocyte clearance (Paredes et al, 2015). Additionally, the cytokine interleukin-11 has been shown to act upstream of stem cell proliferation after tail injury in *Xenopus tropicalis* (Tsujioka et al, 2017), which is evidence for a role in direct immune signalling during tissue regeneration. In ths CNS,immunohistological staining with monoclonal antibody 4F4 has shown that there is a rapid and extensive microglial/macrophage response to crush of the optic nerve. Macrophages are seen in the nerve at the site of the lesion within 1 h. Interestingly, the response peaks between 3-5 days, which is just before axonal regeneration gets under way (Wilson et al, 1992).

While the above studies suggest a pro-regenerative role for the immune system in *Xenopus* CNS and peripheral tissue regeneration, this understanding is complicated by Fukazawa et al., who show that there is no immune response during successful tail regeneration in tadpoles. In contrast, there is a prolonged immune response to tail injury during the refractory period of frog development, during which no regeneration occurs. Notably, suppression of this immune response using genetic or pharmacological tools restored regenerative ability during this refractory period (Fukazawa et al, 2009). This study suggests that the role of the immune system in *Xenopus* regeneration may depend on the temporal dynamics of the immune system in conjunction with the specific developmental stage.

1.9.3 *Acomys*

The African spiny mouse is unique amongst mammals for its regenerative ability which persists even during adulthood. Interestingly, the successful regeneration of the spinal cord after SCI is accompanied by reduced inflammation when compared to SCI in *Mus musculus (Streeter et al, 2020)*. However, there is evidence for the role of immune cells in regeneration of other tissues in African spiny mice. After injury to the ear, there is a stronger and more prolonged period of reactive oxygen species (ROS) production in *Acomys cahirinus* compared to *Mus Musculus*. After experimental ablation of macrophages, this epimorphic regeneration does not occur (Simkin et al, 2017). Whether such a role for macrophages and other immune cells

is evident in the CNS during successful regeneration in African spiny mice is yet to be determined.

1.9.4 *Mus* (Neo-nates)

Neonatal mice, in contrast to adult mice, demonstrate successful regeneration of both the cardiac tissue and spinal cord. Gene expression profiling of cardiac macrophages indicated that regenerative macrophages have a unique phenotype and secrete soluble factors which may facilitate the formation of new myocardium and possibly contribute to angiogenesis. Furthermore, depleting macrophages in neonates resulted in a lack of myocardium regeneration (Aurora et al, 2014).

Similarly, there is direct evidence for the role of microglia in neonatal mice spinal cord injury. The depletion of microglia disrupts axon regrowth after SCI. Single cell sequencing was used to investigate the activation and role of these microglia (Li et al, 2020). These microglia promote successful regeneration in neonates by transiently secreting fibronectin which modulates the ECM. Furthermore, neonatal microglia express peptidase inhibitors and other molecules involved in inflammatory resolution. Applying neonatal microglia to adult spinal cord lesion significantly improved axon regeneration in adult mice (Li et al, 2020). Hence, the innate immune system plays a vital role in both neonatal spinal cord and heart regeneration.

1.10 The immune system in non-regenerating mammals

As discussed above, the immune system is pivotal to successful regeneration in some species. On the other hand, it has also been associated with the inability of many mammalian species to achieve successful CNS regeneration.

Following the initial trauma of the CNS injury (primary injury), secondary injury occurs. This is a cascade of inflammatory processes resulting in the death of neurons, oligodendrocytes and astrocytes (Alizadeh et al, 2019). The death of these cell types inhibits regeneration both directly (e.g dead neurons cannot be involved in motor or sensory pathways) and indirectly (by releasing growth inhibiting molecules) (McKerracher et al, 1994).

One source of these inflammatory signals is macrophages and microglia which are present at the injury site. This includes the activation of resident CNS microglia as well as the infiltration of monocyte-derived macrophages. The presence of these cells begins at three days post injury in mammals and can persist for longer than six

months after injury (Beck et al, 2010). While many of the functions of the macrophages and monocytes are beneficial (e.g prevention of infection, phagocytosis of cellular debris, recruitment of further immune cells), it is possible that this prolonged presence of macrophages and monocytes at the injury site is detrimental to achieving functional regeneration. Indeed, ablation of macrophages/microglia by clodronate loaded liposomes improved functional recovery in the hindlimb (Popovich et al, 1999) and improved myelinated tissue retention (Iannotti et al, 2011) in mice.

Further complexity concerning the role of macrophages and microglia after mammalian SCI is introduced by the presence of different phenotypes of macrophages. Traditionally referred to as M1 and M2, these phenotypes represent two extremes of a spectrum which are also referred to as pro-inflammatory (M1) and anti-inflammatory (M2). Kigerl et al. showed that the SCI site of mice is composed of primarily M1 macrophages with only a small and transient increase of M2 macrophages (Kigerl et al, 2009). Since M1 macrophages can kill nearby cells and prevent cellular proliferation, and M2 macrophages can promote cellular regeneration, it is hypothesised that promoting M2 polarisation at the expense of M1 polarisation of macrophages could aid in spinal cord regeneration. Indeed, in the typical wound healing process elsewhere in an organism, the macrophages are predominantly M2 polarised (Krzyszczyk et al, 2018). Kigerl et al. also demonstrated that in *ex vivo* adult sensory mice neurons, M2 macrophages are growth promoting and M1 macrophages are neurotoxic (Kigerl et al, 2009).

Along with the role of macrophages and microglia in modulating the extracellular environment in a SCI lesion, there is some evidence that they also signal directly to neural progenitors. Activation of microglia by LPS is detrimental for the survival of newly formed hippocampal neurons (Ekdahl et al, 2003; Monje et al, 2003a). Furthermore, immune cells release IL-1β, IL-6 and TNF-α, which all have a negative effect on neural stem/progenitor cells (NSPCs). In contrast, IL-15 is also produced by activated microglia and has been reported to promote proliferation and self-renewal of NSPCs (Gómez-Nicola et al, 2011). This evidence suggests that the role of the immune system in unsuccessful CNS regeneration is complex and may depend on precise temporal dynamics as well as cell-type specific responses.

1.11 Neural progenitor cells

1.11.1 Neural progenitor cells in zebrafish and other regenerating organisms

Ependymo-radial glial cells are a specialised form of glial cell found in the CNS of anamniotes. In the spinal cord, these cells contribute to the ependyma, but also possess characteristics of radial glial cells. They have radial processes which span from the ventricular lumen to the pial surface (Reimer et al, 2008). They also express genes typical of radial glial cells, including glial fibrillary acidic protein (GFAP), glutamine synthase and aquaporin 4. Furthermore, they possess motile cilia (Hui et al, 2015; Kishimoto et al, 2011), another hallmark of ependymal cells. These cells are referred to elsewhere in the literature as 'radial glia' (Fei et al, 2014), and 'ependymoglia' (Kirkham et al, 2014).

Ependymo-radial glial cells share many similarities with the early developmental cell type present in the neural tube, neuroepithelial cells. Hence, they are hypothesised to be the adult form of these cells (Becker & Becker, 2015). Both cell types display location specific identities. Depending on their dorso-lateral positioning within the spinal cord, they express specific combinations of transcription factors, and give rise to specific types of neurons. For example, one of the dorsal domains expresses *nkx6.1*, *pax6* and *vsx1* and specifically gives rise to V2 interneurons (Francius et al, 2016; Kuscha et al, 2012b), and an adjacent domain which expresses *nkx6.1*, *pax6* and *olig2* instead generates motor neurons (Reimer et al, 2009).

It has previously been shown that a mechanical lesion in adult reinitiates the program for neurogenesis resulting in generation of new serotonergic interneurons, V2 interneurons, *pax2*+ interneurons and motor neurons (Kuscha et al, 2012a; Kuscha et al, 2012b; Reimer et al, 2008). Lineage tracing experiments in the zebrafish brain and spinal cord has determined that the source of these newly generated neurons is ERG cells, which react to injury by proliferating and then differentiating into their neuronal progeny. In zebrafish larvae, *olig2* positive ERG cells have the ability to switch between neurogenesis and oligodendrogenesis. Early on in development, the *olig2*+ ERG cells generate neurons (Mori et al, 2005). However, by 48 hours post fertilisation, they switch mainly to an oligodendrocyte generating phenotype. In a healthy post-embryonic CNS these cells continue to generate new oligodendrocytes into adulthood (Park et al, 2007), eventually achieving relative quiescence (Reimer et al, 2008). In response to injury, however, they rapidly return to a neuron-generating phenotype at the expense of

oligodendrogenesis (Ohnmacht et al, 2016). This switch occurs in larval zebrafish even after a lesion at 3 dpf, despite the oligodendrocyte programme being recently induced in these cells.

1.11.2 Equivalent cell types in other organisms

ERG cells in regenerating species share many similarities with ependymal cells in the mammalian spinal cord. Ependymal cells in mammals are highly polarised and maintain long filament-rich processes extending to the pial surface. Some of these cells also have radial processes, similar to ERG cells, however with endfeet connecting to blood vessels rather than the pial surface (as with ERG cells). Their cell bodies are large and those found in the spinal cord have between two and four motile cilia. Importantly, ependymal cells are the main source of proliferative cells in the ependymal zone in the spinal cord during growth (Alfaro-Cervello et al, 2012) and following spinal cord injury (Bruni & Anderson, 1987). Whilst only astrocytes and oligodendrocyte generation has been observed *in vivo* (Meletis et al, 2008), cell fate regulators including *Shh*, *Bmp4* and *Notch1* show higher expression levels after injury (Chen et al, 2005; Yamamoto et al, 2001), suggesting at least partial recapitulation of developmental neurogenesis. Transplantation experiments have demonstrated that progenitors of the adult spinal cord generate mostly glial cells when grafted into the spinal cord, but the same cells can generate neurons when transplanted into a neurogenic environment, the hippocampus (Shihabuddin et al, 2000). Recently, Llorens-Bobadilla et al., demonstrated that ependymal cells can be manipulated to increase oligodendrocyte generation by artificially overexpressing the transcription factor OLIG2, and that this results in improved axon conduction in these mice (Llorens-Bobadilla et al, 2020). Taken together, these findings suggest that ependymal cells in mammals may have the capacity to generate new neurons after spinal cord injury, as occurs with ERG cells in anamniotes. This makes the elucidation of gene regulation in ERGs of zebrafish highly relevant for future experiments aiming to promote neurogenesis in mammals.

Radial glial cells are another cell type which are present in mammals and share some morphological and molecular similarities with the ependymo-radial glial cells found in anamniotes (discussed above, and in (Becker & Becker, 2015)). As in zebrafish, radial glial cells originate from neuroepithelial cells after early development (Aaku-Saraste et al, 1996). An important distinction between ERG cells in anamniotes and radial glial cells in mammals is that radial glial cells in

mammals are a transient population occurring in the brain. Radial glial cells during development are able to generate neurons, oligodendrocytes and astrocytes. Some radial glial cells are consumed during neurogenic division, and later the remaining radial glial cells terminally differentiate to become astrocytes (Malatesta et al, 2000; Voigt, 1989). An exception to this is in the dentate gyrus of mammals where radial glial-like stem cells represent the quiescent stem cell population (Alvarez-Buylla et al, 2001) and can undergo asymmetric divisions to generate neurons and astrocytes in response to a stimuli (Bonaguidi et al, 2011). However, the majority of radial glial cells in mammals do not persist outside of development and thus their potential for neurogenesis after injury is limited.

As discussed, some radial glial cells give rise to astrocytes in mammals. Astrocytes differ from radial glial cells in that they are not tethered to the ventricle and possess a star-shaped morphology. Suprisingly, in many species there are no marker genes differentiating between radial glial cells and astrocytes; instead, they are recognised by morphology alone (Malatesta et al, 2008). Until recently, astrocytes were not thought to be present in zebrafish, but in 2020, cells with astrocyte morphology and functionality were reported in zebrafish (Chen et al, 2020). However, their relevant abundance is as yet unclear, and in contrast to mammals, appear to exist alongside radial glial cells, instead of replacing them. Following injury in mammals, astrocytes can shift to a reactive astrocyte phenotype and become highly proliferative. These reactive astrocytes primarily give rise to further astrocytes in a process known as astrogliosis. In some brain regions, they also have neurogenic potential. This is demonstrated in the subventricular zone where astrocytes give rise to new neurons in the olfactory bulb (Doetsch et al, 1999). Whilst such a phenomenon does not appear to occur unaided in the mammalian spinal cord, *in vivo* reprogramming of astrocytes towards neurogenesis has been achieved using two different methods in mice (Puls et al, 2020; Su et al, 2014).

The lack of neurogenesis from ependymal cells and radial glial cells, in parallel with the generation of reactive astrocytes, are undoubtedly contributors to the lack of regeneration observed after mammalian spinal cord injury. This is in contrast to the generation of new neurons from ERG cells in regenerating organisms such as zebrafish and *Xenopus* and the concurrent lack of reactive astrogliosis in these same organisms.

1.12 Conclusions and statement of aims

Based on the reported influx of innate immune cells to the lesioned zebrafish spinal cord, as well as the reduction in neurogenesis after immune system inhibition, this thesis investigates the role of innate immune cells in promoting neurogenesis in zebrafish larvae.

The overarching hypothesis of this project is that macrophages are important for regeneration of the spinal cord in the zebrafish larvae. The specific hypothesis addressed in this thesis is that macrophages secrete cytokines which promote neurogenesis from ERG cells after spinal cord injury.

In this thesis I investigated the pro-neurogenic signalling between the innate immune cells and the ERG cells in the zebrafish spinal cord following injury. To investigate this, I addressed the following aims:

Chapter 3:

- To characterise the gene expression changes undergone by *mpeg1*+ cells in the zebrafish spinal cord after spinal cord lesion.

Chapter 4:

- To characterise the gene expression changes undergone by the *her4.3*+ cells in the zebrafish spinal cord after spinal cord lesion.

Chapter 5:

- To identify any ligand-receptor pairs in which the ligand was upregulated in the *mpeg1*+ cells and the receptor was upregulated in the *her4.3*+ cells.
- To investigate the role of *tnfa-tnfrsf1a* signalling in regenerative neurogenesis.

Chapter 2: Materials and Methods

Some of the methods in this chapter are also included as a chapter in a Methods in Molecular Biology publication – "Axon Regeneration: Methods and Protocols":

Drake, L. K., Keatinge, M., Tsarouchas, T. M., Becker, C. G., Lyons, D. A. & Becker, T. (2023) Rapid Testing of Gene Function in Axonal Regeneration After Spinal Cord Injury Using Larval Zebrafish. *Methods Mol Biol*, 2636, 263-277.

2.1 Methods

2.1.1 Zebrafish Husbandry

Zebrafish were raised and housed at temperature of 26.5℃ in 14/10 hour light dark cycles, in accordance with standard protocols (Westerfield, 2007). For breeding, adult fish were either kept in a mass breeding tank overnight (with incline and marbles) or housed in opposite sex pairs, kept separate by a removable divider. This allowed precise timing of embryo production for time-sensitive injections. Embryos were kept at 28.5 ℃ until 5 days post fertilisation (dpf) in conditioned aquarium water with 0.0001% methylene blue, with water exchanges performed daily. After 5 dpf the larvae are kept in the same conditions as adults, described above. For the purpose of this study both females and males of the following lines were used (described in Table 2.1).

Line name	Other names	Function	Reference
Tg(mnx1:GFP)	*mnx1*:EGFP *mnx1*:GFP	Visualisation of motor neurons	(Flanagan-Steet et al, 2005)
Tg(her4.3:EGFP)	*her4.1*:EGFP, *her4.3*:GFP	Visualisation of ERG cells	(Yeo et al, 2007)
Tg(olig2:DsRed2)	*olig2*:DsRed	Visualisation of motor neuron and oligodendrocyte progenitors	(Kucenas et al, 2008b; Shin et al, 2003)
Tg(mpeg1:EGFP)	*mpeg1*:GFP	Visualisation of macrophaes and microglia	(Ellett et al, 2011)

Table 2.1: Fish lines used in this study, along with their commonly used names and references.

2.1.2 Ethical considerations

All experiments in this thesis were performed on larval zebrafish of < 5dpf. These are not protected organisms under A(SP)A 1986, which regulates the use of animals in research. This thesis therefore follows the principles of 3Rs (reduction, replacement and refinement) (Tannenbaum & Bennett, 2015).

2.1.3 Larval lesions

Larvae were anaesthetised to a final concentration of 0.01% MS-222. After 2 minutes in 0.01% MS-222, larvae were unresponsive to touch stimuli and removed from anaesthetic to be placed on an agar plate (4%) in a lateral position. Excess water was removed and the sharp point of a 30 ½ gauge needle was used to perform the lesion, at the point of the 15th myotome (or at the end of the yolk extension). Lesions were performed looking through a stereo microscope for improved accuracy. Lesioned larvae were then kept at 28.5℃ at a density of 30 fish per 50 ml petri dish.

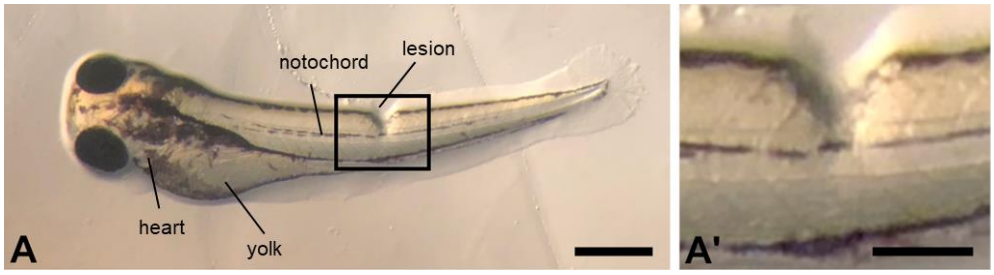

Figure 2.1: A zebrafish larvae at 3 dpf with lesion in dorsal trunk. A: Larvae imaged on agarose surface under stereo microscope. Scale bar 500 µm. **A':** Close-up of lesion area boxed in A. Scale bar 200 µm. Figure adapted from (Drake et al, 2023)

For the large quantity of larval lesions required for the single cell sequencing experiment, a team of four of us (myself, Leonardo Cavone, Themistoklis Tsarouchas and Tahimina Munir) worked together to lesion the larvae. For the single cell sequencing experiment on cells from *mpeg1*:GFP fish, this took place over a time period of four hours. For the single cell sequencing experiment on cells from *her4.3*:GFP fish, this took place over a period of 1.5 hours (the number of GFP positive cells was higher per fish so fewer fish were required to achieve a high yield of GFP positive cells). It was decided to perform the lesions in a team, to perform all the lesions over as short a period of time as possible. This ensured that the larvae

were at a similar stage of regeneration when the tissue was collected the following morning.

2.1.4 Single cell sequencing experiments preparation and processing

2.1.4.1 Tissue collection and dissociation.

At 4 dpf, the larvae were culled using MS-222. This was 24 hours post injury, although an equivalent number of unlesioned larvae were also used. Larvae were placed on agar plate and micro-scissors were used to remove the head and majority of the yolk of each larva. For the *mpeg1*:GFP larvae, the entire trunk (excluding removed head and yolk) was retained in order to maximise the GFP+ cells captured. For the *her4.3*:GFP larvae, micro-scissors were also used to remove the trunk caudal to the lesion site. Hence, only the immediate area surrounding the lesion site was retained (approximately 1 mm). The equivalent site was collected from unlesioned larvae. Trunk sections were immediately transferred to PBS on ice. For each experiment, the process of removing the head and tail was performed by a team of three (myself, Leonardo Cavone and Themistoklis Tsarouchas) and took 1 hour for the *mpeg1*:GFP larvae and 3 hours for the *her4.3*:GFP larvae.

2.1.4.2 FAC sorting

To isolate the cells and prepare for FAC sorting, initially larvae were incubated in 1 mL of 1x Trypsin-EDTA at 37℃ for 5 minutes. Tissue was dis-aggregated by pipetting and digestion was stopped by adding fetal bovine serum (FBS) to a final concentration of 5%. The samples were then centrifuged at 200g for seven minutes. The supernatant was discarded and the pellet resuspended in 500 µl of PBS. This suspension was added to a 40 µM cell strainer and re-centrifuged at 200g for another seven minutes. Finally, the pellet was resuspended in the PBS-FBS buffer (PBS with 5% FBS).

FACS was performed by the SuRF facility at Edinburgh Bioquarter. Wild-type fish with no fluorescence were used as a control to identify true GFP positive cells. After FAC sorting for GFP positive cells, re-running of the fluorescent fraction indicated > 90% purity.

2.1.4.3 10X Chromium sample preparation and processing

Single cell preparation was performed in collaboration with Dr Ross Dobie and Dr Beth Henderson of the Henderson group in QMRI, Edinburgh. Samples from the same cell type were processed in tandem on the same 10 X chromium chip, and

different cell types (*mpeg1:GFP* and *her4.3:GFP*) were processed separately due to time constraints.

The sequency library was generated following the comprehensive protocol provided by the manufacturer (10X Genomics, Pleasanton, USA). Briefly, this consists of preparing an adequately concentrated input sample, generating barcoded GEMs (Gel Bead-In-Emulsions), generation of barcoded, full length cDNA within the GEMs via reverse transcription, pooling of these cDNA molecules and library construction. Library construction generates a Single Cell 3' library which consists of Illumina paired-end constructs. The final library structure includes the details of the original sequence of interest as well the 10x barcode and unique molecular identifier (UMI).

2.1.4.4 Sequencing and data mapping

The sequencing of the libraries and mapping to reference sequence was performed by Edinburgh Genomics (Edinburgh, UK) as a service. The libraries were sequenced on a Novaseq 6000 using a S2 flowcell, and data was processed using the 10x Cell Ranger pipeline to align reads to the zebrafish genome GRCz10 and to generate gene-cell matrices.

2.1.4.5 Seurat

The gene-cell matrices were read into Seurat v3.1.5 for quality control, normalisation, scaling and clustering. This was performed separately for *her4.3:*GFP and *mpeg1:*GFP samples. The basic protocol described by Seurat was followed (Stuart et al, 2019). First, the gene-cell matrices were loaded in from the output provided by Edinburgh Genomics, with filters applied. These filters excluded genes which were expressed in fewer than 3 cells, or cells with fewer than 200 features expressed. Following this, the two separate conditions (lesioned and unlesioned) were merged, and then quality control metrics were plotted for the samples. These distributions allowed further cut-offs to be set for exclusion of poor-quality cells or doublets. Specific cut-offs are outlined in chapters 3 (*mpeg1:*GFP sample) and 4 (*her4.3*:GFP sample).

Following the application of quality control cutoffs, the datasets were normalised using the Seurat function LogNormalize and the default scale factor of 10000 and the top 2000 variable features were identified. The dataset was then integrated using these 2000 variable features as the anchors. Seurat's inbuilt integration function was used for this purpose. Seurat's integration was chosen for continuity

with the other steps of the analysis and as it has been shown to consistently rank well in an analysis of integration methods (Tran et al, 2020). An integrated analysis was then performed on all cells. Principle component analysis dimensionality reduction was performed using 30 principle components. Cells were clustered at a resolution of 0.5 for the *her4.3:*GFP sample and 0.3 for *mpeg1:*GFP sample. tSNE plots were generated using the first 20 dimensions.

The R script containing this code for both datasetsis published online publicly at https://github.com/s1836302/Mpeg1-and-Her4-zebrafish-larval-SCI

2.1.4.6 Differential expression testing and subsequent analysis

Differential expression testing on the single cell dataset was performed using the Wilcoxon Rank Sum test. Genes were considered differentially regulated if the adjusted p-value (Bonferroni correction for comparisons) was < 0.05. To identify differentially regulated gene programmes amongst highly upregulated genes (e.g Gene Ontology pathways, Kyoto Encyclopedia of Genes and Genomes pathways), Metascape webtool was used (Zhou et al, 2019) with the generated lists of significantly differentially expressed genes.

To identify transcription factors within our dataset, gene lists of interest (e.g significantly upregulated in specific clusters after injury) were cross-referenced with the *Danio rerio* transcription factor database AnimalTFDB v3.0 (Hu et al, 2019). The AllianceMine webtool (2022) was used to convert gene names to recent versions and find overlaps between generated gene lists and published zebrafish transcription factors.

In order to find orthologs between zebrafish genes from the GRCz10 assembly and mouse or human genes for analyses in chapters 4 and 5 respectively, Ensembl's BioMart webtool (Kinsella et al, 2011) was used.

2.1.4.7 Monocle

Monocle v3 for Rstudio was used for trajectory inference from the single cell sequencing datasets. The quality control cutoffs were first applied using the Seurat workflow as described above, and then the Seurat object was imported into the Monocle package. Monocle performed pre-processing, dimensionality reduction and cell clustering as described in the standard workflow (Cao et al, 2019). Following the learn_graph function, the root node was assigned manually.

2.1.5 CRISPR/Cas9 mutagenesis

2.1.5.1 Designing gRNAs

In order to identify highly active guide RNAs (gRNAs), initially four guides were designed for each gene. Guide RNAs are also referred to as synthetic RNA Oligo CRISPR guide RNAs (sCrRNAs) in the literature, and therefore highly active gRNAs are also referred to as haCRs (highly active sCrRNAs) (Keatinge et al, 2021).

The sequence for exons of the gene of interest (with 25-50 base pair (bp) flanking intronic material) was loaded into SnapGene Viewer software. Potential gRNA sites were identified based on the presence of the protospacer adjacent motif (PAM) 5'NGG where the preceding 20 bp (known as the 'spacer region') fell exclusively or mostly within the exon sequence. Targeting the exon sequence increases the probability that any changes in sequence induced will effect the protein function. An additional criteria for selecting gRNA sequences was that the region 3 bp 5' of the PAM site coincided with the recognition site of a restriction enzyme. SnapGene Viewer automatically detects and labels restriction enzyme recognition sites. Where more than four potential options were identified for a gene, preference was given to those in early exons and spanning functional domains. Once gRNAs were designed, primers spanning the gRNA target site were designed using primer3 web tool (Untergasser et al, 2012).

The design of one gRNA sequence and accompanying primers in SnapGene Viewer is illustrated in

Figure 2.2. All gRNAs, primers and corresponding restriction enzymes utilised in this project are listed in Table 2.2. Once designed, gRNAs were synthesised by Merck (2nmol, purified by high-performance liquid chromatography).

a

b

	Design in figure 1a
Custom gRNA sequence (5'-3')	AAATACAAAACCTGCAAACC
Forward primer sequence	TGCAAGCCTGGAATGTACTG
Reverse primer sequence	gctccaatattaatgtttgcttcc
Restriction enzyme	MwoI

Figure 2.2: Example gRNA design using SnapGene Viewer. A: An exon and flanking intron sequences are loaded into SnapGene Viewer. Intronic sequences are shown in lower case, exon sequences in upper case. For the sake of clarity, only the restriction enzyme sites used in the design are shown. **B:** The gRNA and primer sequences corresponding to the design in A are listed. Figure adapted from (Drake et al, 2023)

Gene target	Product	Restriction enzyme	Sequence
tnfa	gRNA	BslI	5'- GATGATGGCATTTATTTTGT -3'
	Forward primer		5'- ACCAGGCCTTTTCTTCAGGT -3'
	Reverse primer		3'- ACTTTTCAGTGCAATCCGCT -5'
tnfrsf1a exon 3	gRNA	BsrI	5'- TGATATTGTATATAACTGGC -3'
	Forward primer		5'- CAGACAGGGCACAGCATACA -3'
	Reverse primer		3'- TTCAAGACAATTAACTCCCTTCATAG -5'
tnfrsf1a exon 4	gRNA	BstNI	5'- ATAGTTTGCTTGTTCCAGGT -3'
	Forward primer		5'- CAGGAATGCAGTGCAGAAAA -3'
	Reverse primer		3'- TGACAATCCAGTGCTATTTTGG -5'
tnfrsf1a exon 5	gRNA	BslI	5'- AGGGTGAAGACTCCCTGGAA -3'
	Forward primer		5'- AACATGTGGAGGGTTGGTGT -3'
	Reverse primer		3'- CGAGAGCATTCCCATCCTAA -5'

tnfrsf1a exon 7	gRNA	MwoI	5'- GGGGAATGCTGGTTTTGCAT -3’
	Forward primer		5’- TCACTACTGGACATGGTGAACA -3’
	Reverse primer		3’- CACCTGTGATAGACCCAAATG -5’
control	gRNA	N/A	5’-TTACCTCAGTTACAATTTAT-3'

Table 2.2: Sequences and restriction enzymes for gRNA designs used in this project.

2.1.5.2 Microinjection of gRNA

Between 1 – 4 gRNAs were injected into one-cell-stage embryos. The injection mix consisted of 1 µl of each 20 µM gRNA (up to total of 4 µl), 1 µl 20 µM tracrRNA, 1 µl Cas9 protein 20 µM, 1 µl 1 % Fast Green FCF dye. The injection mix was made fresh for every injection session and kept on ice until embryos were laid. A control injection mix was also made, where the gRNA was based on standard morpholino control (Table 2.2).

Injection needles were made from glass capillaries (with filament), which were made into injecting needles using a needle puller and then cut to the correct diameter (droplets of 10-15 micron diameter) using forceps. Droplets of injection mix was injected into the yolk of individual embryos underneath a stereomicroscope. Embryos were randomly assigned to control injected, target injected, and uninjected groups. Embryos were lined up on petri dish against a glass slide to allow easy injection of multiple embryos in quick succession. Following injection, embryos were kept at 28.5℃ at a density of 30 fish per 50 ml petri dish.

Within 6 hours of initial injection, embryos were checked under stereo microscope for successful incorporation into the dividing cell mass. Embryos were removed if there was unsuccessful incorporation of injection mix into cell mass (Figure 2.3), or if they were unhealthy. Medium exchange and removal of dead, dying or unhealthy embryos was performed daily.

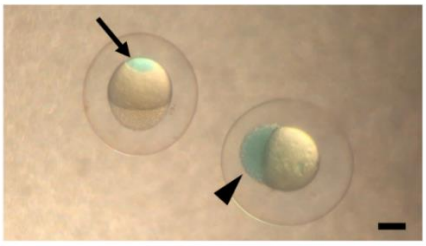

Figure 2.3: Examples of injected embryos. The embryo labelled with the arrowhead is successfully injected, as the green injection mix is incorporated into the cell mass. The embryo marked with the arrow has not had significant injection mix uptake into the cell mass and therefore should be discarded. Scale bar = 250 µm. Figure adapted from (Drake et al, 2023)

2.1.5.3 Checking efficiency of CRISPR/Cas9 mutagenesis

The efficiency of the gRNA injections was tested for each injection session on eight randomly chosen embryos using restriction fragment length polymorphism (RFLP). In the first instance, RFLP was performed to identify the most efficient guides out of the four designed per gene. RFLPs were also performed on eight embryos in all subsequent injection sessions to confirm continuing efficiency of gRNA injections.

Typically, eight control embryos and eight gRNA-injected embryos were included in the RFLP analysis. DNA was extracted from the 16 individual embryos (not pooled) at 1-2 dpf. Individual embryos were added to 100 µl 50 mM sodium hydroxide and heated to 95℃ for 10 minutes. Following a brief vortex, each sample was neutralised with 10 µl 1M-TrisHCL.

Using these DNA samples, the region surrounding the potential gRNA target was amplified using PCR. For each DNA sample, a PCR mix of 5 µl BioMix Red, 2 µl Nuclease free water, 1 µl forwards primer, 1 µl reverse primer, was added to 1 µl DNA sample and gently mixed. The primers used were those designed specifically for each gRNA target site. These samples were then amplified using a thermocycler set to the programme outlined in Table 2.3.

Following amplification, 1 µl of the appropriate restriction enzyme (Table 2.2) was added to 12 of the samples and gently mixed. The remaining four control samples did not have restriction enzymes added. This was followed by incubation of all samples for the recommended temperatures for 120 minutes (Table 2.4).

Step	Temperature	Duration	Function
1	95℃	180 seconds	Initial denaturation
2	95℃	30 seconds	Denaturation
3	55℃	30 seconds	Annealing
4	72℃	60 seconds	Extension
5	*Repeat steps 2-4 35 times*		
6	72℃	300 seconds	Final extension

Table 2.3: Thermocycler programme for PCR amplification.

Restriction enzyme	Temperature
BsrI	65℃
BslI	55℃
BstNI	37℃
MwoI	60℃

Table 2.4: Temperatures used for restriction digest, as per manufacturer's instructions.

2.1.5.4 Gel electrophoresis

Following restriction digest, samples were separated on a 2% agarose gel (with 0.0005 % Gel Red nucleic acid stain) via gel electrophoresis in Tris-acetate-EDTA (TAE) buffer at 100V for 60 minutes. Samples were loaded directly, as BioMix Red can act as a loading buffer. Samples were loaded individually into wells in the agarose gel. The first and last lane of the agarose gel was occupied with 100bp DNA ladder to allow accurate estimation of fragment size.

In order to easily gain information on the efficiency of gRNAs, the samples were loaded in a specific order. The four undigested controls are added to the first four wells, followed by the four digested controls and finally the eight digested injected embryos. This allowed for easy comparisons between the size of the bands. Embryos injected with efficient guides display the same band size/pattern as the first four bands (control undigested) since the restriction enzyme recognition site will have been mutated and hence digestion will not have occurred.

2.1.6 Histology

2.1.6.1 EdU incubation

Larvae were incubated in 50 µM EdU from 3 dpf. Some experiments involved lesions at 3 dpf, in which case larvae were placed in water containing EdU directly

after lesion. For experiments which did not include lesioning, larvae were transferred directly to water with EdU at 3 dpf. In both cases, water and EdU was exchanged after 24 hours until culling at 5 dpf. Larvae were kept at 28.5℃ throughout.

2.1.6.2 EdU detection

EdU detection occurs via the Click-It reaction, described below. All stages were performed with the larvae in 2 ml microtubes, with a maximum of 12 larvae per tube. Volumes used were 1 ml and steps were carried out at room temperature unless stated otherwise.

Larvae were fixed in 4% paraformaldehyde (PFA) at 4℃ overnight or for three hours at room temperature with gentle agitation. PFA was removed and larvae were washed in 5% PBS-Triton X (PBSTx) three times for five minutes each. PBSTx was replaced by methanol for another five minutes, before being replaced again with fresh methanol. This was kept at - 20℃ for a minimum of two hours (longer storage of up to a week was also used with good results).

Larvae were rehydrated through a series of methanol dilutions for five minutes each:

- 75% methanol in PBSTx
- 50% methanol in PBSTx
- 25% methanol in PBSTx

Larvae were then washed three times for five minutes each in PBSTx before their heads and majority of their yolk sac were removed under stereo microscope using micro-scissors. We found that larvae with head and yolks removed displayed greater reagent penetration. Following removal of heads, larvae were washed in PBSTx for another five minutes before incubation in 10 µg/ml Proteinase K in PBSTx for 45 minutes. After removal of as much Proteinase K as possible, embryos were refixed for 15 minutes with 4% para.

Next, larvae were washed in PBSTx three times for 5 minutes each and then incubated in 1% DMSO/0.5% Triton in PBS for 20 minutes. Following another three PBSTx washes for five minutes each, the reaction cocktail was added (Table 2.5) and incubated for 2 hours protected from light, with gradual agitation.

Component	Volume (µl)
Click-iT reaction buffer	9
$CuSO_4$	2
Fluorescent dye azide	0.5
Reaction buffer additive	10
ddH_2O	87.5
Total	**100**

Table 2.5: Reaction mix for Click-iT reaction. Each sample required 100 µl of mix, hence these volumes were scaled up depending on the number of samples used.

Following a further three PBSTx washes, larvae could be mounted in glycerol for imaging. However, for all experiments included in this thesis, antibody detection was performed directly following the final PBSTx wash.

2.1.6.3 Immunohistochemistry

When immunohistochemistry was performed directly after the EdU protocol above, embryos were protected from light during all upcoming incubation steps.

When immunohistochemistry was performed without prior EdU protocol, larvae were fixed and dehydrated then rehydrated in Methanol, and digested using Proteinase K as described above.

Larvae were placed in blocking buffer for one hour at room temperature, or overnight at 4℃, with gentle agitation. Meanwhile, primary antibody was diluted in blocking buffer to desired concentration (see Table 2.6 for concentrations). Following the blocking step, blocking buffer was replaced with this primary antibody solution. Larvae were incubated in primary antibody for two hours at room temperature, or overnight at 4℃, with gentle agitation.

Next, primary antibody solution was removed and three washes in PBSTx were carried out, for 15 minutes each. Meanwhile the secondary antibody was diluted in blocking buffer to the correct concentration. Following the final 15 minute PBSTx wash, larvae were incubated in secondary antibody overnight at 4℃.

Finally, the larvae were washed twice more in PBSTx for 15 minutes, and once in PBS for 15 minutes. Larvae were transferred to 70% glycerol in PBS for a minimum of 30 minutes before mounting for imaging. Larvae were mounted on microscope slides with a thin layer of glycerol and covered gently with a coverslip. The coverslip

was sealed with clear nail polish and stored flat, in the dark at 4℃, before imaging within the following 3 days.

2.1.6.4 Image acquisition and cell counting

For acquisition of fluorescent images, LSM 710 confocal microsocope or Zeiss Axioimager Z1 microscope with apotome attachment was used. Both microsocopes use the Zeiss Zen 2011 software.

Confocal image stacks were taken through the complete thickness of the spinal cord, with the lesion site or equivalent location in unlesioned larvae in the centre of the image. The interval of this z-stack was 1 µm and approximately 30 stacks were needed to cover the entirety of the spinal cord.

After image acquisition, Image J was used to crop the image to a rectangle of 300 µm width and 100 µm height, centred on the lesion site, so that 150 µm rostral and caudal of the lesion site was captured (or equivalent area in unlesioned larvae). Cells were counted in each slice individually, using keyboard shortcuts to switch between fluorescent channels to best identify co-localised cells. Cells were considered as co-localised when the area and shape of staining in the two channels of interest was largely overlapping, with the EdU signal expected to be the smaller of the two. Image J plugin 'Cell counter' was used to mark cells across multiple z-stacks and to keep track of number of cells counted. For all experiments, the observer was blinded to experimental conditions when performing cell counts. This randomisation and blinding was performed manually by a colleague.

2.1.7 Statistical analysis and bias mitigation

Statistical analysis was performed with Graphpad Prism v8. The Shapiro-Wilk normality test was used to test for Gaussian distribution, and the result of this determined whether parametric (T-test and ANOVA) or non-parametric tests (Mann-Whitney) were used. Exact p-values are indicated in the figure legends, and p-value ranges are indicated on the graphs themselves (*P < 0.05, **P < 0.01, ***P < 0.001, n.s. = no significance). Error bars indicate the standard deviation (SD).

Graphpad Prism v7 and v8 were also used to generate graphs of experimental data, and Rstudio was used to generate feature plots, violin plots and t-distributed stochastic neighbour embedding (tSNE) plots of single cell sequencing data using the ggplot2 package.

In experiments involving CRISPR/Cas9 mutagenesis, petri dishes with injected embryos were relabelled with a non-descriptive title (e.g A/B/C) by colleagues to blind me to the experimental conditions . This mitigated bias during the experimental procedures following micro-injection, e.g application of solutions and lesion.

2.2 Materials and Reagents

2.2.1 Antibodies and kits

Kit/Antibody	Source	Catalogue number	Dilution
Chromium Single Cell 3' Library & Gel Bead Kit v2	10X Chromium	PN-120267	-
Click-iT EdU Alexa Flour 647 Imaging Kit	Invitrogen	C10340	-
anti-GFP (chicken)	Abcam	ab13970	1:400
Alexa 488 conjugated donkey anti-chicken IgG(H+L)	Jackson	703-545-155	1:200

Table 2.6: Details of antibodies and kits used in this study

2.2.2 Reagents and products

Product	Catalogue number	Source
30 ½ gauge syringe needle	304000	BD
5-Ethylnyl-2'-deoxyuridine (EdU)	A10044	Invitrogen
Agarose	10688973	Fisher Scientific
Aminobenzoic acid ethylmethylester (MS-222)	A5040	Supelco
BioMix Red	BIO-25006	Meridian Bioscience
Bovine serum albumin	A3912	Sigma-Aldrich
BslI restriction enzyme	R0555	New England Biolabs
BsrI restriction enzyme	R0527	New England Biolabs
BstNI restriction enzyme	R0168	New England Biolabs
Cas9	M0386	New England Biolabs
Custom gRNAs (2nmol, HPLC purified)	VC40003N	Sigma-Aldrich

Custom primers (25 nmole DNA oligo)	-	Integrated DNA Technologies
Dimethyl sulfoxide (DMSO)	D84418	Sigma-Aldrich
Ethylenediamineteraacetic acid disodium slat dihydrate, EDTA	E6635	Sigma-Aldrich
FastGreen Dye FCF	F7258	Sigma-Aldrich
Fetal Bovine Serum	F9665	Roche
GelRed nucleic acid stain	SCT123	Millipore
Glass capillary (with filament)	BF100-58	World Precision Instruments
Glycerol	G5516	Sigma-Aldrich
Hydrochloric acid	320331	Sigma-Aldrich
Methanol	67-56-1	Fischer Chemicals
Methylene Blue	370.0025	VWR International
MwoI restriction enzyme	R0573	New England Biolabs
Normal donkey serum	S30	Millipore
Paraformaldehyde	P6148	Sigma-Aldrich
Precision forceps	MSPP-1125230	VWR International
Quickload 100bp DNA ladder	N0467	New England Biolabs
Sodium hydroxide	30620-M	Sigma-Aldrich
Superpremium microscope slides	631-0116	VWR International
tracrRNA	TRACRRNA05N	Sigma-Aldrich
Triton X-100	327372500	Acros Organics
Tween 20	P1379	Sigma Aldrich

Table 2.7: Products and reagents used in this project, with corresponding catalogue numbers.

2.2.3 Solutions

Solution	Components
Blocking buffer	1x PBS 1% DMSO 1%BSA 1% Normal Donkey serum 0.7% TritonX-100

Paraformaldehyde (4%)	16g Paraformaldehyde 40ml 10X PBS complete with dH2O up to 400ml
50x TAE buffer	484g TrisBase 114.2ml Acetic Acid 1000ml 0.1 EDTA, pH8 Adjust pH to 7.5 with HCl Complete with dH2O up to 2L
10X phosphate buffered saline (PBS)	160g NaCl 28.3g Na2HPO4 4g KCl 4.8g KH2PO4 Complete with dH2O up to 2
PBSTx	50ml PBS, 100ul Triton X-100

Table 2.8: Solutions made in laboratory, used in this project

2.2.4 Software and Packages

Product	Version	Reference
Cell Ranger pipeline	3.0.2	10X Genomics
GraphPad Prism	6 +	GraphPad by Domatics
ImageJ	various	
Monocle package	3 v0.2.1	
R	4.0.0	R core team
Rstudio	1.2.5042	RStudio
Seurat package	3.1.5	
SnapGene Viewer	various	Dotmatics

Table 2.9: Software and package versions used in this project

2.2.5 Data and code availability

Data/code	Repository	Accession
*her4.3:*GFP scRNAseq raw data	ArrayExpress	E-MTAB-10390
*mpeg1:*GFP scRNAseq raw data	ArrayExpress	E-MTAB-10379
R code for generating Seurat plots and Analysis	Github	s1836302/Mpeg1-and-Her4-zebrafish-larval-SCI

Chapter 3: Single cell sequencing of the innate immune cells in naïve and lesioned zebrafish spinal cord

---

Some of the data in this chapter was published as:

Cavone, L.*, McCann, T.*, **Drake, L**.*, Aguzzi, E., Oprişoreanu, A., & Pedersen, E. et al. (2021). A unique macrophage subpopulation signals directly to progenitor cells to promote regenerative neurogenesis in the zebrafish spinal cord. *Developmental Cell*, *56*(11), 1617-1630.e6.

*: Joint first authors

https://doi.org/10.1016/j.devcel.2021.04.031

3.1 Introduction

In order to determine the contribution of the innate immune cells to neurogenesis in the zebrafish spinal cord after lesion injury, I performed a single cell sequencing experiment to characterise this cell type. This chapter characterises the isolated *mpeg1*+ cells and their progeny from the spinal cord of both uninjured and injured zebrafish larvae at 4 dpf (24 hours after injury). *Mpeg1* is a marker for macrophages and microglia cells which contribute to the innate immune system. It is known that macrophages can contribute to axonal regeneration in zebrafish spinal cord, and neurogenesis elsewhere in the CNS. The inclusion of both uninjured and lesioned larvae allows us to describe the injury induced changes in the *mpeg1*+ population and to investigate the role of these cells during spinal cord neurogenesis. This dataset and corresponding analysis has already been published with me as a joint first author (Cavone et al, 2021). Some details such as cell cluster annotations have been refined since publication due to further exploration of the data.

In this chapter, I first describe the single cell sequencing experiment performed to capture the *mpeg1*+ cells. Following quality control of the sequencing data, I characterise the cell types captured in this dataset. Finally, I compare the populations before and after injury, both in terms of relative composition of cell types and gene expression changes within these cell types following injury.

3.1.1 Mpeg1 as a marker for macrophages

Mpeg1 is a protein coding gene first identified in humans and mice (Spilsbury et al, 1995), but also present in zebrafish (Zakrzewska et al, 2010), sea sponges (Wiens et al, 2005), and pacific oysters (Renault et al, 2011). It is upregulated after bacterial (McCormack et al, 2013; McCormack et al, 2015), viral (Renault et al, 2011) and prion infections (Kopacek et al, 2000) and its subsequent protein, perforin-2, is hypothesised to aid in host defence by pore formation in invading pathogens (McCormack et al, 2015).

In zebrafish, there are three *mpeg1* isoforms: *mpeg1.1*, *mpeg1.2* and *mpeg1.3*. The similarity between the amino acid sequences are 80-90%, and their similarity with murine and human MPEG1 is 70-80%. In general and for the rest of this thesis, *mpeg1.1* is referred to as *mpeg1* (Benard et al, 2015).

Due to mpeg1's role in monocytes, it is frequently used as a marker to identify circulating and tissue-specific macrophages (Ellett et al, 2011). In zebrafish, a mpeg1 reporter line exists in which GFP is expressed in mpeg1 expressing cells. While the line was originally believed to identify monocytes specifically, it has since been understood that some neutrophils also express *mpeg1* (Kaveh et al, 2020), as do B cells and NK-like cells in adult zebrafish (Ferrero et al, 2020; Moyse & Richardson, 2020).

Despite the growing appreciation of *mpeg1* expression in a limited selection of non-macrophages, *mpeg1* is still regarded as an acceptable macrophage marker, particularly in larval zebrafish prior to the development of the adaptive immune system (Rougeot et al, 2019). Since the aim of this chapter is to investigate changes in macrophages and microglia (CNS-specific macrophages), the *mpeg1*:GFP reporter line is used to identify this population in this thesis.

3.1.2 Single cell sequencing as a technology for understanding immune cell populations

One way to investigate the neurogenic promoting role of innate immune cells is to characterise the gene expression of these cells in the spinal cord of uninjured and injured zebrafish larvae. Differences in the gene expression profiles of these cells could highlight pro-neurogenic signals secreted by infiltrating immune cells. Furthermore, identification of changes in the numbers or gene programmes of specific cell subtypes could point towards potential roles of these cells in

regeneration. Modern techniques allowing large scale and comprehensive analysis of gene expression profiles include bulk sequencing and single cell sequencing.

Since the inception of high-throughput sequencing in 2005, the technology has become increasingly accessible and affordable. Now, bulk sequencing is used routinely to look at the transcriptome of groups of cells. In bulk sequencing, cells from a particular tissue or organ are pooled and the RNA transcriptome is described for the sample as a whole. This technique is used extensively, particularly when comparing the global gene expression of two conditions or disease states.

Bulk sequencing has the disadvantage that its homogenous approach may mask subtler, subtype-specific changes or processes. Single cell sequencing can address this disadvantage. The transcription of specific mRNA molecules can be traced back to the cell of origin. Hence, single cell sequencing can detect smaller or more transient cell types which are likely to be lost in bulk sequencing approaches (Figure 3.1). Due to the heterogenous nature of immune cells, single cell sequencing is therefore often the preferred choice from understanding immune cell characteristics and behaviour.

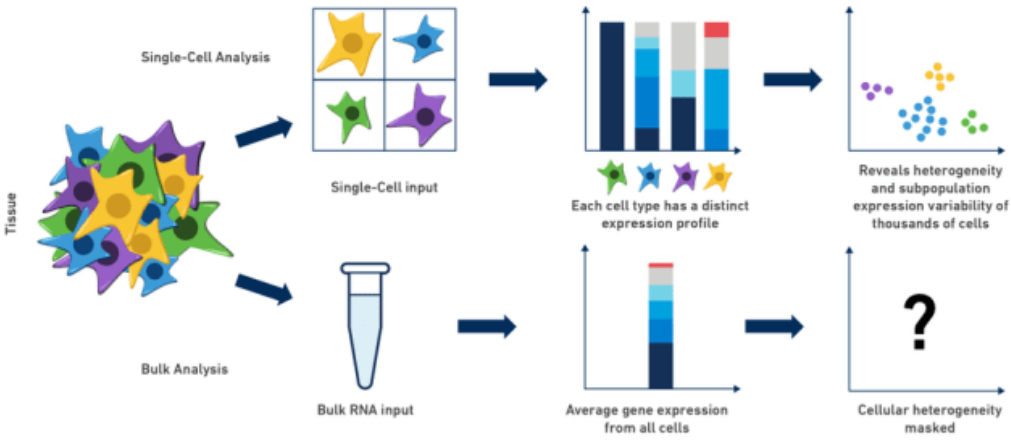

Figure 3.1: A diagram comparing bulk and single cell transcriptomics. Bulk expression profiling masks the heterogeneity within samples. Figure from 10x Genomics, LIT000027 Getting Started with Single Cell Gene Expression.

One example of the power of single cell sequencing to investigate immune cell populations is a study conducted by See *et al.* in 2017 (See et al, 2017). Previously, the source of two subtypes of plasmacytoid dendritic cells in humans was unknown. Single cell sequencing found that these subtypes shared a developmental origin, and identified the group of pre-dendritic cells which were the source of both of these

subtypes. This population contained unique markers and displayed unique abilities including production of IL-2, which were confirmed by mass spectrometry techniques and cell functional studies. This study has lead to revisions of some previous conclusions about plasmacytoid dendritic cells (Cao et al, 2020).

3.1.2.1 Technologies for single cell isolation and library construction

For both bulk and single cell sequencing experiments, cells need to be dissociated from their surrounding tissues. This process involves either physical or chemical dissociation but varies significantly between organism and tissue type. In single cell sequencing experiments, the cells in these samples then need to be captured individually before library construction occurs. Library construction is the processing of reverse transcribing the captured mRNA molecules into cDNA which are stable enough to sequence. Presently, there are two main technologies in widespread use for single cell capture and the subsequent library construction: plate-based technologies, and droplet-based technologies. Plate-based techniques use manual or microfluidic techniques to separate the cells into individual wells on a plate. Droplet-based technologies instead capture individual cells within an oil nanodrop. Both techniques have advantages and disadvantages making them more suited for specific experimental aims.

The most popular plate-based single cell experimental platform is SMART-seq (and subsequent versions SMART-seq2 and SMART-seq3). These technologies generally come at a lower cost but are able to capture only a few hundred cells per sample (Baran-Gale et al, 2017). During library construction, SMART-seq systems capture the full length mRNA and therefore is well placed to detect gene fusions or isoforms (Picelli et al, 2014).

In contrast, the 10x Genomics single-cell controller is a popular platform for droplet-based capture of single cells. This system can assess larger numbers of cells and therefore can detect rare cell types successfully (Wang et al, 2021b). However, the use of 3’ tags to convert mRNA to cDNA have the disadvantage that they are not cannot capture all the instances of gene fusion and gene isoforms.

For this experiment, due to the desire for large numbers of cells to be captured, and the possibility of rare cell types involved, I utilised the 10x Genomics system at the expense of capturing the complexity of gene isoforms and gene fusion events.

3.1.2.2 Tools for the analysis of single cell sequencing datasets

One difficulty accompanying the use of single cell sequencing is the complicated analysis. With the rise in popularity of single cell sequencing experiments in recent years, the options for analysis of such datasets has grown in parallel. While there are some commonalities with the bulk sequencing analysis tools, the vast quantities of data generated in single cell sequencing experiments, along with its high degree of dimensionality, means that it is often better suited to specific tools.

A recent cataloguing of tools for analysing and processing raw single cell sequencing datasets found there are more than 1000 tools (Zappia & Theis, 2021). These vary from tools which are specific to one form of analysis, or those which offer a more generalised toolbox. Furthermore, there are a variety of software platforms for such tools. R and Python are the most popular choices, perhaps because of their dominance in the field of data science as a whole, but Matlab, C++ and workflow managers such as Nextflow are also used (Zappia & Theis, 2021).

For the analysis of this dataset, the R package Seurat (version 3) was used (Stuart et al, 2019). Seurat offers an end-end package, including quality control of data, exploration and analysis. It also allows integration and comparison of different conditions, which is a vital component of our research question. An emphasis is made on clear and interpretable visualisations and the package is comprehensively documented.

3.2 Results

3.2.1 Experimental Design

To investigate the transcriptome of the infiltrating innate immune cells at the lesion site, I raised *mpeg1*:GFP larvae until 3 dpf. At 3 dpf, the larvae were randomly assigned to two groups of 1800 larvae each. The larvae in one group underwent spinal cord transection injury. The remaining larvae were kept uninjured as the unlesioned control group. Twenty-four hours later, the head and yolk sac were removed from all fish. The trunk was retained for cell dissociation, followed by FACS preparation for the 10x Genomics system. The subsequent 10x library of tagged cDNA molecules was sent to Edinburgh Genomics for sequencing. A schematic of the experimental design is shown in Figure 3.2.

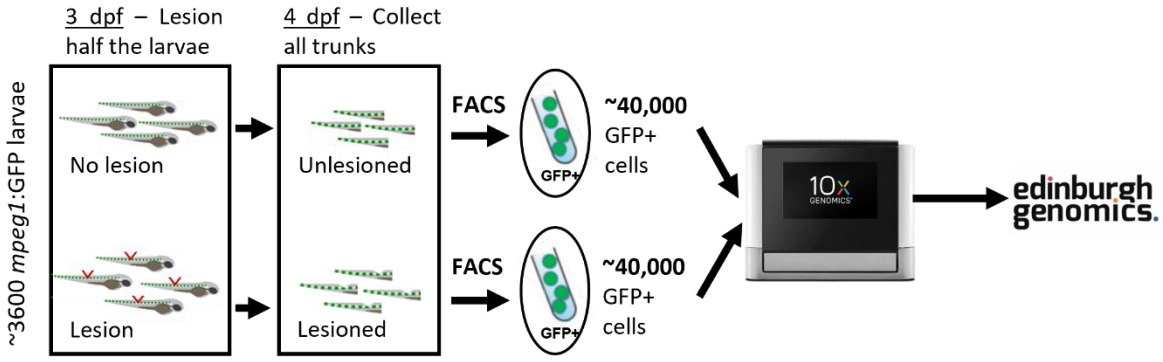

Figure 3.2: A schematic diagram demonstrating the preparation and timeline of samples for single cell sequencing. At 3 dpf, spinal cord lesion was inflicted on approximately 1800 larvae. Another 1800 were uninjured. The trunks of all larvae were collected 22-24 hours later and following cell dissociation, GFP+ cells were captured using FACS. These GFP+ cells were processed by 10x for single cell suspension and library construction and the resulting library was sent for sequencing by Edinburgh genomics.

3.2.2 Quality control

The single cell dissociation and isolation protocols inevitably introduce some technical noise to the dataset. For example, the processing of dissociating cells from the tissue causes cellular stress, which is likely to lead to some cell death. Furthermore, it is possible for multiplets to be generated, in which two or more cells are captured together. Before downstream analysis of the sequencing dataset, it is necessary to filter cells based on quality control parameters in order to be as confident as possible that the remaining data is a true reflection of the underlying biology of the sample.

The two datasets originating from the two conditions are treated equally here, since the samples were prepared concurrently and represent comparable underlying cell populations.

Due to the heterogeneous nature of such experiments and the variety of protocols used, there are no strict rules to follow when performing quality control. Instead, cut-offs are decided on an experiment-by-experiment basis, in the context of the dataset as a whole. Hence, before deciding on quality control parameters, I first visualised the distribution of the three main attributes looked at when performing quality control: feature depth, count depth, and mitochondrial fraction (Figure 3.3).

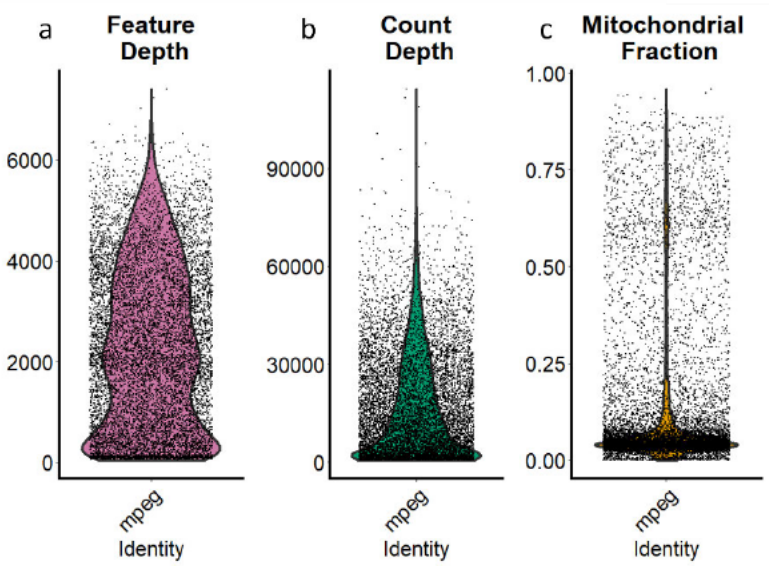

Figure 3.3: Distribution of all cells based on three quality control metrics. Each dot represents a single cell. A: The majority of cells have fewer than 6000 features. B: The majority of cells have a count depth of less than 60,000. C: The majority of cells captured have between 2-10% of their transcriptome corresponding to mitochondrial genes

Term	Definition
Barcode	Every read captured in a droplet is labelled by the same barcode. Due to technical issues in droplet capture, a barcode may mistakenly tag multiple cells (multiplet) or not tag any cells (empty droplet).
Feature	The entity that the DNA sequence is mapped to. In the case of this dataset, all features are genes.
Multiplets	Multiple cells can be captured within one droplet, and will therefore be assigned to the same barcode. These are multiplets and should be filtered out by quality control.
Mitochondrial reads	Reads originating from mitochondria, in zebrafish these are prefixed with “mt-“
Feature depth	The number of genes detected in each cell
Count depth	The number of molecules detected in each cell
Mitochondrial fraction	The ratio of reads mapped to mitochondrial DNA compared to the total number of reads mapped in a cell or barcode

Table 3.1: Definitions of the technical terms used relating to single cell sequencing data quality information.

In the first instance, barcodes with fewer than 200 features were removed. These are likely empty droplets and account for 9.7% of all cells in the dataset. Cells with more than 6000 features were also removed from further analyses as these are likely to be multiplets. Multiplets are a type of technical error in which two or more cells are captured in the same droplet, and can skew the downstream analysis. Finally, cells with more than 20% of their reads corresponding to mitochondrial transcripts were removed as cells with a high proportion of mitochondrial reads can indicate dead or dying cells.

When taken together, these quality control parameters resulted in 8346 cells being retained for downstream analysis, 81.5% of the original captured barcodes.

3.2.3 Pre-processing and clustering for mpeg1 dataset

Data normalisation, scaling and dimensionality reduction was performed as recommended in the Standard pre-processing workflow (Stuart et al, 2019) (see Chapter 2 for more details). Unsupervised clustering generated sixteen clusters which are displayed in a t-distributed stochastic neighbour embedding (tSNE) plot (Figure 3.4a). In these plots, each point represents an individual cell, and the cells are the location of each cell is based on its gene expression. tSNE plots are a way of visualising high-dimensional datasets in a two dimensional space.

To investigate the distribution of potentially low-quality cells, I plotted the quality control data for each of the sixteen clusters generated (Figure 3.4 c-e). In these violin plots, each cell is represented by a point. The purpose of these plots was to identify any clusters with an unusual distribution of features, for example excessively high feature depth or a high proportion of mitochondrial reads. These violin plots highlight that cells in clusters 1 and 8 have a high feature depth, however as these are normally distributed and peak below the threshold it is likely this is a biological characteristic of this cluster type rather than an indication of multiplet detection.

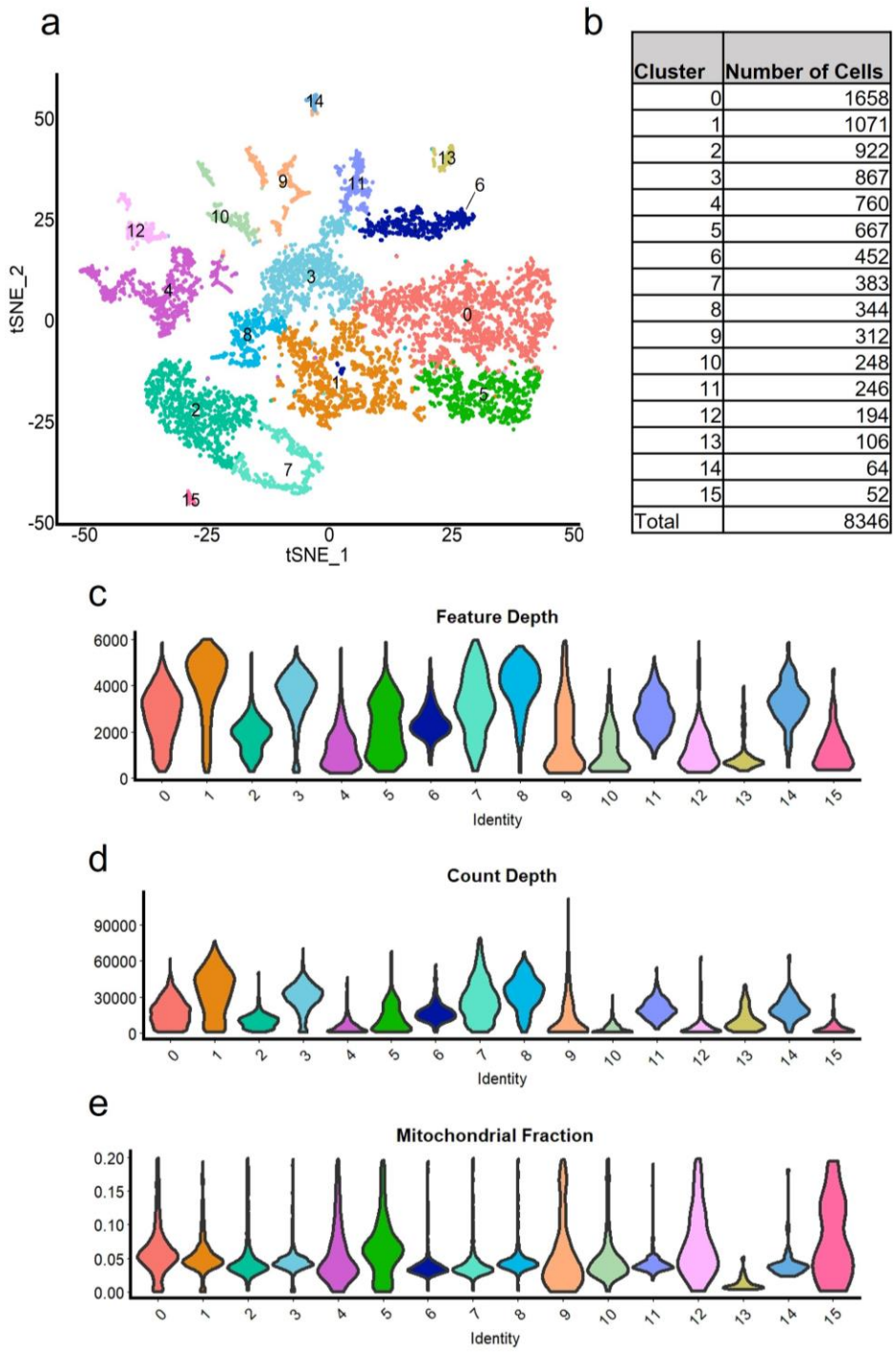

Cluster	Number of Cells
0	1658
1	1071
2	922
3	867
4	760
5	667
6	452
7	383
8	344
9	312
10	248
11	246
12	194
13	106
14	64
15	52
Total	8346

Figure 3.4: Clustering and quality control data following pre-processing of combined dataset. A: Unsupervised clustering created 16 clusters, displayed on a tSNE plot. **B:** The number of cells in each cluster ranges from 1658 cells (cluster 0) to 52 cells (cluster 15). **C-E:** Quality control data is plotted for each cluster.

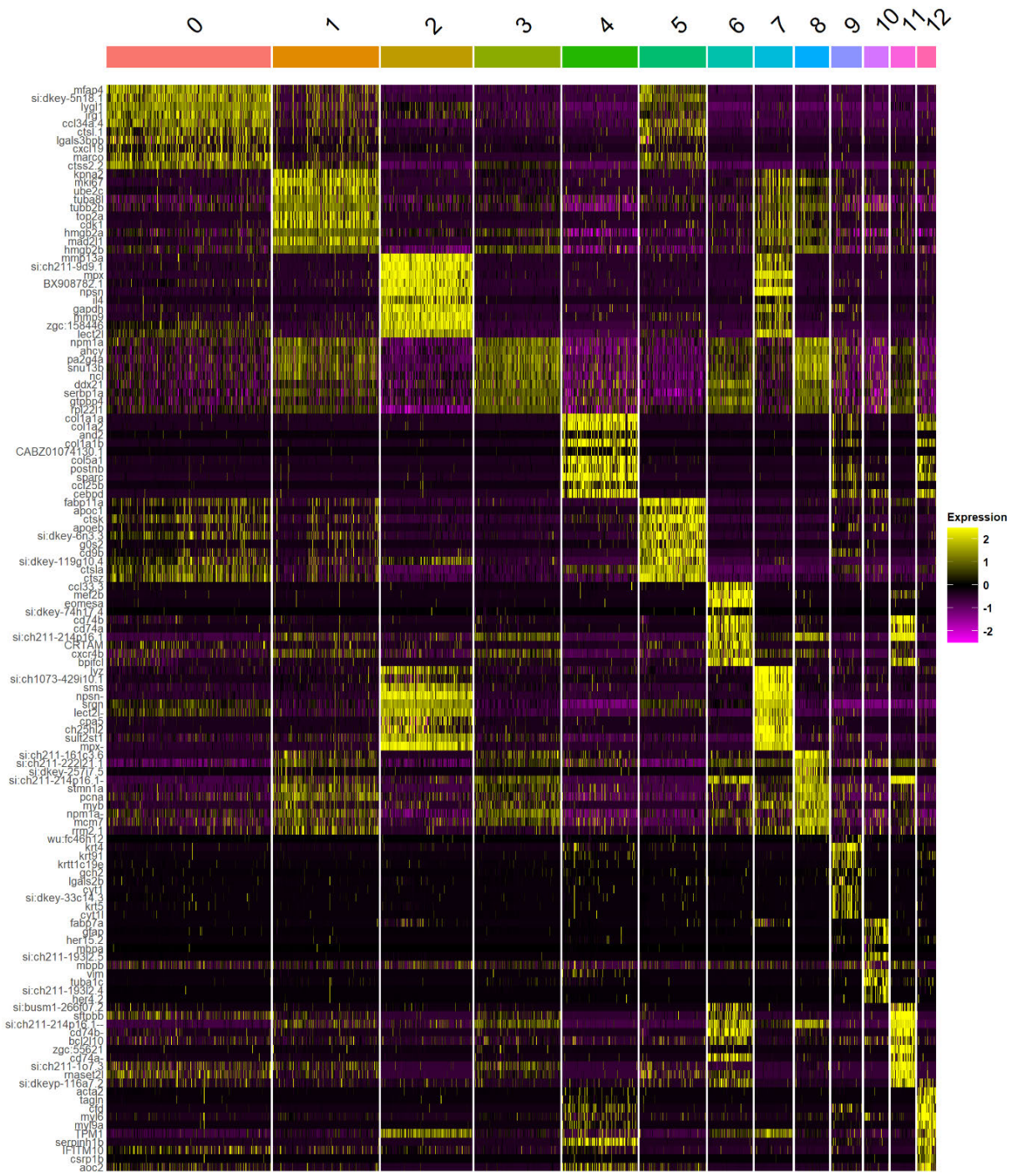

Figure 3.5: A heatmap displaying the top 10 most highly enriched genes for the top 13 clusters.

To assign identities to cell clusters, the Seurat function FindMarkers was used to identify genes which are highly enriched in a specific cluster compared to the rest of the dataset as a whole. The Wilcoxon test was used to calculate adjusted p-values for the enrichment of these genes. The top 10 significant genes for the main clusters are plotted in Figure 3.5. This heatmap allows us to recognise immediate similarities

between specific clusters, based on which genes are strongly expressed (and thus appear yellow) in more than one cluster. For example, the genes most enriched in cluster 0 are also highly expressed in cluster 5, and hence their corresponding cell types may be similar.

In the following sections, we consider the identity of the main clusters generated based on these top ten highly enriched genes, as well as the expression of known cell-type associated genes.

3.2.3.1 Clusters 0 and 5: Macrophages and microglia cells

Based on our FAC sorting for *mpeg1*:GFP^{+} cells, we primarily expected our dataset to capture macrophages and microglia cells. In accordance with this, two interconnecting clusters (clusters 0 and 5) both show strong and specific expression of *mpeg1*, *mfap4* and *marco*, which are all genes known to be essential in macrophage and microglia development and/or function (Benard et al, 2014; Ellett et al, 2011; Rougeot et al, 2019; Svahn et al, 2013) (Figure 3.6 b-e).

In addition to the shared expression of these marker genes, there are differences between cluster 0 and cluster 5. a*poeb*, known to be a marker specific to microglia cells (Herbomel et al, 2001; Mazzolini et al, 2020), is significantly enriched in cluster 5 but not cluster 0 (Figure 3.6e). It is expressed in 71.2% of cluster 5 cells compared to only 20.9% of cluster 0. While other microglial markers such as *p2ry12* (Sieger et al, 2012) and *slc7a7* (Rossi et al, 2015) are enriched in both clusters 0 and 5 when compared to the dataset as whole, their enrichment is stronger in cluster 5 than cluster 0 (Figure 3.6 f, g). Based on these patterns of expression it can be deduced that cluster 5 is comprised of microglial cells and cluster 0 of macrophages.

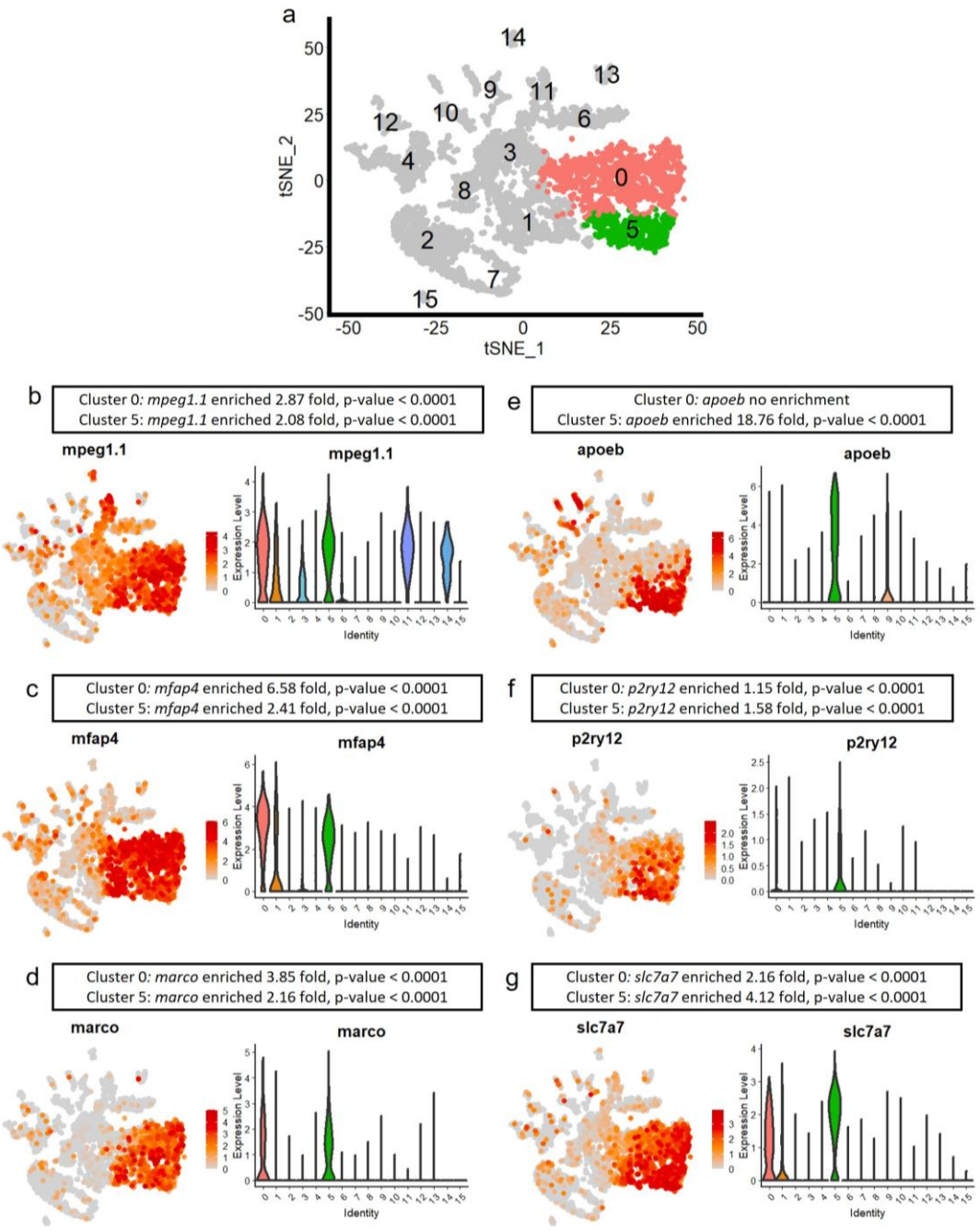

Figure 3.6: Expression patterns of marker genes for clusters 0 and 5. A: tSNE plot highlighting clusters 0 and 5. **B-D**: Expression patterns and levels for genes *mpeg1, mfap5* and *marco* show enrichment in clusters 0 and 5. **E-G:** Expression patterns and levels for microglia genes *apoeb, p2ry12* and *slc7a7* show stronger enrichment in cluster 5 than in cluster 0.

3.2.3.2 Clusters 2 and 7: Neutrophils

Clusters 2 and 7 are interconnected to each other and express many of the same genes. Their expression of transcripts including *mpx*, *mmp9*, *lyz* and *npsn*

distinguish them from the rest of the dataset. Since these are all known to be involved in neutrophil development and function (Bennett et al, 2001; Bradley et al, 2012; Di et al, 2017; Lieschke et al, 2001; Meijer et al, 2008; Song et al, 2004; Yang et al, 2012), we have assigned these clusters the neutrophil identity. Despite these shared markers, there are some differences between the populations which has led them to be clustered separately. The smaller of the two clusters, cluster 7, expresses cell cycle and proliferation related transcripts including *mki67* and *cdk1* which are not present in cluster 2. Conversely, cluster 2 expresses a number of secreted and activation factors which are not enriched in cluster 7, including *m17* (previously known as *lif*), *tnfb* and *fth1a*. Another secreted factor, *il4,* is enriched in both clusters but much more strongly in cluster 2 than 7. Importantly, *fth1a* (ferritin) is associated with inflammation (Recalcati et al, 2008; Torti & Torti, 2002), and *m17* directly induces neutrophil degranulation (exocytosis of secretory granules including inflammatory mediators) (Conti et al, 1990; Schainberg et al, 1988). Taken together, this may suggest that cluster 7 is comprised of more immature neutrophils which are still proliferating and have yet to take on an inflammatory phenotype, whilst cluster 2 have ceased proliferation and are playing a more active role in the inflammatory response.

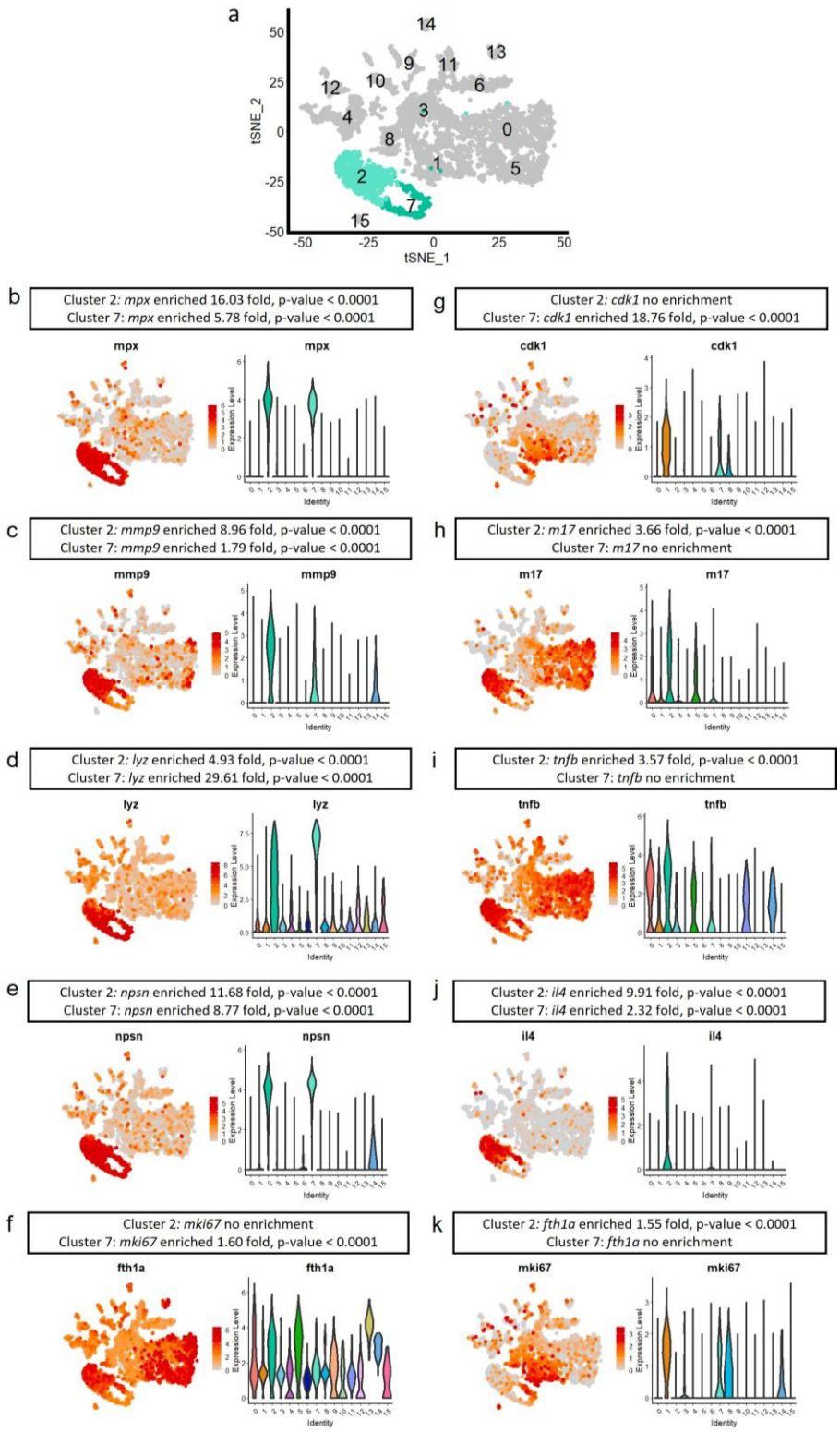

Figure 3.7: Expression patterns of marker genes for clusters 2 and 7. A: tSNE plot highlighting clusters 2 and 7. **B-E:** Canonical neutrophil genes *mpx*, *mmp9*, *lyz* and *npsn* show strong enrichment in both clusters 2 and 7. **F-G**: Proliferation and cell-cycle related transcripts *mki67* and *cdk1* are enriched in cluster 7 but not cluster 2. **H-K:** Secreted and activation factors *m17, tnfb, il4* and *fth1a* are all more strongly enriched in cluster 2 than cluster 7.

3.2.3.2 Clusters 6 and 11: Dendritic Cells

Dendritic cells are a subtype of antigen-presenting innate immune cells known to express *mpeg1* in mammals (McCormack et al, 2015).

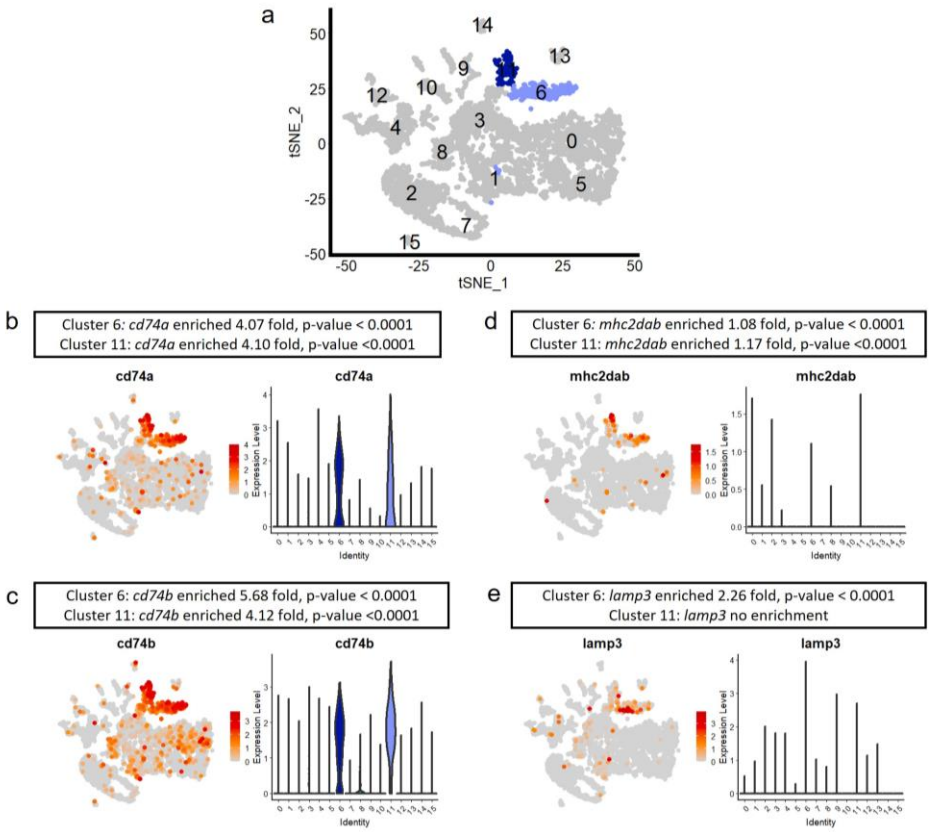

Figure 3.8: Expression patterns of marker genes for clusters 6 and 11. A: tSNE plot highlighting clusters 6 and 11. **B-E:** *cd74a, cd74b* and *mhc2dab* are all enriched in both clusters 6 and 11. *lamp3* is enriched in cluster 6 but not cluster 11.

To see if any had been captured within our dataset, I looked for expression of genes associated with the major histocompatibility complex. Indeed, enrichment of *cd74a*, *cd74b* (previously known as *iclp1*/*2*) and *mhc2dab* is evident in both clusters 6 and 11 (Figure 3.8 b-d). These genes are associated with antigen presenting cells in zebrafish (Lugo-Villarino et al, 2010; Wittamer et al, 2011). Since B cells do not start to develop in zebrafish until 3wpf (Lam et al, 2004; Lewis et al, 2014), we can assume that these cells are dendritic cells, which were originally identified in zebrafish in 2010 (Lugo-Villarino et al, 2010). Additionally, *lamp3* (cd208*)* is enriched in cluster 6 (Figure 3.8e) and is also considered a dendritic cell marker in humans and trout (Johansson et al, 2012).

3.2.3.3 Clusters 1,3 and 8: Hematopoietic stem cells

Clusters 1, 3 and 8 are similar in that they all lack markers of differentiated immune cells, including *mpeg1* (Figure 3.6b*)*, *lyz* (Figure 3.7d*)* and *mhc2dab* (Figure 3.8d). Despite this, their expression of *ptprc* (*cd45*) (Figure 3.9b) implies that these are of hematopoietic cell lineage (Thomas, 1989; Wittamer et al, 2011).

The enrichment of some genes in these clusters points towards the identity of these cells being hematopoietic stem cells. For example, nucleophosmin (*npm1a*) is enriched 2.77 fold (pvalue < 0.0001) when comparing clusters 1,3 and 8 to the remainder of the dataset (Figure 3.9c) and is known to play a critical role in hematopoietic stem cells (HSCs) (Ito et al, 2010; Mahony et al, 2021). Similarly, there is specific expression of stathmin (*stmn1a*) (Figure 3.9d) which is a microtubule destabiliser known to be expressed in hematopoietic stem cells and involved in hematopoiesis (Iancu-Rubin et al, 2009; Machado-Neto et al, 2014). The expression of these markers combined with the sparse but fairly specific labelling by transcription factor *c-myb* in these clusters (Figure 3.9e) has cemented the identification of these clusters as HSCs (Soza-Ried et al, 2010). Interestingly, cluster 1 expresses cell cycle markers (e.g *mki67*, *cdk1*) (Figure 3.9 f-g) along with the HSC specific genes, hence these can be considered a proliferating HSC population.

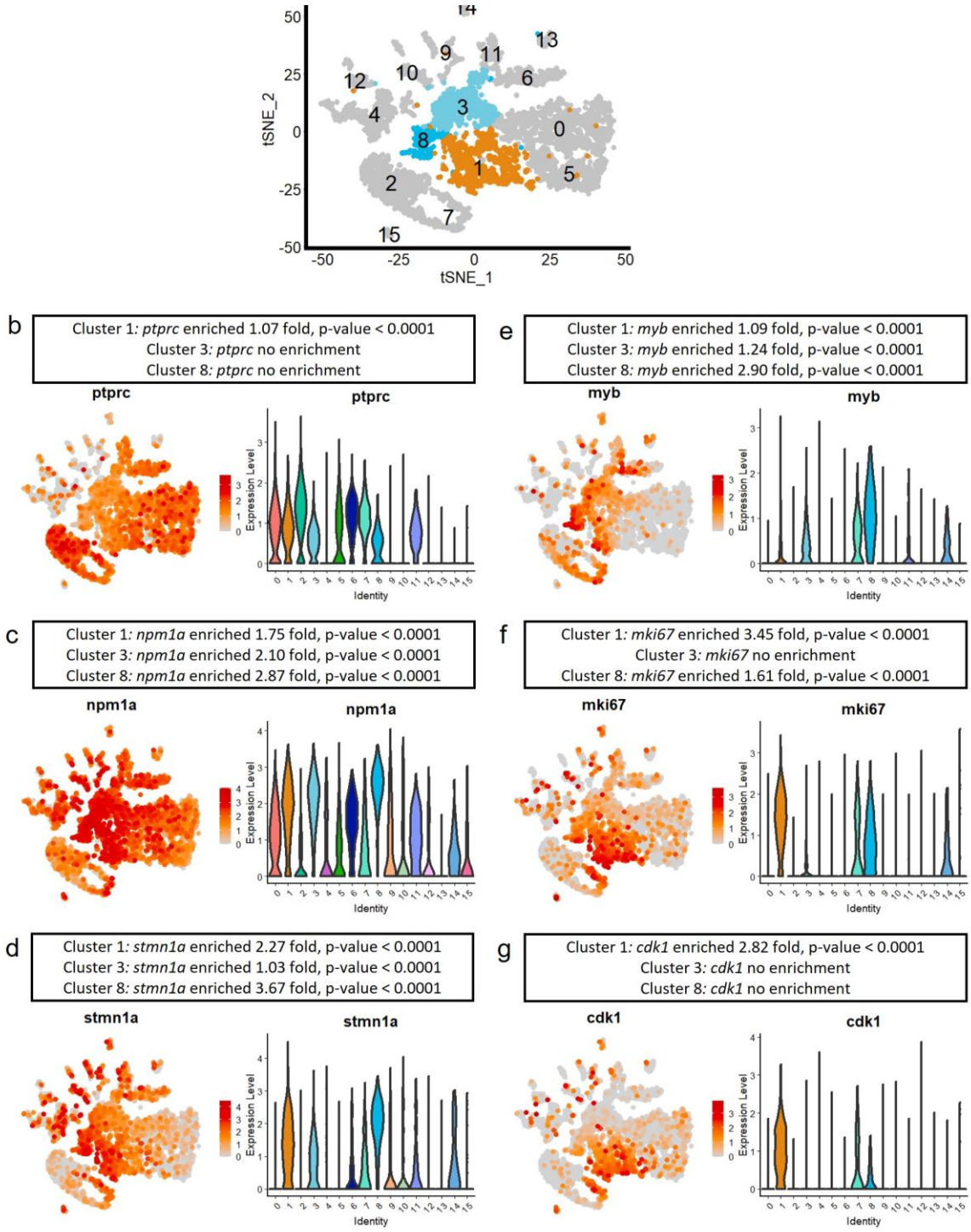

Figure 3.9: Expression patterns of marker genes for clusters 1, 3 and 8. A: tSNE plot highlighting clusters 1,3 and 8. **B:** The expression of *ptprc* in these clusters confirms these cells are likely of a hematopoietic lineage. **C-E:** Hematopoietic stem cell markers *npm1a, stmn1a* and *myb* are all enriched in clusters 1, 3 and 8. **F-G:** Cell cycle and proliferation markers *mki67* and *cdk1* are enriched in cluster 1.

3.2.3.4 Clusters 4, 9, 10, 12: Other clusters

The remaining clusters show little to no expression of *ptprc* (Figure 3.9b) and therefore do not appear to be of hematopoietic lineage (Iancu-Rubin et al, 2009; Wittamer et al, 2011). Furthermore, they show markers which confirm their identity as non-hematopoietic.

Clusters 4 and 12 show strong expression of *pmp22a (*Figure 3.10b). This, combined with their expression of collagen genes (*col1a2* and *col6a1*) and *pdgfra* suggests a fibroblast identity (Figure 3.10c-e) (Lee et al, 2014; Li et al, 2000).

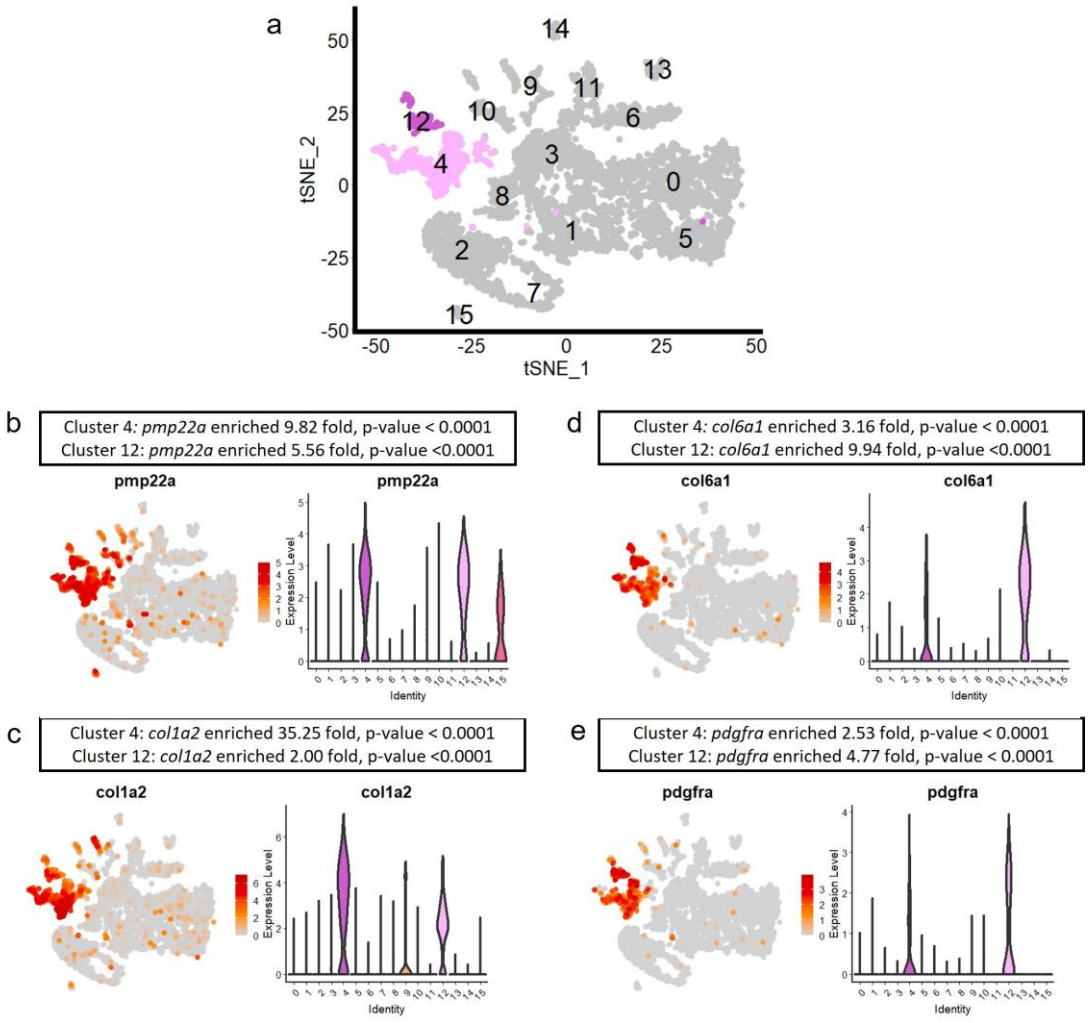

Figure 3.10: Expression patterns of marker genes for clusters 4 and 12. A: tSNE plot highlighting clusters 4 and 12. **B-E:** Clusters 4 and 12 both show strong and enrichment of fibroblast markers *pmp22a, col1a, col6a1* and *pdgfra.*

Cells in cluster 9 have highly specific expression of keratin genes including *krt4* and *krt91* (Figure 3.11 b-c) and hence are likely keratinocytes. Finally, cluster 10 appears to consist of neural progenitor cells based on their expression of *fabp7a*, *gfap*, *elavl4* and *her4.1* (Figure 3.12 b-e) (Anderson et al, 1984; Johnson et al, 2016; Kurtz et al, 1994; Wang et al, 2015).

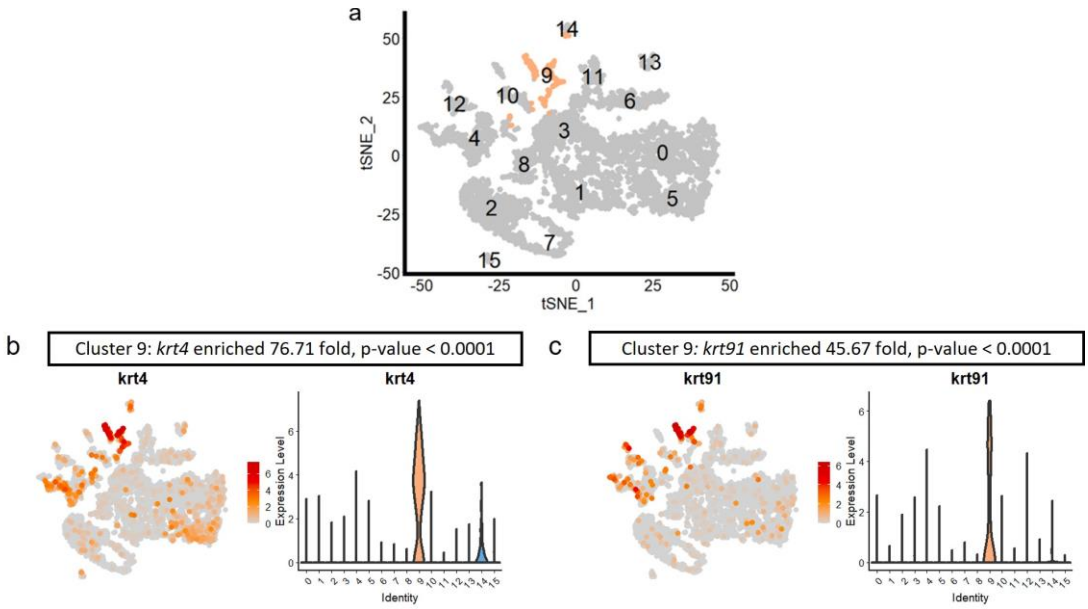

Figure 3.11: Expression pattern of marker genes for cluster 9. A: tSNE plot highlighting cluster 9. **B-C:** *krt4* and *krt91* are both significantly enriched in cluster 9.

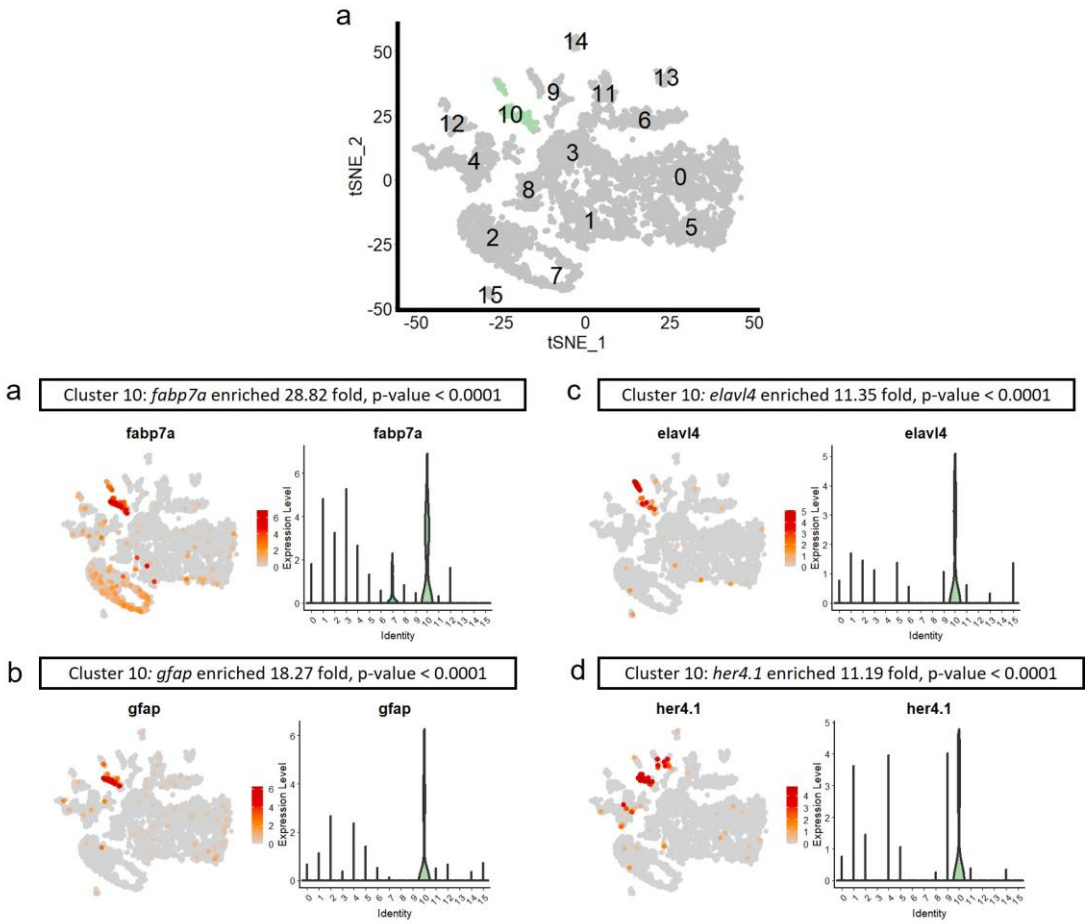

Figure 3.12: Expression pattern of marker genes for cluster 10. A: tSNE plot highlighting cluster 10. B-E: *fabp7a, gfap, elavl4* and *her4.1* are all significantly enriched in cluster 10.

3.2.3.5 Cluster assignments for *mpeg1*+ dataset

Based on the expression patterns of marker genes discussed above, cell type identities were assigned to each cluster. These are summarised in Figure 3.13. Exceptions are the smallest clusters (13, 14 and 15) which were not assigned identities due to the small numbers of cells included.

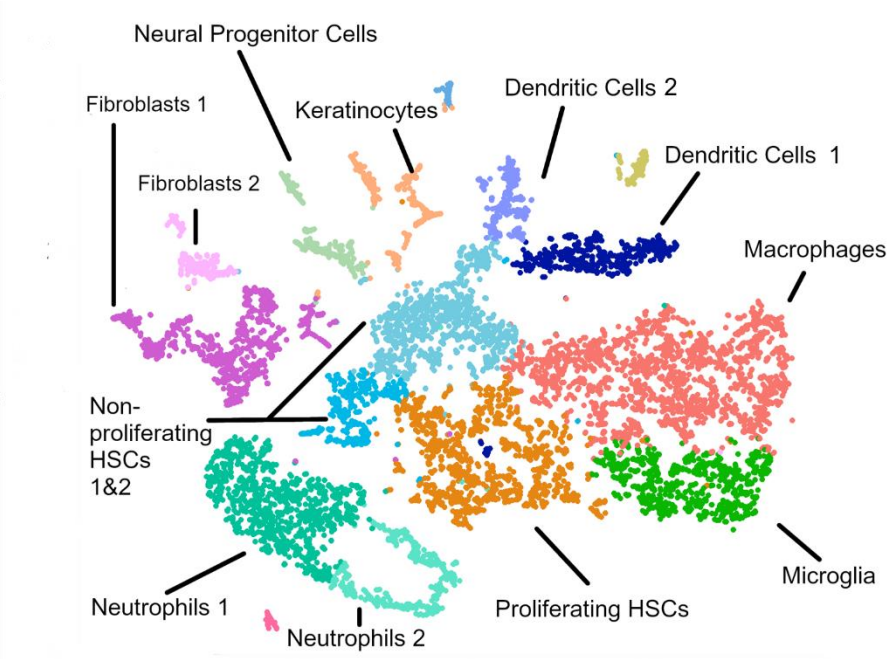

Figure 3.13: The tSNE plot for the mpeg1+ dataset with major cell types identified and labelled.

3.2.4 Changes in proportion of cell types in spinal cord after injury

Comparing the proportion of a specific cell type in the unlesioned spinal cord to the proportion of the same type of the uninjured spinal can reveal basic information about the cell type's response to injury. For example, the microglia cells only make up a small percentage of the total captured cells from the unlesioned fish (2.6%, 99 out of 3767). However, they make up a much larger proportion of the total captured cells from the lesioned larvae (12.4%, 568 out of 4579) (Figure 3.14). Hence, we can deduce that there is either a large influx of microglia cells to the trunk, an increase in the number of microglia being generated, or a combination of the two.

Similarly, the proportion of proliferating HSCs increases after lesion, perhaps at the expense of the non-proliferating HSCs, as the two non-proliferating HSC clusters contribute proportionally less to the lesioned sample than the naïve sample.

The proportion of neutrophils and dendritic cells in the spinal cord is slightly lower in the injured fish than the unlesioned fish.

a

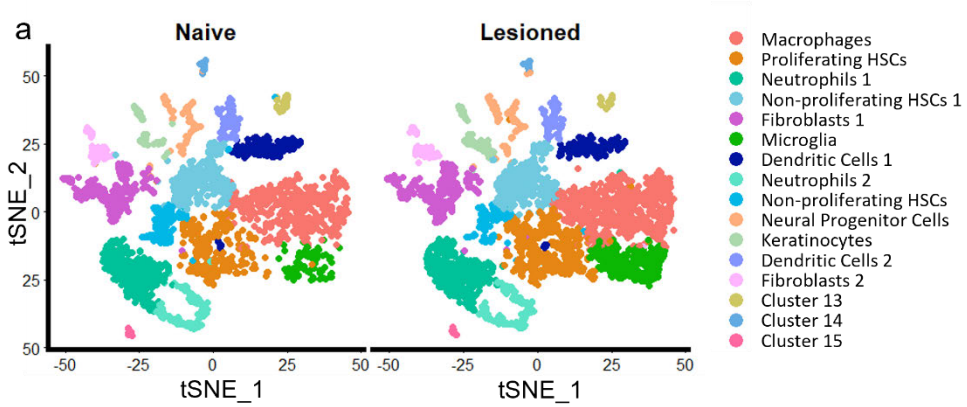

b

Cluster	Percentage of entire naïve sample	Percentage of entire lesioned sample	Difference
Macrophages	19	20.6	1.6
Microglia	2.6	12.4	9.8
Neutrophils 1	12.7	9.7	-3
Neutrophils 2	5.2	4.1	-1.1
Non-proliferating HSCs 1	12	9.1	-2.9
Non-proliferating HSCs 2	5.9	2.7	-3.2
Proliferating HSCs	9.3	15.8	6.5
Dendritic Cells 1	7.4	3.8	-3.6
Dendritic Cells 2	3.9	2.2	-1.7
Keratinocytes	4.2	3.3	-0.9
Neural Progenitor Cells	2.3	3.6	1.3
Fibroblasts 1	9.5	8.8	-0.7
Fibroblasts 2	2.5	2.1	-0.4
Cluster 13	2	0.6	-1.4
Cluster 14	0.9	0.7	-0.2
Cluster 15	0.6	0.6	0
Total	100	100	0

Figure 3.14: A comparison of the cell numbers in each cluster of the naïve and lesioned samples. A: Two tSNE plots of the dataset, displaying the cells originating from the naïve dataset separately from those originating from the lesioned dataset. An expansion of the microglia cluster and the proliferating HSCs is evident. **B:** A table displaying the percentage each cell type contributes to the entire captured dataset for each condition. The third column displays the difference for each cell proportion between lesioned and naïve. Rows highlighted in green are cell types which contribute proportionally more to the lesioned sample than the naïve. Rows highlighted in red contribute proportionally more to the unlesioned sample than to the lesioned sample.

3.2.5 Gene expression changes in macrophages and microglia following injury

3.2.5.1 Similarities between gene expression changes in microglia and macrophages following injury

Another facet of the response to injury is the differential regulation of genes following injury. This can be investigated by comparing the expression of genes in a particular cluster from the unlesioned larvae with the expression of genes in the same cluster from the lesioned larvae.

The gene expression changes undergone by the macrophage and microglia clusters after injury share many similarities with each other. Of the 369 significantly upregulated genes in microglia after injury, 343 are also significantly upregulated after injury in the macrophage population (Figure 3.15). Notably, of all the genes which are significantly upregulated in one of the populations, none of them are significantly downregulated in the other population; instead they are not significantly differentially regulated in the other group.

A further indication of the degree of conservation in the gene expression response to injury between both cell types is the similarity between the top 20 upregulated genes after injury (Table 3.2). Of the 20 genes with the strongest upregulation in the macrophage cluster, 12 of these are also found in the top 20 upregulated genes in the microglia cluster. Of the other eight, five are also significantly upregulated after injury in the microglia cluster (although not within the 20 most strongly upregulated) and three are not significantly different in the microglia cluster.

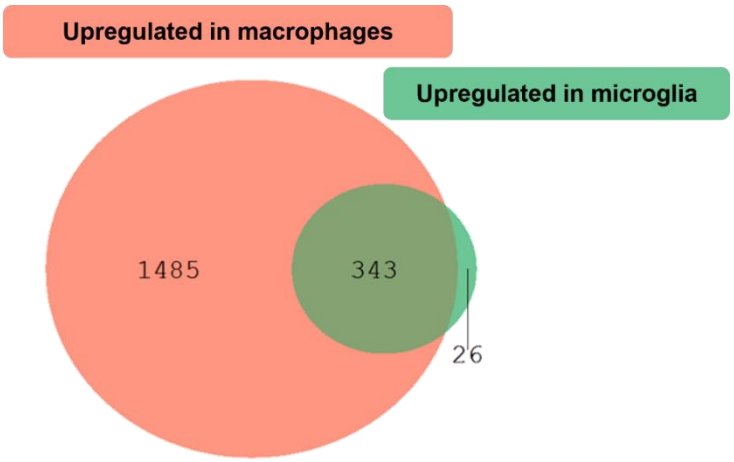

Figure 3.15: Venn diagram displaying the number of genes upregulated in macrophages and microglia. In total, 369 genes are upregulated in microglia and 1828 are upregulated in macrophages. 343 of these genes are upregulated in both macrophages and microglia.

Gene symbol	Rank upregulated in macrophages	Rank upregulated in microglia
apoeb	1	No significant difference
fth1a	2	1
si:dkey-119g10.4	3	4
fabp11a	4	6
si:dkey-6n3.3	5	12
apoc1	6	No significant difference
stoml3b	7	14
cd9b	8	2
s100a10b	9	16
si:ch211-198c19.3	10	13
lgals9l1	11	53
anxa2a	12	3
ctsla	13	37
gapdhs	14	52
anxa1a	15	17
txn	16	18
srgn	17	65
cldni	18	9
fthl28	19	No significant difference
atp6v1g1	20	83

Table 3.2: A table displaying the top 20 most strongly upregulated genes in macrophages after injury, with rank information about the same gene in the microglia cluster. Rows highlighted in green indicate that the gene is within the top 20 most strongly upregulated genes in both cell types.

Of the twelve genes which are highly upregulated in both macrophages and microglia (Table 3.2), three are unnamed *(si:dkey-119g10.4, si:dkey-6n3.3, si:ch211-198c19.3*). One of these, *si:dkey-119g10.4*, has been identified as a long intervening/intergenic non-coding RNA (lincRNA). Another, *si:dkey-6n3.3,* is a close ortholog to a zinc finger protein in mice. No known function is assigned to *si:ch211-198c19.3* and a BLAST search did not find any likely candidates for orthologues in other species, however according to the Alliance of Genome Resources automated gene description, it is predicted to localize to integral component of membrane. Due

to the lack of information about these three genes, it is difficult to make any assumptions about their role in macrophages and microglia after injury.

Of the remaining nine genes, *fth1a, fabp11a, txn, anxa1a, anxa2a, cd9b* and *s100a10b* have established roles associated with immune activation and modulation of cytokine secretion (Bertini et al, 1999; Kim et al, 2008; Makowski et al, 2005; Moraes et al, 2017; Suzuki et al, 2009; Torti & Torti, 2002). Additionally, *cd9b, anxa1a, anxa2a* and *s100a10b* have roles in migration and recruitment to the injury site (Brownstein et al, 2004; Falcone et al, 2001; McArthur et al, 2015; Powner et al, 2011), whilst glycoproteins *anxa1a* and *anxa2a* are also associated with phagocytosis (Dalli et al, 2012; Fan et al, 2004).

Two genes which are within the top 20 most upregulated in both microglia and macrophages are less well studied, and currently their role in macrophages and microglia are not understood. *stoml3b* encodes a cholesterol binding protein which, in sensory neurons, controls membrane mechanics and facilitates force transfer (Qi et al, 2015). *Cldni* encodes a claudin protein orthologous to human claudins 6,9, and 17. Claudins are associated with tight junctions, but as yet no role in macrophages or microglia has been reported.

To further understand the main functions and pathways of the 343 upregulated genes after injury, I used Metascape (Zhou et al, 2019) to perform gene ontology (GO) analysis to find any overarching patterns in the functions of these genes

Performing gene ontology (GO) analysis on these shared genes primarily revealed an enrichment of metabolic processes (e.g Oxidative phosphorylation, ATP metabolic process, proton transmembrane transport) (Figure 3.16). Other enriched processes indicate the immune response of these cells. The enrichment of genes relating to GO term ‘regulation of cellular extravasation’ indicates the migration of macrophages and microglia into the injury site. The enrichment of genes relating to GO term ‘Lysosome’ indicates both cell types participate in phagocytosis.

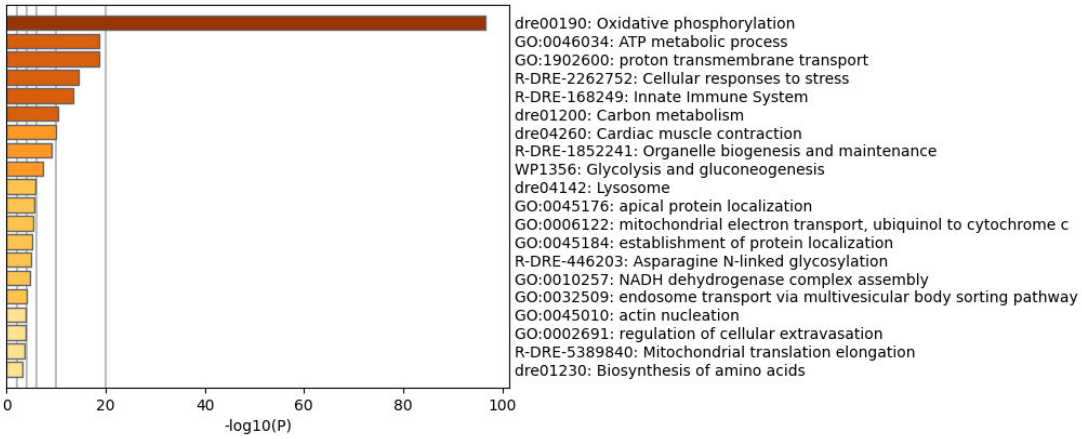

Figure 3.16: Gene ontology enrichment analysis of the 343 genes upregulated in both the macrophages and microglia after injury

Taken together, these upregulated genes demonstrate many commonalities between the response of macrophages and microglia to spinal cord lesion at this time point, including immune cell activation, migration and phagocytosis.

3.2.5.2 Macrophage specific upregulated genes

Interestingly, three of the genes in Table 3.2 are strongly upregulated in macrophages but not significantly different in microglia. These are *apoc1*, *apoeb*, and *fthl28*. Apolipoproteins encoded by *apoc1* and *apoeb* are both known to be specific to microglia in the zebrafish CNS (Mazzolini et al, 2020; Thiel et al, 2022). This could be indicative of transdifferentiation of macrophages into microglia following infiltration of the lesion site.

Further investigation of genes specifically upregulated in macrophages reveals a large number of secreted factors. The top 20 genes which are the most strongly upregulated in macrophages after injury but not significantly differentially regulated in microglia are displayed in Table 3.3. These genes include three secreted cathepsins (*ctsl.1, ctsz, ctsba*) (Vidak et al, 2019), and an array of signalling molecules (*hbegfb, hmgb2a, ccl38*, *cxcl19, il1r2*). Other upregulated genes include those with a role in macrophage migration (tubulin genes *tuba8l4* and *tubb2b*) (Hanania et al, 2012) and antioxidants *atox1* and *prdx1*. Along with *fthl28*, this combination of genes suggests macrophages become activated and highly secretory following injury, perhaps with different mechanisms or combinations of secreted factors than microglia cells.

Gene symbol	Fold change in macrophages after injury
fthl28	6.82
apoc1	3.70
zgc:198419	2.15
lgmn	2.08
hbegfb	2.00
zgc:109934	1.93
prdx1	1.92
ctsl.1	1.89
atox1	1.86
tuba8l4	1.86
ccl38.6	1.84
cxcl19	1.83
lacc1	1.81
CABZ01064972.2	1.79
hmgb2a	1.78
ctsz	1.77
ctsba	1.76
IL1R2	1.76
slc35f6	1.76
tubb2b	1.75

Table 3.3: Top 20 genes which are significantly upregulated in macrophages after injury but not significantly different in microglia cluster following injury.

GO analysis of all 1485 genes which are upregulated in macrophages but not significantly changed in microglia after injury reveals an enrichment for genes involved in metabolic pathways (e.g Mitochondrial and tricarboxylic acid cycle related pathways). There is an enrichment of terms relating to protein synthesis (Proteasome, Protein processing, Protein folding), which is consistent with the increase in secreted signalling molecules. Additionally, some of the enriched terms are linked to phagocytosis (Membrane Trafficking, Endocytosis).

Taken together, this suggests that one of the main roles specific to macrophages is secretion of signalling molecules. Genes relating to phagocytosis and metabolic pathways are also found upregulated in this gene set, however as these terms were also enriched in the set of genes upregulated in both macrophages and microglia after injury, these roles are not specific to macrophages.

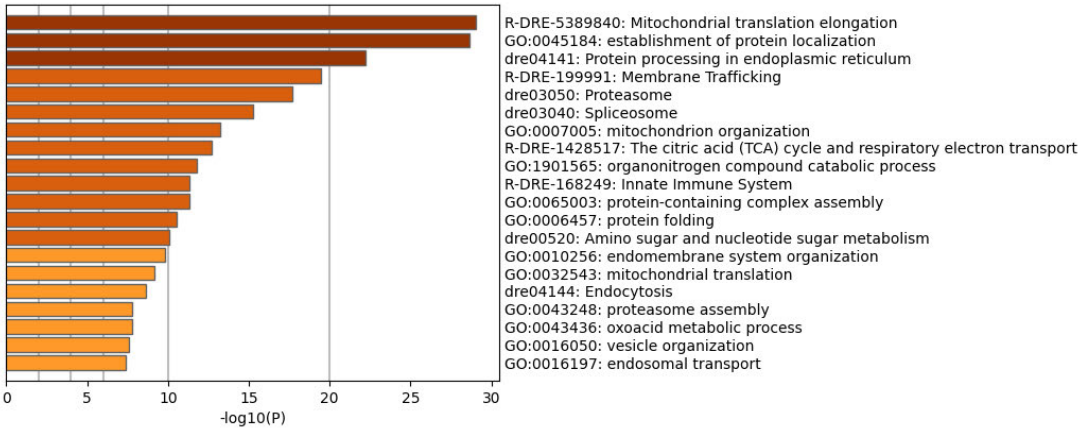

Figure 3.17: Gene ontology enrichment analysis of the 1485 genes specifically upregulated in the macrophages after injury

3.2.5.3 Microglia specific upregulated genes

To identify any possible pathways activated specifically in microglia after injury, I analysed the genes which were strongly upregulated in microglia but not upregulated in the macrophage population after injury. There were no genes which are upregulated in microglia and downregulated in macrophages, however 26 were significantly upregulated in microglia but not differentially regulated in macrophages (Figure 3.15). The top 20 of these are displayed in Table 3.4.

In contrast to the macrophage specific upregulated genes discussed above, there is not an abundance of secreted factors upregulated specifically in microglia. Interestingly, many of the top 20 microglia specific upregulated genes have functions related to the extracellular matrix (ECM). Two obvious examples of these are the ECM protein *fn1a* (fibronectin 1a) and intermediate filament *krt8* (keratin 8). Interestingly, they also both are involved in integrin signalling, as is *fermt3b* (Malinin et al, 2010; Wu et al, 1995). Integrins interact with the actin cytoskeleton, and two actin-related genes are also found overexpressed - *coro1ca* (coronin 1c) (Chan et al, 2012) and *fmnl1a* (formin-like protein 1a, previously known as *frl1*) (Harris et al, 2006). Furthermore, *ahnak*, the most strongly upregulated gene in Table 3.4, interacts with the annexin 2/S100A10 complex to regulate actin cytoskeleton organisation (Benaud et al, 2003). Actin cytoskeleton remodelling is also involved in microglia motility and migration (Franco-Bocanegra et al, 2019).

Aside from ECM and integrin signalling cell functions, these sets of genes can also give insight to intracellular processes. Three genes (*yaf2*, *mcl1* and *rtn3*) are known inhibitors of apoptosis (Stanton et al, 2006; Wan et al, 2007; Yang et al, 1996). Other upregulated genes include those which encode intracellular enzymes (*rnf128* and *ptp4a1*), cell cycle regulation (*plk3)* (Ouyang et al, 1997) and cell polarisation and migration (*fam65a)* (Mardakheh et al, 2016). The remaining genes are less well annotated and their functional significance is as yet unknown.

Overall, these gene expression changes suggest that microglia function after spinal cord injury differs from macrophages mainly due to their association with the ECM.

Gene symbol	Fold change in microglia after injury
ahnak	2.44
pigrl2.3	2.29
ccr12b.2	2.23
zgc:77517	2.18
hopx	2.14
fn1a	1.78
krt8	1.69
fermt3b	1.54
plk3	1.46
yaf2	1.45
ptp4a1	1.43
mcl1b	1.40
dicp3.1	1.37
MAP4K4	1.37
coro1ca	1.36
rnf128a	1.35
fam53b	1.30
fmnl1a	1.30
rtn3	1.30
fam65a	1.27

Table 3.4: Top 20 genes which are upregulated in the microglia cluster after injury but not differentially regulated in the macrophage cluster following injury

3.2.5.4 Trajectory analysis of lesioned *mpeg1*:GFP cells

The strong upregulation of microglia-associated genes *apoeb* and *apoc1* in macrophages after injury indicates that some macrophages may differentiate into microglia following migration to the lesion site. To investigate this computationally, I performed trajectory inference on the lesioned *mpeg1*:GFP sample.

One benefit of the capture and sequencing of individual cells is the ability to study complex cellular dynamic processes such as differentiation. It is possible to computationally order cells along trajectories in an unbiased manner. Here, I used monocle3 R package (Cao et al, 2019) to plot the cells from the lesioned *mpeg1*:GFP sample on a Uniform manifold approximation and projection (UMAP) plot. I then identified where each cell type is plotted on the UMAP plot (Figure 3.18a), using known marker genes associated with the Seurat-generated clusters as described in previous sections. Following this, I used monocle3 to construct a trajectory for the lesioned dataset, and to calculate where each cell sits along the reconstructed pseudotime (Figure 3.18b). The pseudotime trajectory (overlaid in grey in Figure 3.18b) was constructed after manually specifying the root node (chosen to be the *cdk1* positive HSC), as is standard in monocle3.

The trajectory inferred by this method suggests that HSCs give rise to two main branches – one which consists of the dendritic cells, and the other which consists of the macrophage and microglia clusters. The positioning of microglia cells after the macrophages in the trajectory suggests microglia are generated by transdifferentiation of macrophages after injury (Figure 3.18b). This is supported by the strong upregulation of microglia-associated genes *apoc1* and *apoeb* in the macrophage cluster after injury (Table 3.2).

Interestingly, whilst the HSCs, dendritic cells, macrophages and microglia are placed along the same trajectory as eachother, the neutrophils and other cell types are separate – they are not found to be connected by a differentiation pathway to these main cell types (macrophages, microglia, HSCs and dendritic cells). This may suggest the captured neutrophils do not originate from the same cell types as the macrophages/microglia/dendritic cells.

This trajectory inference indicates that macrophages may transdifferentiate into microglia at the lesion site. It also provides insight into the ontogeny of the dendritic cell populations and neutrophil populations in our datasets. It suggest that whilst the

dendritic cells are derived from the same progenitor cells as the macrophage and microglia cells, the neutrophils may originate from an alternative progenitor state not captured in our dataset.

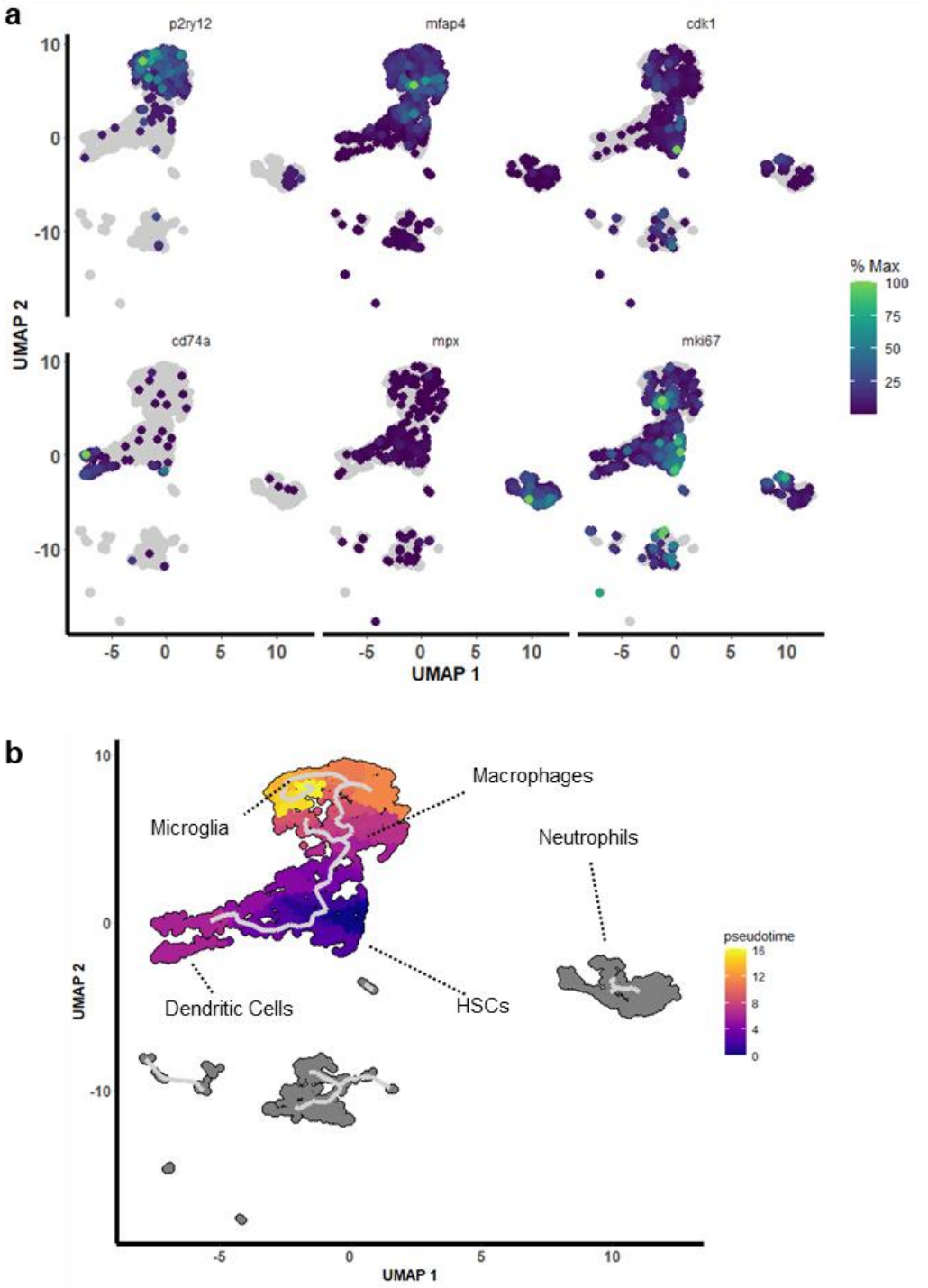

Figure 3.18: Trajectory analysis of the lesioned *mpeg1*:GFP dataset. **A:** The UMAP plots display the expression of specific genes, in order to identify where the major cell types are positioned in the plot. %Max refers to the levels of expression of each gene relative to the highest level of expression of the specific gene in our dataset. **B:** The UMAP is coloured

according the pseudotime, and labelled according to inferred cell types, based on marker gene expression. The trajectory graph is overlaid on the UMAP in light grey. Clusters of cells shaded in dark grey are those not connected to the root node, the HSCs.

3.2.6 Data Availability

Both unlesioned and lesioned datasets are available on ArrayExpress, accession code E-MTAB-10379.

Additionally, I have created and published an application allowing easy exploration of the dataset. Users can input a gene symbol of interest to visualise expression of the gene within the dataset. Basic expression data of the gene input across the naïve and lesioned dataset is also provided. An example output is provided in Figure 3.19. This is publicly available at https://louisakdrake.shinyapps.io/beckerlab-mpeg/

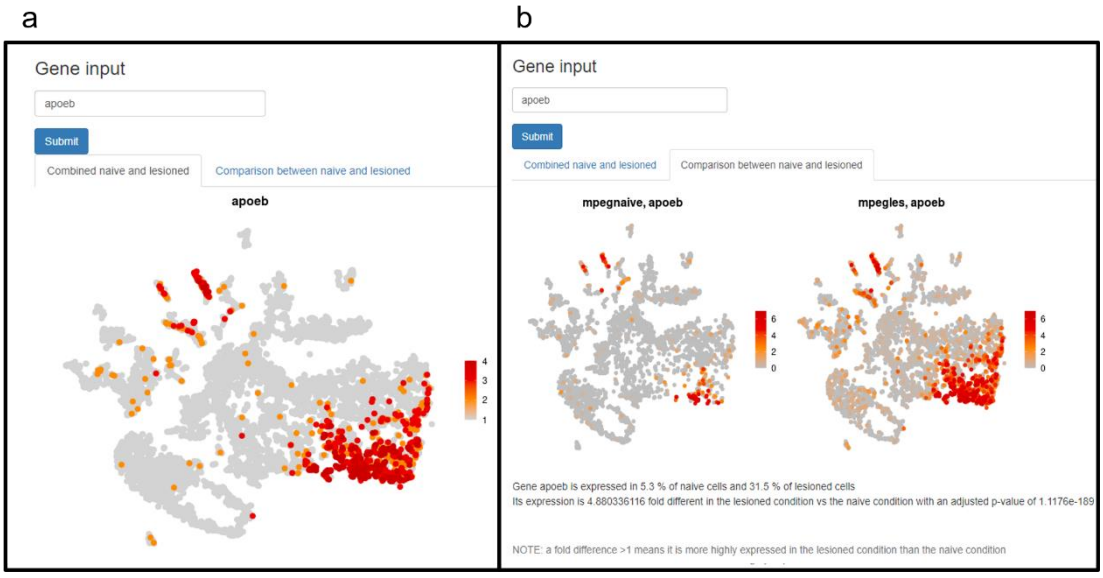

Figure 3.19: An example output of the web application allowing exploration of this dataset.

3.3 Discussion

In summary, I have performed single cell sequencing on *mpeg1*+ cells isolated from the spinal cord of uninjured and injured zebrafish larvae. Following quality control and clustering of the cells, putative cell type identities were assigned to the clusters. Finally, comparisons of gene expression profiles of these cell types helped to elucidate injury-induced changes in these cell types. In this dataset, microglia specifically upregulate genes involved in the ECM, integrin signalling and the actin cytoskeleton after injury. Macrophages upregulate genes which indicate they shift to an activated and secretory phenotype in response to lesion.

3.3.1 Microglia cell cluster assignment

The assignment of cell types to specific clusters is based on the presence of specific marker genes or combinations of marker genes. In some cases however, marker genes from the literature are not found in our dataset, or not distributed as would be expected based on the proposed cell type. For example, an analysis of the transcriptome of zebrafish larval microglia cells at various developmental timepoints confirmed the enrichment of marker genes *sall1a* and *mafb* (alongside other microglia marker genes) (Mazzolini et al, 2020). However, neither of these genes are found widely expressed in our microglia cluster, nor in our dataset as a whole (data not shown). Other marker genes identified are either expressed specifically in our microglia cluster (*apoeb, p2ry12*) or more broadly (*hexb, csfr1b*).

One explanation for this discrepancy could be the differences in tissue of origin; whilst *sall1a* and *mafb* were co-expressed with other microglia genes in the brain, they were not found in high numbers in our sample isolated from the spinal cord. While differences in the gene expression profiles of brain resident and spinal cord resident microglia have not been investigated so far in zebrafish, a comparison of brain derived and spinal cord microglia in mice did highlight some transcriptional differences between populations (Gosselin et al, 2017).

To confirm whether there is differential expression of *sall1a* and *mafb* between spinal cord and brain microglia at this timepoint it would be useful to perform qRT-PCR on mpeg1+ cells isolated from the spinal cord and brain individually to check for expression of *sall1a* and *mafb* at 4 dpf. Alternatively, *in situ* hibridisation could be used to confirm the localisation of these transcripts. To further characterise molecular differences between brain and spinal cord derived microglia, isolating the populations using the same marker gene (e.g *apoeb*) and then comparing sequencing results directly would help to elucidate region-specific microglia populations.

3.3.2 Dendritic cells

Clusters 6 and 11 were putatively assigned the dendritic cell identity based on expression of marker genes *mhc2dab* and *cd74a/b*. It is only within the last 15 years that dendritic cells have been identified in zebrafish (Lugo-Villarino et al, 2010). Interestingly, their presence in larval zebrafish has not yet been reported. Since their role is to bridge the innate and adaptive immune system by presenting antigens to

T-cells, their potential presence in our dataset (before development of the adaptive immune system) is surprising. It is possible their development is not linked to that of the adaptive immune system, and they may have as-yet unreported roles in the innate immune system.

Another possibility is that this cluster represents an antigen presenting macrophage cluster instead of a dendritic cluster. Antigen presenting macrophages also express genes relating to the major histocompatibility complex (e.g *mhc2dab*, *cd74a/b*) (Wittamer et al, 2011) as well as *mpeg1* (which is also expressed in our putative dendritic cell clusters – see Figure 3.6b). Since clusters 6 and 11 do not express any other common marker genes of macrophages, and cluster separately from the 'traditional' macrophage cluster, I putatively assigned these cells as dendritic cells.

To investigate the presence of dendritic cells in larval zebrafish, the *mhc2dab*:GFP;*cd45*:DsRed transgenic reporter lines could be utilised (Wittamer et al, 2011). Live *in vivo* imaging would confirm whether they display the stereotypical branched morphology of dendritic cells. Co-expressing putative dendritic cells could be isolated using FACS based on their fluorescence, and May-Grünwald-Giemsa staining would then allow visualisation of the intracellular cellular structure. A high nuclear/cytoplasmic ratio is typical for dendritic cells (Lugo-Villarino et al, 2010; Wittamer et al, 2011)

3.3.3 Neutrophils

The presence of neutrophils in such high numbers in the *mpeg1*:GFP dataset was unexpected, as *mpeg1* is not widely considered to be associated with neutrophils (Ellett et al, 2011). One explanation is that a large number of cells bypassed the FAC sorting gating for GFP+ cells, including many neutrophils. Alternatively, it is possible that these neutrophils were included correctly, and they were GFP positive. Since the input of FACS was *mpeg1*:GFP fish, this suggests that the neutrophil cluster also express *mpeg1*. At the time of sequencing, the neutrophil clusters do not broadly express the *mpeg1* transcript (Figure 3.6b), however due to the relative stability of the GFP protein it can act as a short term lineage tracer. This means that GFP positive cells do not have to be actively expressing the transcript of the GFP promoter. In this case, it would suggest that the captured neutrophils recently expressed the *mpeg1* transcript, or that their expression of *mpeg1* is below detection level.

In support of this, human neutrophils have been found to constitutively express *mpeg1* (McCormack et al, 2015). Furthermore, a population of co-positive *mpx*:GFP+ *mpeg1*:mCherry+ neutrophils were recently observed in zebrafish larvae after tail transection injury and cardiac injury (Kaveh et al, 2020). Together, this suggests that the population of neutrophils in our cluster are derived from *mpeg1* expressing cells. Whether this is true of all neutrophils in zebrafish is unknown, however lineage tracing with neutrophil and macrophage reporter lines (e.g *mpeg:GFP* and *mpx:mCherry*) during development and injury models may help to address this.

3.3.4 Contamination

The putative identification of two fibroblast clusters, neural progenitor cells, keratinocytes and HSCs indicates some contamination of the sorted cells. For some forms of downstream analysis (e.g bulk comparisons between unlesioned and lesioned samples) it may be worthwhile to exclude clusters consisting of contaminated cells. Future experiments may use more stringent gating strategies to ensure only the inclusion of true GFP positive cells.

3.3.5 Cell type expansion after injury

One of the most notable changes in our cell populations following injury is the observed expansion of the microglia cluster. The source of these new microglia is unclear. During development, it is known that primitive macrophages colonize the CNS before differentiating into mature microglia (Prinz et al, 2017). Outside of developmental systems, local expansion of microglia is believed to be a result of self-renewal of resident CNS cells instead of replenishment from the periphery (Ajami et al, 2007). In our dataset, the most significant upregulation of genes in macrophages following injury are apolipoproteins *apoeb* and *apoc1* which are associated with a microglia lipid processing. This may suggest some macrophages are transdifferentiating to microglia following injury. This is supported by the trajectory inference in Figure 3.18 which indicates that microglia may be derived from the macrophage population.

Alternatively, it is possible that microglia numbers in the spinal cord increase due to migration of microglia from elsewhere in the CNS, and that the upregulation of *apoeb* and *apoc1* in macrophages is not indicative of their transdifferentiation to microglia. Indeed, macrophages are also known to upregulate *apoeb* synthesis in response to inflammatory stimuli (Werb et al, 1986). Apolipoprotein E (*apoeb*) has

multiple roles in macrophages including lipid clearance and immune regulation, although its precise function in regeneration is so far unclear. Indeed, migration-related genes are upregulated in both macrophages and microglia after injury, which is congruent with the migration of microglia to the injury site (Table 3.2).

Further clarification of the method of microglia population expansion at the lesion site could be gained by utilising *csfr1a/b* mutant zebrafish which lack microglia. In these mutants, macrophages are unable to transdifferentiate into microglia. If macrophages in these larvae fail to show increased expression of *apoeb* and *apoc1*, this would suggest that the increase in microglia observed after SCI in normal larvae is due to transdifferentiation of macrophages into microglia.

3.3.6 Shared macrophage and microglial response to injury

Macrophages and microglia are derived originally from the same progenitor cells, however later occupy different tissues, display different morphology and express specific combinations of genes. This dataset shows that their response to injury in terms of gene expression changes is broadly similar. Notably, no genes were regulated in opposite directions in macrophages and microglia after injury.

According to GO analysis, the primary function of the set of genes upregulated in both macrophages and microglia are involved in metabolic processes. This is unsurprising as many shared functions of these cells including motility, ROS production and membrane turnover are highly energy intensive. Indeed, pro-inflammatory and anti-inflammatory phenotypes of both macrophages and microglia are accompanied by increased metabolic activity. Interestingly, different metabolic pathways are involved in the generation of energy for pro- and anti- inflammatory phenotypes. Aerobic glycolysis can provide immediate energy utilisation and is therefore the main pathway used by pro-inflammatory macrophages and microglia. Since anti-inflammatory systems require sustained energy production for functions such as transcription and fatty acid breakdown, oxidative phospohorylation is favoured (reviewed in (Devanney et al, 2020)). The GO analysis based on shared macrophage and microglia upregulated genes show an enrichment of mitochondrial respiratory processes, although glycolysis terms are also present. This suggests that the macrophages and microglia captured are displaying an anti-inflammatory phenotype. This is in agreement with previous work showing that at 24 hours post injury, the peak of pro-inflammatory cytokines il-1β and tnf-α expression in macrophages has passed, and anti-inflammatory cytokines tgf-β1a and tgf-β3 are

increasing (Tsarouchas et al, 2018). However, it is noteworthy that in this single cell dataset, there is no significant increase in either tgf-β1a or tgf-β3 in the macrophage cluster, possibly due to the retention of the entire trunks in this dataset compared to only the smaller lesion site in (Tsarouchas et al, 2018). This field of immunometabolism is a rapidly developing one and understanding the reprogramming undergone by macrophages and microglia will be invaluable in understanding the complexities of macrophage and microglia activation.

3.3.7 Individual macrophage and microglial responses to injury

While there is vast overlap between macrophage and microglial gene responses to injury, genes were identified which are significantly upregulated in one population but not the other. In macrophages, many of these genes encoded for secreted factors, although genes relating to macrophage activation and migration were also found. In contrast, genes specifically upregulated in microglia primarily involved those coding for ECM-interacting genes. This is of interest because previous work by our group (unpublished data; Anna Underhill, MSc thesis) has shown that specific knockdown of microglia results in lower levels of neurogenesis after injury. It is possible therefore that the ECM remodelling undergone specifically by microglia is necessary for neurogenesis.

This dataset shows that macrophages upregulate many secreted factors. The role of some secreted factors from macrophages in spinal cord regeneration is already known. For example, il-1β and tnf-α promote axonal regrowth (Tsarouchas et al, 2018). Furthermore, it is known that secreted factors from macrophages can promote the recruitment and eventual clearance of other immune cells (Keatinge et al, 2021; Prame Kumar et al, 2018). It is proposed that some secreted factors from macrophages can directly promote neurogenesis from ERG cells in spinal cord (Becker & Becker, 2022). The possible candidates for this signalling are investigated in Chapter 5 and the role of one secreted factor is tested experimentally.

Chapter 4: Single cell sequencing of the ependymo-radial glial cells in naïve and lesioned zebrafish spinal cord

---

Some of the data in this chapter was published as:

Cavone, L.*, McCann, T.*, **Drake, L**.*, Aguzzi, E., Oprişoreanu, A., & Pedersen, E. et al. (2021). A unique macrophage subpopulation signals directly to progenitor cells to promote regenerative neurogenesis in the zebrafish spinal cord. *Developmental Cell*, 56(11), 1617-1630.e6.

*: Joint first authors

https://doi.org/10.1016/j.devcel.2021.04.031

4.1 Introduction

In order to determine the transcriptional changes undergone in these progenitor populations in response to injury, I performed a single cell sequencing experiment to capture this cell type. This chapter characterises the isolated *her4.3*+ cells and their progeny from the spinal cord of both uninjured and injured zebrafish larvae. *Her4.3* is a marker for ependymo-radial glial (ERG) cells, the resident progenitor cells in the zebrafish spinal cord. Following zebrafish spinal cord injury, these cells can produce new neurons. This dataset and some accompanying analysis have already been published with me as a joint first author (Cavone et al, 2021). Some details such as cell cluster annotations have been refined since publication due to further exploration of the data.

4.1.1 *Her4.3:*GFP as a reporter line for ERG cells

The main signalling pathway responsible for the maintenance of the ERG population is the Notch pathway. By means of lateral inhibition, activation of Notch receptors in ERG cells by Jagged and Delta ligands from their neuronal progeny prevent the differentiation of cells towards a neuronal identity (Pierfelice et al, 2011). Hence, target genes of Notch can be used to identify ERG cells. One particular target gene of Notch, *her4.3*, is specifically expressed in ERG cells in the brain and spinal cord in zebrafish and anamniotes (Kroehne et al, 2011; Yeo et al, 2007). Therefore, fish which express fluorescent proteins under the control of the *her4.3* promoter have been generated, and can be used to study ERG cells (Yeo et al, 2007). The

transgenic fish *her4.3*:GFP is interchangeably referred to as *her4.1*:GFP and *her4.3*:GFP, although *her4.3*:GFP is the current preferred designation on zfin.org and is what will be used in this thesis. *Her4.3* is one of nine orthologs of the *Hes5* gene in humans.

The *her4.3*:GFP reporter line has previously been used to identify radial glial cells in the zebrafish brain (Kroehne et al, 2011) as well as ERG cells in the spinal cord (Chang et al, 2021). *Her4.3* has the advantage of being a general reporter of ventricular ERG cells; other studies have instead utilised reporter lines which identify specific ERG subtypes. For example, *dbx1a* expressing ERG cells in the zebrafish spinal cord specifically regenerate interneurons after injury (Briona & Dorsky, 2014), whilst motor neurons progenitors express *olig2* (Kuscha et al, 2012b).

4.1.2 Overview

In this chapter, I first describe the single cell sequencing experiment performed to capture the *her4.3*+ cells. Following quality control of the sequencing data, I characterise the cell types captured in this dataset, and identify the major gene expression changes undergone by the captured cells. Finally, I compare the response of ERG cells in zebrafish after spinal cord injury to that of similar cell types after spinal cord injury in mice.

4.2 Results

4.2.1 Experimental Design

In order to compare the transcriptome of ERG cells in both the healthy and lesioned spinal cord, a transection injury was performed on the spinal cord of 600 3 dpf *her4.3*:GFP zebrafish larvae. Another 600 were left unlesioned. Twenty-four hours later, the spinal cord lesion site was collected from the lesioned fish, and the equivalent area of the trunk was collected in unlesioned fish. Following cell dissociation, FAC sorting was performed to capture GFP positive cells. These GFP positive cells are subject to the 10x library preparation protocol which consists of reverse transcription of mRNA, amplification of resultant cDNA, and tagging with unique molecular identifiers (UMIs). These libraries were multiplexed and pooled for sequencing by Edinburgh Genomics.

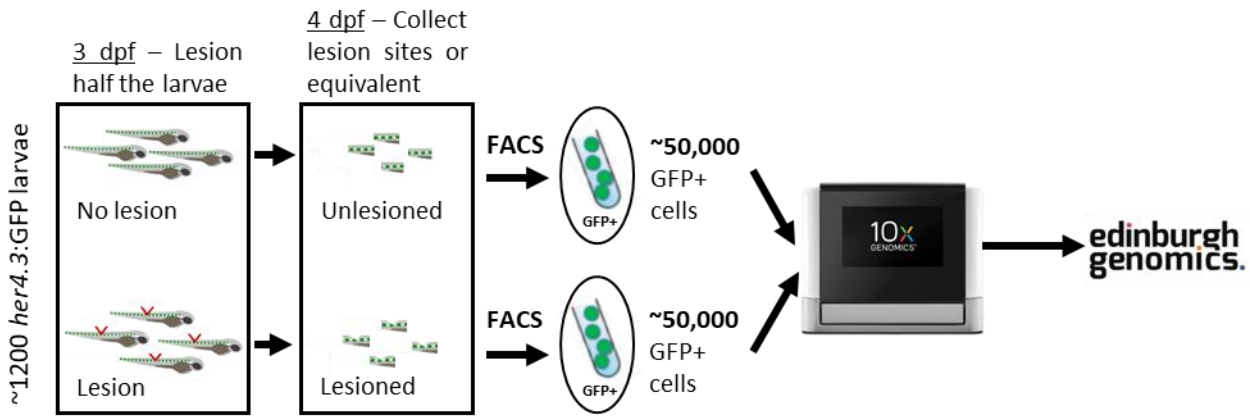

Figure 4.1: A schematic diagram describing the capture and processing of *her4.3*+ cells for single cell sequencing.

4.2.2 Quality control

The sequencing data received from Edinburgh Genomics includes the sequenced transcripts linked to barcodes. During the 10x library construction protocol, individual cells are captured in droplets, and the droplets are tagged with barcodes. In theory, every barcode therefore represents an individual cell, and hence each sequenced transcript can be linked to the cell it originated from. However, due to inevitable variation during the library construction process, sometimes two or more cells are captured within one droplet and are consequently tagged with the same barcode. In addition, some captured cells are of poor quality (e.g dead or dying) due to the stresses of the cell dissociation and FACS protocol. Hence, quality control parameters are applied to ensure that only barcodes which correspond to individual cells are included in downstream analysis, and that these captured cells included are of sufficient quality.

The same quality control parameters will apply for both datasets (naïve and lesioned) since the samples were prepared concurrently and represent comparable underlying cell populations.

In order to select appropriate quality control parameters, I first visualised the distribution of three indicators of cell quality: feature depth, count depth and mitochondrial fraction (Figure 4.2). This allows understanding of the context of this specific dataset and the spread of cell attributes before deciding on which barcodes represent poor quality cells or multiplets.

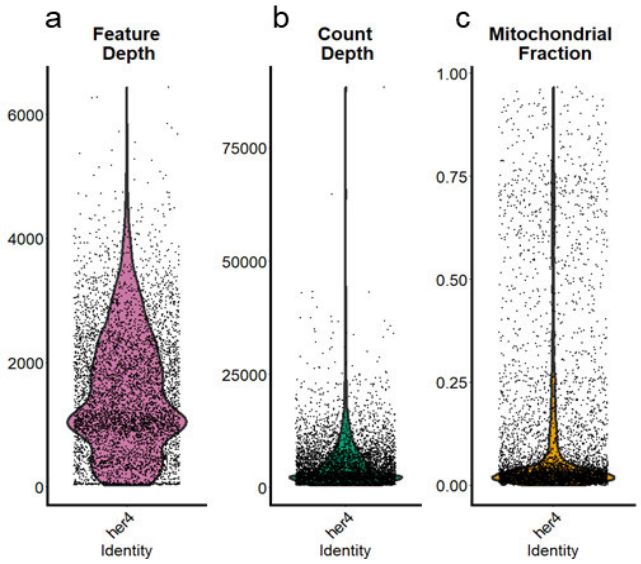

Figure 4.2: Distribution of all captured barcodes based on three quality control metrics. Each dot represents a single captured barcode (expected to correspond to a cell). **A:** The majority of barcodes have fewer than 4000 features. **B:** The majority of barcodes have a count depth of less than 25,000. **C:** The majority of barcodes captured have between 0 – 10 % of their transcriptome corresponding to mitochondrial genes.

Before quality control, 5588 barcodes were present in the dataset. In the first instance, barcodes with fewer than 200 features were removed. These are the result of droplets created without capturing any cells, and account for 368 barcodes (6.6% of the original dataset). Following this, cells with more than 4500 features were also removed from further analysis as these likely represent mulitplets, based on the distribution of barcodes in Figure 4.2. Finally, cells whose transcriptome was comprised of more than 5% of their reads corresponding to mitochondrial transcripts were removed as cells with a high proportion of mitochondrial reads can indicate dead or dying cells.

When all above parameters were applied, 3680 cells were retained for downstream analysis, 65.8% of the original captured barcodes. This proportion of cells retained for downstream analysis is comparable to other single cell sequencing experiments of the same cell type (Lange et al, 2020).

4.2.3 Pre-processing and clustering for her4.3 dataset

Data normalisation, scaling and dimensionality reduction was performed as recommended in the standard pre-processing workflow (Stuart et al, 2019) (see Chapter 2 for more details). Sixteen clusters were generated by unsupervised

clustering and these are displayed in a tSNE plot (Figure 4.3a). These clusters range in size from 22 cells to 1059 cells (Figure 4.3b).

The quality control data for each cluster was then plotted individually for each cluster (Figure 4.3 c-e). This is to confirm if any cluster has an unusual distribution of cells with particularly high values for a specific quality control metric. This is useful as low quality cells are likely to cluster together and any cluster with particularly high values for the quality control metrics can therefore be excluded. In this dataset, no clusters of concern were identified.

To assign identities to cell clusters, the Seurat function FindMarkers was used to identify genes which are highly enriched in a specific cluster compared to the rest of the dataset. The Wilcoxon test was used to calculate adjusted p-values for the enrichment of each gene in each cluster. Genes with an adjusted p-value of < 0.05 are considered significant. The top ten genes which are most highly upregulated in each of the main clusters are plotted in Figure 4.4. Due to space constraints, only 13 of the 16 clusters are included in this figure. As well as displaying the top ten genes and their expression patterns for each cluster, this heatmap allows us to recognise immediate similarities between specific clusters. This information, combined with prior knowledge of marker genes, is used to assign cell types to the clusters.

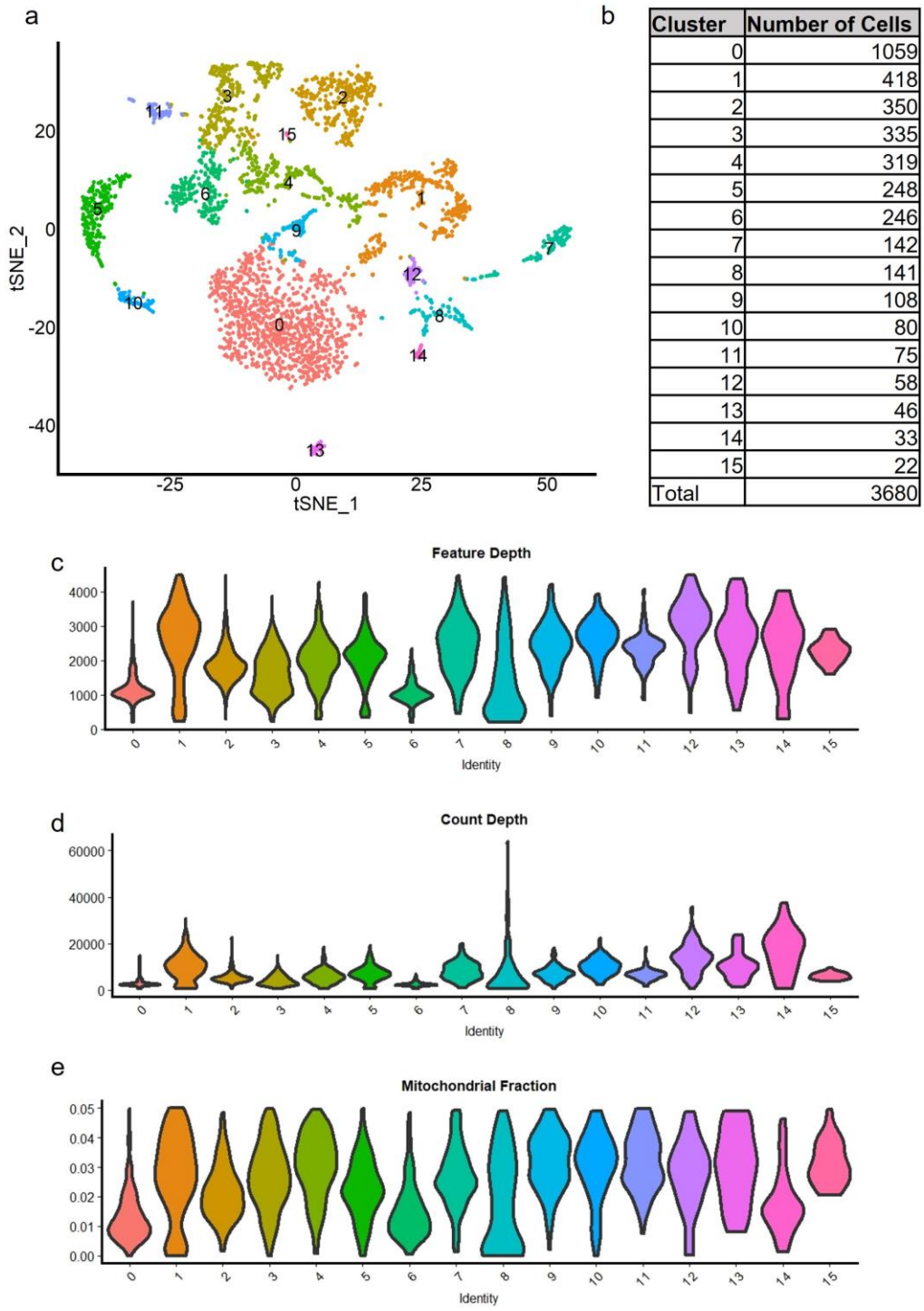

Cluster	Number of Cells
0	1059
1	418
2	350
3	335
4	319
5	248
6	246
7	142
8	141
9	108
10	80
11	75
12	58
13	46
14	33
15	22
Total	3680

Figure 4.3: Clustering and quality control data following pre-processing of dataset. A: Unsupervised clustering created 16 clusters, displayed on a tSNE plot. **B:** The number of cells in each cluster ranges from 1059 (cluster 0) to 22 (cluster 15). **C-E:** Quality control data is plotted for each cluster.

Figure 4.4: A heatmap displaying the expression data for the top 10 most highly enriched genes of 13 clusters.

4.2.3.1 Clusters 1 and 12: ERG Cells

In the first instance, I wanted to identify which of the clusters represented the ERG cell population. Since *her4.3* was the marker we used to identify these progenitor cells, I looked at the expression of this transcript. Figure 4.5b shows the expression is specific to clusters 1 and 12.

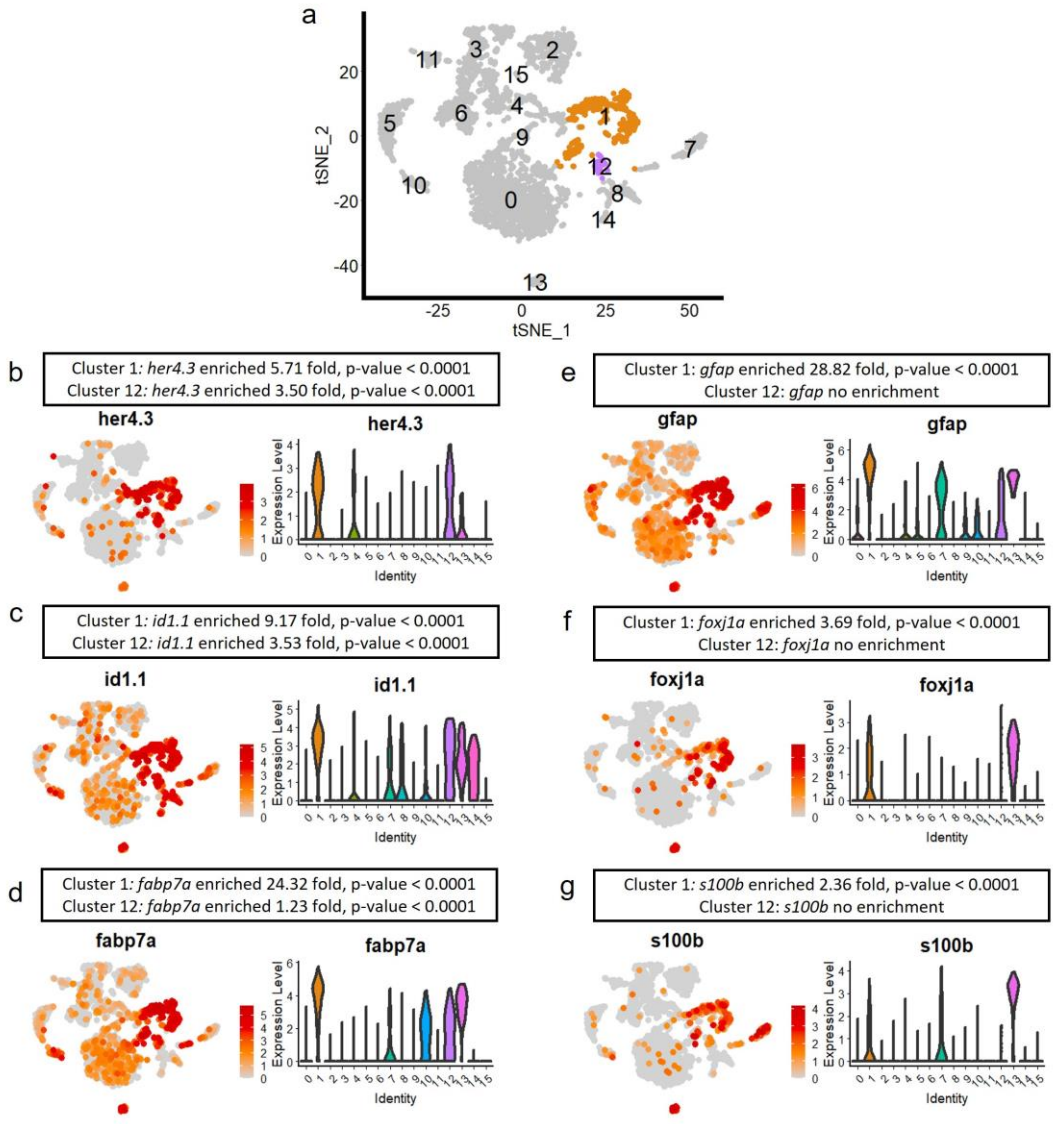

Figure 4.5: Expression patterns of marker genes for cluster 1. A: tSNE plot highlighting cluster 1 and 12. **B-D:** Genes *her4.3, id1* and *fabp7a* are all enriched in both clusters 1 and 12. **E-G:** *gfap, foxj1a* and *s100b* are all enriched in cluster 1 but not cluster 12.

To further confirm the identity of cluster 1, I looked at the top enriched genes in this cluster (Figure 4.4). Confirmation of the ERG cell identity of these is obvious in some of the top genes. *GFAP*, *fabp7a* (also known as BLBP) and *id1* are all

canonical radial glial markers in other systems (Anderson et al, 1984; Feng et al, 1994; Johnson et al, 2016; Kurtz et al, 1994; Lange et al, 2020; Malatesta et al, 2000; Zhang et al, 2020a). Other known ERG cell markers, *foxj1a* and *s100b*, are also highly enriched in this cluster (Figure 4.5).

Probing the identity of cluster 1 was inextricably linked to that of cluster 12, a much smaller but interconnecting cluster. Some of the canonical progenitor cell markers expressed in cluster 1 (*her4.3, fabp7a, id1*) also showed high levels of expression in cluster 12 (Figure 4.5 b-d). However, one unique feature of this cluster is the expression of proliferation markers and cell cycle genes. Transcripts *pcna*, *mki67* and *kiaa0101* (also known as *pcna clamp associated factor*; *pclaf*) are all associated with proliferation (Emanuele Michael et al, 2011; Gerdes et al, 1991; Gerdes et al, 1983; Wullimann & Puelles, 1999). Whilst *mki67* expression appears to be highly specific to cluster 12, *pcna* and *kiaa0101* expression is also expressed sporadically in other clusters. This perhaps reflects the long-lasting property of *pcna* and the more transient nature of mki67. Other cell cycle associated genes including *ccna2*, *cdk1* and *top2a* (Jin et al, 2021) are also highly specific to cluster 12 (Figure 4.6 d-f). These genes, combined with the strong expression of ERG markers, suggest that this cluster represents a proliferating progenitor cell subtype.

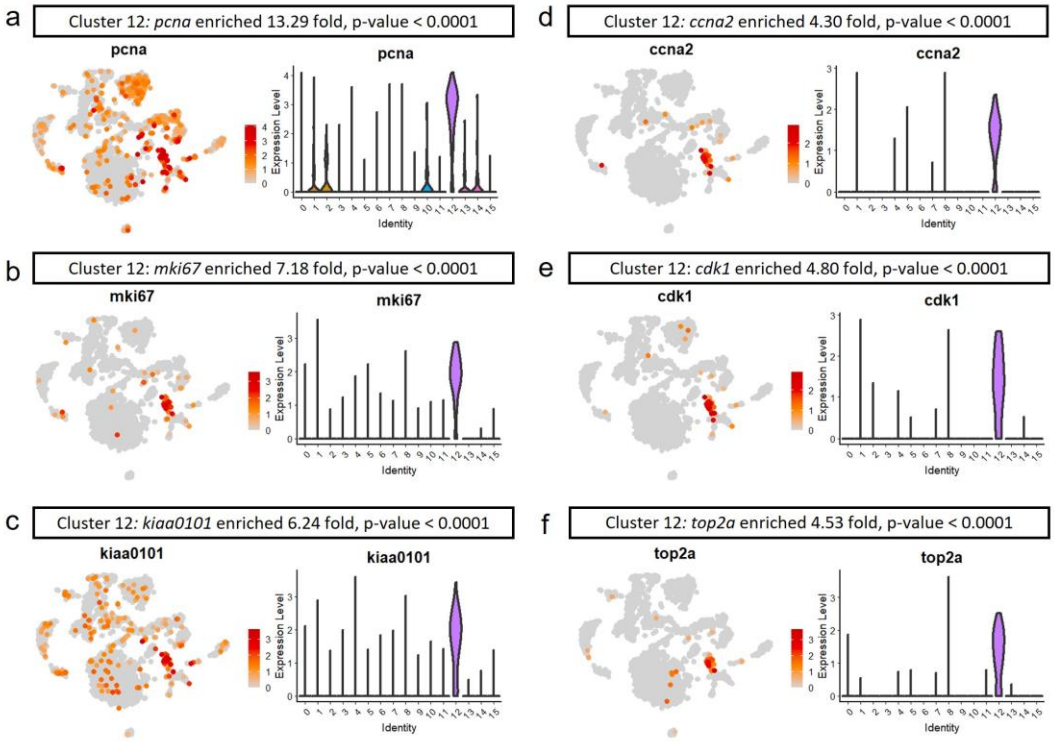

Figure 4.6: Expression patterns for marker genes of cluster 12. A-F: Proliferation and cell cycle associated genes are highly specific to cluster 12.

4.2.3.2 Clusters 0 and 9: Motor Neurons

Cluster 0 is the largest of the clusters. Based on the most highly enriched genes in this cluster, *isl1* and *isl2a* initially suggest a motor neuron identity [54-57] (Figure 4.4, Figure 4.7 b,c). I therefore looked to see if this cluster expressed the canonoical motor neuron marker, *mnx1*, and found that it is enriched in cluster 0 compared to the rest of the dataset (Figure 4.7d). Similarly, *lhx4* is enriched in cluster 0 (Figure 4.7 e) and is known to be a marker of motor neuron identity in zebrafish and mice (Sharma et al, 1998; Thor et al, 1999).

It is notable that the motor neuron markers enriched in cluster 0 also show strong expression in the smaller but connected cluster 9 (Figure 4.7 b-e). This is confirmed by the top enriched genes in cluster 9, which includes *lhx4* (Figure 4.4), *mnx1* and *isl1*. These genes suggest cells in cluster 9 are also of a motor neuron identity, however since they have clustered separately and do express differing genes it is possible they are either a specific subtype of motor neurons or of a different developmental stage.

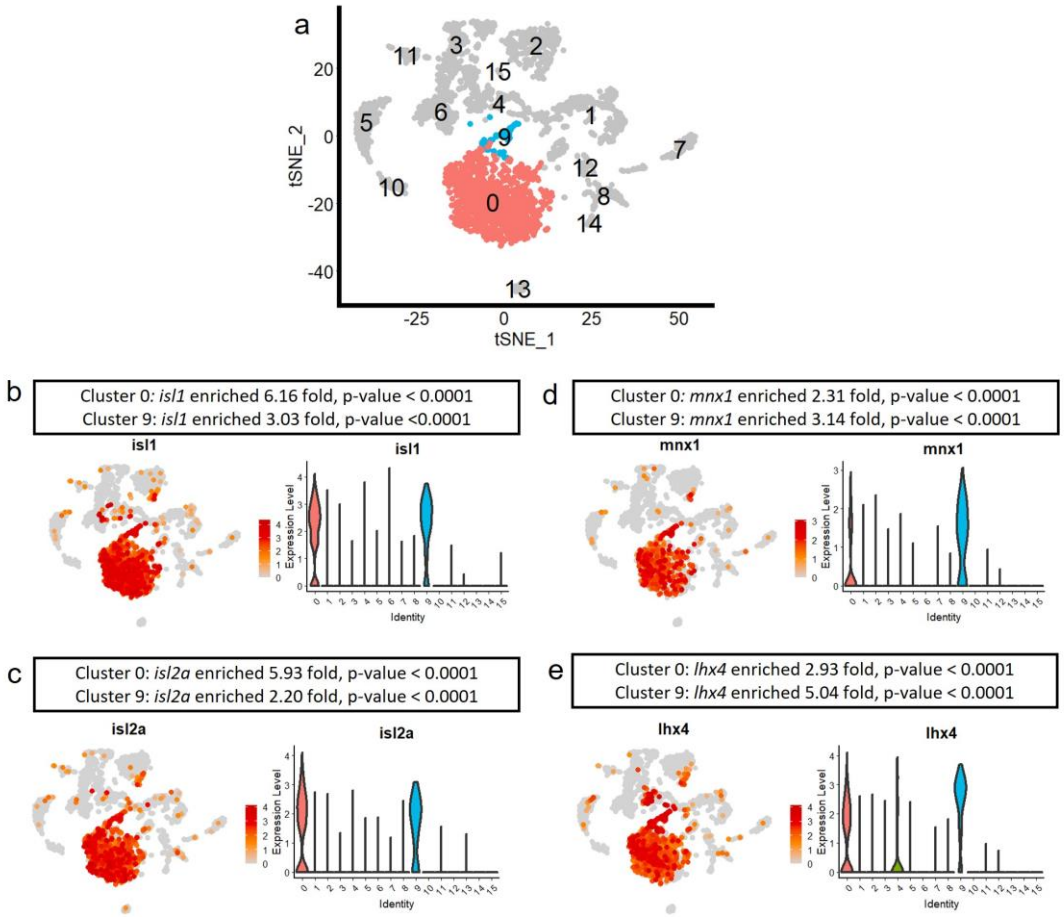

Figure 4.7: Expression patterns for motor neuron marker genes. A: tSNE plot highlighting clusters 0 and 9. **B-E:** Expression of motor neuron marker genes *isl1, isl2a, mnx1* and *lhx4* are enriched in clusters 0 and 9.

4.2.3.3 Clusters 3,4,6,11: Interneurons

Since the same population of *her4.3*$^{+}$ progenitors are known to generate many types of neurons, it is not a surprise that we found clusters of cells with interneuron markers within our dataset. Indeed, the enrichment of *lhx1a* and *lhx5* across clusters 3, 4, 6 and 11 (Figure 4.8) suggest these all represent interneuron cells (Pillai et al, 2007).

Based on the combination of specific markers in specific clusters, it is possible to assign putative interneuron subtypes to specific clusters. For example, cluster 11 can be assumed to consist of V2b interneurons based on the highly specific expression of *gata3* and *tal2*, along with *gad1b* and *glyt2* (Achim et al, 2013; Callahan et al, 2019; Karunaratne et al, 2002) (Figure 4.9).

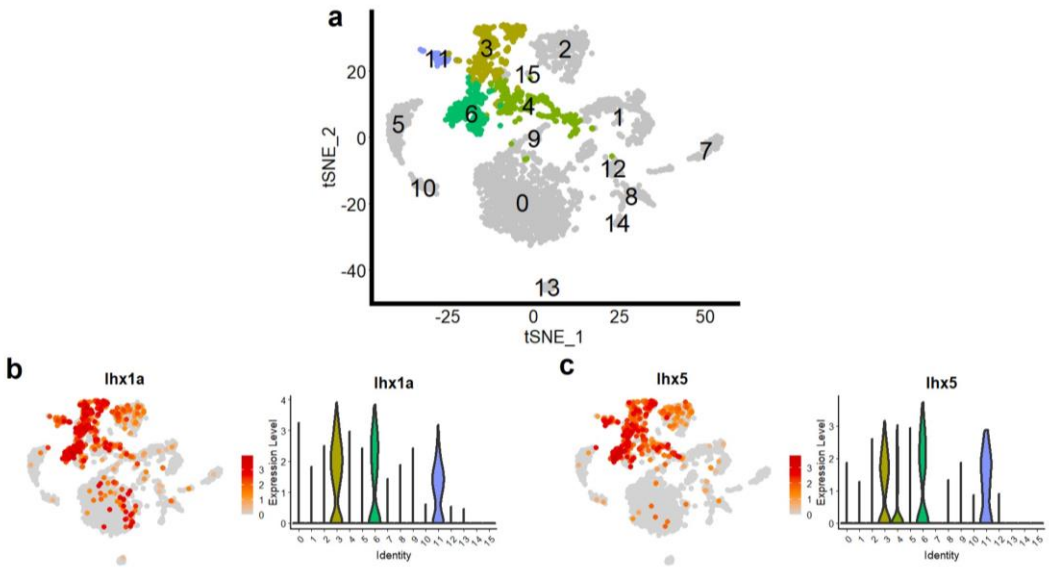

Figure 4.8: Expression of interneuron marker genes. A: tSNE plot highlighting clusters 3,4,6 and 11. **B-C:** Clusters 3,4,6 and 11 all express *lhx1a* and *lhx5*

Other clusters are not so straightfoward. The co-expression of *vsx2* and *sox14* in some cells in cluster 4 suggests that these cells may be v2a interneurons (Clovis et al, 2016; Hargrave et al, 2000; Kimura et al, 2006). However, only a subset (~20%) of this cluster expresses these markers (Figure 4.10 b,c), which may suggest other cell types contribute to this cluster too. Indeed, genes which play key roles in neuronal differentiation *neurod1* and *nrn1a* are both also among the top ten enriched genes in this cluster (Figure 4.4) and are expressed in a larger proportion of cells within cluster 4 than V2a markers *vsx2* and *sox14* (Figure 4.10 d,e) One possibility is that the cells expressing neurod1 and/or nrn1a without *vsx2* and *sox14* are immature V2 neurons which are yet to express V2a markers *vsx2* and *sox14*. Alternatively, these cells may indeed express vsx2 and sox14 but not at high enough levels to be detected in this dataset.

Similarly, cluster 6 is unlikely to consist of a single subtype of interneuron. The expression of *evx2* in some of this cluster suggests that at least some of these cells are v0 interneurons (Moran-Rivard et al, 2001) (Figure 4.11b). However, the *evx2* labelling is sparse (14.6% of cluster 6) and consequently it can be assumed other interneuron subtypes contribute towards this cluster. The expression of *barhl2* in 21.1% of cluster 6 suggests the contribution of dI1 interneurons to this cluster (Ding et al, 2012) (Figure 4.11c). Similarly, *tfap2a* is known to be expressed in GABAergic neurons (Zainolabidin et al, 2017), and is expressed in 36.6% of the cells in cluster 6 (Figure 4.11d).

Cluster 3 is notable for its expression of *pax2a* and *pax8* (Figure 4.12 b-c). These genes have been shown to be expressed in both GABAergic and glycinergic interneurons in zebrafish (Batista & Lewis, 2008). Since both *gad1b* and *gad2* are expressed in > 50% of the cells in this cluster (Figure 4.12 d-e), it is likely these cells represent GABAergic cells.

Due to the varied combination of subtype specific markers in clusters 3, 4 and 6 which prevent any definitive cell type identity assigning, these cells will be referred to as Interneurons 1, 2 and 3 respectively.

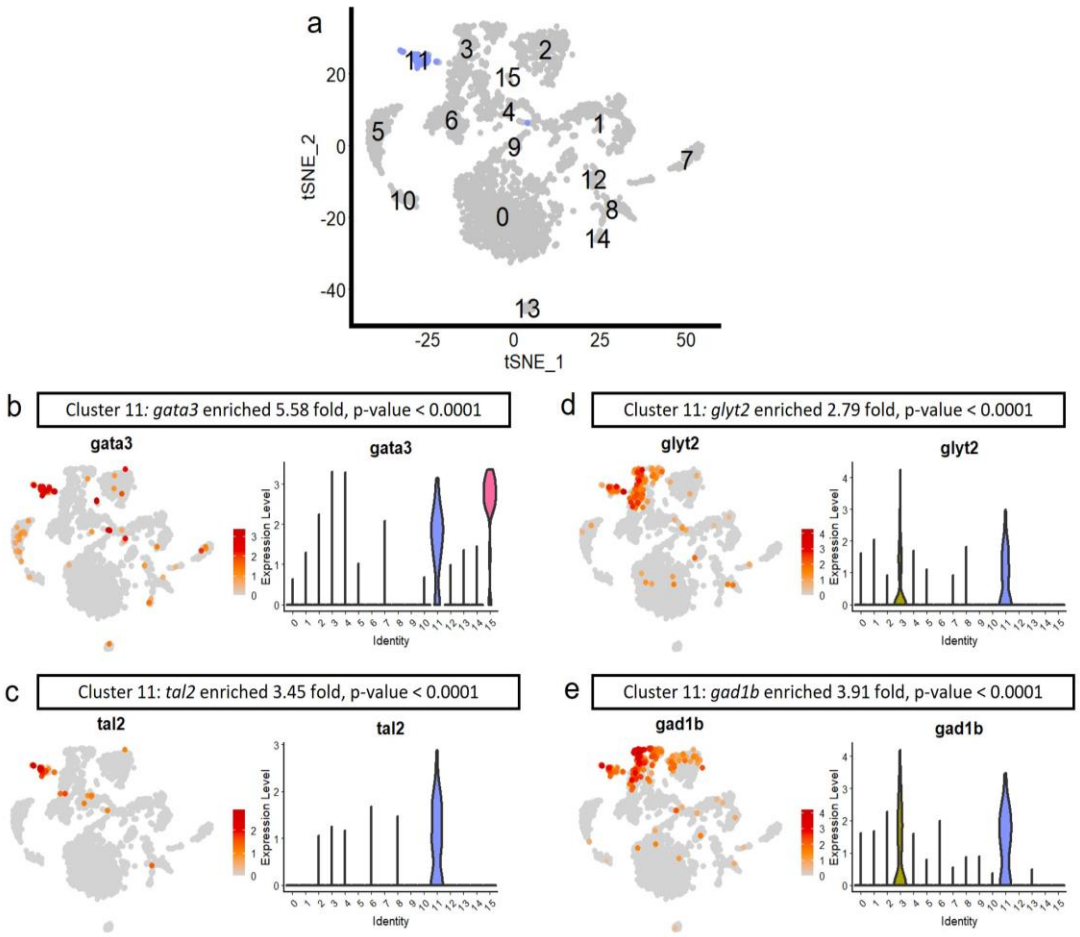

Figure 4.9: Expression patterns for V2b interneuron marker genes. A: tSNE plot highlighting cluster 11. **B-C:** Expression of *gata3* and *tal2* are highly specific to cluster 11. **D-E:** *glyt2* and *gad1b* are also enriched in cluster 11.

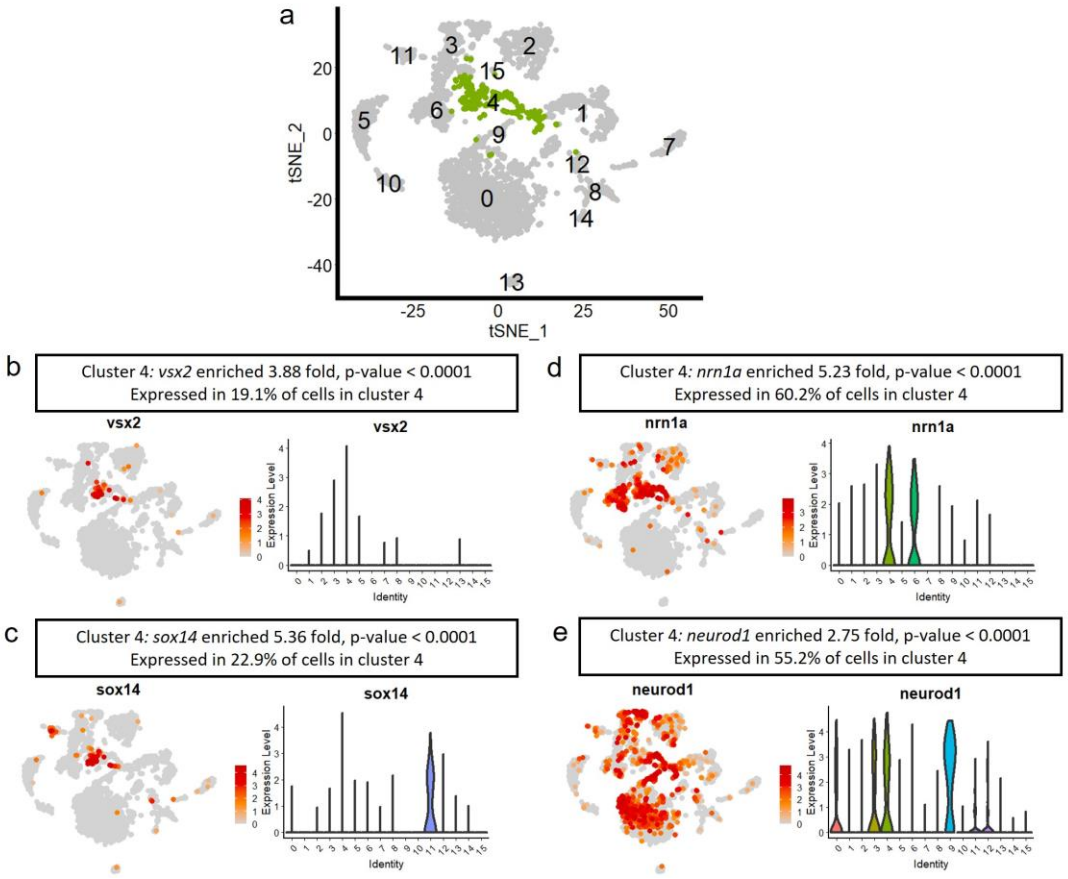

Figure 4.10: Expression pattern for cluster 4 marker genes. A: tSNE plot highlighting cluster 4. **B-C:** V2a interneuron markers *vsx2* and *sox14* are enriched in cluster 4, although they are expressed by <25% of cells in this cluster. **D-E:** *neurod1* and *nrn1a* are both also enriched in cluster 4.

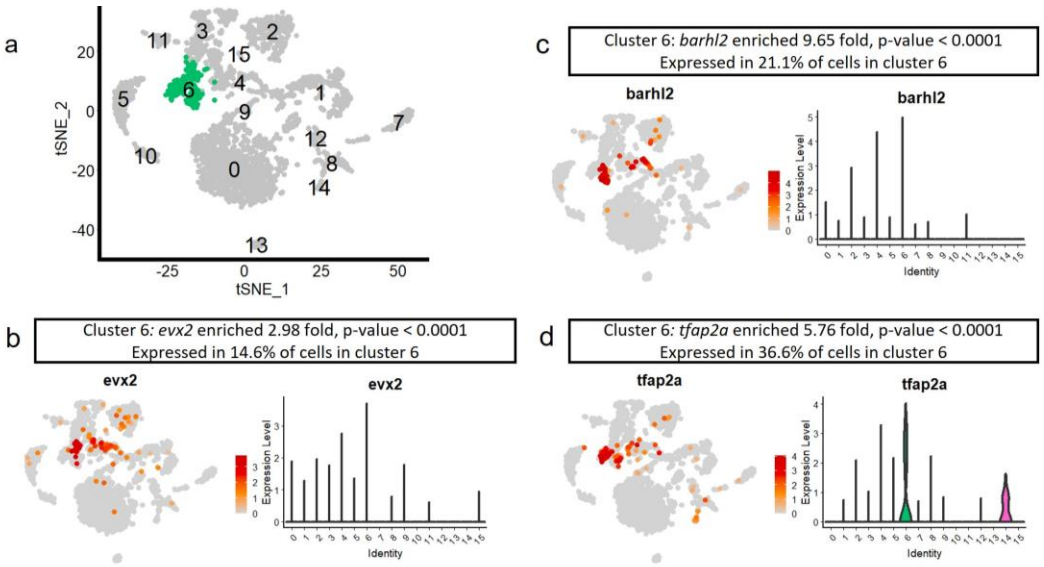

Figure 4.11: Expression patterns of genes enriched in cluster 6. A: a tSNE plot highlighting cluster 6. **B-D:** *evx2*, *barhl2*, and *tfap2a* are all enriched in cluster 6 compared to the dataset as a whole, however all are expressed in less than 40% of cluster 6 cells, with little overlap. This suggests that this cluster consists of multiple subtypes of interneurons.

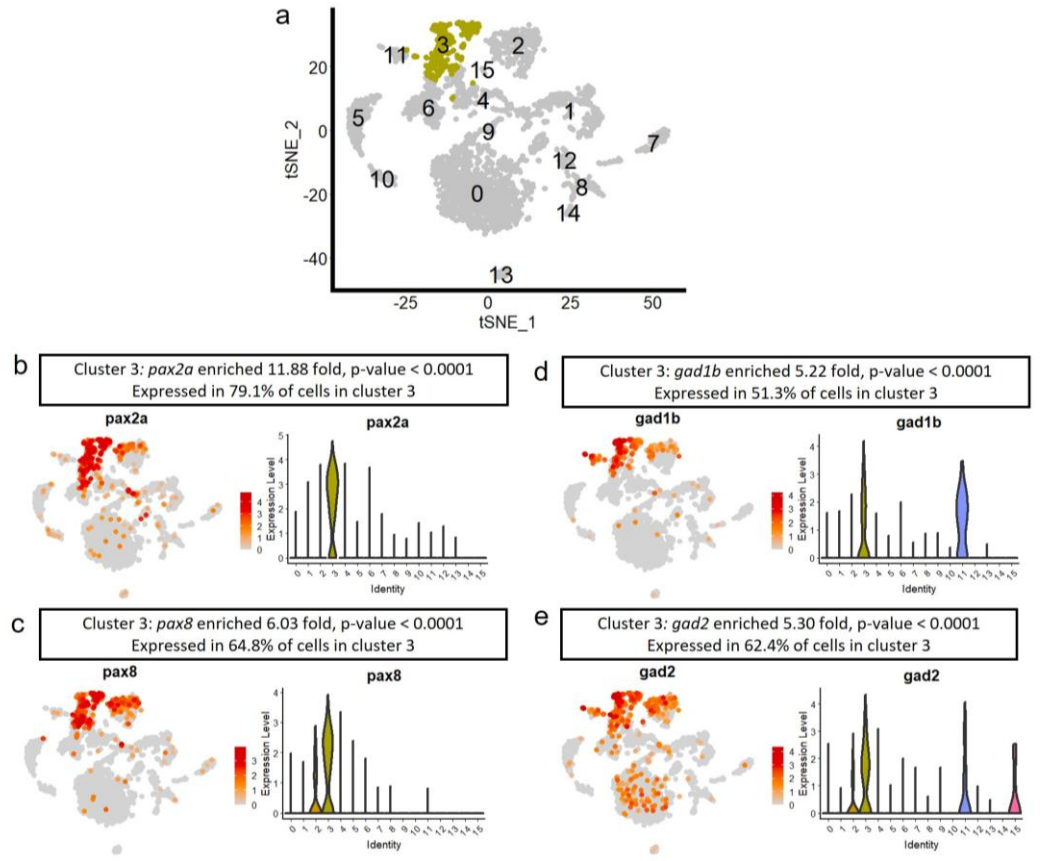

Figure 4.12: Expression patterns of genes highly expressed in cluster 3. A: tSNE plot highlighting cluster 3. **B-C:** Markers of glycinergic and GABAergic neurons, *pax2a* and *pax8*, are highly expressed in cluster 3. **D-E:** GABAergic markers *gad1b* and *gad2* are both enriched in cluster 3.

4.2.3.4 Clusters 5, 7 and 10: Oligodendrocytes and Schwann cells

Another cell type generated from her4.3^{+} cells is oligodendrocytes; therefore we would expect to see a population of these in the dataset. Indeed, multiple markers of myelinating cells including *sox10* (Stolt et al, 2002), *mbpa* (Early et al, 2018; Jung et al, 2010) and *nkx2.2a* (Kucenas et al, 2008a) are expressed in clusters 5,7 and 10 (Figure 4.13 b-d).

In addition to these markers of myelinating cells, cluster 7 is also enriched for the Schwann cell specific marker *pmp22a* (Wulf et al, 1999) (Figure 4.13e). In contrast, clusters 5 and 10 show much lower expression of this gene. Consequently, the identity of oligodendrocytes is putatively assigned to interconnecting clusters 5 and 10, and cluster 7 is a population of Schwann cells.

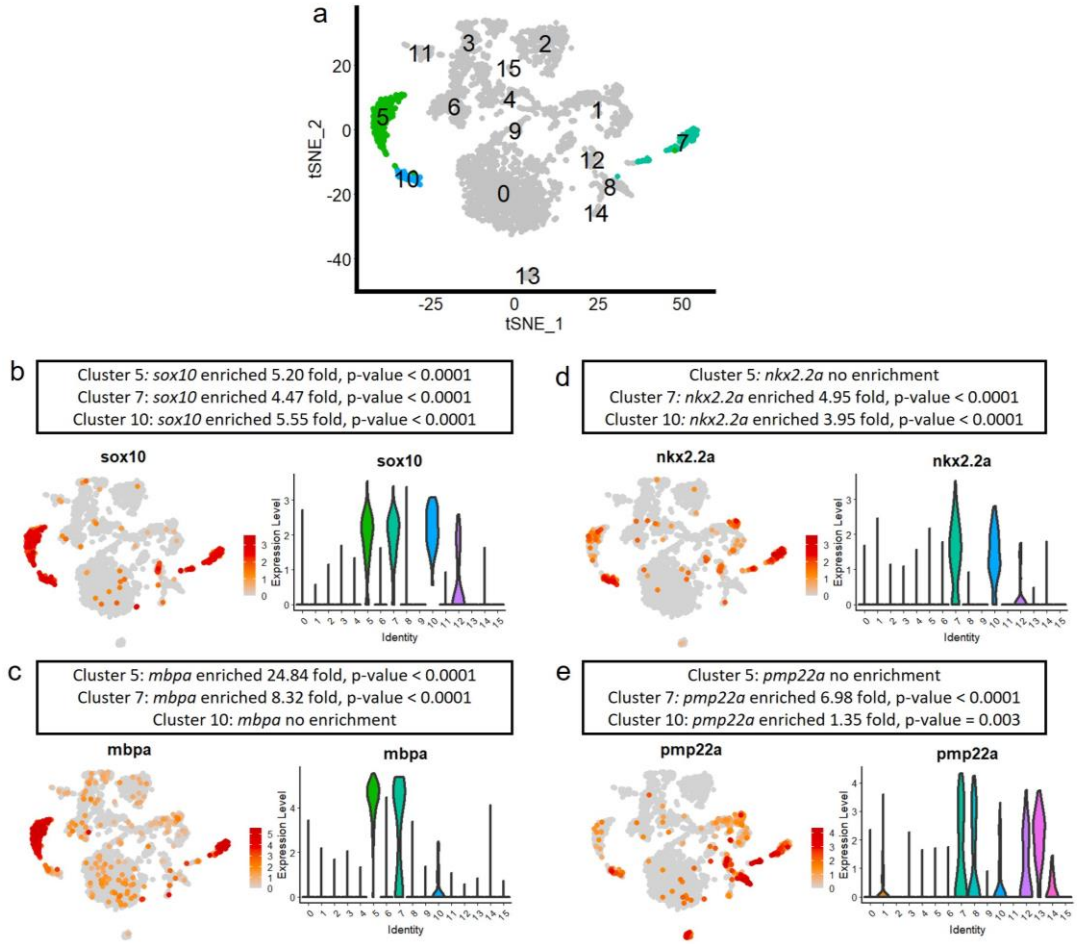

Figure 4.13: Expression patterns of genes expressed in clusters 5, 7 and 10. A: tSNE plot highlighting clusters 5, 7 and 10. **B:** Myelination marker *sox10* is enriched in clusters 5,7 and 10. **C:** *mbpa* is enriched in clusters 5 and 7. **D-E:** *nkx2.2a* and *pmp22a* are both enriched in clusters 7 and 10.

4.2.3.5 Cluster 2: Neurosecretory cells

The identity of cluster 2 has proven elusive. While these cells do widely express pan-neuronal markers, e.g *snap25a* and *elavl3* (

Figure 4.14 b-c), there is no widespread of either interneuron markers (Figure 4.12) or motor neuron markers (Figure 4.7). Instead, secreted molecules including leptin-a (*lepa*), peptide YYb (*pyyb*) and secretogranin II (*scg2b*) are expressed in a highly specific manner in this cluster (

Figure 4.14 d-f). In addition, there is strong enrichment for regeneration associated genes including *gap43* (

Figure 4.14g).

Taking these features into account, these cells are putatively labelled as neurosecretory cells.

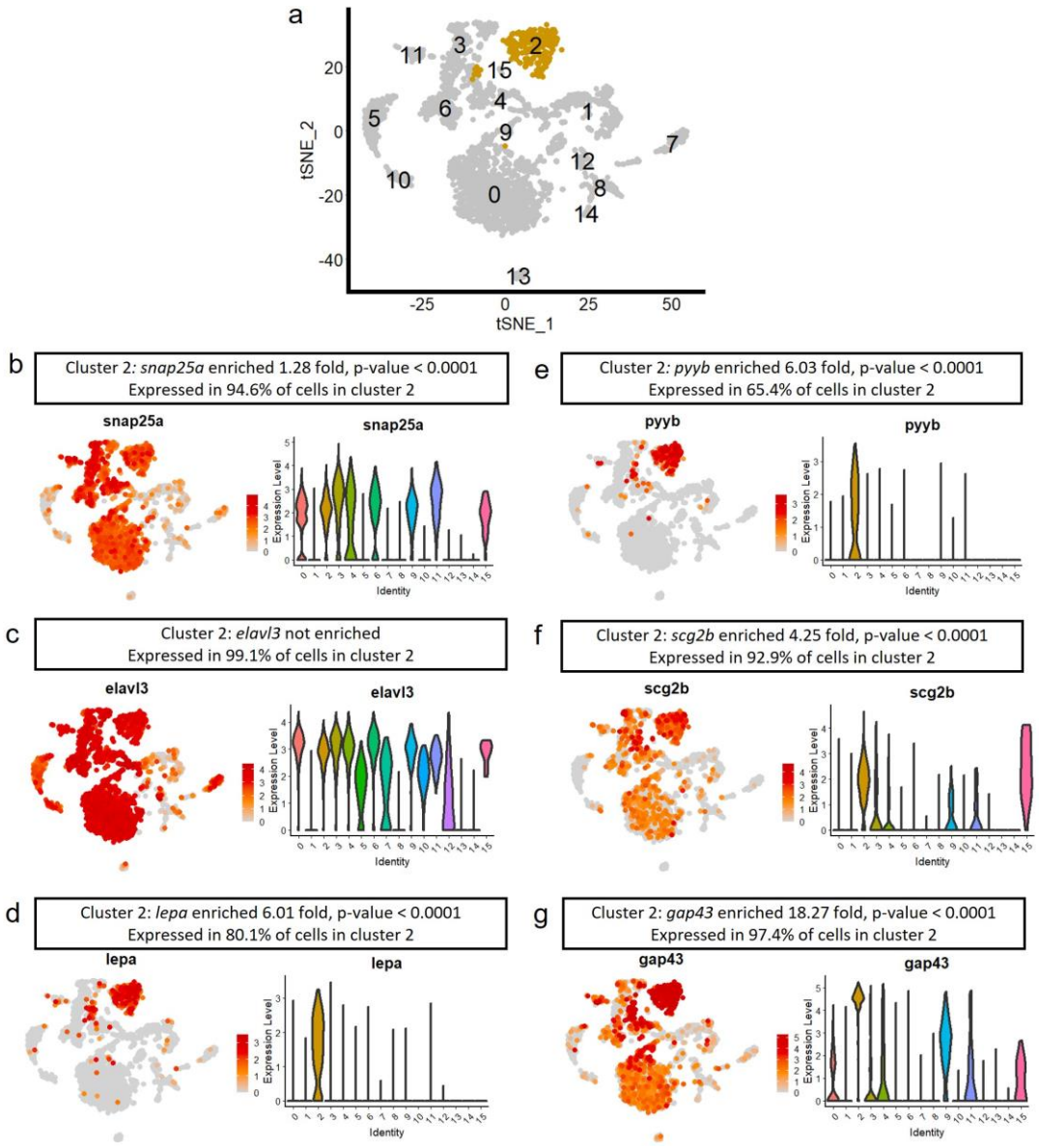

Figure 4.14: Expression pattern of genes highly expressed in cluster 2. A: tSNE plot highlighting cluster 2. **B-C:** Pan-neuronal markers *snap25a* and *elavl3* are expressed in cluster 2. **D-F:** Genes for secreted molecules *lepa*, *pyyb* and *scg2b* show specific expression in cluster 2. **G:** Regeneration associated gene *gap43* is enriched in cluster 2.

4.2.3.6 Clusters 8, 13, 14, 15: Other cell types

The remaining clusters 8, 13, 14 and 15 do not appear to display any of the marker genes associated with any cell types of expected *her4.3*$^{+}$ progeny. Analysing the top enriched genes in each cluster is helpful at elucidating their identity (Figure 4.4, Appendix). A number of collagen related genes (e.g *col1a1a*, *col5a1*) are enriched in cluster 8 (Figure 4.15 b-c). This raises the possibility that these cells may be

fibroblasts, as fibroblasts are known to deposit collagen to contribute to the ECM. Indeed, there is some localised expression of known fibroblast-associated genes *pdgfra* (Li et al, 2000) and *prrx1b* (de Bakker et al, 2021) in this cluster (Figure 4.15 c-d).

The likely identity of cluster 13 is clear from the expression of known floorplate markers *foxa1*, *foxa2* and *shha/b* (Odenthal & Nüsslein-Volhard, 1998; Odenthal et al, 2000), which all show strong and specific expression in this cluster (Figure 4.16).

Similarly, the highly specific and strong enrichment of multiple keratin genes (e.g *krt5*, *krt91*) in cluster 14 makes the identification of this cluster fairly straightforward (Figure 4.17 b-c). In addition, keratinocyte specific markers including *epcam* and *tp63* (previously known as delta-np63) (Slanchev et al, 2009) are also enriched in this cluster (Figure 4.17 c-d).

Finally, the smallest cluster is cluster 15, which comprises of only 22 cells. Their expression of *tph2* (Lillesaar et al, 2007) and *fev* (Maurer et al, 2004) demarcate these as potential serotonergic neurons (Figure 4.18).

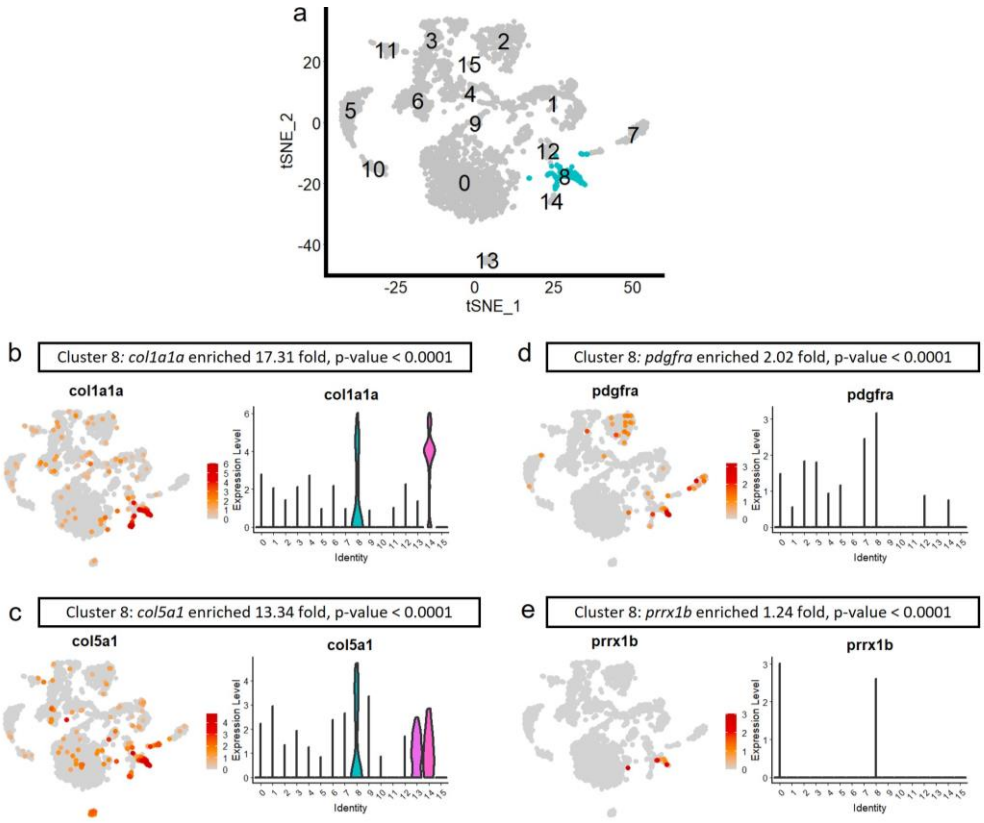

Figure 4.15: Expression pattern of fibroblast related genes. A: tSNE plot highlighting cluster 8. **B-E:** Collagen genes and fibroblast markers are enriched in cluster 8.

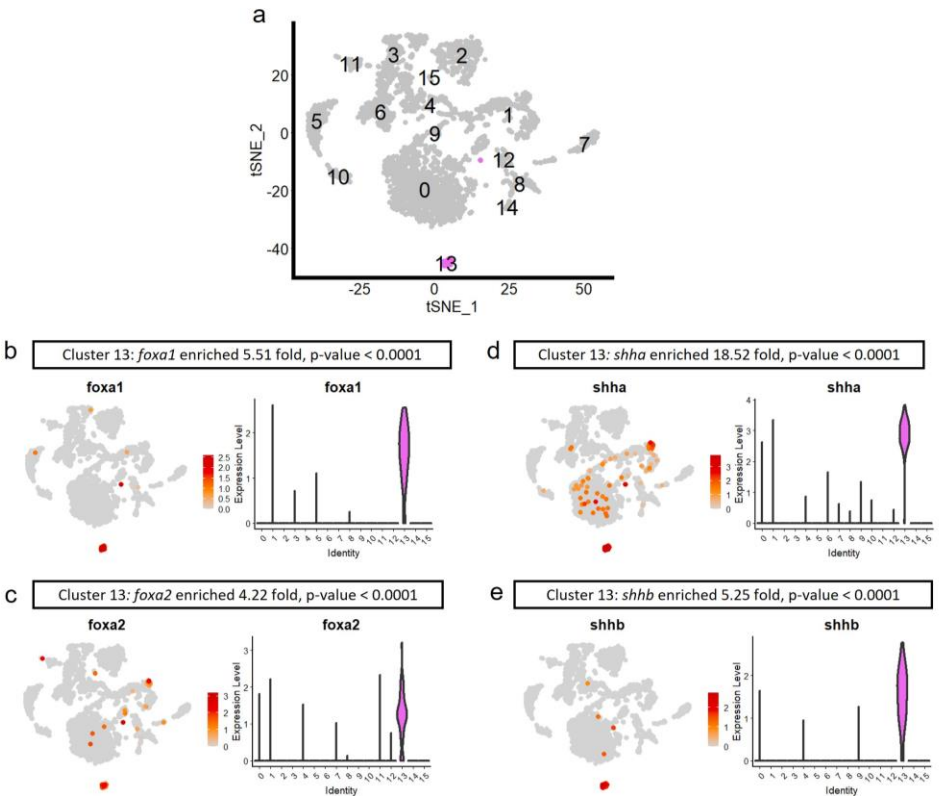

Figure 4.16: Expression of floorplate marker genes. A: tSNE plot highlighting cluster 13. **B-E:** Floorplate markers *foxa1, foxa2, shha* and *shhb* are enriched in cluster 13.

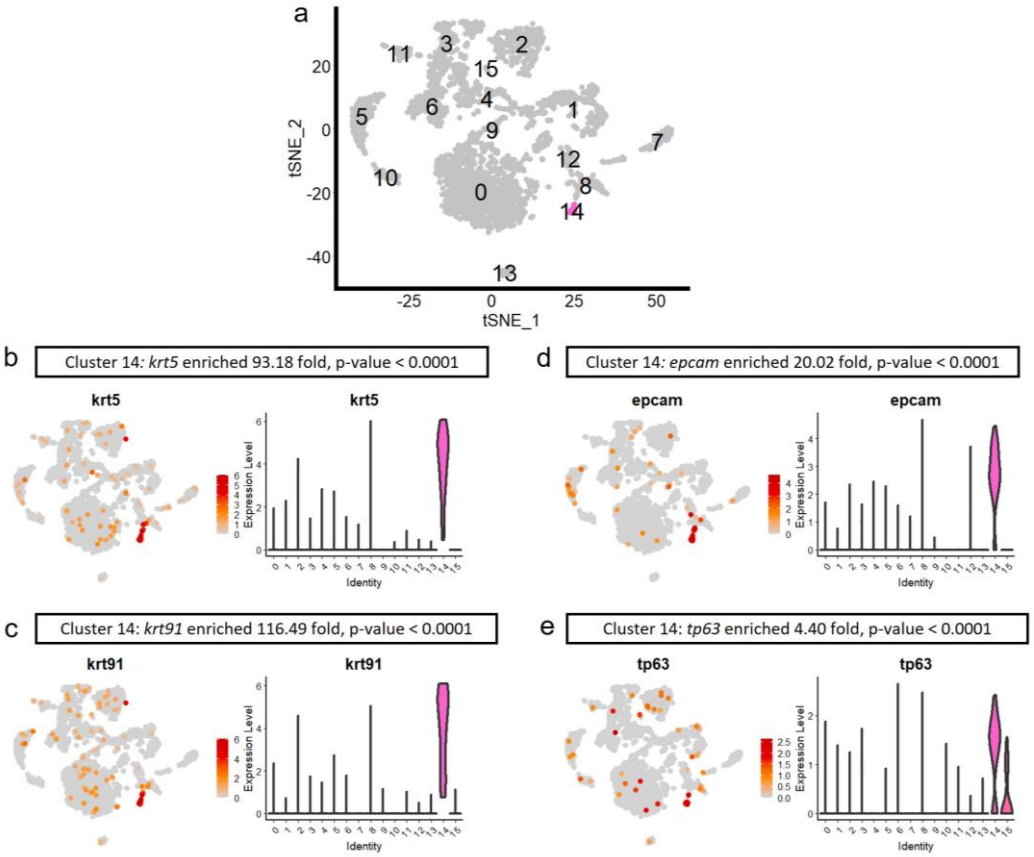

Figure 4.17: Expression of keratinocyte marker genes. A: tSNE plot highlighting cluster 14. **B-E:** Keratinocyte marker genes *krt5, krt91, epcam* and *tp63* are enriched in cluster 14.

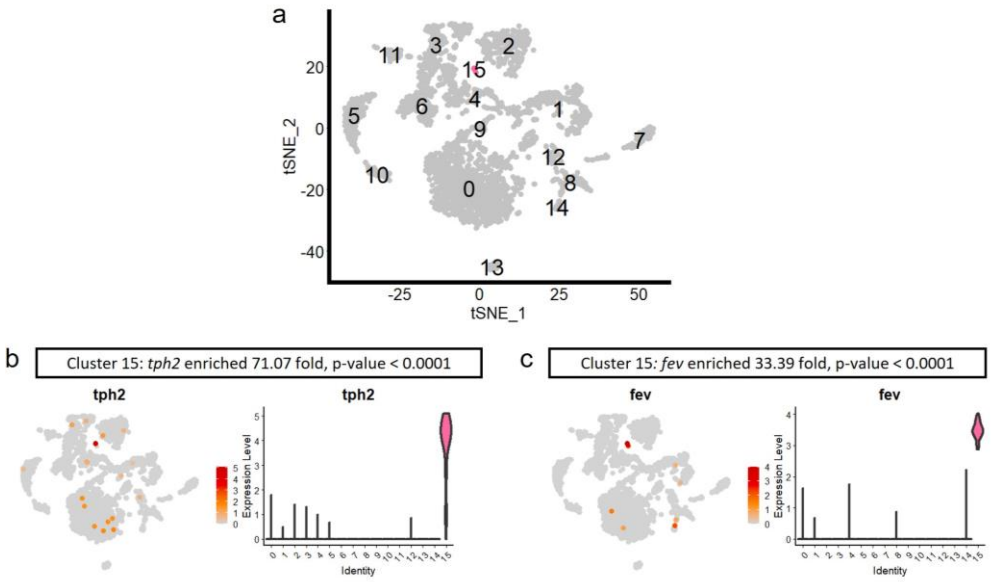

Figure 4.18: Expression of serotonergic marker genes. A: tSNE plot highlighting cluster 15. **B-C:** Serotonergic neuron marker genes *tph2* and *fev* are strongly enriched in cluster 15 compared to the dataset as a whole.

4.2.3.7 Cluster assignments for her4.3+ dataset

Based on the expression patterns of marker genes discussed above, cell type identities were assigned to each cluster. These are summarised in Figure 4.19.

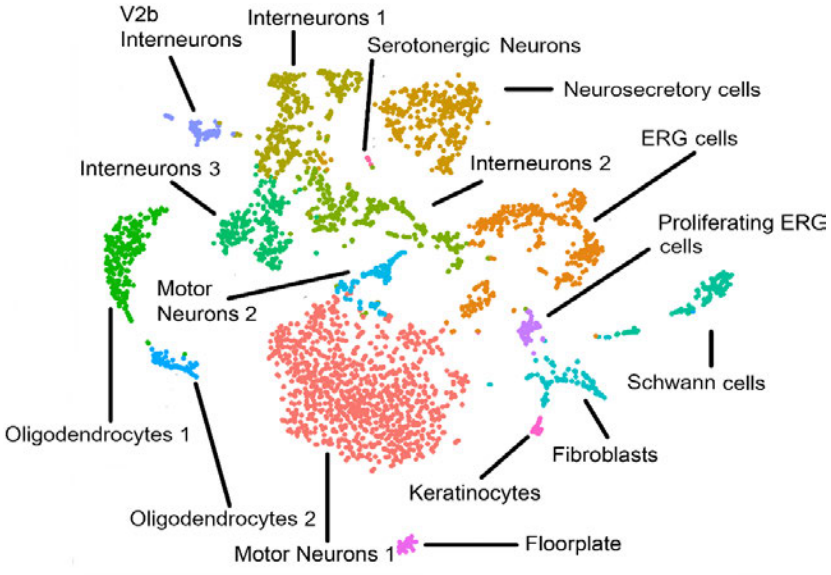

Figure 4.19: The tSNE plot for the her4.3+ dataset with assigned cell types labelled.

4.2.4 Injury induced changes in her4.3+ cells and their progeny

4.2.4.1 Changes in proportion of cell types in spinal cord after injury

One important piece of information about the reaction of a cell type to injury is the relative proportions of the cells present before and injury. The most striking change between the cell type proportions before and after injury is the large increase in the number of putative neurosecretory cells after injury (Figure 4.20). This cell type contributes only negligibly to the captured naïve dataset (2.79% of the captured naïve cells are neurosecretory cells), however in the lesioned sample, 20.57% of the captured cells are neurosecretory cells.

Oligodendrocytes, motor neurons and interneurons all display decreases in their proportion to the total captured cells in the spinal cord after injury when compared to the naïve sample. To some extent this can be explained by the expansion of neurosecretory cells (meaning even if the number of cells is unchanged, the relative proportion of the entire sample is smaller due to the additional neurosecretory cells in the lesioned sample). The lack of increase in cells which express motor neuron markers in the lesioned larvae compared to the unlesioned larvae is surprising, as it has been previously reported that new motor neurons are preferentially generated after injury at the expense of oligodendrocytes from specific ERG cell subtypes by 48 hpf (Ohnmacht et al, 2016). One explanation may be that the increase in motor neurons in the lesioned fish may not occur until after 24 hpi.

a

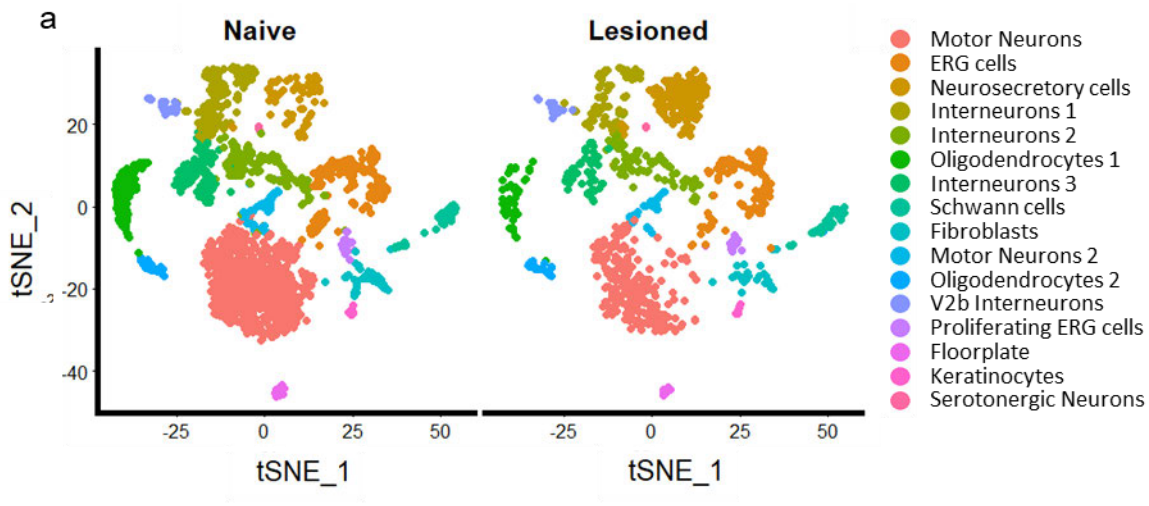

b

Cluster	Percentage of entire naïve sample	Percentage of entire lesioned sample	Difference
Motor Neurons	31.81	22.53	-9.29
ERG cells	11.79	10.47	-1.31
Neurosecretory cells	2.79	23.36	20.57
Interneurons 1	9.89	7.48	-2.41
Interneurons 2	8.76	8.48	-0.28
Oligodendrocytes 1	8.16	3.82	-4.33
Interneurons 3	7.71	4.57	-3.14
Schwann cells	3.75	4.07	0.32
Fibroblasts	3.71	4.07	0.36
Motor Neurons 2	3.19	2.41	-0.78
Oligodendrocytes 2	2.14	2.24	0.10
V2b Interneurons	2.18	1.75	-0.43
Proliferating ERG cells	1.45	1.83	0.38
Floorplate	1.21	1.33	0.12
Keratinocytes	1.01	0.67	-0.34
Serotonergic Neurons	0.44	0.91	0.47

Figure 4.20: A comparison of the cell numbers in each cluster of the naïve and lesioned samples. A: Two tSNE plots of the dataset, displaying the cells originating from the naïve dataset separately from those originating from the lesioned dataset. An expansion of the neurosecretory cells is evident. **B:** This table displays the percentage each cell type contributes to the entire captured dataset for each condition. Cell types which are present in a higher proportion in the lesioned condition than the naïve condition are highlighted in green, and those which are present in a lower proportion in the lesioned condition than the naïve condition are highlighted in red.

One potential explanation for the increase in number of neurosecretory cells but lack of increase in motor neurons is that the neurosecretory cell identity could be a transitionary stage between the progenitor cells and the motor neurons, and at this timepoint the majority of cells on the pathway are at the neurosecretory stage. To

investigate whether this is indeed the trajectory of progenitor cells to motor neuron generation, I performed trajectory analysis on the dataset.

4.2.4.2 Trajectory analysis of lesioned sample

To gain insight into the differentiation pathway of cell populations from the *her4.3:GFP* dataset, trajectory inference was performed on the lesioned dataset. Initially cell types were identified using known marker genes associated with the Seurat-generated clusters as described in previous sections (Figure 4.21a). Following this, I used monocle3 to construct a trajectory for the lesioned dataset, and to calculate where each cell sits along the reconstructed pseudotime (Figure 4.21b). The pseudotime trajectory was constructed after manually specifying the root node, as is standard in monocle3.

This trajectory analysis suggests that ERG cells may initially become proliferative, before transitioning either to a myelinating cell identity or a neuronal identity. Cells which are transitioning towards a neuronal identity initially express both motor neuron markers (*isl1*) and interneuron markers (*pax2a*) before committing to a particular fate. This trajectory then places the neurosecretory as a further state after cells proceed through an interneuron cluster. Therefore, neurosecretory cells could be a differentiated cell type and and not an immature transitory state.

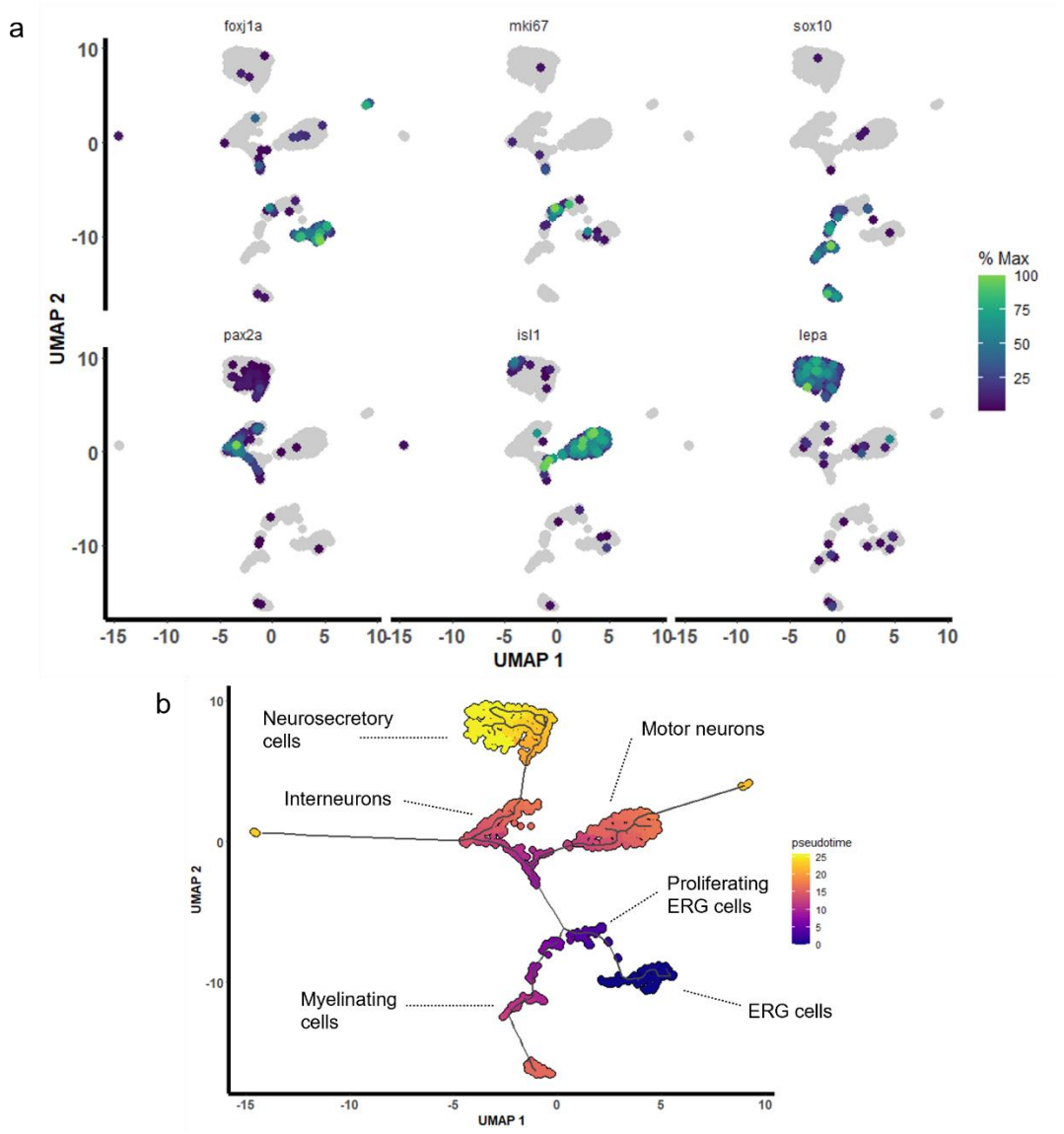

Figure 4.21: Trajectory analysis of the lesioned dataset. A: The UMAP plots display the expression of specific genes, in order to identify where the major cell types are positioned in the plot**.** %Max refers to the levels of expression of each gene relative to the highest level of expression of the specific gene in our dataset. **B:** The UMAP is coloured according the pseudotime, and labelled according to inferred cell types, based on marker gene expression. The trajectory graph is overlaid on the UMAP.

4.2.4.3 Gene expression changes undergone by ERG cells following injury

The relative contribution of ERG cells to the entire sample is not drastically different before and after injury in terms of the number of cells present (Figure 4.20b). This is in line with previous findings that these cells are a self-renewing population (Rothenaigner et al, 2011). Since these cells react to injury by switching from an oligodendrocyte generating programme to a neuron generating programme, it is

expected that widespread gene expression changes are undergone in the ERG cells. To investigate this, I compared the gene expression between the populations before and after injury. Using the Wilcoxon Rank Sum test, 207 genes were found which are significantly upregulated in the lesioned sample compared to the naïve sample. The top ten strongest upregulated genes are displayed in Table 4.1.

Gene symbol	Fold Change	Adjusted p-value	% of cells from unlesioned sample expressing this gene	% of cells from lesioned sample expressing this gene
anxa2a	8.09	6.21E-27	0.7	42.9
txn	6.22	1.38E-25	70.2	92.1
timp2b	5.80	7.63E-14	13.7	50.8
cxcl18b	3.36	5.95E-09	16.4	48.4
vmp1	3.05	1.17E-07	50.3	70.6
si:dkey-153m14.1	3.01	1.12E-02	72.9	87.3
fosl2	3.01	5.76E-19	31.5	73
hbegfa	2.90	1.74E-03	54.5	71.4
ppp1r1c	2.55	2.97E-20	0	32.5
krt18b	2.54	5.27E-27	1.7	46

Table 4.1: The top ten most strongly upregulated genes in the ERG cell cluster after injury.

Understanding the function of these most strongly upregulated genes can provide insight into the changes undergone by the ERG cells in response to injury. For example, *vmp1*, *txn, fosl2* and *hbegfa* are implicated in neuronal survival. Thioredoxin is a cytoprotective antioxidant enzyme which protects against oxidative stress and cell death. Specifically in neurons it is a neurotrophic cofactor and has roles in neuroprotection (Masutani et al, 2004). Similarly, *vmp1* codes for an autophagy protein, vacuole membrane protein 1, which in mammals plays a role in modulating neuronal survival and maintaining axonal homeostasis (Wang et al, 2021a). Fos family members including *fosl2* have a plethora of roles in proliferation

and differentiation of cells, and *fosl2* specifically has been shown to be involved in the transcriptional control of neuroprotective genes (Butler & Pennypacker, 2005). Finally, the neurotrophic factor HB-EGF (mammalian ortholog of *hbegfa*) has been shown to play a neuroprotective role against ischemic injury *in vitro* (Zhou & Besner, 2010).

Another recurring function played by some of these top genes is differentiation. Along with roles in neuroprotection, *fosl2* and *txn* have both been shown to promote or augment neuronal differentiation in PC12 cells *in vitro*. Similarly, it has been suggested that TIMP-2 (mammalian ortholog of *timp2b*) promotes neuronal differentiation and neurite outgrowth *in vitro* (Pérez-Martínez & Jaworski, 2005). This is supported by the observation that TIMP-2 mRNA is expressed in the nervous system at the onset of neuronal differentiation in rats (Fager & Jaworski, 2000). Annexin A2 (*anxa2a*), the most strongly upregulated gene, has also been shown to have similar roles in neuronal differentiation and neurite outgrowth on PC12 cells *in vitro* (Jacovina et al, 2001).

The gene *ppp1r1c* is also amongst the ten top upregulated in ERG cells after injury. This gene codes for a subunit of the enzyme protein phosphatase 1. This role of this subunit is not well understood, however, in cell models of glioblastoma PPP1R1C potentiates proliferation (Liu et al, 2017). HB-EGF, which in zebrafish is transcribed from the *hbegfa* gene, has a much better understood role in proliferation. In rats, HB-EGF stimulates the proliferation of CNS astrocytes and progenitors during development (Kornblum et al, 1999; Nakagawa et al, 1998). Furthermore, HB-EGF has well characterised roles in neurogenesis in the adult mice and rat brains when applied intracerebroventricularly (Jin et al, 2002; Jin et al, 2003). Interestingly, *hbegfa* is strongly upregulated in muller glia after zebrafish retina injury and HB-EGF promotes regeneration by stimulating the dedifferentiation of muller glia into their neurogenic progenitors (Wan et al, 2012).

Two of the genes which are highly upregulated in the ERG cluster following injury don't have well characterised roles in the CNS. One of these, *krt18b*, is normally associated with epithelial cells, but has been identified in radial glial cells in axlotl (Holder et al, 1990). It's role following injury is unknown. Similarly, since *cxcl18b* is an inflammatory chemokine, it is normally associated with immune cells. Interestingly, it has previously been isolated from non-phagocytic uninfected cells in

the stroma of granuloma (Torraca et al, 2017). Cxcl18b is found in zebrafish and amphibians and doesn't have a close mammalian ortholog. It is known to be a chemoattractant for neutrophils, and any further roles specific to neuronal progenitors are not yet known.

One of the genes in Table 4.1 is unannotated; *si:dkey-153m14.1*. It is a long intervening non-coding RNA with unknown function.

To further understand the main functions and pathways of the 207 upregulated genes after injury, I used Metascape (Zhou et al, 2019) to perform gene ontology (GO) analysis to find any overarching patterns in the functions of these genes (Figure 4.22). GO analysis returned an enrichment of GO terms associated with expected functions such as 'regeneration', 'neuron projection regeneration' and 'regulation of cell population proliferation'. Additionally, many terms associated with the immune response were enriched, including 'Innate Immune System', 'response to wounding' and 'Cytokine-cytokine receptor interaction'. This suggests a role for cell-cell communication between the immune cells and ERG cells after injury which will be further explored in chapter 5.

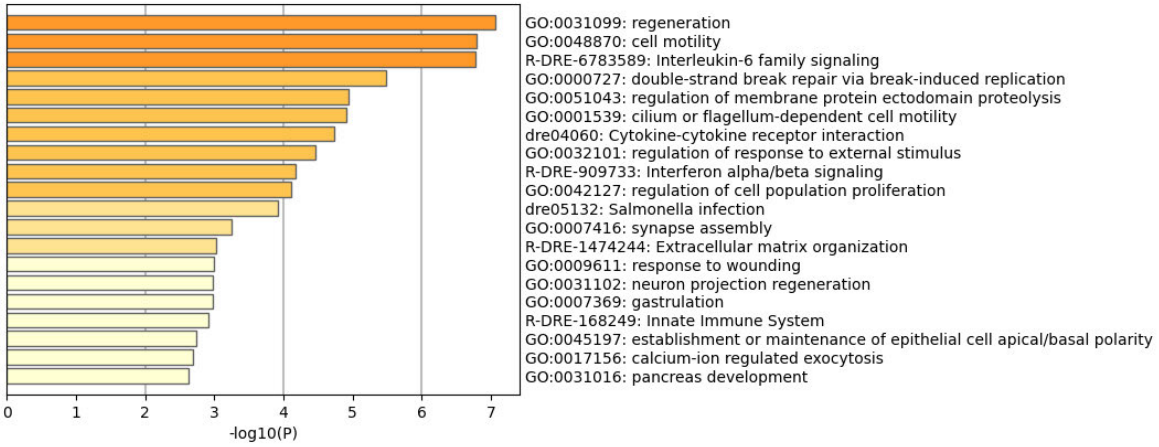

Figure 4.22: Gene ontology enrichment analysis of the 207 upregulated genes in the lesioned ERG cells compared to the unlesioned ERG cells.

4.2.4.4 Transcription factors differentially regulated in ERG cells after injury

Within the upregulated genes in ERG cells following injury, those which code for transcription factors have potentially the largest opportunity to effect large scale changes in the ERG population. To investigate which transcription factors are up- or downregulated in the ERG cells after injury, I cross referenced the differentially

regulated genes with the list of all zebrafish transcription factors obtained from AnimalTFDB 3.0 (Hu et al, 2019). Of the 207 genes which are significantly upregulated in the injured ERG cluster compared to the unlesioned ERG cluster, 12 of these are genes for transcription factors. Of the 88 genes which are significantly downregulated in the lesioned ERG cluster compared to the unlesioned sample, 16 of these are transcription factors.

Gene symbol	Gene name	Fold differentially regulated
fosl2	FOS like 2, AP-1 transcription factor subunit	3.01
junbb	JunB proto-oncogene, AP-1 transcription factor subunit b	2.08
foxj1a	forkhead box J1a	1.82
zfp36l1b	zinc finger protein 36, C3H type-like 1b	1.78
nme2b.1	NME/NM23 nucleoside diphosphate kinase 2b, tandem duplicate 1	1.67
mideasb	mitotic deacetylase associated SANT domain protein b	1.49
lin28a	lin-28 homolog Ab	1.25
cbfb	core-binding factor subunit beta	1.24
irf9	interferon regulatory factor 9	1.21
fosl1b	FOS like 1, AP-1 transcription factor subunit b	1.18
bcl6ab	BCL6A transcription repressor b	1.17
glis3	GLIS family zinc finger 3	1.11
srebf2	sterol regulatory element binding transcription factor 2	0.80
tfe3a	transcription factor binding to IGHM enhancer 3a	0.73
vdrb	vitamin D receptor b	0.71
hes6	hes family bHLH transcription factor 6	0.68
klf11a	Kruppel-like factor 11a	0.68
tsc22d1	TSC22 domain family, member 1	0.67
si:dkeyp-68b7.7	si:dkeyp-68b7.7	0.65
heyl	hes related family bHLH transcription factor with YRPW motif like	0.64
mycn	MYCN proto-oncogene, bHLH transcription factor	0.63
nfia	nuclear factor I/A	0.62
her4.1	hairy-related 4, tandem duplicate 1	0.59
ddit3	DNA-damage-inducible transcript 3	0.58
hoxb9a	homeobox B9a	0.57

her4.3	hairy-related 4, tandem duplicate 3	0.55
znf395a	zinc finger protein 395a	0.54
hoxb8a	homeobox B8a	0.52

Table 4.2: A table of the transcription factors which are differentially regulated in the ERG cells after injury. Genes which are upregulated after injury are highlighted in green, those downregulated after injury are highlighted in red.

Amongst the upregulated transcription factors, three transcription factors involved in the AP-1 pathway are present (*fosl2*, *junbb* and *fosl1b*). AP-1 signalling mediates gene regulation in response to a range of stimuli including cytokines and growth factors and effects a plethora of cell processes including differentiation, proliferation and apoptosis. In Xenopus development it has a role in neurogenesis via its regulation of *foxd5b* expression (Yoon et al, 2013). One of the main activators of the AP-1 signalling pathway is TNF, whose role in neurogenesis will be discussed in chapter 5.

Other transcription factors upregulated in our dataset with known roles in neurogenesis include *bcl6ab* (Bonnefont et al, 2019), *lin28a* (Hu et al, 2022), *glis3* (Calderari et al, 2018) and *mideasb* (Mondal et al, 2020). In contrast, roles for *zfp36l1b, nme2b* and *cbfb* in neurogenesis have not yet been reported.

It is interesting that *foxj1a* is upregulated after injury, where *her4* duplications *her4.3* and *her4.1* are both downregulated. Both *foxj1a* and *her4* are used to identify the ERG population. The upregulation of *foxj1a* suggests that new ERG cells are generated. This is expected, as ERG cells are a self-renewing population (Rothenaigner et al, 2011). The downregulation of Notch target genes *her4.1* and *her4.3* is indicative of progenitor cells becoming neurogenic. Together, this differential regulation of *her4* and *foxj1a* may suggest that new ERG cells are being generated transiently before differentiation into their neurogenic progeny.

Other downregulated genes support the previous evidence that the ERG progenitors become neurogenic after injury. The mouse ortholog of *tfe3a*, Tfe3, has been shown to have a role in the maintenance of neural stem-progenitor cells in the embryonic mouse telencephalon (Yuizumi et al, 2021).

Interestingly, *mycn* has recently been shown to inhibit the survival of adult neuronal progenitor cells and to promote the generation of oligodendrocytes in the brains of adult mice. Hence, the downregulation of *mycn* in zebrafish may help to maintain the

ERG cell population as well as to help reprogramme the cells from an oligodendrocyte generating programme to a neurogenic programme (Chen & Guan, 2022). Similarly, the downregulation of *nfia* may also contribute to this reprogramming, as during mouse spinal cord development *nfia* controls the onset of gliogenesis (Deneen et al, 2006).

Two hes family transcription factors, *hes6* and *heyl*, are downregulated in the lesioned ERG population compared to the lesioned ERG population. *Hes6* promotes neuronal differentiation in *Xenopus* embryos (Koyano-Nakagawa et al, 2000) and in primary cultures of neural progenitor cells isolated from mouse embryos (Gratton et al, 2003). Similarly, *heyl* promotes neuronal differentiation of neural progenitor cells both *in vitro* and in the embryonic mouse brain. The difference in apparent roles of these genes in this dataset compared to the above examples is likely a result of the complexity of Notch signalling, as Hes genes are effectors of Notch signalling. It is already known that tight control of Notch signalling is important for the balance between the self-renewal and differentiation of neuronal progenitors (Chapouton et al, 2010).

The remaining downregulated transcription factors include both hox genes, *hoxb8a* and *hoxb9a*, whose spinal cord expression is well reported due to their role in conferring the axes identity to neurons (Charité et al, 1995; Graham et al, 1991). Their downregulation after injury may suggest an involvement in establishing spatial identity of newly generated neurons.

4.2.5 Cross-species comparisons of the response of spinal cord progenitors to injury

The regenerative ability of zebrafish is not shared by all organisms. Mammals do not have the same potential for regeneration and do not generate new neurons after injury, nor achieve functional recovery (with the recently reported exception of the spiny mouse (Nogueira-Rodrigues et al, 2021)). The creation and analysis of this dataset in the regenerating zebrafish, along with similar datasets in non-regenerative species such as *Mus musculus*, allows comparative analyses to be performed. Comparisons of similar cell types and their response to injury in different species could provide insight into the underlying gene programmes responsible for the success or failure of regeneration. With this in mind, I have compared the gene changes undergone in zebrafish ERG cells after injury to the gene changes undergone in comparable cell types in mice at varying time points post injury.

4.2.5.1 Mouse ependymal cells at three days post injury

Recently, Stenudd et al. performed single cell sequencing on spinal cord cells isolated from adult mice from two conditions: three days after a dorsal funiculus incision and uninjured age-matched mice (Stenudd et al, 2022). They used *Tnfrsf19* as a marker for spinal ependymal cells and captured around 2300 cells. Analysis of their dataset showed that the five biggest clusters have widespread expression of *Foxj1*. These clusters consist of 1226 cells from the lesioned condition and 716 from the uninjured condition. Using a Wilcoxon Rank Sum test, I compared these two sets of cells and found 3684 genes were significantly upregulated in the lesioned condition, while 1203 were significantly downregulated.

I also performed the same Wilcoxon Rank Sum test on the *foxj1a*+ positive clusters from our dataset (ERG cluster and proliferating ERG cluster). These clusters consist of 148 lesioned cells and 328 naïve cells and the differential expression test found 207 genes upregulated in the lesioned cells and 104 genes downregulated in the lesioned cells compared to the naïve cells.

To investigate how similar the response to injury is between the mouse ependymal cells and zebrafish ERG cells, I looked for genes which were significantly differentially regulated in one species after injury, whose ortholog was also significantly differentially regulated in the other species. This returned 129 sets of orthologs which were significantly different in both samples after injury. Of these, the biggest group of genes were those which were upregulated in both samples following injury. This group consisted of 60 genes (Figure 4.23 a, b). Gene ontology enrichment analysis was applied to these 60 genes to gain an overview of the shared pathways that both samples upregulated after injury. This analysis returned expected results such as ‘regeneration’ and ‘regulation of response to external stimulus’. It also gave some indication of the indication of other pathways involved in both species, including ‘Innate Immune System’ and ‘Interleukin-6 family signaling’ (Figure 4.23c). Interestingly, only two genes are significantly downregulated in both samples after injury: defender against apoptotic cell death 1 (*dad1*) and *mdh1* (*mdh1aa* in zebrafish; malate dehydrogenase 1). These genes are known to be involved in the control of cell survival via regulation of apoptosis (Brewster et al, 2000) and autophagy (New et al, 2019) .

While it is interesting to look at the conserved response to injury, it is perhaps more revealing to investigate the genes which are regulated in different directions following injury in a regenerating species compared to a non-regenerating species. In our two datasets, there were 39 genes found which were significantly upregulated in mice after injury but whose ortholog was significantly downregulated in zebrafish (Figure 4.23 a, b). It is therefore possible that these genes contribute to pathways which are detrimental to regeneration. Gene ontology enrichment reveals an overrepresentation of terms include those involved in membrane protein targeting, autophagy and glycoprotein metabolic processes (Figure 4.23d).

Conversely, 28 genes were found to be significantly downregulated in mice but upregulated in zebrafish (Figure 4.23 a-b). These genes may contribute to pathways which are beneficial to successful spinal cord regeneration. The enrichment of genes relating to ‘cell motility’ is indicative of the self-renewal of ciliated ERG cells in zebrafish and may suggest similar renewal of the ependymal cells in mice does not occur (Figure 4.23e).

Genes which code for transcription factors are likely to be those whose differential regulation after injury has the greatest overall effect on biological processes due to their ability to affect transcription of multiple other genes. I cross-referenced the list of 129 differentially regulated genes in both species against the database of transcription factors, AnimalTFDB 3.0 (Hu et al, 2019). This returned a list of 11 genes out of the 129 differentially regulated genes in both species which are transcription factors (Table 4.3).

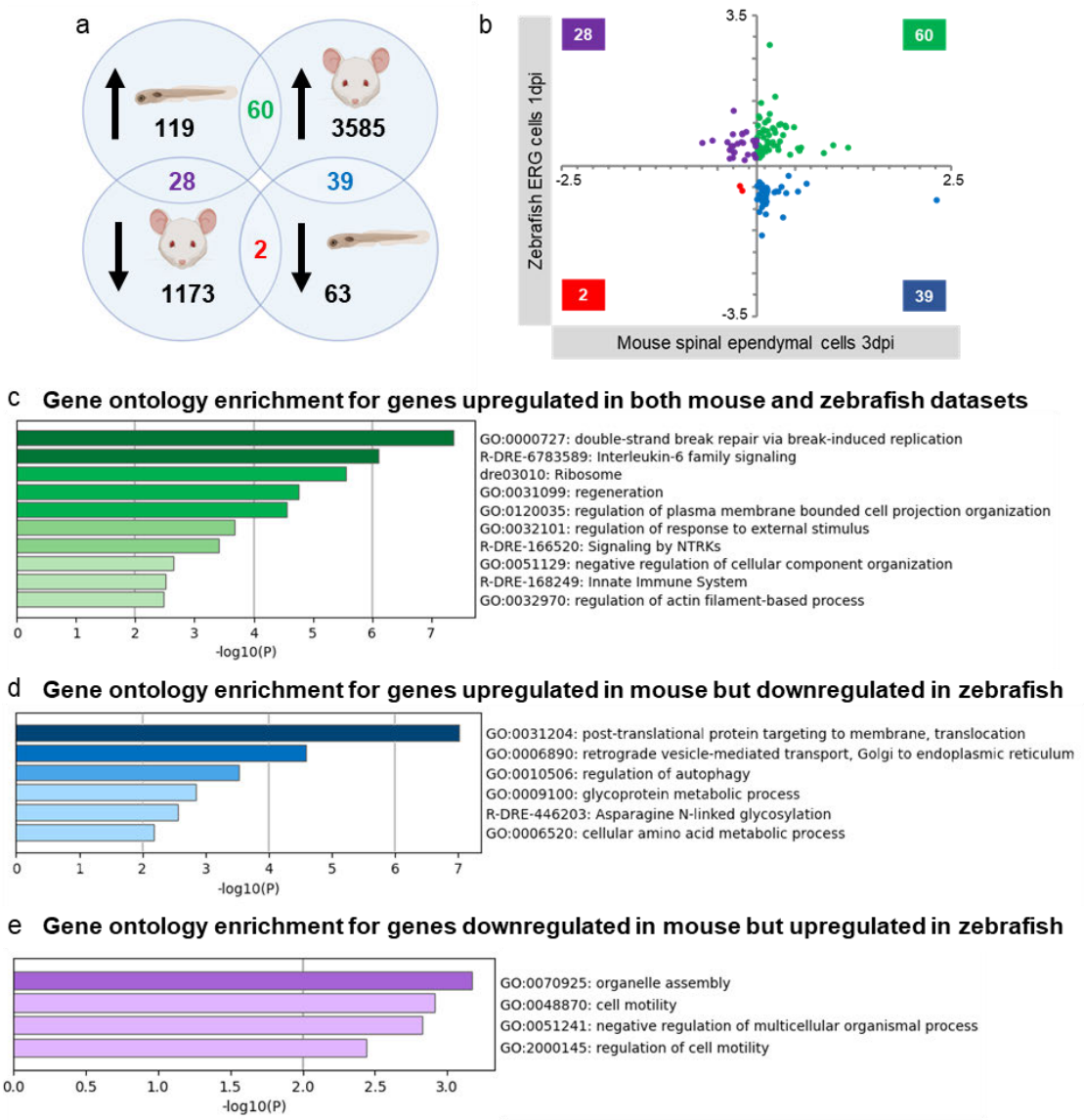

Figure 4.23 A comparative analysis of the injury response of zebrafish ERG cells 1dpi and mouse ependymal cells 3 dpi. A: A Venn diagram displaying the number of up- and down- regulated genes following injury in both datasets. The overlaps display genes whose orthologs are differentially regulated in both species. **B:** A quadrant scatter plot displaying all genes which are differentially regulated in both species following injury. Each point represents a gene and the axis and Log2(fold enrichment) for the mouse dataset and zebrafish dataset are displayed on the x and y axes respectively. **C-E:** Gene ontology analysis was performed on the sets of genes which were differentially regulated in both species. No ontology analysis was performed on the two genes which were downregulated in both datasets as the number of genes is too small.

Mouse gene	Zebrafish gene	Fold Change Mouse	Fold Change Zebrafish
Hes6	hes6	1.102	0.674
Hoxb9	hoxb9a	1.088	0.537
Ddit3	ddit3	1.054	0.556
Irf9	irf9	1.053	1.241
Tfe3	tfe3a	1.049	0.738
Fosl2	fosl2	1.039	2.759
Klf11	klf11a	1.031	0.701
Junb	junbb	1.025	2.173
Bcl6	bcl6ab	1.023	1.141
Cbfb	cbfb	0.980	1.202
Foxj1	foxj1a	0.880	1.669

Table 4.3: Transcription factors differentially regulated after spinal cord injury in mice (3 dpi) and zebrafish larvae (1 dpi).

Of these 11 transcription factors, none were strongly differentially regulated in either direction in mice. Of particular interest are *Fosl2* and *Junb(b)*, which are both upregulated in the zebrafish and mouse datasets, as both are involved in the AP-1 pathway. The upregulation of two transcription factors which play a role in the same pathway suggests that this pathway is particularly important in the response to regeneration in both mice and zebrafish.

4.2.5.2 Mouse ependymal cells at two and four weeks post injury

Another recent study investigated the response of Foxj1+ spinal cord cells to injury (Llorens-Bobadilla et al, 2020). In this study, the authors isolated cells from uninjured adult mice and those two weeks and four weeks after a dorsal funiculus incision. Separately, I compared the injury induced changes after two weeks and four weeks to the injury induced changes in our zebrafish dataset (1 dpi).

In the first instance, I compared the 895 cells from the mice at two weeks post injury to the 362 cells from the uninjured mice. Using a Wilcoxon Rank Sum test, I

compared these two sets of cells and found 871 genes which are significantly ($p < 0.05$) differentially regulated in the 2 wpi dataset compared to the uninjured dataset. As above, I compared the differentially regulated genes in the mouse dataset to the 311 differentially regulated genes in our ERG and proliferating ERG clusters in order to identify which gene responses are conserved between species and which differ between the regenerating zebrafish and non-regenerating mice.

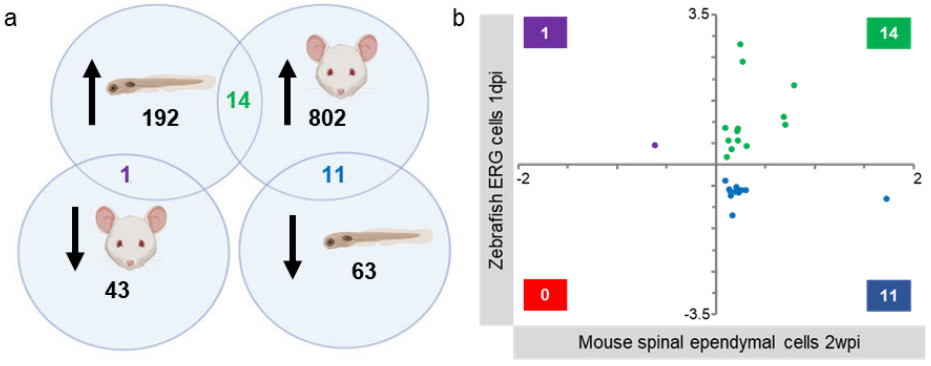

c

Mouse gene	Zebrafish gene	Gene name	Fold Change Mouse	Fold Change Zebrafish
Anxa2	anxa2a	annexin A2	1.188	7.048
Timp2	timp2b	tissue inhibitor of metalloproteinase 2	1.203	5.299
Apoe	apoeb	apolipoprotein E	1.732	3.628
Junb	**junbb**	**jun B proto-oncogene**	1.608	2.173
Socs3	socs3b	suppressor of cytokine signaling 3	1.626	1.914
Actg1	actb1	actin gamma, cytoplasmic 1	1.578	1.871
Lmna	lmna	lamin A	1.067	1.804
Nfkbia	nfkbiaa	nuclear factor of kappa light polypeptide gene enhancer in B cells inhibitor, alpha	1.169	1.786
Npdc1	npdc1b	neural proliferation, differentiation and control 1	1.161	1.712
cfap299	cfap299	cilia and flagella associated protein 299	1.165	1.472
Cotl1	cotl1	coactosin-like 1 (Dictyostelium)	1.090	1.469
Pierce1	si:ch211-248e11.2	piercer of microtubule wall 1	0.650	1.375
Gm10073	rplp1	ribosomal protein, large, P1	1.24	1.34
Rbms1	rbms1a	RNA binding motif, single stranded interacting protein 1	1.115	1.277
Fbxo36	fbxo36b	F-box protein 36	1.079	1.134
Gpr108	gpr108	G protein-coupled receptor 108	1.065	0.772
Creb3	**creb3l3l**	**cAMP responsive element binding protein 3**	**1.151**	**0.692**
Jtb	jtb	jumping translocation breakpoint	1.094	0.665
H3f3a	h3f3b.1	H3.3 histone A	1.195	0.664
H3f3b	h3f3b.1	H3.3 histone B	1.236	0.664
Copb2	copb2	coatomer protein complex, subunit beta 2 (beta prime)	1.103	0.648
Dap	dap	death-associated protein	1.146	0.642
Hmgn3	hmgn3	high mobility group nucleosomal binding domain 3	1.175	0.640
Ndrg3	ndrg3a	N-myc downstream regulated gene 3	1.107	0.606
Gfap	gfap	glial fibrillary acidic protein	3.307	0.573
Sulf2	sulf2a	sulfatase 2	1.120	0.438

Figure 4.24: A comparative analysis of the injury response of zebrafish ERG cells 1 dpi and mouse ependymal cells 2 wpi. A: A Venn diagram displaying the number of up-

regulated and down-regulated genes following injury in both datasets. The overlaps in the Venn diagram display genes whose orthologs are differentially regulated in both species. **B:** A quadrant scatter plot displaying all genes which are differentially regulated in both species following injury. Each point represents a gene-ortholog pair and the Log2(fold enrichment) for the mouse and zebrafish genes are displayed on the x and y axes respectively. **C:** A table of all gene-ortholog pairs in which both genes are differentially regulated. Fold changes are coloured based on upregulation (green) or downregulation (red). Genes highlighted in bold with grey backgrounds are transcription factors.

Interestingly, only 26 genes are differentially regulated in both species following injury (Figure 4.24 a, b). Of these, 14 genes are upregulated in both species, one is upregulated in zebrafish but downregulated in mice, and the remaining 11 are upregulated in mice but downregulated in zebrafish. No genes are downregulated in both datasets.

Due to the small number of genes found differentially regulated in both species, gene ontology enrichment analysis was not possible. Instead, all differentially regulated genes are listed in Figure 4.24c. Two of these genes encode for transcription factors: *Junb(b)*, which is upregulated in both zebrafish and mice, and *Creb3(l3l)* which is upregulated in mice two wpi but downregulated in zebrafish one dpi. *Junb* is a member of the AP-1 pathway involved in gene regulation in response to a range of cell processes, and has previously been linked to neurogenesis in developing Xenopus (Yoon et al, 2013). Interestingly, *Creb3* (also known as Luman) has a role in promoting axon outgrowth in cultured rat sensory neurons following injury, however the genetic mechanism for this has not been determined (Ying et al, 2014). It is also proposed to have an inhibitory role in astrocyte to neuron differentiation in cultured mice neural progenitor cells (Saito et al, 2012). Whether this applies to ERG cell to neuron conversions in zebrafish is unclear, but this would be supported by the downregulation of *creb3l3l* in the zebrafish dataset.

Within the same study, Llorens-Bobadilla et al. also sequenced Foxj1+ cells from mice four weeks post injury (Llorens-Bobadilla et al, 2020). After quality control, 992 cells remained in the lesioned condition, and their transcriptomes were compared to the 362 cells in the uninjured condition, using a Wilcoxon Rank Sum test. Overall, 3422 genes were significantly upregulated in the lesioned cells compared to the unlesioned sample, and 711 were significantly downregulated. Of these 4,133

differentially regulated genes in mice, 79 have orthologs which were also differentially regulated in zebrafish (Figure 4.25 a, b).

It is notable that the number of differentially regulated genes between the uninjured mice ependymal cells and the 4 wpi dataset is nearly five times the number of differentially regulated genes between the uninjured mice ependymal cells and the 2 wpi ependymal cells (871 differentially regulated genes 2 wpi, 4133 differentially regulated genes 4 wpi). Given that all experimental and statistical conditions are otherwise equal between the mice datasets, this suggests that the transcriptome differences undergone by ependymal cells in mice become greater with time. Due to the larger number of differentially regulated genes at 4 wpi, there is also a bigger overlap between these genes and those differentially regulated in zebrafish ERG cells after injury than there was at 2 wpi.

Looking at these overlapping gene orthologs and which pathways they participate in can reveal some commonalities between the two species at the different time points. Gene ontology enrichment analysis of the 42 genes upregulated in both datasets suggests that some of the pathways involved in both cell types are those responsible for apoptosis and regulation of neuronal death. Indeed, neuronal death is an important part of the early response to spinal cord injury to remove damaged cells. However, prolonged and extensive death of neurons in mice after injury is one of the factors leading to expansion of the lesion site during secondary degeneration (Crowe et al, 1997). Apoptotic cell death has previously been shown to peak at 24 hpi in adult zebrafish (Hui et al, 2014), but whether this timeframe is similar for larval zebrafish is currently unclear. Interestingly, some of the genes involved in autophagy are upregulated in the mice dataset but downregulated in the zebrafish dataset at this timepoint. Autophagy is also linked to regulation of cell death as it can prevent the apoptosis of unhealthy cells by instead digesting the damaged organelles. How the downregulation of autophagy related genes in ERG cells after zebrafish injury may contribute to their successful regeneration is not known. Interestingly, in 2021 Beckers et al. showed that inhibition of autophagy pathways in the injured zebrafish optic nerve results in accelerated retinal ganglion cell target innervation via a proposed role in axonal outgrowth (Beckers et al, 2021). This suggests that limiting autophagy after injury is beneficial to successful regeneration in zebrafish via its role in axonal regeneration. However, it is notable that the roles for cell death in neuronal cells is not necessarily directly related to the roles for cell

death in the ERG cell populations investigated here. The function and frequency of ERG cell death in healthy and injury conditions has not yet been investigated.

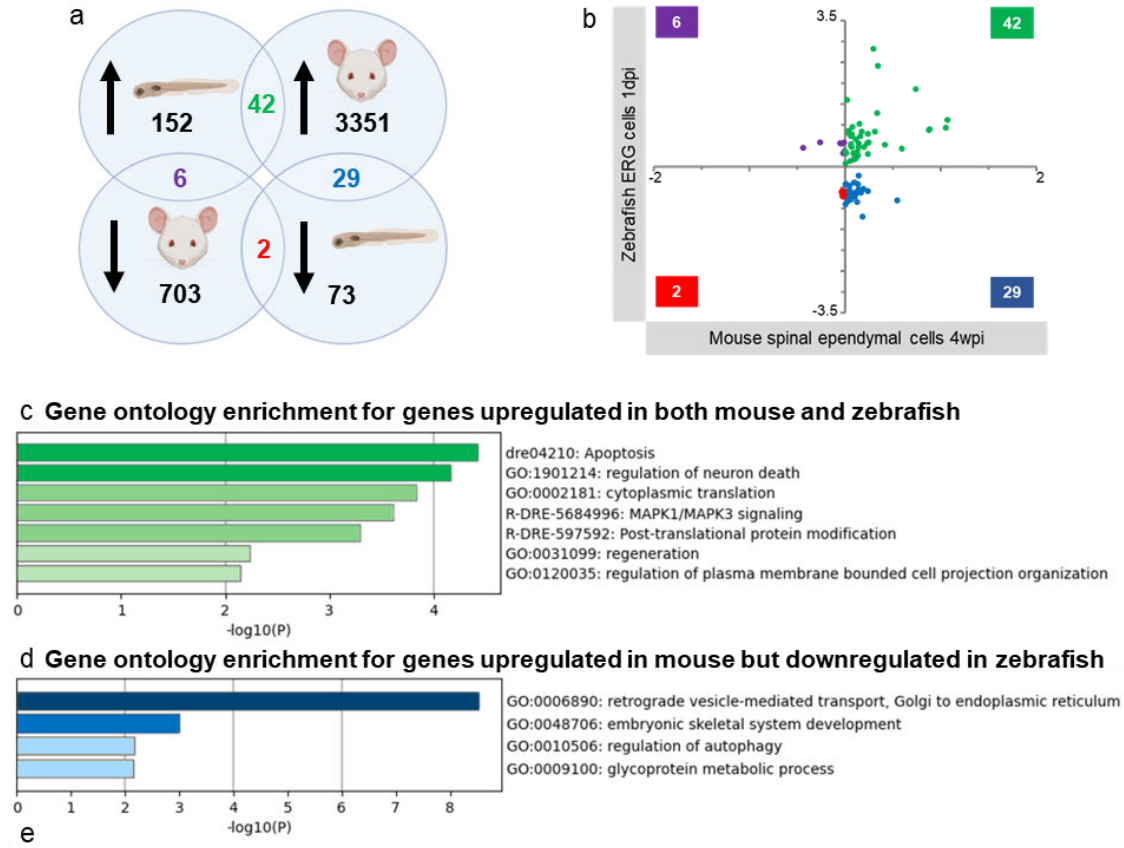

e

Mouse gene	Zebrafish gene	Gene name	Fold Change Mouse	Fold Change Zebrafish
Kpnb1	kpnb1	karyopherin (importin) beta 1	0.994	1.503
Rplp2	rplp2l	ribosomal protein, large P2	0.836	1.489
Jak1	jak1	Janus kinase 1	0.965	1.480
Pierce1	si:ch211-248e11.2	piercer of microtubule wall 1	0.738	1.375
Got1l1	got1l1	glutamic-oxaloacetic transaminase 1-like 1	0.999	1.298
Rnps1	rnps1	RNA binding protein with serine rich domain 1	0.984	1.244
Calu	calua	calumenin	0.984	0.658
Psat1	psat1	phosphoserine aminotransferase 1	0.989	0.615

Figure 4.25: A comparative analysis of the injury response of zebrafish ERG cells 1 dpi and mouse ependymal cells 4 wpi. A: A Venn diagram displaying the number of upregulated and downregulated genes following injury in both datasets. The overlaps in the Venn diagram display genes whose orthologs are differentially regulated in both species. **B:** A quadrant scatter plot displaying all genes which are differentially regulated in both species following injury. Each point represents a gene-ortholog pair and the Log2(fold enrichment) for the mouse and zebrafish genes are displayed on the x and y axes respectively. **C:** Gene ontology enrichment analysis was performed on the 42 genes which are upregulated in both datasets after injury. **D:** Gene ontology enrichment analysis was performed on the 29 genes which are upregulated in the mouse dataset after injury but whose ortholog was downregulated in the zebrafish dataset. **E:** The remaining genes which are differentially regulated in both datasets

are listed. Those highlighted in red are downregulated in the injured dataset compared to the uninjured dataset. Those highlighted in green are upregulated in the injured dataset compared to the uninjured dataset.

Other pathways found to be upregulated in mice but downregulated in zebrafish include retrograde transport from the Golgi to the endoplasmic reticulum (ER) and glycoprotein metabolism (Figure 4.25d). To some extent, these functions are likely interlinked as glycoproteins are synthesised in the ER and Golgi apparatus. It is not clear the specific role of retrograde transport after spinal cord injury in mice and zebrafish, however induction of the ER stress response after SCI has previously been reported in rats (Penas et al, 2007), and attenuation of this response in mice has been shown to improve functional recovery after SCI (Ohri et al, 2011).

The remaining genes which are differentially regulated in both datasets are listed in Figure 4.25e. Six of these are downregulated in mice but upregulated in zebrafish. No gene ontology enrichment analysis is performed on such a small number of genes. One gene which may point to a functional difference between the species is the downregulation of *Pierce1* in mice, and the upregulation of its ortholog in zebrafish. *Pierce1* has recently been identified for its role in motile ciliogenesis (Anujan et al, 2018), and this is consistent with the upregulation of *foxj1a,* which is also involved in cilia function (Hellman et al, 2010). It is interesting that genes involved in cell motility were also found to be enriched amongst the dataset of genes downregulated in mice at 3 dpi and upregulated in zebrafish (Figure 4.23e).

Finally, Table 4.4 lists all transcription factors which are differentially regulated in mouse ependymal cells 4 wpi and zebrafish ERG cells 1 dpi. It is notable than *Junb(b)* is strongly upregulated in all mice datasets looked at as well as in zebrafish ERG cells. In terms of transcription factors which are consistently regulated in opposite directions between species, *Creb3(l3l)* is upregulated in mice at both 2 wpi and 4 wpi but downregulated in zebrafish ERG cells at 1 dpi. *Hoxb9(a)* is also upregulated in mice, at both 3 dpi and 4 wpi, but shows strong downregulation in zebrafish ERG cells. These transcription factors which are consistently upregulated in the unsuccessfully regenerating mice cells but downregulated in the zebrafish ERG cells may provide some insight into the gene programmes which prevent successful regeneration in non-regenerating species.

Mouse gene	Zebrafish gene	Fold Change Mouse	Fold Change Zebrafish
Hoxb9	hoxb9a	1.002	0.537
Zfp395	znf395a	1.022	0.564
Creb3	creb3l3l	1.133	0.692
Glis3	glis3	1.039	1.092
Irf9	irf9	1.179	1.240
Junb	junbb	2.095	2.173

Table 4.4 All transcription factors which are differentially regulated in both the zebrafish ERG cells 1 dpi and the mouse ependymal cells 4 wpi are listed. Those highlighted in green are upregulated after injury, and those highlighted in red are downregulated after injury.

4.2.6 Data Availability

Unlesioned and lesioned *her4.3*+ datasets are available separately on ArrayExpress, accession code: E-MTAB-10390.

To allow easy exploration of the data for those without prior coding knowledge or specific software requirements, I have created and published an R shiny app. This app, which is publicly available at https://louisakdrake.shinyapps.io/beckerlab-her4/, allows users to input a gene symbol of interest and provides two main outputs based on the gene input. Firstly, the expression pattern of the gene on the combined naïve and lesioned tSNE plot is presented (Figure 4.26a). Secondly, the tSNE plots of the naïve and lesioned are presented individually, to allow users to compare the expression patterns of their gene of interest before and after injury. Accompanied by the comparative tSNE plots is basic expression data for their gene of interest in terms of fold change after injury and accompanying adjusted p-value (Figure 4.26b).

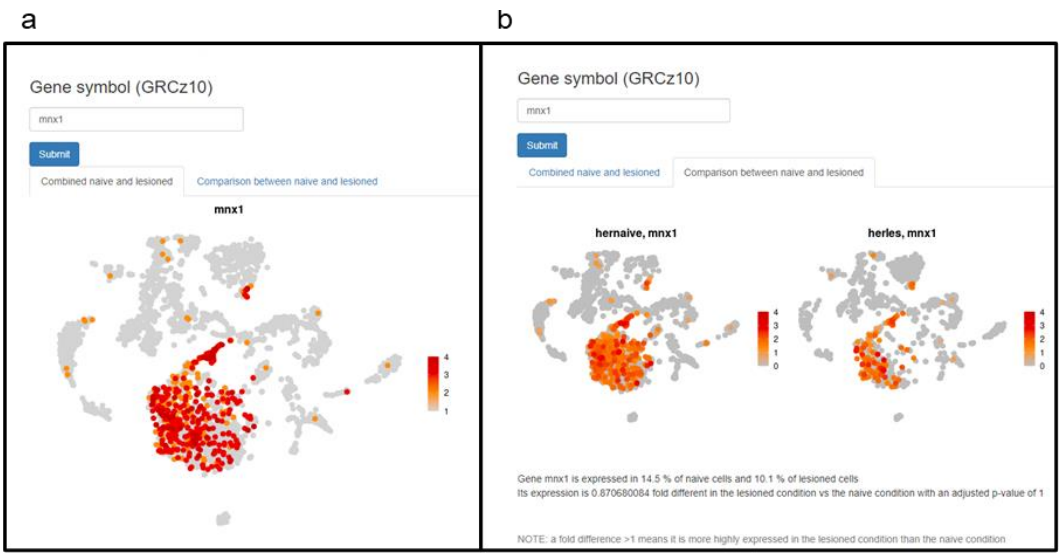

Figure 4.26 Screenshots of the app which allow exploration of the her4.3+ dataset. A: The default view provides expression data of the input gene in the tSNE plot of the combined lesioned and naïve datasets. **B:** The user can also access expression data for the gene input on the tSNE plots for the naïve and lesioned datasets separately. Global expression change of the input gene between naïve and lesioned samples is provided, along with the adjusted p-value calculated by Wilcoxon Rank Sum Test.

4.3 Discussion

In summary, I have performed single cell sequencing on *her4.3*+ cells isolated from the spinal cord of uninjured and injured zebrafish larvae. Following quality control and clustering of the cells, putative cell type identities were assigned to the clusters. Notably, a neurosecretory cell cluster was identified which comprises many more cells in the lesioned sample than the unlesioned sample. Comparisons of gene expression profiles of ERG cells from the unlesioned and lesioned samples helped to elucidate injury-induced changes in ERG cells. As well as an upregulation of regeneration associated genes in this population of injury, there is also evidence of immune system signalling. Finally, the gene expression changes undergone in zebrafish ERG cells at 1 dpi were compared to published mouse datasets of similar cell types. This revealed that the transcription factor *Junbb* was consistently upregulated in injured zebrafish and mouse datasets compared to their uninjured counterparts. Gene ontology enrichment analysis also revealed that genes involved in regulation of autophagy were consistently upregulated in mice but downregulated in zebrafish after injury. Conversely, genes upregulated in zebrafish but consistently downregulated in mice after injury were involved in cell motility.

4.3.1 Neurosecretory cells

One surprising finding from this dataset is the presence of the neuronal subpopulation putatively assigned as neurosecretory cells. These cells have an interesting combination of characteristics. Whilst they express pan-neuronal markers, no markers of specific neuronal subtypes (e.g motor neurons or interneurons) are strongly enriched. Instead, regeneration associated genes are highly enriched in this cluster, and the size of the cluster is much expanded in the lesioned condition compared to the naïve condition. Looking at the combination of genes enriched in this cell type, in particular the secreted molecules leptin (*lepa*), peptide yyb (*pyyb*) and secretogranin II (*scg2b*) may imply that these cells are neurosecretory cells. Neurosecretory cells have been identified in the spinal cord of zebrafish previously (Parmentier et al, 2006) as well as skates (Bennett & Fox, 1962) and eels (Morita et al, 1961), but not in mammals. Their function and physiology is not widely understood, nor their response to CNS injury reported.

While their identity as neurosecretory cells is one possibility, it is not a definitive assignment. One of the characteristics of neurosecretory cells in zebrafish is expression of peptides urotensin I and II, which are largely absent from our dataset. Furthermore, one of the most strongly enriched genes in this cluster, lymphocyte specific protein 1 (*lsp1*), does not easily fit into the narrative of neurosecretory cells. Another potential identity of these cells is neuroblasts. This is largely due to their expansion after injury, and the strong enrichment of regeneration associated genes including *gfap* and *atf3.* A neuroblast identity may also explain their expression of *pcna* but lack of *mki67* or other cell cycle markers; one explanation for this could be that these cells are postmitotic but have recently proliferated. However, the presence of neuronal markers e.g *snap25a* as well as the strong enrichment of secreted factors is not aligned with the neuroblast identity, and hence these cells are putatively assigned as neurosecretory cells.

Outside of characterising the gene expression of these cells, considerable *in vivo* work is in progress by other members of the Becker lab to confirm the presence of these cells in the regenerating zebrafish. Generation of transgenic reporter lines for these cells, e.g *pyyb*:GFP is underway which will confirm the presence of these cells before and after injury and help to determine if this is a transient or permanent cell type. So far, an injury induced population of *sall1b* positive cells has been identified using RNAscope near the lesion site but not in unlesioned fish (Claire Richmond,

unpublished data). In this dataset, the expression of transcription factor *sall1b* is specific to the neurosecretory cells. Further *in vivo* work includes manipulating some of the key genes using CRISPR/Cas9 and measuring the effect on regenerative neurogenesis. It would also be valuable to examine these cells morphologically as the previously reported neurosecretory cells have reported differences to regular neurons. They have a single, sometimes branching axon and a limited number of shorter dendrites from the soma. Notably, they have large electron-dense vesicles which act as storage for the peptides and hormones (Brown et al, 2013). Confirmation of whether the cells identified in this dataset display these same morphological features may help to cement their neurosecretory cell identity.

4.3.2 Trajectory analysis

Trajectory analysis was performed on the lesioned dataset to understand the progression of cells from ERG cells to differentiated neurons. This analysis also supports the putative identity of cluster 2 as neurosecretory cells rather than neuroblasts, as the cluster is positioned at the end of the trajectory, instead of between ERG cells and neurons as would be expected for neuroblasts. Interestingly, the neurosecretory cells are positioned after the interneuron clusters on the trajectory, suggesting the neurosecretory cells may be differentiated from interneuron cells.

While trajectory analysis is a useful tool, in the case of our dataset it should be considered only as a starting point for further experimental investigation. Trajectory predictions rely on the capture of intermediate cell states which can then be used to infer the progression of one cell type to another. Since our dataset captured minimal intermediate states, in particular between interneurons and neurosecretory clusters, the trajectory inference relies on more assumptions and the conclusions drawn are therefore less robust. For future trajectory inference, it would be optimal to have larger datasets including multiple timepoints in order to maximise chances of capturing transitionary cell states.

Lineage tracing *in vivo* could be used to confirm whether the differentiation trajectory presented in this chapter is a true representation of the biological differentiation pathway. This may involve live imaging of reporter lines which express different fluorophores under promoters for interneuron markers e.g *lhx5* and neurosecretory cell markers e.g *pyyb*. Reporter lines for interneurons e.g *lhx5*:GFP

and *pax2a*:GFP are already available (Gao et al, 2012; Picker et al, 2002; Turner et al, 2016), and the generation of reporter lines for neurosecretory cells is currently underway by other members of the Becker group. Time-lapse or live imaging would allow observation of these cells in normal conditions and after injury, and the sequential activation of different fluorophores in the same cell would clarify the differentiation trajectory.

4.3.3 Comparisons with mice ependymal cells

One of the benefits of the growing popularity of sequencing as well as the culture of open access of the subsequent datasets is the ability to compare gene responses in different conditions and even different species. Comparing gene responses between species can be valuable in identifying conserved and diverging pathways responsible for species-specific effects including successful functional regeneration. Notably, this approach has previously identified similarities in the responses of *ctgfa+ gfap+* glial cells in adult zebrafish to those of mouse astrocytes in a separate study in spinal cord injury (Klatt Shaw et al, 2021).

Whilst this comparative approach is valuable, there are also limitations to this approach as applied in this chapter. Ideally the compared datasets would consist of like-to-like samples. In practise this is rare, except when the comparative analysis is the aim of the original experiment and hence the experimental design facilitates this. In most cases, including this study, researchers instead make use of previously published datasets. In the case of the comparative analyses reported here, one result of this is the cell type captured may not be exactly equivalent in the datasets. While the zebrafish dataset uses the *her4.3* reporter to capture the ERG cells, the mice studies use *Tnfrsf19* and *Foxj1*. The discrepancies induced by these differences is minimised by the downsampling applied by selection of *Foxj1(a)* positive clusters for the comparison in both datasets. Nevertheless, the potential for differences based on the initial marker gene selection still exists. In particular, the comparison with the *Tnfrsf19* 3 dpi sample is less robust, since the authors report that *Tnfrsf19* is a marker for a specific subtype of ependymal cells. Whether this subtype is important in zebrafish is unclear, although the expression of this gene in the *her4.3*+ dataset is sparse and not specific to particular clusters (data not shown).

Another factor to consider when comparing responses to injury is which timepoints to include. This comparison used the datasets available at the time of analysis,

which consisted of the 1 dpi zebrafish dataset and mice datasets at 3 dpi, 2 wpi and 4 wpi. Ideally, further zebrafish datasets would be included so the time course of gene responses in zebrafish could be compared to the time course of gene responses in mice. One of the observations in the mouse dataset is that there are more differentially regulated genes at 4 wpi than there were at 2 wpi. Considering injuries in mice are non-regenerative and involve long periods of chronic injury this is unsurprising. Capturing further timepoints from regenerating zebrafish would allow us to investigate if the ERG cells in zebrafish revert back to the gene programme of uninjured fish soon after injury, or if this population is altered long-term as it appears to be in mice. Additionally, including further species in the comparisons would be interesting. For example, finding gene pathways which are shared between regenerating species such as zebrafish and *Xenopus* but divergent in non-regenerating species such as mice or rats would further implicate such pathways in successful regeneration. Indeed, a suitable dataset in regenerating *Xenopus* tadpoles is available (Pelzer et al, 2021) and could be utilised for this purpose, assuming the relevant differences in species and injury model are taken into consideration. The cells in the dataset from Pelzer *et al* are from the spinal cord, extracted during epimorphic regeneration of the amputated tail, in *Xenopus laevis* at 3 days post injury.

Overall, this comparative approach did reveal some interesting differences between mice and zebrafish which may play a role in their differing levels of neurogenesis after injury. For example, the upregulation of genes involved in motile ciliogenesis in zebrafish after injury but downregulation of similar genes in the mice samples may be notable. Since ependymal cells and ependymo-radial glial cells have motile cilia, this might suggest that while zebrafish ERG cells are successfully replenishing their ERG cells following injury, mice ependymal cells are consumed. For further value to be gained from similar comparative approaches, ideally samples would be taken at a variety of timepoints post injury in both species, and the initial cell selection should be as consistent as possible (for example, both samples should be isolated using the same marker gene).

Chapter 5: Tnf mediated signalling promotes neurogenesis from ERG cells

---

Some of the data in this chapter was published as:

Cavone, L.*, McCann, T.*, **Drake, L**.*, Aguzzi, E., Oprişoreanu, A., & Pedersen, E. et al. (2021). A unique macrophage subpopulation signals directly to progenitor cells to promote regenerative neurogenesis in the zebrafish spinal cord. *Developmental Cell*, 56(11), 1617-1630.e6.

*: Joint first authors

https://doi.org/10.1016/j.devcel.2021.04.031

5.1 Introduction

This chapter first uses the datasets characterised in chapters 3 and 4 to identify signalling candidates involved in injury induced neurogenesis. Receptor-ligand pairs are identified in which ligands are upregulated in response to injury in innate immune cells at the injury site and their corresponding receptors are upregulated in response to injury in ERG cells. One of these receptor-ligand pairs, *tnfa* and *tnfrsf1a*, is investigated experimentally to determine its role in injury induced neurogenesis. The *in vivo* work in this chapter has already been published with me as joint first author (Cavone et al, 2021). Some experiments included in this chapter were performed by my co-authors; where this is the case, it is explicitly indicated in the text.

5.1.1 Cell-cell communication after zebrafish CNS injury

The regeneration of neurons following injury depends both on intrinsic qualities of the neurons themselves and extrinsic factors from the environment surrounding the injury site. Intrinsic qualities include neuronal expression of regeneration-promoting genes and their subsequent proteins. For example, Gata3 is a transcription factor expressed in radial glial cells after injury and is required for their proliferation and subsequent neurogenesis in the zebrafish brain (Kizil et al, 2012b). Similarly, Foxm1 is expressed in *Xenopus* neuronal progenitors and is essential for regulating their

fate after tail amputation by promoting neuronal differentiation (Pelzer et al, 2021). Extrinsic factors include not only structural components of the injury site, but also molecular signals which may be detected by cells of the injury site and consequently promote successful regeneration. The most parsimonious source of these extrinsic signals is cells and tissues in close proximity to the injury site, either through normal tissue organisation or due to injury-induced cell influx.

External signalling from a variety of surrounding cell types has already been reported to promote injury induced neurogenesis. This includes both neuronal cells and non-neuronal cells. Pro-neurogenic signals from neuronal cells include serotonin and dopamine from descending axons in the spinal cord (Barreiro-Iglesias et al, 2015; Reimer et al, 2013). Additional neuron- and glia-derived neurogenesis promoting molecules include Fgf3 (Goldshmit et al, 2012; Goldshmit et al, 2018), Shh (Reimer et al, 2009) and Ctgf (Mokalled et al, 2016). Furthermore, Bmp1 signalling from neurons in the zebrafish telencephalon promotes neurogenesis from radial glial cells (Zhang et al, 2021).

The contribution of non-neuronal cells towards regenerative neurogenesis is also significant. Indeed, activation and proliferation of immune cells is among the first responses detected after a severe CNS injury in zebrafish (Martin & Feng, 2009). Kyritsis *et al.,* showed that inflammation is required and sufficient for enhancing neurogenesis in the zebrafish brain even in the absence of CNS injury, and that these inflammation-induced neurogenic programs are distinct from constitutive neurogenesis in the adult brain (Kyritsis et al, 2012). Similarly, after retina injury, microglia are necessary for retina regeneration, likely due to the signalling from microglia to Müller glia (Conedera et al, 2019). In the larval spinal cord after injury, immune cells contribute to neurogenesis as fewer new neurons are generated after pharmacological suppression of the immune system in the injured zebrafish (Ohnmacht et al, 2016).

Since one of the major roles performed by immune cells is release of cytokines, it is plausible that cytokines may be responsible for neurogenesis. Indeed, there is evidence for the involvement of specific cytokines and chemokines in regenerative neurogenesis. For example, chemokine receptors *cxcr4* and *cxcr5* are both expressed on radial glial cells in the zebrafish brain, and *cxcr5* was shown to regulate injury induced neuronal differentiation from activated radial glial cells (Diotel et al, 2010; Kizil et al, 2012a). In a zebrafish model of neurodegeneration,

Interleukin-4 is activated in neurons and microglia/macrophages and increases neurogenesis in the endogenous neural stem/progenitor cells via the Il4 receptor and STAT6 phosphorylation (Bhattarai et al, 2016). Intriguingly, Il4-STAT6 mediated neurogenesis appears to be specific to neurodegeneration and is not induced in lesioned brains, suggesting context dependent signalling axes between immune cells and neuronal progenitors.

5.1.2 Tnf signalling in neurogenesis

One cytokine signalling pathway implicated in regenerative neurogenesis is Tnf signalling. Tnf is already known to be involved in facilitating acute inflammation via its role as a pro-inflammatory cytokine. Indeed, it is involved in the recruitment of further immune cells (including additional macrophages) to the injury site (Vassalli, 1992). In mammals, the contribution of TNF to neurogenesis is highly context-dependent. In neonatal subventricular zone cell cultures from mice, TNF induces survival, proliferation and neuronal differentiation (Bernardino et al, 2008). On the other hand, *in vivo* exposure to TNF in postnatal mice resulted in impairment of hippocampal precursor proliferation and a depletion of neural precursor cells (Wang et al, 2018). Similarly, TNF increased astroglia number and reduced neurogenesis in two human neural stem/progenitor lines (Johansson et al, 2008). These differing results suggest the contribution of TNF towards neurogenesis is highly variable and may depend on species, cell type and developmental stage.

In zebrafish, there is some evidence to suggest that Tnf signalling leads to increased neurogenesis after injury. A role for Tnf signalling in neurogenesis has been revealed after retina injury in adult zebrafish. Dying retinal neurons produce Tnf which signal to Müller glia to re-enter the cell cycle via increased expression of *ascl1a* and *stat3* (Nelson et al, 2013). In zebrafish larval injured spinal cord, *tnfa* expression is strongly increased within 4 hours post injury, and remains increased above unlesioned levels for 72 hours or longer (Tsarouchas et al, 2018). Despite this, the role of Tnf signalling in regenerative neurogenesis after SCI has not yet been elucidated.

5.1.3 Tnf signalling pathway

Along with the specific roles in neurogenesis and axonal growth as described above, TNF signalling is responsible for a large array of cellular events, including immune response, apoptosis, cell senescence, cell growth and cell proliferation. This diversity of cellular events is possible due to the cascade of intracellular molecular

events which occur after binding of TNF to its receptors (TNFR1 and TNFR2) (see Figure 5.1 for schematic overview of TNF signalling). Following binding of TNF to its receptors, the receptors form trimers. In the case of TNFR1, this conformational change allows the adaptor protein TNFR1-associated via death domain (TRADD) to bind intracellularly. Subsequently, a variety of cellular cascades can be initiated. To initiate apoptosis, TRADD binds to another protein, Fas receptor-associated death domain (FADD), which begins a sequence of caspase signalling resulting in apoptosis. Alternatively, TRADD recruits TNF receptor-associated factor 2 (TRAF2) and the pathways leading to transcription factor activation are initiated. TRAF2 can also be activated directly by TNFR2 signalling without the recruitment of TRADD due to differences in the intracellular domains between the two receptors. Regardless, the pathways downstream of TRAF2 activation after binding of TNF to either receptor is shared.

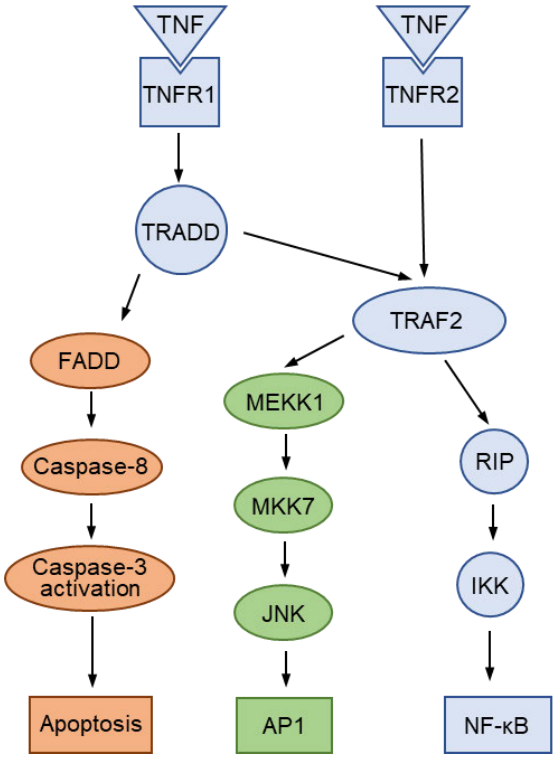

Figure 5.1: A schematic diagram displaying downstream signalling after TNF binding to its receptors TNFR1 and TNFR2. Figure adapted from (Aggarwal, 2003)

To activate the transcription factor NF-κB, TRAF2 recruits receptor-interacting kinase (RIP), which activates IκB kinase (IKK). IKK phosphorylates the inhibitory protein IκB which normally is found bound to NF-κB, and this leads to its ubiquitination and degradation (Wajant & Scheurich, 2011). Following the

degradation of IκB, NF-κB can translocate to the nucleus and promote the transcription of a large variety of genes, notably those involved in inflammatory and immune responses, cell survival, proliferation and differentiation.

The activation of transcription factor activator protein 1 (AP-1) is also initiated by TRAF2. TRAF2 sequentially recruits and activates MAP/ERK kinase kinase 1 (MEKK1) and MAPK kinase 7 (MKK7). This leads to Jun N2-terminal kinase (JNK) activation by phosphorylation. Phosphorylated JNK translocates to the nucleus and activates transcription factor c-Jun. The dimerization of Jun family proteins with Fos and ATF family proteins results in the transcription factor AP-1. The intricacies of AP-1 activation by TNF are discussed in detail in (Kyriakis, 1999). Following activation, AP-1 binds and trans-activates a large number of genes, hence it can mediate large scale gene expression changes.

In this chapter, receptor-ligand pairs which are upregulated after injury in the *her4.3* and *mpeg1* datasets respectively are identified. One of these pairs, tnfa-tnfrsf1a is then investigated experimentally and the knockdown of the receptor tnfrsf1a is demonstrated to reduce injury-induced neurogenesis.

5.2 Results

5.2.1 Receptor-ligand pairs upregulated in macrophages and ERG cells

It is hypothesised that in lesioned zebrafish, infiltrating macrophages promote neurogenesis by directly signalling to ERG cells. To investigate this, I used the lists of transcripts upregulated after injury in lesioned macrophages and ERG cells to identify receptor-ligand pairs which may be involved in this process.

While there is no published list of receptor-ligand interactions in zebrafish, a resource has been created compiling the known and putative receptor-ligand interactions in humans (Ramilowski et al, 2015). This resource consists of 2557 pairs compiled from five sources (Ben-Shlomo et al, 2003; Franceschini et al, 2013; Graeber & Eisenberg, 2001; Keshava Prasad et al, 2009; Sharman et al, 2013). Based on this, I created an equivalent list for zebrafish, where each human receptor-ligand interaction in the original resource was mapped to its zebrafish orthologs. Since there are often multiple orthologs for each human gene, the zebrafish receptor-ligand list consists of 5394 pairs.

I then refined the list to identify only pairs in which the ligand was significantly upregulated in the macrophage lesioned cluster compared to the unlesioned macrophage cluster, and which the receptor was significantly upregulated in the lesioned ERG cluster compared to the unlesioned ERG cluster. This resulted in a list of 10 receptor-ligand pairs (Table 5.1).

Zebrafish ligand	Ligand fold change	Zebrafish receptor	Receptor fold change
hbegfa	1.06	cd44a	1.08
hbegfb	2.00	cd44a	1.08
mmp9	1.97	cd44a	1.08
pkma	1.55	cd44a	1.08
vcanb	1.47	cd44a	1.08
il11b	1.24	il6st	1.60
m17	1.98	lifrb	1.49
gnai2a	1.32	s1pr5a	1.20
tnfa	1.13	tnfrsf1a	1.44
tnfa	1.13	tnfrsf21	1.76

Table 5.1: Receptor-ligand pairs where the ligand is significantly upregulated in the macrophage cluster after injury and the receptor is significantly upregulated in the ERG cluster after injury.

The nature of these lists, some of which are based on computationally predicted interactions of molecules, means some of the receptor-ligand pairs are not likely candidates for macrophage-ERG cell signalling in zebrafish. These include *gnai2a-s1pr5a*, *pkma-cd44a and tnfa-tnfrsf21*. Pyruvate kinase M1/2a (*pkma*) is a cytosolic enzyme involved in glycolytic processes and no secretion has been reported. Similarly, *gnai2a* is an intracellular protein involved in G protein signalling and is not reported to be secreted. Hence, the opportunity for macrophage derived *pkma* or *gnai2a* to interact with receptors on ERG cells is unlikely. Finally, the interaction between *tnfa* and *tnfrsf21* is reported by only one of the compiled receptor-ligand sources and is based on a combination of evolutionary genomics and sequence homology (Ben-Shlomo et al, 2003). Indeed, experimental evidence shows that TNF does not bind to TNFRSF21 in either human or mouse cells (Bossen et al, 2006).

Of the remaining seven pairs, *cd44a* is the receptor for four. Cd44 is a cell surface glycoprotein involved in cell-cell interactions, cell adhesion and migration. Inspecting

the gene expression of *cd44a* (Figure 5.2b) shows that even though it is significantly upregulated after injury, the number of cells expressing *cd44a* even in the lesioned conditions is very small (11 cells in lesioned ERG cluster express *cd44a*). Similarly, expression of its paralog *cd44b* is limited (4 cells in lesioned ERG cluster express *cd44b*) (Figure 5.2c). Based on this sequencing dataset and the low level of expression of *cd44a* and *cd44b*, *cd44a/b* are not considered top candidates for further manipulation. However, since single cell sequencing has high levels of dropout (Kharchenko et al, 2014), and because receptors may be able to amplify signals effectively without being themselves highly expressed, the function of Cd44 and corresponding ligands should not be entirely eliminated as possible mediators of immune cell to ERG cell signalling.

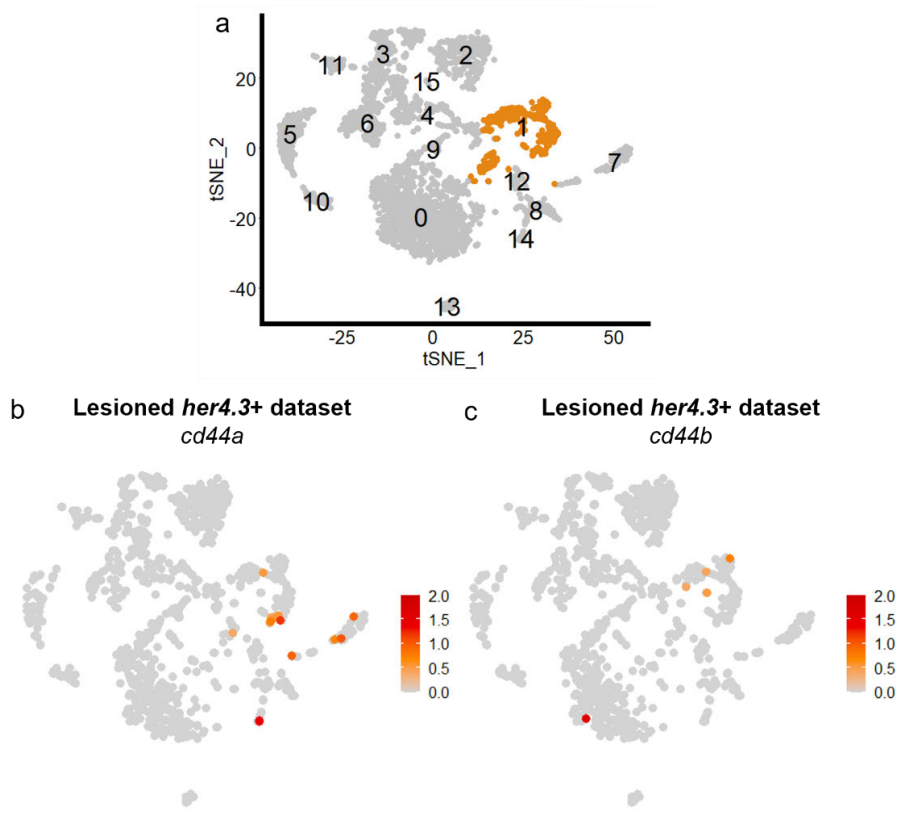

Figure 5.2: Expression of cd44a and cd44b in the lesioned *her4.3*+ dataset. A: tSNE plot highlighting the ERG cluster. **B-C:** Feature plot displaying the expression of *cd44a* and *cd44b* amongst the lesioned her4.3+ dataset.

Two of the receptor-ligand pairs*, m17-lifrb* and *il11b-il6st,* consist of members of the Il6 family. Both bind to receptor complexes including Il6st (also known as Gp130). The cytokine M17 (also known as Lif) binds to a receptor complex comprising of Lifrb and Il6st. Similarly, the cytokine Il11-b binds to a complex consisting of Il6st

and Il11r (Rose-John, 2018). While the gene *il6st* is strongly expressed and upregulated in the ERG cells after injury, *il11ra* is only expressed at low levels (only 19 cells in the lesioned ERG cluster express *il11ra*) (Figure 5.3f). Since the presence of Il11r is essential for Il11 signalling, the axis of Il11-Il6st signalling from macrophages to ERG cells is considered here to have less chance of making a strong contribution to injury induced neurogenesis. On the other hand, *m17* and its receptor components *lifrb* and *il6st* are both relatively strongly expressed and upregulated after injury (Figure 5.3b-d, Table 5.1) and hence it is a promising candidate for injury induced signalling from macrophages to ERG cells.

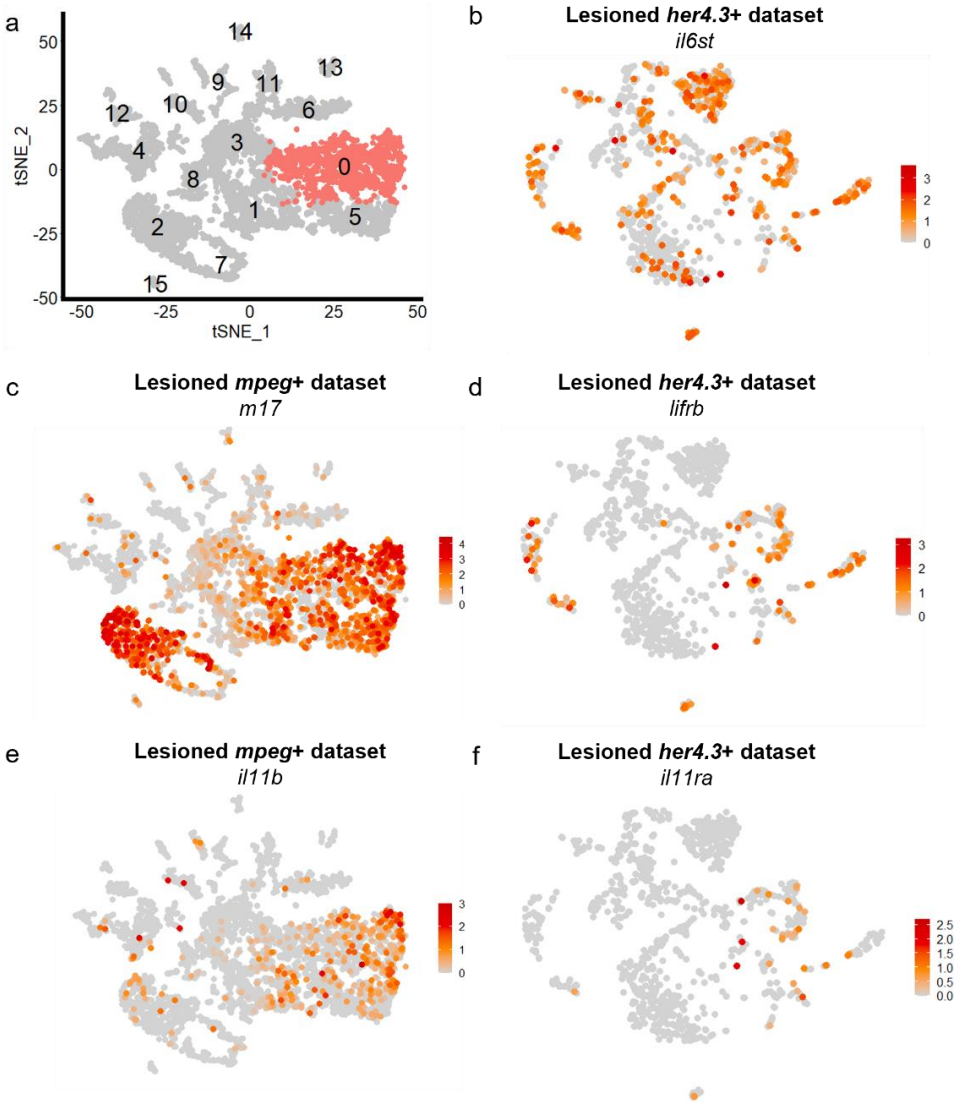

Figure 5.3: Expression of Il6 family genes in the lesioned datasets. A: A tSNE plot highlighting the macrophage cluster. **B:** Expression of *il6*st is widespread in the lesioned *her4.3*+ dataset, including in the ERG cluster. **C:** Expression of *m17* is strong in the

macrophage cluster, as well as in the neutrophils and microglia. **D:** The gene *lifrb*, which is the receptor for *m17*, is expressed amongst the lesioned ERG cluster. **E:** Expression of *il11b* is present amongst the lesioned macrophage cluster. **F:** Expression of *il11ra* is limited in our dataset.

Another strong candidate for signalling pathways between macrophages and ERG cells after injury is *tnfa-tnfrsf1a*. Its interaction is confirmed elsewhere *in vivo* (Bossen et al, 2006) and previous roles for Tnf signalling to Tnfr1 (*tnfrsf1a*) to promote zebrafish larvae fin regeneration has been reported (Nguyen-Chi et al, 2017). While Tnf can also bind to Tnfr2 (*tnfrsf1b*) (Bossen et al, 2006), no expression of *tnfrsf1b* was found in our lesioned ERG cluster. It is also notable that transcripts for the Tnf were not detectable within the *her4.3*+ dataset, suggesting absence of auto- or paracrine signalling within this population. As well as significant upregulation of *tnfa* and *tnfrsf1a* in the relevant populations after injury (1.13 fold and 1.44 fold respectively, Table 5.1), it is also important the gene of interest is widely expressed in the cell type. Figure 5.4 shows that macrophages have widespread expression of *tnfa* after injury, and similarly the lesioned ERG cluster has strong and specific expression of *tnfrsf1a*.

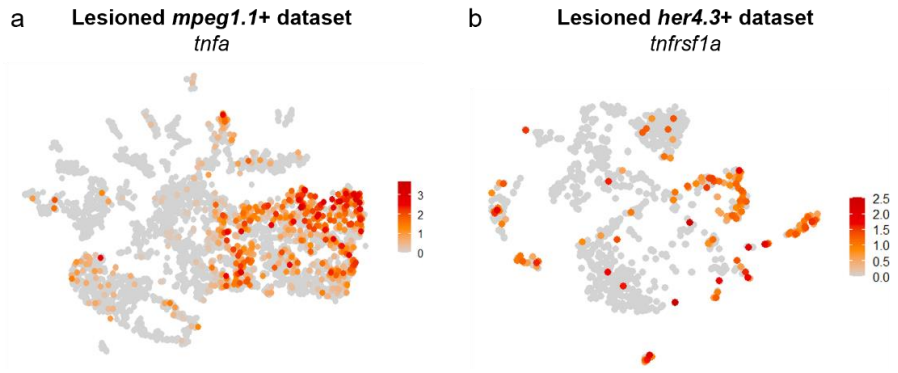

Figure 5.4: Expression of tnf family genes. A: *tnfa* is strongly expressed in lesioned macrophage cluster. **B:** One of the receptors for Tnfa, *tnfrsf1a*, is strongly expressed in the lesioned ERG cluster.

5.2.2 Receptor-ligand pairs upregulated in microglia and ERG cells

Since other immune cells were captured at the injury site, it is possible that these cells are also involved in signalling to ERG cells after lesion. In particular, large populations of microglia and neutrophils are present at the injury site.

To identify any receptor-ligand pairs involved in microglia to ERG signalling, I utilised the same receptor-ligand resource as described above to see if any of the

genes significantly upregulated in microglia after injury had a corresponding receptor which was significantly upregulated in the lesioned ERG cluster.

This approach returned five pairs of interest (Table 5.2). Three of these involve the *cd44a* receptor, which is only lowly expressed in our ERG cluster. The receptor ligand pair *m17-lifrb* is also identified here, suggesting this signalling pathway is not exclusive to macrophage-ERG cells. The final pair of interest is *fn1a-itga2.2* (fibronectin 1 – integrin α2 subunit). This supports a role for a physical interaction between microglia and ERG cells. Indeed, many of the microglia specific genes involve physical interactions with the ECM (discussed in chapter 3). However, the number of cells in the lesioned ERG cluster expressing *itga2.2* is low (10/126 cells) and therefore this ligand-receptor signalling axis is not likely to be a strong contributor towards neurogenesis.

Zebrafish ligand	Ligand fold change	Zebrafish receptor	Receptor fold change
fn1a	1.78	cd44a	1.08
mmp9	2.59	cd44a	1.08
vcanb	2.70	cd44a	1.08
fn1a	1.78	itga2.2	1.10
m17	1.78	lifrb	1.49

Table 5.2: Ligand-receptor pairs in which the ligand is upregulated in the microglia cluster after injury and the receptor is upregulated in the ERG cluster after injury.

5.2.3 Receptor-ligand pairs upregulated in neutrophils and ERGs

Similarly, I looked if any genes upregulated in neutrophils have a known receptor which is upregulated in the ERG cluster after injury. This returned seven pairs (Table 5.3), of which only *hsp90aa1.2-cftr* and *psen1-cd44a* are unique to the neutrophil-ERG axis. Since neither *cftr* nor *cd44a* are expressed in high numbers in our ERG cluster (*cftr*: 18/126 cells; *cd44a*: 11/126) neither of these pathways are considered likely to play a role in ERG response to injury.

Zebrafish ligand	Ligand fold change	Zebrafish receptor	Receptor fold change
hbegfb	1.18	cd44a	1.08
mmp9	1.89	cd44a	1.08
pkma	1.43	cd44a	1.08
psen1	1.08	cd44a	1.08

gnai2a	1.31	s1pr5a	1.20
m17	1.67	lifrb	1.49
hsp90aa1.2	1.51	cftr	1.86

Table 5.3: Ligand-receptor pairs in which the ligand is upregulated in the neutrophil clusters after injury and the receptor is upregulated in the ERG cluster after injury.

5.2.4 Downstream signalling in ERG cells

Following injury, ERG cells undergo massive transcriptional changes in order to generate new neurons. These downstream signalling processes can reveal information about the signalling pathway responsible for the activation of the cells. For example, *tnfaip2b* and *tnfaip6* are both significantly upregulated in the ERG cells after injury (1.99 and 1.59 fold respectively), suggesting a role for Tnf signalling (Figure 5.5).

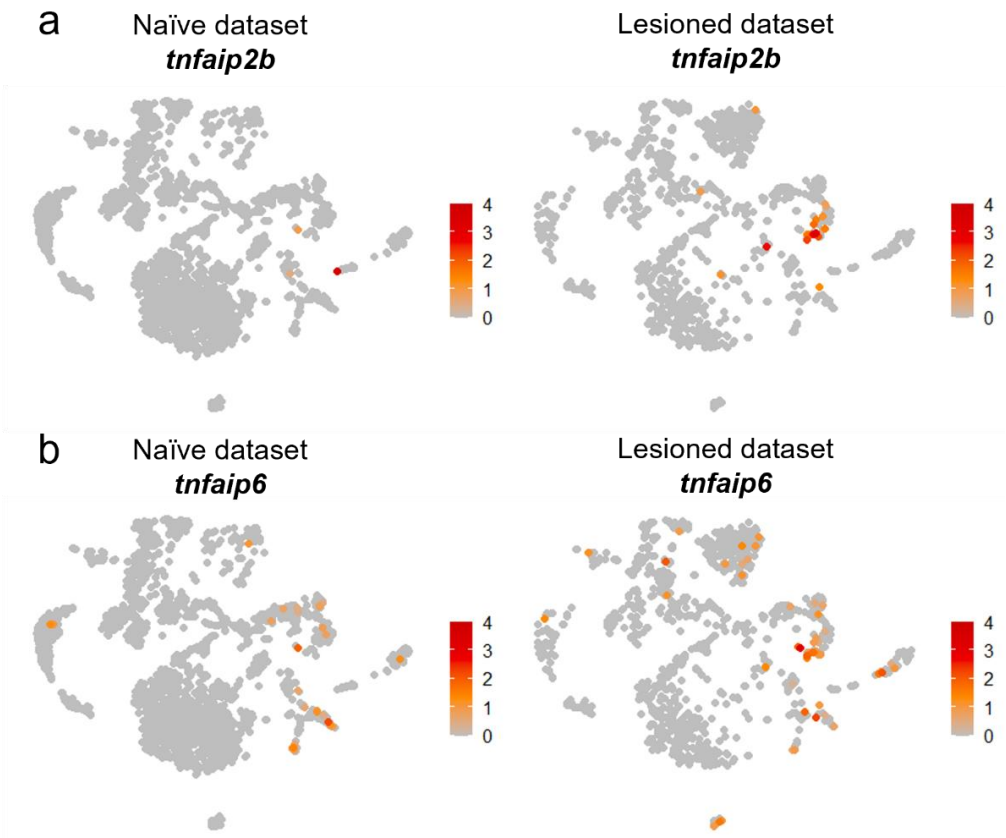

Figure 5.5: Expression of tnf induced genes *tnfaip2b* (a) and *tnfaip6* (b) is increased in lesioned ERG cells compared to unlesioned ERG cells.

It is also notable that two components of AP-1 signalling, *fosl2* and *junbb,* are amongst the most highly upregulated genes in the ERG population after injury.

Fosl2 is upregulated 3.01 fold in the lesioned ERG cells compared to the unlesioned ERG cells (rank 8), whilst *fosl2* is upregulated 2.08 fold (rank 28) (Figure 5.6). These encode the Jun-B protein from the JUN family and Fra-2 from the Fos family of proteins, which together can dimerise to form the AP-1 transcription factor. Whilst Tnf is well known for activating gene transcription changes via AP-1 signalling (Kyriakis, 1999), AP-1 activation can occur downstream of a plethora of cytokine and growth factor signals (Shaulian & Karin, 2001).

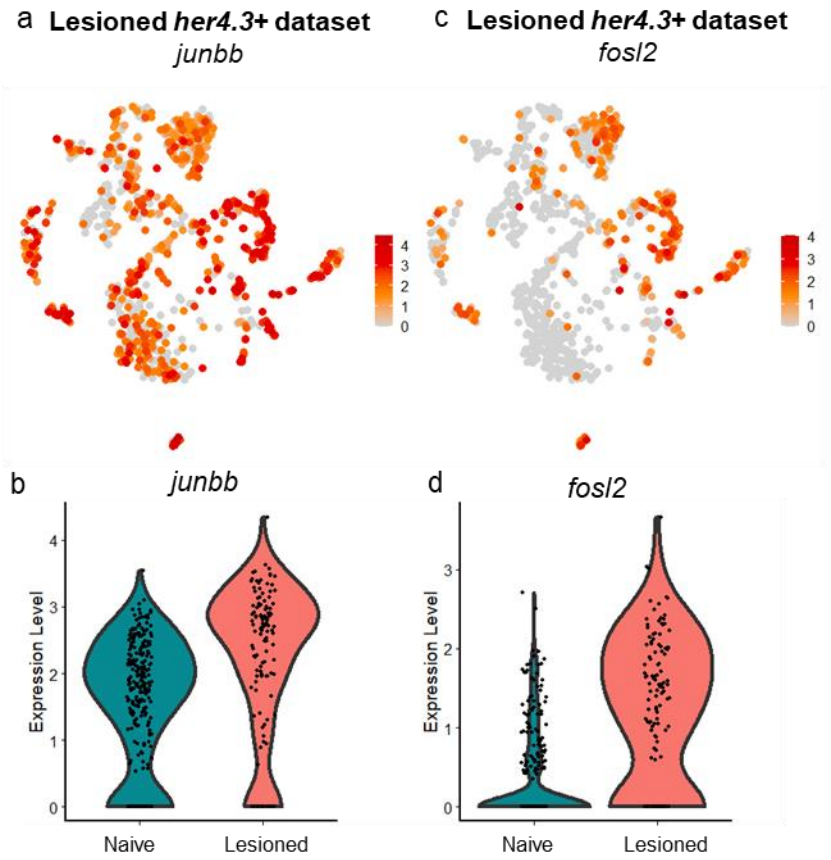

Figure 5.6: Expression of AP-1 protein components, *junbb* and *fosl2*, is present in ERG cells (a,c) and is increased after lesion (b,d).

To find out if other signalling pathways could be responsible for the upregulation of AP-1 components *junbb* and *fosl2* in the ERG cluster, the expression and upregulation of other receptors proposed to mediate AP-1 signalling (Gaiddon et al, 1996; Lau et al, 2016; Monje et al, 2003b; Persson et al, 2005; Shaulian & Karin, 2001; Sundqvist et al, 2020; Zeng et al, 2002) was investigated (Table 5.4). In total, 26 receptors were identified as expressed in the ERG cells, and six of these are expressed in a substantial proportion (30% or more) of the lesioned ERG cells. Of these six highly expressed genes, only two were also significantly upregulated in the

ERG cells after injury – *tnfrsf1a*, and *il6st*. Of note, *met* (receptor for HGF) is the only other receptor found to be upregulated after injury, although the overall expression is fairly low (18.3% of lesioned ERG cells express *met*).

Receptor	Percentage of lesioned ERG cells expressing this receptor	Significantly upregulated after injury?
il6st	61.1	Yes
met	18.3	Yes
tnfrsf1a	49.2	Yes
egfra	29.4	No
fgfr1a	24.6	No
fgfr1b	43.7	No
fgfr2	41.3	No
fgfr3	34.1	No
fgfr4	22.2	No
flt1	1.6	No
igfr1ra	4	No
igfr1rb	31.7	No
il11ra	15.1	No
il4r.1	31	No
kdrl	0.8	No
ntrk2a	4	No
ntrk2b	4	No
ntrk3a	11.1	No
ntrk3b	3.2	No
pdgfra	0.8	No
PDGFRB	2.4	No
tgfbr1a	3.2	No
tgfbr1b	5.6	No
tgfbr2	5.6	No
tgfbr3	0.8	No
tnfrsf1b	0	No

Table 5.4: Expression of receptors known to activate pathways involving AP-1 in the ERG cells. Six of these genes are expressed by more than 30% of lesioned ERG cells

(highlighted in green in column 2) and three are significantly upregulated in lesioned ERG cells compared to unlesioned ERG cells (highlighted green in column 3).

5.2.5 Candidates for immune cell to ERG cell signalling

Based on all the pairs identified in Tables 5.1-5.3, two sets of signalling pairs are likely candidates to participate in immune cell to ERG signalling after spinal cord injury. *m17-lifrb* is a promising candidate as *m17* is upregulated in all immune cell types investigated (macrophages, microglia and neutrophils) and the transcripts for both of the proteins in the receptor complex are upregulated in lesioned ERG cells (*lifrb* and *il6st*). Notably, although members of the *il6* signalling pathway have also been reported to activate AP-1 signalling in specific cell types (Leu et al, 2001), this is reported to be via the IL6-IL6ST receptor complex. Currently, M17/LIF signalling via LIFR/IL6ST complexes has not been reported to stimulate AP-1 signalling.

The other pair of interest is *tnfa-tnfrsf1a*. Since *tnfa* is upregulated in the macrophage cells but not widely expressed in microglia or neutrophils (Figure 5.4a), it is suggested to be specifically involved in signalling from the macrophages to the ERG cells. The activation of AP-1 signalling in the ERG cells also supports a role for Tnfa-Tnfrsf1a signalling, although it is likely other signalling molecules contribute to this signalling too. The contribution of Tnfa to neurogenesis after SCI is investigated experimentally in the upcoming sections.

5.2.6 Macrophages are found in close proximity to the lesioned spinal cord

In order for macrophage to ERG cell signalling to occur, it is necessary for macrophages to come into close proximity with ERG cells. To quantify the influx of macrophages and microglia, the number of *mpeg1*+ cells close to the lesion site was counted in injured larvae at 24 hpl. The corresponding area was counted in uninjured larvae of the same age. Frequently more than 20 *mpeg1*+ cells were found in the injured larvae, compared to only 1 or 2 in the equivalent uninjured spinal cord (Figure 5.7). This is complemented by direct immunolabeling of Tnf in close proximity to macrophages and motor neuron progenitors at the lesion site at 1 dpl (Cavone et al, 2021). The presence of macrophages in close proximity to the lesioned spinal cord but not the uninjured spinal cord supports the hypothesis that macrophages signal to lesioned progenitors in the spinal cord to promote injury-induced neurogenesis.

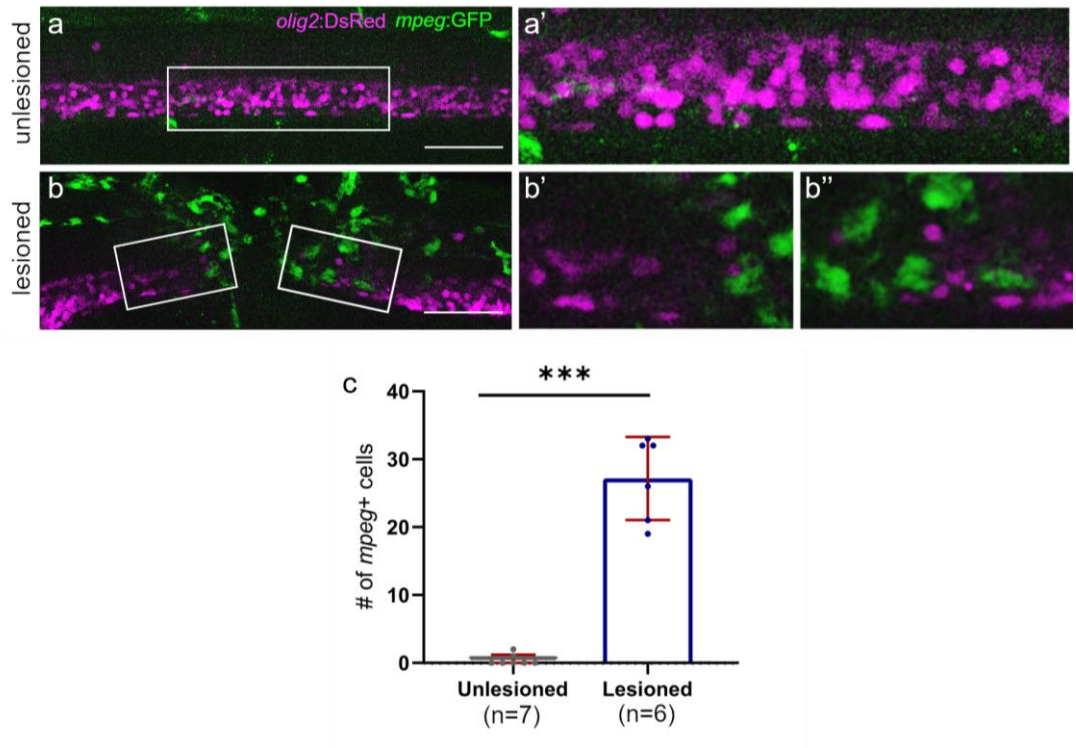

Figure 5.7: Macrophages and microglia cells accumulate at the injured spinal cord, but not the uninjured spinal cord. A, B: *mpeg1+* cells were counted within the area of interest (indicated with the white rectangles) and displayed separately to the right (marked with ‘ and ‘’). Lateral view of spinal cord is shown; rostral is left, dorsal is up**.** Scale bar is 50 µm**. C:** Quantification of *mpeg1+* cells in the selected regions, 140x40x40 µm, showed an increase d presence of *mpeg1+* cells in the vicinity of the *olig2+* cells of lesioned fish than unlesioned fish. Data shown as mean±SD, as a bar and scatter plot. N numbers shown on graph, each dot is a fish (Mann-Whitney U-test: P = 0.0012). Post-hoc power analysis: 0.99. Figure adapted from (Cavone et al, 2021).

5.2.7 Knockdown of *tnfrsf1a* reduces injury induced neurogenesis but not developmental neurogenesis

The injury induced upregulation of *tnfa* in the macrophage cluster, along with the upregulation of Tnf pathway genes in the ERG and the close proximity of *mpeg1+* cells and Tnf immunolabelling to ERG cells after spinal cord injury indicates a role for Tnf signalling after spinal cord injury. Work by colleagues has shown that both after acute somatic mutation and stable knock out of Tnf, neurogenesis is impaired (Cavone et al, 2021).

In order for Tnf signalling to be directly responsible for new neuron generation from ERG cells, the ERG cells must be able to detect Tnf. Based on the single cell sequencing dataset, it is proposed that ERG cells express the Tnf receptor Tnfr1

(encoded by *tnfrsf1a*) which allows the detection of Tnf and subsequent increase in neurogenesis.

To test the role of *tnfrsf1a* in regenerative neurogenesis, *tnfrsf1a* was mutated using Crispr/Cas9 mutagenesis. Four guide RNAs (gRNAs) targeting four separate exons of *tnfrsf1a* were designed initially, with the aim of identifying one or two efficient gRNAs. Since the guides were designed to target restriction enzyme recognition sites, the efficiency of the guides was tested by the success or failure of restriction enzyme digest, observed by gel electrophoresis of the DNA from eight injected embryos. Based on the resulting gels (Figure 5.8), the guides targeting exons 4, 5 and 7 all show reasonable efficiency. In order to reduce the chance of inducing off-target effects, it is recommended to co-inject a maximum of two guides (Keatinge et al, 2021). Since there is no clear difference in the efficiency of the gRNAs for exons 4, 5 and 7, the guides for exons 4 and 5 were chosen as their gels show clearer resolution, and early exons are generally considered more likely to disrupt resultant gene product function.

To investigate the effects of the knockdown of this receptor on injury induced neurogenesis, the two most efficient guides (targeting exons 4 and 5 of *tnfrsf1a*) were co-injected into 1 cell stage *mnx1*:GFP embryos. An equivalent number were injected with a control (nonsense) gRNA. A spinal cord lesion was inflicted at 3 dpf.

Following lesion, larvae were treated with EdU, which incorporates into newly proliferating cells. Larvae were left to recover for 48 hours, at which point the larvae were fixed and stained for EdU detection and GFP fluorescence. Larvae were whole-mounted and then the area near to the lesion site was imaged. Cells which showed co-localisation of the proliferation marker, EdU, and motor neuron marker, *mnx1*, are new motor neurons, generated after the application of EdU (and therefore generated after lesion). Larvae injected with *tnfrsf1a* gRNA displayed significantly fewer new motor neurons after injury than those injected with a control gRNA (Figure 5.9), suggesting Tnfr1 is involved in injury induced neurogenesis. This experiment was performed together with Elisa Pedersen, an undergraduate student who I was supervising in the lab.

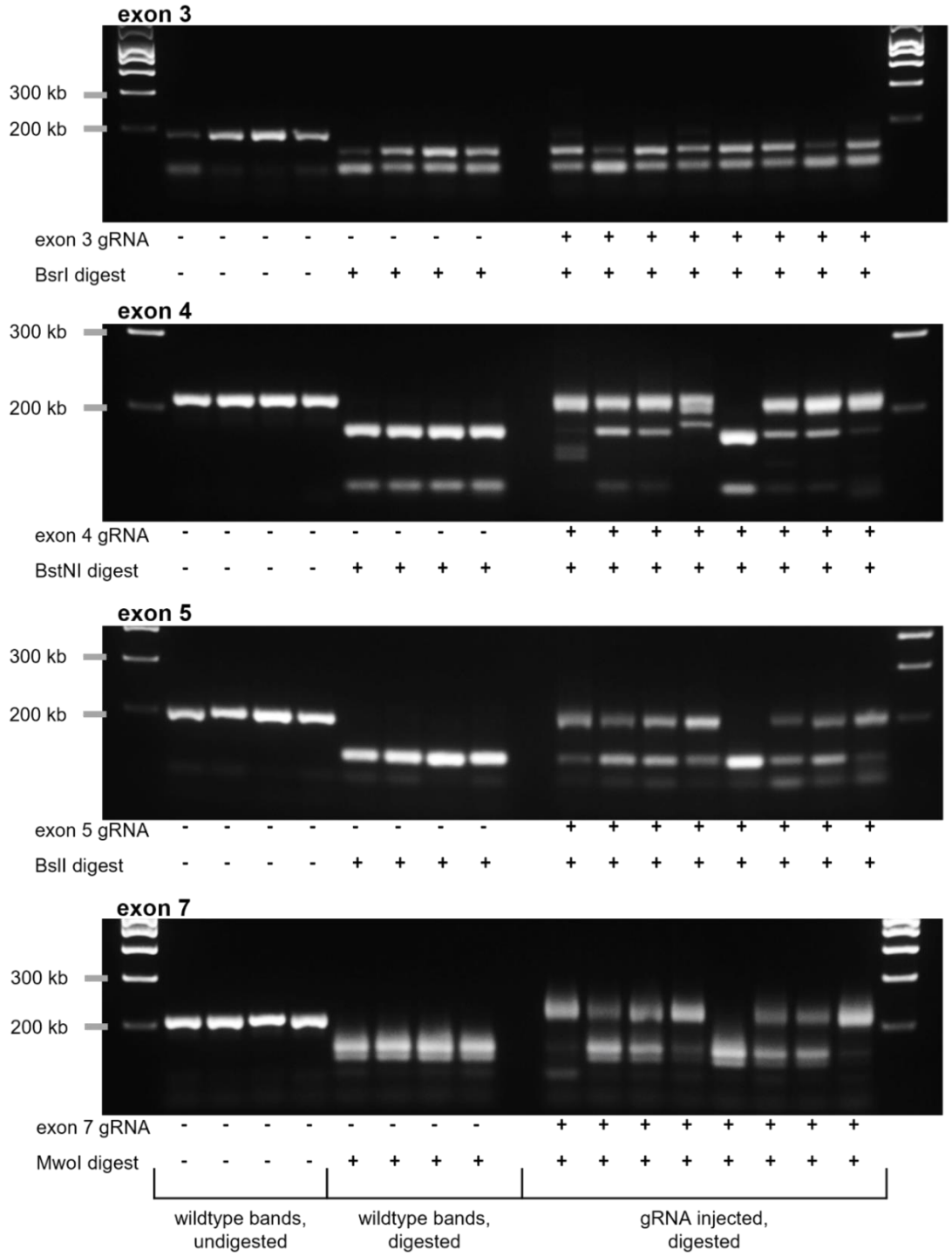

Figure 5.8: RFLP analysis to test the efficiency of four gRNAs targeting *tnfrsf1a*. The first eight lanes include DNA from uninjected larvae. Half of these samples are digested with the appropriate restriction enzyme. The latter eight lanes include DNA from injected larvae (four gRNAs co-injected), all of which have undergone restriction enzyme digest. The ratio of undigested to digested band in the latter eight lanes indicates the efficiency of the guide.

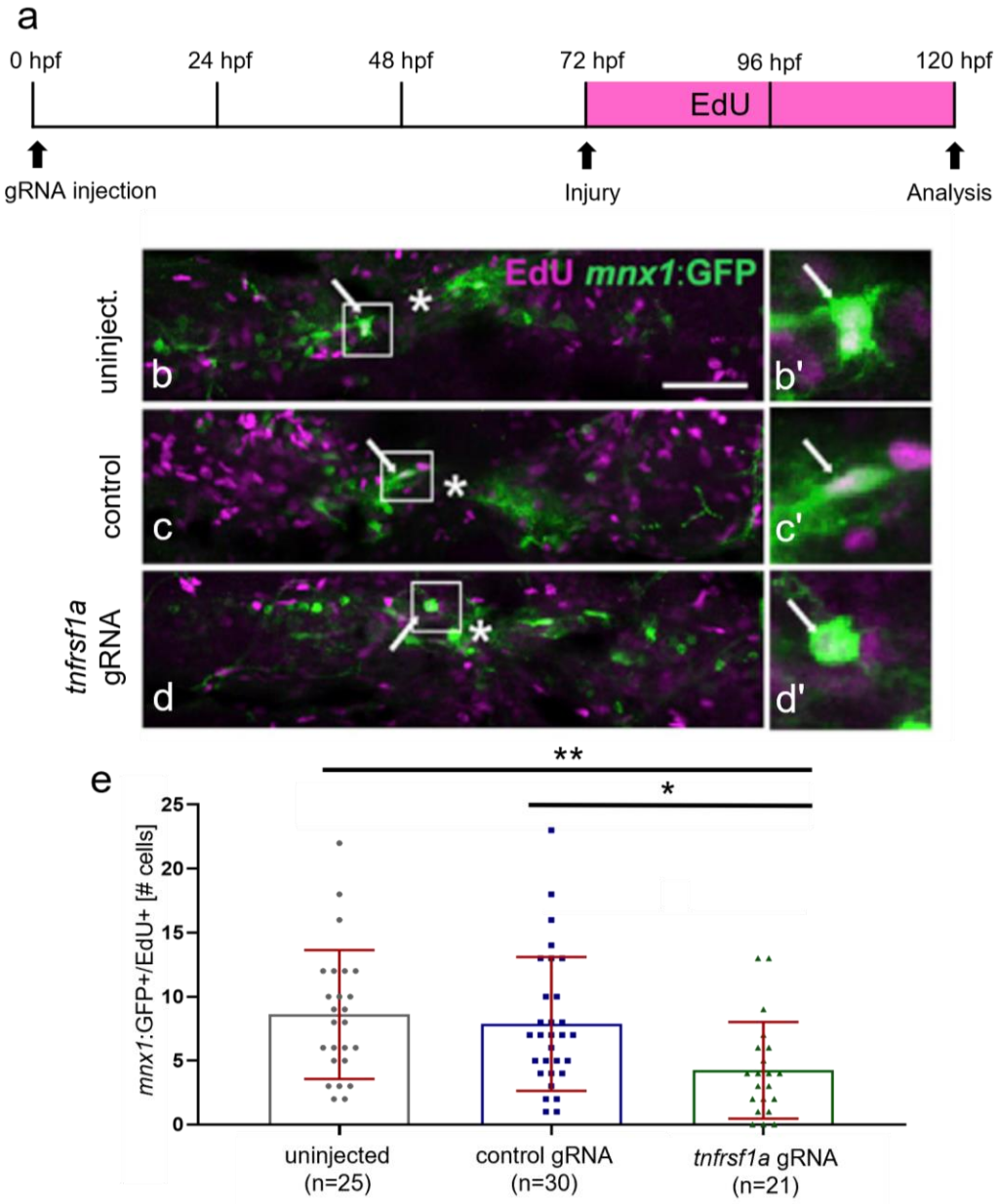

Figure 5.9: CRISPR knockdown of *tnfrsf1a* reduces injury induced neurogenesis. A: The experimental timeline is shown. **B-D:** Representative images showing EdU and *mnx1* positive cells. Lateral view of spinal cord is shown; rostral is left, dorsal is up. Site of lesion indicated with * and arrows indicate examples of cells which colocalise. Inset (‘) is higher magnification of area marked with white square. Scale bar: 50 µm. **E:** Number of colocalised cells within 300 µm of the lesion site in each larvae is displayed. Larvae injected with gRNAs targeting *tnfrsf1a* have fewer new motor neurons compared to control injected fish and uninjected fish. Data is shown as mean±SD, as a bar and scatter plot. N numbers shown on graph, each dot is a fish; 3 independent experiments. ANOVA and Tukey post-test, **P = 0.0085, *P = 0.026. Post-hoc power analysis: 0.94. Experiments and analysis performed with Elisa Pedersen under my supervision and figure adapted from .

To confirm whether the reduction in neurogenesis seen in *tnfrsf1a* knockdown larvae is due to the role of *tnfrsf1a* in injury induced neurogenesis as opposed to developmental neurogenesis, the number of new motor neurons in uninjured larvae over the same developmental timepoint was compared between *tnfrsf1a* knockdown larvae and control injected larvae. This showed no significant difference between the number of new motor neurons over this time period, as measured by number of cells with co-expression of *mnx1* and EdU (Figure 5.10). Hence, it is concluded that Tnfr1 is not involved in constitutive neurogenesis.

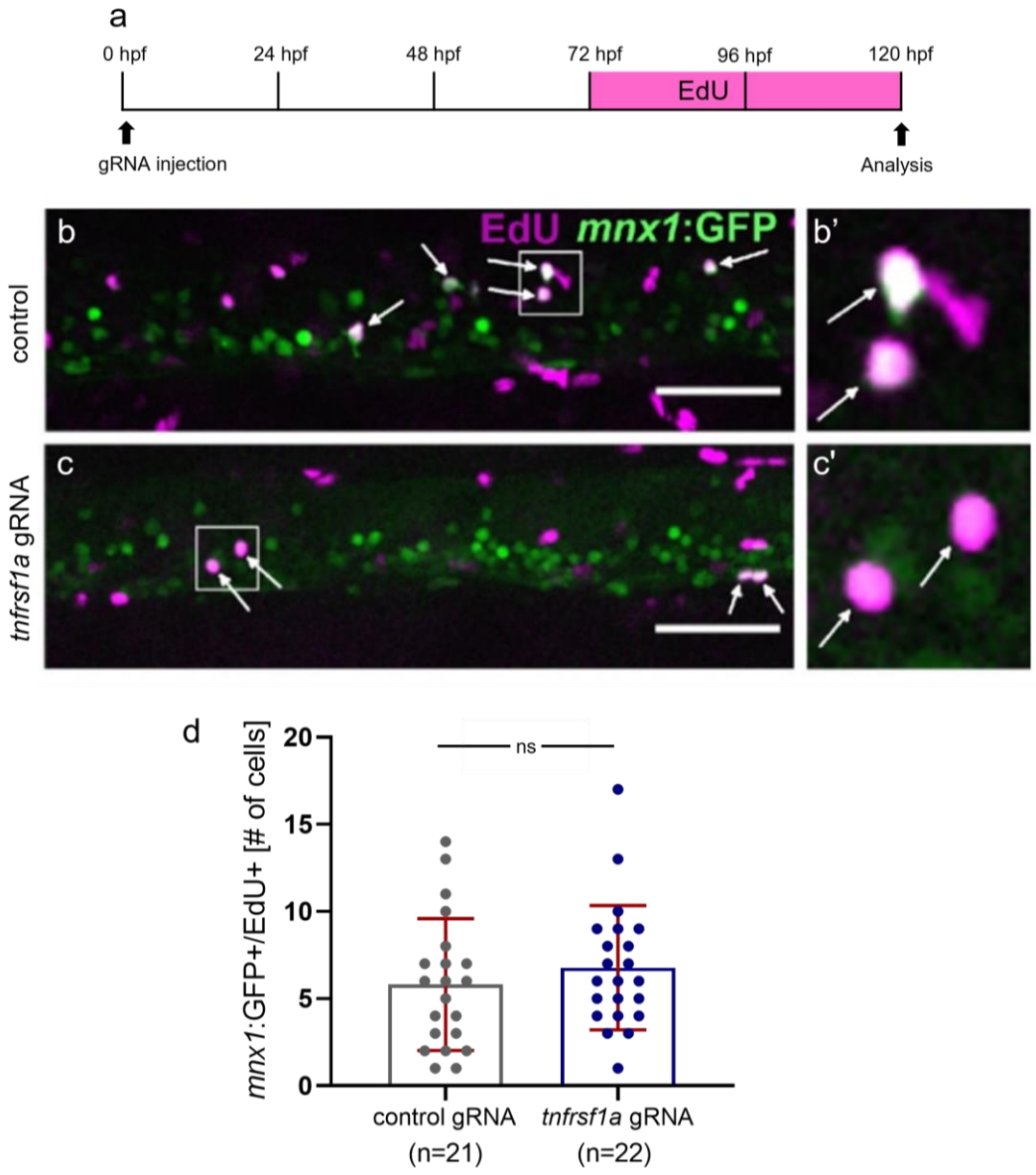

Figure 5.10: CRISPR knockdown of *tnfrsf1a* does not affect developmental neurogenesis. A: The experimental timeline is shown. **B,C:** Representative images showing EdU positive cells and expression of GFP. Lateral view of spinal cord is shown; rostral is left,

dorsal is up. Arrows indicate examples of cells which have expression of both *mnx1* and *EdU*. Scale bar: 50 µm. **D:** Number of co-localised cells is not significantly different in larvae injected with gRNAs targeting *tnfrsf1a* compared to those injected with control gRNA. Data is shown as mean±SD, as a bar and scatter plot. N numbers shown on graph, each dot is a fish; 3 independent experiments. Unpaired t-test, P=0.8001. Post-hoc power analysis: 0.89. Figure is adapted from (Cavone et al, 2021).

5.2.8 Overview

These experiments were my contribution to a larger study to show direct signalling from macrophages to ERGs via Tnf signalling (Cavone et al, 2021). Figure 5.11 summarises the overall study. After lesion, macrophages in the injury site produce Tnf. Genetic and pharmacological inhibition of Tnf resulted in decreased neurogenesis after spinal cord injury, and application of Tnf on *ex vivo* ERG cells resulted in an increase in readouts for neurogenesis in these cells. Tnf signalling is detected by ERG cells via Tnfr1, which increase their production of new neurons via AP-1 activation and regulation of histone deacetylase 1 (*hdac1*). Experiments using dominant negative *hdac1* and pharmacological manipulations of *hdac1* demonstrated the necessity of *hdac1* for regenerative neurogenesis downstream of immune system activity.

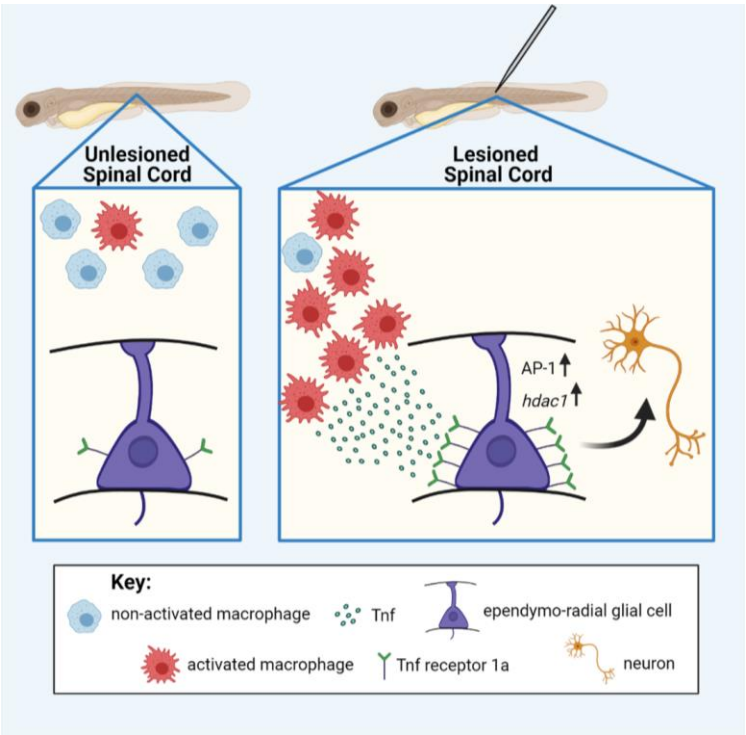

Figure 5.11: A graphical representation of the findings in this chapter and (Cavone et al, 2021) . Adapted from .(Cavone et al, 2021).

5.3 Discussion

5.3.1 Overview

In this chapter, receptor-ligand pairs are identified which are upregulated after injury in the lesioned spinal cord. This highlighted the Tnf-Tnfr1 signalling pathway as a potential signalling axis between macrophages and ERG cells to promote regenerative neurogenesis. Experimental manipulations of Tnfr1 demonstrated the involvement of this pathway in regenerative but not constitutive neurogenesis.

The overall findings of this chapter have contributed to elucidating a signalling pathway for regenerative neurogenesis as summarised above (Figure 5.11).

5.3.2 Receptor-ligand pairs

Early in this chapter, receptor-ligand pairs were identified by the criteria of the ligand being upregulated in specific *mpeg1*+ clusters after injury with the corresponding receptor upregulated in the ERG cluster after injury. These included *tnf-tnfrsf1a* signalling which was consequently demonstrated to be involved in regenerative neurogenesis. Other receptor-ligand pairs are also highlighted as potential signalling pathways by which immune cells signal to ERG cells after lesion. These have not yet been tested experimentally. Of note, *m17-lifrb* is a promising pair for future investigation into its role in neurogenesis. Indeed, Il6 family signalling was returned as a significantly enriched GO term amongst the upregulated genes after lesion in ERG cells in chapter 4 (Figure 4.22). In contrast to Tnf (whose expression is specific to the macrophage cluster), M17 expression is expressed widely in all immune clusters investigated (macrophages, microglia, and neutrophils), as well as being significantly upregulated in those populations. *lifrb*, along with its co-receptor *il6st*, are both strongly upregulated in ERG cells after lesion. Consequently, this pair is another promising candidate for receptor-ligand signalling from the immune system and may contribute to neurogenesis. In support of this, *il6st* knockdown by CRISPR results in fewer new motor neurons generated after injury (Themistoklis Tsarouchas, unpublished data), however since Il6st is a co-receptor for many Il6 family cytokines this does not directly implicate M17 involvement in neurogenesis. Futhermore, the mammalian ortholog of *m17*, leukemia inhibitory factor (*lif*) is necessary for injury-induced neurogenesis in the adult mouse olfactory epithelium due to its role as a stimulus for proliferation of neuronal progenitor cells after injury (Bauer et al, 2003). Interestingly, *m17* was induced in zebrafish retinal ganglion cells as early as 6 hpi

and activated the signal transducer and activator of transcription 3 (STAT3), although its role in axonal outgrowth not neurogenesis was investigated (Elsaeidi et al, 2014; Ogai et al, 2014). Additionally, functional recovery was significantly decreased in adult zebrafish after spinal cord injury with CRISPR/Cas9 mediated *m17* knockdown (Klatt Shaw & Mokalled, 2021). Hence, further investigation of M17 signalling from immune cells to ERG cells after SCI would be worthwhile. Initially, CRISPR/Cas9 knockdown of *m17*, as utilised previously (Klatt Shaw & Mokalled, 2021), could be used to measure the impact of *m17* signalling on the number of new neurons after SCI.

As well as *tnfa-tnfrsf1a* and *m17-lifrb* signalling, a variety of other receptor-ligand pairs were highlighted as being upregulated after injury in in their respective populations of interest. Besides from those dismissed due to biological properties (e.g proteins present exclusively intracellularly), some were dismissed due to their scarcity: whilst their expression was significantly upregulated, the number of cells expressing the transcript was small. This is true for *cd44a*, as several of its ligands are upregulated and highly expressed by immune cells after injury, but *cd44a's* transcript was found expressed in only 11 cells. However, it must be considered that the only timepoint examined was 24 hpi. It is possible that expression of *cd44a* is induced immediately after injury and hence mRNA production has decreased by 24 hpi, although the protein itself may be present in large numbers and involved in cell-cell signalling over this time period. Furthermore, single cell sequencing technology is not especially sensitive for lowly expressed transcripts and therefore it is possible that further cells express *cd44a*. Although resolving this question for *cd44a* would be fairly straightforward, for example by quantitative PCR from 0 hpi onwards, or through protein measurement such as western blot, this would not remove the possibility of other signalling receptors being excluded due to the 24 hpi timepoint. Designing and performing a single sequencing experiment looking at ERG cells covering an array of timepoints between 0-48 hours post injury is likely to reveal further signalling pathways involved in neurogenesis which are not identified in this chapter.

It is interesting that our dataset only highlighted a relatively small number of signalling pairs of interest, even when other immune cells were considered (microglia and neutrophils). It is possible that this reflects the true biology of the system: that few immune signals are detected by the ERG cells following injury.

However, another possibility is that signalling pairs were excluded by the criteria applied when compiling the lists of candidates for immune – ERG signalling. Genes were included based on their upregulation, rather than their expression. One disadvantage of this is discussed above: the inclusion of lowly expressed transcripts such as *cd44a,* which may not be expressed in enough cells to be of consequence. Additionally, this criterion excludes transcripts which may be highly expressed but not significantly upregulated after injury. This is particularly relevant for receptors, which may be stably present in high numbers without need for constant gene transcription as would be necessary for secreted molecules from immune cells. Hence, if one wishes to extract further possible signalling candidates it may be worthwhile to compile lists in which the ligand is upregulated after injury, where the corresponding receptor is highly expressed (by more than 50% of cells, for example) in ERG cells. This would detect further ligand-receptor pairs with potential signalling roles.

5.3.3 Tnf-Tnfrsf1a signalling

Tnf signalling is known to enact a plethora of responses, particularly related to inflammation. For example, inhibiting *tnfa* expression using *tnfa* gRNA increases neutrophil numbers at 24 hpi, and *il1b* mRNA is also increased more in *tnfa* gRNA injected fish at 2 dpi than control fish (Tsarouchas et al, 2018). Hence, it is difficult to be certain whether Tnf enacts its effects directly by signalling from macrophages to ERG cells, or via another more indirect mechanism. The decreased neurogenesis displayed after Tnfr1 knockdown implies at least some direct signalling is involved, however since the *tnfrsf1a* knockdown is not cell-specific the possibility of indirect signalling cannot be excluded. Some experiments performed by other group members and published in the same paper address this issue (Cavone et al, 2021). Purified *ex vivo* ERG cells respond to Tnf with upregulation of *hdac1* and *mnx1* mRNA, which are both critical for neurogenesis. Additionally, manipulations of the immune system and Tnf levels *in vivo* also correlate with *hdac1* expression in ERGs. Together, these experiments suggest that some of the effects of Tnf on neurogenesis are mediated by direct signalling. Additionally, since more than 90% of the Tnf+ cells at the lesion site are also Mfap4+ (Tsarouchas et al, 2018), it can be assumed that the source for the majority of the Tnf detected by ERG cells is released from blood derived macrophages.

In order for neurogenesis to occur, large scale gene expression changes must be induced in ERG cells. This is likely to occur by induction of transcription factor signalling by Tnf induced pathways. In this chapter we propose AP-1 is the likely transcription factor responsible for the induction of a neurogenic programme based on the upregulation of AP-1 components *junbb* and *fosl2* (Figure 5.6). Further experiments to support the role of AP-1 expression in Tnf induced neurogenesis was performed by my colleagues and reported in (Cavone et al, 2021). The application of AP-1 inhibitor SR 11302 completely abolished Tnf mediated upegulation of *hdac1* (used as a readout for neurogenesis) in *ex vivo* ERG cells.

Despite this, it is possible that other genes are also involved in the activation of AP-1. In this dataset, six receptors were identified to be widely expressed in the ERG cluster (Table 5.4). One of these receptors, Il6st, is also significantly upregulated in lesioned ERGs after injury. Members of the *il6* signalling pathway have also been reported to activate AP-1 signalling, although so far this has only been reported in liver cells (Leu et al, 2001). Interestingly, no specific link to AP-1 has so far been reported specifically for LIF-LIFRB signalling, which would be notable as LIF and LIFRB are strong candidates for additional immune to ERG signalling. However, *il6* ligand and secreted *il6* receptor are both expressed in lesioned mpeg datasets (data not shown), and although they are not significantly upregulated in response to injury, could nevertheless be involved in injury-induced neurogenesis. Interestingly, genes related to Il6 signalling were also upregulated in mice ependymal cells at 3 dpi (Figure 4.23), which may suggest a conserved response to Il6 between zebrafish and mice.

Chapter 6: General Discussion

The overall aim of this thesis was to identify signals from the innate immune system which promote neurogenesis from ERG cells after spinal cord lesion in larval zebrafish. To do this, the transcriptomes of *mpeg1*+ cells and *her4.3*+ cells from naïve and lesioned larvae were analysed in chapters 3 and 4 respectively. In chapter 5, ligand-receptor pairs were identified as potential signalling pathways between the *mpeg1*+ cells and the *her4.3*+ cells from lesioned larvae. One of the candidates, *tnfa-tnfrsf1a*, was investigated experimentally, and the CRISPR/Cas9 mediated knockdown of *tnfrsf1a* resulted in decreased neurogenesis after spinal cord injury. These results supported the hypothesis that macrophages signal to ERG cells to promote neurogenesis after spinal cord injury.

6.1 Quality control

Quality control of sequencing data, and particularly single cell sequencing data, is highly context dependent. The quality control metrics applied to the *mpeg1* dataset may be considered overly permissive. In particular, the criteria of <20% of the genes being derived from mitochondria in the *mpeg1* dataset is higher than standard recommendations of <5%.

The reason for choosing a higher threshold of mitochondrial fraction in the *mpeg1* cells is due to the biology of our cells of interest. Cells with high energy demands have elevated mitochondrial gene expression (AlJanahi et al, 2018). Immune cells generally have high energy requirements, and many of the functions of immune cells specifically involve mitochondrial processes, including phagocytosis (Park et al, 2011), efferocytosis (Wang et al, 2017b) and reactive oxygen species (ROS) production (Hall et al, 2013). While no studies have looked at the proportion of mitochondrial fraction in zebrafish, a systematic analysis recently found that human macrophages have an average of more than 10% of their transcripts derived from mitochondria (Osorio & Cai, 2020). This, combined with the distribution of our cells in Figure 3.3c, informed the decision to apply a permissive quality control boundary of 20%.

It is advised to reconsider quality control metrics after further processing of the data (Luecken & Theis, 2019). When looking at the mitochondrial fraction across all clusters of the *mpeg1* dataset (Figure 3.4c) it is reassuring that none of the clusters comprise cells with high mitochondrial fraction. This is one piece of evidence

suggesting that none of our clusters contain primarily dead or dying cells which could bias downstream analysis.

The mitochondrial cutoffs for the *her4.3* dataset applied here are less permissive. Here, the standard recommendations of <5% of transcripts being of mitochondrial origin was applied. The distribution of the mitochondrial proportion of each cell before quality control (Figure 4.2c) shows the majority of cells have a low proportion of mitochondrial reads. Additionally, after the 5% cutoff was applied, the distribution of cells and their mitochondrial fraction (Figure 4.3e) does not suggest a higher cutoff would be necessary. In accordance with guidelines, the basic analyses was re-performed using more permissive quality control but no major differences to clustering or downstream analyses were observed (data not shown). It is notable that published comparable single cell datasets use varied mitochondrial cutoffs, from around 5% (Klatt Shaw et al, 2021) (Cosacak et al, 2019) up to 20% (Lange et al, 2020). This highlights the need to decide quality control metrics on a case-by-case basis while maintaining transparency about the decision.

6.2 Developmental stage of experimental model

A major factor to consider regarding the findings in this thesis is the developmental stage at which the experiments were performed at. Since these experiments were performed at 3 dpf, there are some unique considerations regarding the physiology of the zebrafish at this point. One of these is the state of the immune system in zebrafish larvae, which is comprised of a functioning innate immune system but no adaptive immune system at 3 – 5 dpf.

The main advantage of larval zebrafish in this project is the presence of the innate immune system in isolation from an adaptive immune system. However the use of larval zebrafish does raise some unique difficulties. While the innate immune system is thought to be fully developed in zebrafish from 2 dpf, whether all cells can perform the full range of their potential functions so early is unclear. Additionally, due to the relative newness of zebrafish and zebrafish larvae as model organisms, the innate immune system has not yet been fully characterised. For example, the presence of natural killer cells in zebrafish is unclear. This dataset, which is openly accessible, will contribute to further understanding of populations and molecular signatures of immune cells in both the healthy and regenerating larvae. Indeed, it would be interesting to compare and contrast the cell types recognised in this dataset to the

capture immune cells in 5-6 dpf larvae captured by Rougeot et al. (Rougeot et al, 2019).

It is also important to consider the levels of constitutive neurogenesis occurring in larvae of 3 – 5 dpf. The larval zebrafish model is gaining popularity in terms of its use in investigating injury induced neurogenesis, as it is widely considered to have reached most fundamental milestones of spinal cord development by 3 dpf (Alper & Dorsky, 2022), although functional locomotor circuits are not established until 4 dpf (Buss & Drapeau, 2001). Indeed, the constitutive generation of neurons has been measured in zebrafish larvae at 3 dpf and was found to be at low levels both in *dbx1* expressing progenitors (Briona & Dorsky, 2014) and motor neuron progenitors (Ohnmacht et al, 2016). However, in this project, the number of proliferative motor neurons in unlesioned larvae (5 dpf) was substantial (Figure 5.11). This may suggest that developmental neurogenesis is still occurring at this timepoint and hence the single sequencing experiments described in this thesis may capture a mixture of injury-induced and developmental neurogenesis. This finding, if replicated elsewhere, would have implications for the use of 3 – 5 dpf larvae in studies investigating neurogenesis after SCI. In some cases this can be addressed by utilising controls to separate developmental and regenerative neurogenesis (as in this project). However, this is perhaps an unnecessary complication of using the larval model and it must be considered whether the benefits of the larval model (in particular the short experimental timeline) outweigh the disadvantage of the potentially parallel modes of developmental and regenerative neurogenesis in these juvenile fish.

6.3 Timepoint post injury

It is also relevant to consider the post injury timepoint sequenced. In this dataset, cells were isolated and sequenced 24 hours after injury. Based on previous work (Tsarouchas et al, 2018), we know that this is past the peak of neutrophil recruitment (2 hpi) and before the peak of microglia and macrophage recruitment (48 hpi) to the lesion site. Since large numbers of new neurons are detected by 48 hpi and larvae achieve functional recovery by this timepoint (Ohnmacht et al, 2016), it is assumed that much of the underlying cellular and molecular changes allowing this have occurred by this timepoint. Hence, 24 hpi was chosen as a timepoint where innate immune cells are present in high numbers (and likely actively

contributing to regeneration), and ERG cells are undergoing the changes necessary for neurogenesis.

However, this highlights an important limitation of this study, in that only a snapshot of the regeneration process is captured. Ideally, samples would be taken at a variety of timepoints, ranging from immediately following injury, to 48 hpi. This would allow further resolution of the pro and anti-inflammatory stages of immune response, as well as a more complete understanding of the changes undergone by ERG cells as they respond to the injury. Of particular interest would be the initial 6 hours following injury. Here, the macrophages undergo a rapid increase in numbers and likely gene expression changes, and ERG cells may begin their initial injury response.

6.4 Differential expression testing

One of the considerations of using single cell sequencing data to compare samples from different conditions is the choice of differential expression tests. Testing for differentially expressed genes, even in conventional bulk RNA-sequencing datasets, is a well- documented problem (Luecken & Theis, 2019; Scholtens & von Heydebreck, 2005). Single cell sequencing expression datasets have further technical challenges, such as dropout and high cell-to-cell variability (Hicks et al, 2018; Vallejos et al, 2017). A plethora of different tools are available to measure differential gene expression which all have different trade-offs between sensitivity, precision and computing power.

For all the comparisons in this project, the Wilcoxon Rank Sum test was used. This test is well regarded for giving robust results without requiring long processing times (Soneson & Robinson, 2018). Perhaps for these reasons, it is the most widely used differential expression test for single cell sequencing data (Squair et al, 2021). Despite this, it does have some flaws. In particular, one study has found it has a high false discovery rate – it incorrectly detects some genes as significantly differentially regulated (Squair et al, 2021). Hence, while the lists of differentially regulated genes are a good starting point for uncovering pathways involved in our dataset, it is important to consider that individual genes may be reported falsely as being up or downregulated between condition. By focusing instead on pathways where multiple genes are reported as differentially regulated, this risk is minimised. Additionally, differential expression testing is ideally used a starting point to identify genes which may be biologically important and worth validating by experimental

manipulation *in vivo*. In chapter 5, some of the genes identified as differentially regulated are investigated experimentally.

6.5 Innate immune cells

In chapter 3, the *mpeg1*+ cells isolated from naïve and lesioned zebrafish were characterised by single cell RNA sequencing. Whilst there is growing appreciation for the role of immune cells in regeneration, to my knowledge this was the first study to capture the transcriptome of immune cells in injured and uninjured zebrafish larvae to characterise their injury response.

Zebrafish larvae are becoming established as a useful system for investigating the innate immune system, due to work characterising the contributing cell populations (Mazzolini et al, 2020; Rougeot et al, 2019). The temporal separation of the innate and adaptive immune system in larval zebrafish means they are a powerful model for understanding innate immune responses in isolation from the more complex adaptive immune system. However, there is still much to be understood about the innate zebrafish immune system. The presence of eosinophils, dendritic cells and natural killer cells has been reported in adult zebrafish, but their developmental timeline in zebrafish is unknown, and their existence has not yet been reported in larval zebrafish. In chapter 3, a putative dendritic cell population is identified, based on the expression of *mhc2dab*, *cd74a/b* and *lamp3*. Further confirmation *in vivo* by morphological experiments may clarify their presence and potential role in the larval zebrafish before the maturation of the adaptive immune system. Interestingly, no eosinophil, natural killer cells or mast cells were identified within this dataset. Natural killer cells are derived from lymphocyte progenitors, hence even if these are present in larval zebrafish it would not be expected to capture these in the *mpeg1*:GFP dataset. Since our dataset extracted only GFP positive cells from *mpeg1*:GFP transgenic fish, it is still possible that eosinophils and natural killer cells are present in larval zebrafish, but if so, this dataset suggests that they are not derived from *mpeg1*+ progenitors. Similarly, mast cells have previously been reported to be present in larval zebrafish, but were not detected in this dataset, perhaps due to lack of *mpeg1* expression. This is unsurprising considering that *mpeg1* is considered to be specific to the macrophage lineage.

Intriguingly, neutrophils were captured in our dataset. The accepted dogma is that neutrophils do not express *mpeg1*. Indeed, in our dataset, there is no substantial expression of *mpeg1* in the neutrophil cluster. However, their presence in the

dataset indicates that they are GFP positive, and therefore it could be assumed that they recently expressed *mpeg1*, e.g they are derived from *mpeg1* expressing cells. Another possibility is that they are a contaminant cell population which bypassed FAC sorting and are therefore included in the dataset despite a lack of *mpeg1* expression. This would be consistent with the trajectory inference (Figure 3.18) in which no differentiation pathway existed between the captured HSCs and neutrophils. However, since a large population of neutrophils were captured, and because the presence of *mpeg1*+ neutrophils has previously been noted in zebrafish during cardiac and tail fin regeneration (Kaveh et al, 2020), the possibility cannot be discounted that these neutrophils are indeed derived from an *mpeg1*+ population. If this is the case, it would be interesting to investigate whether the entirety of the neutrophils in the lesion site are derived from *mpeg1*+ cells, or just a subset (as is found in (Kaveh et al, 2020)). This, combined with the capture of dendritic cells from *mpeg1*:GFP cells may suggest that the *mpeg1* transgene is expressed in progenitors to these cells, e.g common myeloid progenitors. To clarify this, lineage trajectory tools such as GESTALT or CellTag could be used to faithfully reconstruct the trajectories of these cell types (Biddy et al, 2018; Raj et al, 2018).

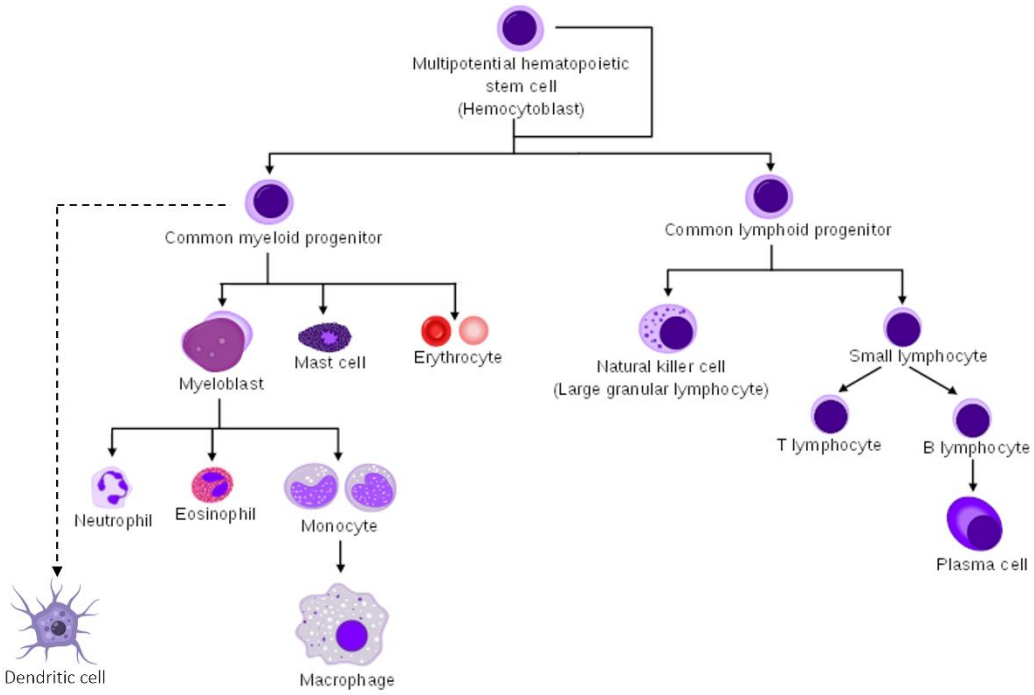

Figure 6.1: Ontogeny of the major cells in the immune system. Dendritic cells are displayed connected by a dashed line in lieu of the intermediary cell types. Figure adapted from original image by M. Häggström & A. Rad

The response of macrophages and microglia to injury were broadly similar. However, it was still possible to identify some differences. Macrophages showed increased expression of activation and secreted molecules. Microglia, on the other hand, upregulated genes relating to structural proteins including both cytoskeletal proteins and ECM proteins, as well as integrin signalling. This is congruent with our recent unpublished work in the lab which showed that microglia physically interact with astrocyte-like glial cells in the zebrafish larval brain to encourage wound healing, which is dependent upon microglia cytoskeletal dynamics (El-Daher et al, in preparation). Indeed, integrin signalling is reported to be specifically important for microglia dynamics (but not macrophage dynamics) after laser injury in larval brains, due to their roles in elongation of microglial processes towards the injury site and formation of phagosomes (Meller et al, 2017). Previous work in our group has shown that larvae which lack microglia have comparable axon regrowth across the lesion site to wildtype larvae (Tsarouchas et al, 2018), but do have reduced neurogenesis (unpublished data; Anna Underhill, MSc thesis). Whether this effect of microglia on neurogenesis can be fully explained by changes in microglia dynamics and ECM changes is unclear. Alternative ways in which microglia could induce neurogenesis include cytokine signalling (as reported by (Kanagaraj et al, 2022) in the zebrafish telencephalon) and/or phagocytosis of inhibitory debris.

6.6 Ependymo-radial glial cells

In chapter 4, the transcriptome of ERG cells from the naïve and lesioned spinal cord were characterised. Cell populations corresponding to ERG cells, oligodendrocytes, motor neurons and interneurons were identified based on enrichment of specific genes.

One particularly intriguing finding from this dataset was the existence of putative neurosecretory cells, which exist in much larger numbers in the lesioned dataset than the unlesioned dataset. They were assigned neurosecretory cells identity due to their expression of some unspecialised neuronal markers, along with strong enrichment of some secreted molecules. Indeed, neurosecretory cells have been previously noted in the spinal cord of adult zebrafish (Parmentier et al, 2006). More work is required to confirm whether the cell population recognised after injury in larval zebrafish is the same population assigned as neurosecretory cells in adult uninjured zebrafish, although due to the lack of urotensin II expression and substantial absence of this cell type in our uninjured larval zebrafish it is likely these

are two separate cell types. Interestingly, a leptin expressing population of neuronal cells has been identified by three separate groups after tail amputation in *Xenopus* (Aztekin et al, 2019; Kakebeen et al, 2020; Pelzer et al, 2021). In all cases, this leptin expressing population is virtually absent in the uninjured *Xenopus* tail and immediately after injury but is abundant at 24 hours post amputation and later. It is significant that this leptin expressing neuronal population is present even in regeneration-incompetent *Xenopus*, therefore its presence in *Xenopus* after tail amputation is not sufficient for regeneration. More research to understand this cell population in the regenerating zebrafish is currently being undertaken by other members of the Becker group.

6.7 Immune cell to ERG signalling

Whilst it had been previously established that immune system activation promoted neurogenesis, it was not clear whether this was due to direct immune cell signalling to the ERG cells, or through activation of known developmental signalling pathways. In chapter five, receptor-ligand pairs were identified in which the ligand was upregulated in the immune cells after lesion and the receptor was upregulated in the ERG cells after lesion. It was hypothesised that these were signalling pathways by which immune cells could stimulate neurogenesis after spinal cord injury. One pair identified, *tnfa-tnfrsf1a*, was tested experimentally, and the knockdown of *tnfrsf1a* using CRISPR/Cas9 suggests that this pathway is involved in injury-induced neurogenesis. Indeed, other experiments by colleagues targeting other stages of the *tnfa-tnfrsf1a* pathway showed direct signalling between Tnf-producing macrophages and ERG cells to stimulate neurogenesis.

Other possible signalling candidates were also identified in this chapter. In particular, *m17* was upregulated in macrophages, microglia and neutrophils after injury and its corresponding receptors, *lifrb* and *il6st,* are both upregulated in the ERG cells after injury. CRISPR/Cas9 mediated knockdown of *m17* in adult zebrafish has already shown defects in functional recovery after SCI in these fish (Klatt Shaw & Mokalled, 2021). It would be interesting to further investigate the role of *m17* specifically in neurogenesis by measuring the number of newly generated neurons in these *m17* mutant zebrafish after SCI. Furthermore, direct application of *m17* on *ex vivo* ERG cells as performed with Tnf (Cavone et al, 2021) would help to determine if *m17* promotes neurogenesis by direct signalling to ERG cells or through an indirect mechanism.

6.8 Tnf signalling in regenerative and non-regenerative species

In this thesis and accompanying publication, Tnf from macrophages was found to signal to ERG cells to directly stimulate neurogenesis in zebrafish larvae. However Tnf appears to have contrasting roles in regenerating and non-regenerating species.

The distinct roles that Tnf plays in non-regenerating and regenerating species after SCI can be highlighted by comparing the inhibition of Tnf in these species. As shown in the Becker lab and discussed elsewhere in this thesis, Tnf inhibition in zebrafish reduces spinal cord bridging and neurogenesis after SCI (Cavone et al, 2021; Tsarouchas et al, 2018). Furthermore, knocking down Tnf using morpholino strategies reduces fin regeneration in zebrafish larvae (Nguyen-Chi et al, 2017) and muller glial proliferation after retinal injury (Conner et al, 2014; Nelson et al, 2013).

In contrast, pharmacological and genetic TNF inhibition in mice significantly reduced spinal cord inflammation and tissue injury, neutrophil infiltration and apoptosis after spinal cord compression injury in mice (Genovese et al, 2008) Similarly, TNF receptor antagonist and TNF antiserum application immediately after SCI in rat is neuroprotective and reduces apoptosis in neurons and oligodendrocytes (Chen et al, 2011; Sharma et al, 2003).

However, there is evidence for an additional degree of complexity for TNF signalling in mammals. Indeed, one study showed that TNF deficient mice had no reported differences after SCI in mice compared to wild type mice (Farooque et al, 2001). Additionally, application of recombinant TNF to adult sensory neurons and rabbit optic nerve *in vitro* demonstrated growth promoting properties during neurite outgrowth (Saleh et al, 2011; Schwartz et al, 1991).

It is possible that the timing of TNF induction and resolution is key to its pro and anti-regenerative effects. To support this, Tnf mRNA levels quickly return to near baseline levels in wildtype zebrafish larvae after SCI (Tsarouchas et al, 2018), where Lund et al recently found that TNF is significantly increased in both acute and delayed phases of SCI (Lund et al, 2022) and it is known that the general proinflammatory response is sustained for weeks after injury (Kigerl et al, 2009).

It is possible that the temporal resolution of Tnf signalling is therefore responsible for the neurogenesis promoting role of Tnf after zebrafish SCI. Stimulation of the immune system by incubation with bacterial lipopolysaccharides in the 24 hours following SCI in zebrafish larvae leads to increased neurogenesis (Ohnmacht et al,

2016), however it would be interesting to investigate whether prolonged LPS stimulation also promotes regenerative neurogenesis in the larval zebrafish after SCI or instead leads to poor outcomes as in mammalian systems.

6.9 AP-1 signalling

In this thesis it is proposed that the Tnf induced neurogenesis in zebrafish larvae after SCI is mediated by the AP-1 complex, which comprises of dimers of JunB and c-Fos. In axlotl, the role of the AP-1 complex has also been investigated after SCI. Axlotl ependymoglial cells upregulate c-Fos after injury, and inhibition of this c-Fos upregulation leads to defects in spinal cord regeneration (Sabin et al, 2015). Recently, the mechanism by which non-canonical AP-1 (JunB/cFos) is favoured and promotes regeneration in axlotl was discovered to be via upregulation of microRNA miR-200a. This microRNA suppresses c-Jun in the ependymoglial cells and hence the non-canonical AP-1 is (JunB/cFos) present to a larger extent than canonical AP-1 (c-Jun/c-Fos). It is hypothesised that this difference is responsible for the lack of reactive gliosis in axlotl after injury. Interestingly c-Jun and c-Fos proteins are reported to be upregulated after mammalian spinal cord injury, and dimerise in the canonical AP-1 complex (Gadea et al, 2008; Gao et al, 2013). In mammals, this complex contributes to the formation of the glial scar after SCI (Di Giovanni et al, 2003). Interestingly however, JunB is consistently upregulated in mice ependymal cells (including up to 4 wpi) in the datasets analysed in this thesis. Whether the JunB protein is incorporated into the AP-1 complex or c-Jun is still preferentially relied upon is unclear. It is possible that the different reliance on either canonical or non-canonical AP-1 can explain some of the difference in neurogenesis and regenerative success between mammals and anamniotes

6.10 Tnf signalling – future outlook

Despite these experiments and those presented in (Cavone et al, 2021), there is still more to be understood about the pathway initiated in ERG cells by Tnf signalling, and how this results in regenerative neurogenesis. Experimental manipulations including expression of dominant negative *hdac1* show that expression of *hdac1* is essential for neurogenesis to occur. It is hypothesised that the AP-1 signal transducer complex may be responsible for the upregulation of *hdac1* following Tnf signalling, as pharmacological inhibition of AP-1 in *ex vivo* ERG cells stimulated by Tnf inhibited the upregulation of *hdac1*. Whether this is a direct result of AP-1 upregulating *hdac1* or a more indirect mechanism involving other transcription

factors and signalling transducers is not clear. This could be further investigated by comparing the transcriptomes of ERG cells stimulated by Tnf in the presence and absence of AP-1 inhibitor SR 11302 (Ye et al, 2014). Additionally, exactly how *hdac1* leads to neurogenesis in ERG cells has not been established. It is known that *hdac1* is an epigenetic modifier, and thus can regulate the transcriptional accessibility of many genes simultaneously. Techniques such as assay for transposase-accessible chromatin using sequencing (ATAC-seq) combined with the established dominant negative *hdac1* fish could be used to determine which gene regulatory networks are altered by *hdac1* and consequently are associated with neurogenesis. Improving our fundamental understanding of lesion-induced neurogenesis after SCI in zebrafish provides potential areas of intervention in non-regenerating species such as humans.

6.11 Contribution of ERG cells and ependymal cells to the spinal cord after injury in zebrafish and mammals

One perspective on the value of the findings is this thesis is that this communication between innate immune cells and ERG cells may be applicable to the mammalian system, either by manipulating signalling pathways already present or by exogenous application of agonist/antagonists of specific pathways. In order for the findings of this thesis to be directly applicable to the mammalian system, it is necessary for there to exist a cell type in the mammalian spinal cord that has the potential to mirror the neurogenesis undergone by ERG cells in the zebrafish spinal cord.

In chapter 4 the expression changes after SCI undergone by zebrafish larval ERG cells are compared to the expression changes undergone by mammalian ependymal cells. Indeed, ependymal cells have much in common with ERG cells, and along with the transient radial glial cells in mammalian brain, are likely the closest equivalent cells across the two different species. Along with some shared morphological and molecular characteristics (Moreno-Manzano et al, 2009), one salient similarity is the shared potential of ependymal cells and ERG cells to generate both new neurons and glial cells (Becker et al, 2018; Weiss et al, 1996). Interestingly, some of the signals stimulating this transition and the subsequent subtypes of cells generated are shared between zebrafish and mammalian systems (Moreno-Manzano et al, 2009).

While it is true that some ependymal cells have demonstrated *in vitro* neurogenic ability, *in vivo* these cells contribute very few of the newly formed astrocytes and no

cells of any other identity (Ren et al, 2017). It has been posited that only a small subpopulation of ependymal cells, termed EpA cells, display multipotentiality *in vivo*, and that these cells contribute less than 0.1% of the spinal cord residing cells in mice (Stenudd et al, 2022). This is in contrast with zebrafish where the contribution of ERG cells to the regenerating spinal cord is substantial (Briona et al, 2015; Ohnmacht et al, 2016). Already, genetic manipulations have allowed ependymal cells to contribute myelinating oligodendrocytes to the spinal cord after injury in mice (Llorens-Bobadilla et al, 2020). Whether signals derived from the immune system could also promote neurogenesis from mammalian ependymal cells via AP-1 or other transcription factors is a potential future area of study.

6.12 Future directions

These scRNA-seq experiments have allowed the characterisation of two major cell populations involved in regenerative neurogenesis, and the gene expression changes involved in these cell types after injury. Despite the large number of larvae involved in the preparation for this experiment, the number of cells retained after the single cell sequencing preparation and 10x processing was modest. For future experiments, it would be worthwhile to optimise the 10x pre-processing steps to allow for maximum retention of cells. This may involve utilising alternative buffers or shorter centrifuge times. By optimising these factors, it is likely a larger sample of cells would be captured, and this would allow for further insight into the cell populations. In particular, it would be interesting to capture transition states of cells as this would allow us to more confidently infer cell lineage trajectories. For example, understanding how ERG cells transition into the putative neurosecretory cluster would answer questions about this population's origin and function. Furthermore, this may highlight essential transcription factors or pathways involved in this regeneration-specific trajectory and hence the presence of these cells could be experimentally manipulated.

RNA-sequencing technology could be further utilised to answer outstanding questions about regenerative neurogenesis after SCI. It would be beneficial to capture a larger array of timepoints post injury, as this would further aid in the determination of the trajectories of specific populations. Particularly interesting would be to sequence ERG populations from larvae immediately after injury, to capture the immediate gene expression changes undergone in these populations. Capturing immune cells at earlier timepoints could help to understand the specific

roles of neutrophils in injured larvae, as neutrophils are the first responders at the injury site and their numbers peak at 6 hpi (Tsarouchas et al, 2018). Performing single-cell sequencing on mutant larvae would also provide insight into the roles of specific cell types in regenerating larvae. For example, performing single-cell sequencing on ERG cells in *csf1ra/b* larvae which lack microglia would help to clarify the role of microglia in regenerative neurogenesis.

Other single cell sequencing technologies have recently become accessible for academic research and could be utilised to further our understanding of regenerative neurogenesis. Fixed RNA profiling could be utilised to help in large scale experiments where multiple timepoints are involved. Applying a fixative to the samples would allow the samples to be processed in tandem after completion of the final timepoint rather than individually after each timepoint. However, fixed RNA profiling has currently only been optimised for human and mouse samples, and it is likely that adjustments to the protocol would need to be applied to samples from zebrafish larvae. Another exciting development in RNA sequencing is the development of transposase-accessible chromatin sequencing assay (ATAC-seq). This assay identifies open chromatin regions and transcription factor binding sites, and hence can be used to identify transcriptionally active genes and important genetic pathways in the cell type of interest. ATAC-seq has previously been performed on regenerating zebrafish fins and found changes in chromatin accessibility in cells contributing to the blastema (Lee et al, 2020). Applying this technology to the regenerating zebrafish spinal cord will allow the epigenetic changes in ERG cells to be further elucidated. Similarly, spatial trancriptomics is an emerging technology which combines single cell sequencing with spatial information. Due to its recent increase in accessibility and profiling resolution, it is growing in popularity and could be a powerful tool for addressing questions regarding spinal cord regeneration. In a recent preprint, spatial transcriptomics was used to reveal a specific subtype of radial glial cells activated in early regenerative stages in the axolotl telencephalon (Wei et al, 2021). If applied to the zebrafish spinal cord, this technique could reveal insights into rare cell types such as the putative neurosecretory cells and also help to reveal possible physical interactions of interacting immune cells at the injury site.

6.13 Therapeutic relevance

Using the successful regenerating zebrafish larvae to understand regenerative neurogenesis has a number of advantages. Their quick regeneration time allows us to efficiently study the mechanisms involved, and their lack of an adaptive immune system at this stage means the input of the innate immune system can be studied in isolation. Additionally, the availability of transgenic reporter lines allows visualisation and selection of cell types of interest for appropriate experiments. It must be considered, however, that many of these qualities of zebrafish larvae can also be detrimental when considering the therapeutic relevance of any findings in zebrafish to human medicine. Indeed, we know that SCI activates B and T cells in mammals and adult zebrafish, and that these cells contribute to the inflammatory response and downstream processes after SCI (Ankeny & Popovich, 2009; Hui et al, 2017). Furthermore, the differences in regenerative outcomes are so stark that it could be argued that any findings from zebrafish larvae are not applicable to the non-regenerating mammalian system. For example, the neuronal progenitors in mammalian spinal cords do not generate neurons to replace those lost in injury without significant experimental manipulation.

Despite the differences in complexity and regenerative outcomes between zebrafish and mammalian systems, zebrafish are a valuable model for uncovering therapeutic interventions and disease insights which are relevant to humans (reviewed in (Patton & Tobin, 2019)). In terms of regenerative neurogenesis, whilst it is true that new neurons are not generated in the mammalian spinal cord after injury, the endogenous progenitors in mammals do have stem cell potential (Shihabuddin et al, 2000), and proliferate in response to injury (Meletis et al, 2008). Furthermore, in mice, these can be programmed to increase production of oligodendrocytes *in vivo* (Llorens-Bobadilla et al, 2020). Understanding the signals and cell populations which prompt neurogenesis in zebrafish could help to uncover therapeutic interventions to promote neurogenesis in more complicated systems.

List of Abbreviations

AP-1	Activator Protein 1
bp	base pair
BMP	Bone morphogenetic protein
cDNA	Complementary DNA
CNS	Central nervous system
CRISPR	Clustered regularly interspaced short palindromic repeats
DNA	Deoxyribonucleic acid
dpf	Days post fertilisation
dpi	Days post injury
ECM	Extracellular matrix
EdU	5-Ethylnyl-2'-deoxyuridine
ER	Endoplasmic reticulum
FACS	Fluorescence-activated cell sorting
FADD	Fas receptor-associated death domain
FBS	Fetal bovine serum
FGF	Fibroblast growth factor
GEM	Gel Bead-in-Emulsion
GFAP	Glial fibrillary acidic protein
GFP	Green fluorescence protein
GO	Gene ontology
gRNA	guide RNA
hdac1	Histone deacetylase 1
Hh	Hedgehog
hpf	hours post fertilisation
hpi	hours post injury
HSCs	Hematopoietic stem cells
IKK	IkB kinase
Il1b	Interleukin 1β protein
Il-2	Interleukin 2 protein
JNK	Jun N2-terminal kinase
KEGG	Kyoto Encyclopedia of Genes and Genomes
MEKK1	MAP/ERK kinase kinase 1
MKK7	MAPK kinase 7

mRNA	Messenger ribonucleic acid
NETs	Neutrophil extracellular traps
OPC	Oligodendrocyte progenitor cells
PCR	Polymerase chain reaction
PNS	Peripheral nervous system
RA	Retinoic acid
rcf	relative centrifugal force
RIP	Receptor-interacting kinase
RNA	Ribonucleic acid
ROS	Reactive oxygen species
SCI	Spinal cord injury
SMA	Spinal muscular atrophy
STAT3	signal transducer and activator of transcription 3
TBI	Traumatic brain injury
Tnf	Tumour necrosis factor protein
Tnfr1	Tnf Receptor 1
Tnfr2	Tnf Receptor 2
TRADD	Tnfr1-associated via death domain
TRAF2	TNF receptor-associated factor 2
tSNE	t-distributed stochastic neighbour embedding
UMAP	Uniform manifold approximation and projection
UMI	Unique molecular identifier
wpf	Weeks post fertilisation
wpi	Weeks post injury

References

(2022) Harmonizing model organism data in the Alliance of Genome Resources. *Genetics*, 220(4).

Aaku-Saraste, E., Hellwig, A. & Huttner, W. B. (1996) Loss of occludin and functional tight junctions, but not ZO-1, during neural tube closure--remodeling of the neuroepithelium prior to neurogenesis. *Dev Biol*, 180(2), 664-79.

Achim, K., Peltopuro, P., Lahti, L., Tsai, H.-H., Zachariah, A., Astrand, M., Salminen, M., Rowitch, D. & Partanen, J. (2013) The role of Tal2 and Tal1 in the differentiation of midbrain GABAergic neuron precursors. *Biology open*, 2(10), 990-997.

Aggarwal, B. B. (2003) Signalling pathways of the TNF superfamily: a double-edged sword. *Nature Reviews Immunology*, 3(9), 745-756.

Ajami, B., Bennett, J. L., Krieger, C., Tetzlaff, W. & Rossi, F. M. V. (2007) Local self-renewal can sustain CNS microglia maintenance and function throughout adult life. *Nature Neuroscience*, 10(12), 1538-1543.

Alfaro-Cervello, C., Soriano-Navarro, M., Mirzadeh, Z., Alvarez-Buylla, A. & Garcia-Verdugo, J. M. (2012) Biciliated ependymal cell proliferation contributes to spinal cord growth. *Journal of Comparative Neurology*, 520(15), 3528-3552.

Alizadeh, A., Dyck, S. M. & Karimi-Abdolrezaee, S. (2019) Traumatic spinal cord injury: an overview of pathophysiology, models and acute injury mechanisms. *Frontiers in neurology*, 10, 282.

AlJanahi, A. A., Danielsen, M. & Dunbar, C. E. (2018) An Introduction to the Analysis of Single-Cell RNA-Sequencing Data. *Molecular Therapy - Methods & Clinical Development*, 10, 189-196.

Allende, M. L. & Weinberg, E. S. (1994) The Expression Pattern of Two Zebrafish achaete-scute Homolog (ash) Genes Is Altered in the Embryonic Brain of the cyclops Mutant. *Developmental Biology*, 166(2), 509-530.

Alper, S. R. & Dorsky, R. I. (2022) Unique advantages of zebrafish larvae as a model for spinal cord regeneration. *Frontiers in Molecular Neuroscience*, 15.

Alvarez-Buylla, A., García-Verdugo, J. M. & Tramontin, A. D. (2001) A unified hypothesis on the lineage of neural stem cells. *Nature Reviews Neuroscience*, 2(4), 287-293.

Amantea, D., Nappi, G., Bernardi, G., Bagetta, G. & Corasaniti, M. T. (2009) Post-ischemic brain damage: pathophysiology and role of inflammatory mediators. *The FEBS Journal*, 276(1), 13-26.

Anderson, M. J., Swanson, K. A., Waxman, S. G. & Eng, L. F. (1984) Glial fibrillary acidic protein in regenerating teleost spinal cord. *Journal of Histochemistry & Cytochemistry*, 32(10), 1099-1106.

Andrzejczuk, L. A., Banerjee, S., England, S. J., Voufo, C., Kamara, K. & Lewis, K. E. (2018) Tal1, Gata2a, and Gata3 Have Distinct Functions in the Development of

V2b and Cerebrospinal Fluid-Contacting KA Spinal Neurons. *Frontiers in Neuroscience*, 12.

Ankeny, D. P. & Popovich, P. G. (2009) Mechanisms and implications of adaptive immune responses after traumatic spinal cord injury. *Neuroscience*, 158(3), 1112-1121.

Anujan, P., Roy, S., Bingle, L. & Bingle, C. D. (2018) Functional analysis of PIERCE1, in motile ciliogenesis. *European Respiratory Journal*, 52(suppl 62), OA507.

Appel, B. (2000) Zebrafish neural induction and patterning. *Developmental Dynamics*, 219(2), 155-168.

Appel, B. & Eisen, J. S. (1998) Regulation of neuronal specification in the zebrafish spinal cord by Delta function. *Development*, 125(3), 371-380.

Appel, B., Givan, L. A. & Eisen, J. S. (2001) Delta-Notch signaling and lateral inhibition in zebrafish spinal cord development. *BMC developmental biology*, 1, 13-13.

Araya, C., Ward, L. C., Girdler, G. C. & Miranda, M. (2016) Coordinating cell and tissue behavior during zebrafish neural tube morphogenesis. *Developmental Dynamics*, 245(3), 197-208.

Aurora, A. B., Porrello, E. R., Tan, W., Mahmoud, A. I., Hill, J. A., Bassel-Duby, R., Sadek, H. A. & Olson, E. N. (2014) Macrophages are required for neonatal heart regeneration. *J Clin Invest*, 124(3), 1382-92.

Aztekin, C., Hiscock, T. W., Marioni, J. C., Gurdon, J. B., Simons, B. D. & Jullien, J. (2019) Identification of a regeneration-organizing cell in the Xenopus tail. *Science*, 364(6441), 653-658.

Balla, K. M., Lugo-Villarino, G., Spitsbergen, J. M., Stachura, D. L., Hu, Y., Bañuelos, K., Romo-Fewell, O., Aroian, R. V. & Traver, D. (2010) Eosinophils in the zebrafish: prospective isolation, characterization, and eosinophilia induction by helminth determinants. *Blood*, 116(19), 3944-3954.

Baran-Gale, J., Chandra, T. & Kirschner, K. (2017) Experimental design for single-cell RNA sequencing. *Briefings in Functional Genomics*, 17(4), 233-239.

Barreiro-Iglesias, A., Mysiak, K. S., Scott, A. L., Reimer, M. M., Yang, Y., Becker, C. G. & Becker, T. (2015) Serotonin Promotes Development and Regeneration of Spinal Motor Neurons in Zebrafish. *Cell Rep*, 13(5), 924-32.

Batista, M. F. & Lewis, K. E. (2008) Pax2/8 act redundantly to specify glycinergic and GABAergic fates of multiple spinal interneurons. *Developmental biology*, 323(1), 88-97.

Bauer, S., Rasika, S., Han, J., Mauduit, C., Raccurt, M., Morel, G., Jourdan, F., Benahmed, M., Moyse, E. & Patterson, P. H. (2003) Leukemia Inhibitory Factor Is a Key Signal for Injury-Induced Neurogenesis in the Adult Mouse Olfactory Epithelium. *The Journal of Neuroscience*, 23(5), 1792.

Beattie, M. S., Bresnahan, J. C. & Lopate, G. (1990) Metamorphosis alters the response to spinal cord transection in Xenopus laevis frogs. *J Neurobiol*, 21(7), 1108-22.

Beck, K. D., Nguyen, H. X., Galvan, M. D., Salazar, D. L., Woodruff, T. M. & Anderson, A. J. (2010) Quantitative analysis of cellular inflammation after traumatic spinal cord injury: evidence for a multiphasic inflammatory response in the acute to chronic environment. *Brain*, 133(Pt 2), 433-47.

Becker, Catherina G. & Becker, T. (2015) Neuronal Regeneration from Ependymo-Radial Glial Cells: Cook, Little Pot, Cook! *Developmental Cell*, 32(4), 516-527.

Becker, C. G., Becker, T. & Hugnot, J. P. (2018) The spinal ependymal zone as a source of endogenous repair cells across vertebrates. *Prog Neurobiol*, 170, 67-80.

Becker, C. G., Lieberoth, B. C., Morellini, F., Feldner, J., Becker, T. & Schachner, M. (2004) L1.1 is involved in spinal cord regeneration in adult zebrafish. *The Journal of neuroscience : the official journal of the Society for Neuroscience*, 24(36), 7837-7842.

Becker, T. & Becker, C. G. (2001) Regenerating descending axons preferentially reroute to the gray matter in the presence of a general macrophage/microglial reaction caudal to a spinal transection in adult zebrafish. *J Comp Neurol*, 433(1), 131-47.

Becker, T. & Becker, C. G. (2020) Dynamic cell interactions allow spinal cord regeneration in zebrafish. *Current Opinion in Physiology*, 14, 64-69.

Becker, T. & Becker, C. G. (2022) Regenerative neurogenesis: the integration of developmental, physiological and immune signals. *Development*, 149(8).

Becker, T., Wullimann, M. F., Becker, C. G., Bernhardt, R. R. & Schachner, M. (1997a) Axonal regrowth after spinal cord transection in adult zebrafish. *J. Comp. Neurol.*, 377, 577-595.

Becker, T., Wullimann, M. F., Becker, C. G., Bernhardt, R. R. & Schachner, M. (1997b) Axonal regrowth after spinal cord transection in adult zebrafish. *J Comp Neurol*, 377(4), 577-95.

Beckers, A., Vanhunsel, S., Van Dyck, A., Bergmans, S., Masin, L. & Moons, L. (2021) Injury-induced Autophagy Delays Axonal Regeneration after Optic Nerve Damage in Adult Zebrafish. *Neuroscience*, 470, 52-69.

Ben-Shlomo, I., Yu Hsu, S., Rauch, R., Kowalski, H. W. & Hsueh, A. J. (2003) Signaling receptome: a genomic and evolutionary perspective of plasma membrane receptors involved in signal transduction. *Sci STKE*, 2003(187), Re9.

Benard, E. L., Racz, P. I., Rougeot, J., Nezhinsky, A. E., Verbeek, F. J., Spaink, H. P. & Meijer, A. H. (2015) Macrophage-Expressed Perforins Mpeg1 and Mpeg1.2 Have an Anti-Bacterial Function in Zebrafish. *Journal of Innate Immunity*, 7(2), 136-152.

Benard, E. L., Roobol, S. J., Spaink, H. P. & Meijer, A. H. (2014) Phagocytosis of mycobacteria by zebrafish macrophages is dependent on the scavenger receptor Marco, a key control factor of pro-inflammatory signalling. *Dev Comp Immunol*, 47(2), 223-33.

Benaud, C., Gentil, B. t. J., Assard, N., Court, M., Garin, J., Delphin, C. & Baudier, J. (2003) AHNAK interaction with the annexin 2/S100A10 complex regulates cell membrane cytoarchitecture. *Journal of Cell Biology*, 164(1), 133-144.

Bennett, C. M., Kanki, J. P., Rhodes, J., Liu, T. X., Paw, B. H., Kieran, M. W., Langenau, D. M., Delahaye-Brown, A., Zon, L. I., Fleming, M. D. & Look, A. T. (2001) Myelopoiesis in the zebrafish, Danio rerio. *Blood*, 98(3), 643-51.

Bennett, M. V. L. & Fox, S. (1962) Electrophysiology of caudal neurosecretory cells in the skate and fluke. *General and Comparative Endocrinology*, 2(1), 77-95.

Bernardino, L., Agasse, F., Silva, B., Ferreira, R., Grade, S. & Malva, J. O. (2008) Tumor Necrosis Factor-α Modulates Survival, Proliferation, and Neuronal Differentiation in Neonatal Subventricular Zone Cell Cultures. *Stem Cells*, 26(9), 2361-2371.

Bernardos, R. L. & Raymond, P. A. (2006) GFAP transgenic zebrafish. *Gene Expression Patterns*, 6(8), 1007-1013.

Bernstein, J. J. (1964) Relation of spinal cord regeneration to age in adult goldfish. *Experimental Neurology*, 9(2), 161-174.

Bernut, A., Nguyen-Chi, M., Halloum, I., Herrmann, J. L., Lutfalla, G. & Kremer, L. (2016) Mycobacterium abscessus-Induced Granuloma Formation Is Strictly Dependent on TNF Signaling and Neutrophil Trafficking. *PLoS Pathog*, 12(11), e1005986.

Bertini, R., Howard, O. M., Dong, H. F., Oppenheim, J. J., Bizzarri, C., Sergi, R., Caselli, G., Pagliei, S., Romines, B., Wilshire, J. A., Mengozzi, M., Nakamura, H., Yodoi, J., Pekkari, K., Gurunath, R., Holmgren, A., Herzenberg, L. A., Herzenberg, L. A. & Ghezzi, P. (1999) Thioredoxin, a redox enzyme released in infection and inflammation, is a unique chemoattractant for neutrophils, monocytes, and T cells. *J Exp Med*, 189(11), 1783-9.

Bhattarai, P., Thomas, Alvin K., Cosacak, Mehmet I., Papadimitriou, C., Mashkaryan, V., Froc, C., Reinhardt, S., Kurth, T., Dahl, A., Zhang, Y. & Kizil, C. (2016) IL4/STAT6 Signaling Activates Neural Stem Cell Proliferation and Neurogenesis upon Amyloid-β42 Aggregation in Adult Zebrafish Brain. *Cell Reports*, 17(4), 941-948.

Bhattarai, P., Thomas, A. K., Zhang, Y. & Kizil, C. (2017) The effects of aging on Amyloid-β42-induced neurodegeneration and regeneration in adult zebrafish brain. *Neurogenesis*, 4(1), e1322666.

Biddy, B. A., Kong, W., Kamimoto, K., Guo, C., Waye, S. E., Sun, T. & Morris, S. A. (2018) Single-cell mapping of lineage and identity in direct reprogramming. *Nature*, 564(7735), 219-224.

Blader, P., Fischer, N., Gradwohl, G., Guillemont, F. & Strahle, U. (1997) The activity of neurogenin1 is controlled by local cues in the zebrafish embryo. *Development*, 124(22), 4557-4569.

Bohaud, C., Johansen, M. D., Jorgensen, C., Ipseiz, N., Kremer, L. & Djouad, F. (2021) The Role of Macrophages During Zebrafish Injury and Tissue Regeneration Under Infectious and Non-Infectious Conditions. *Frontiers in immunology*, 12, 707824-707824.

Bonaguidi, Michael A., Wheeler, Michael A., Shapiro, Jason S., Stadel, Ryan P., Sun, Gerald J., Ming, G.-l. & Song, H. (2011) In Vivo Clonal Analysis Reveals Self-Renewing and Multipotent Adult Neural Stem Cell Characteristics. *Cell*, 145(7), 1142-1155.

Bonnefont, J., Tiberi, L., van den Ameele, J., Potier, D., Gaber, Z. B., Lin, X., Bilheu, A., Herpoel, A., Velez Bravo, F. D., Guillemot, F., Aerts, S. & Vanderhaeghen, P. (2019) Cortical Neurogenesis Requires Bcl6-Mediated Transcriptional Repression of Multiple Self-Renewal-Promoting Extrinsic Pathways. *Neuron*, 103(6), 1096-1108.e4.

Borla, M. A., Palecek, B., Budick, S. & O'Malley, D. M. (2002) Prey Capture by Larval Zebrafish: Evidence for Fine Axial Motor Control. *Brain, Behavior and Evolution*, 60(4), 207-229.

Bossen, C., Ingold, K., Tardivel, A., Bodmer, J.-L., Gaide, O., Hertig, S., Ambrose, C., Tschopp, J. & Schneider, P. (2006) Interactions of Tumor Necrosis Factor (TNF) and TNF Receptor Family Members in the Mouse and Human *. *Journal of Biological Chemistry*, 281(20), 13964-13971.

Bradley, L. M., Douglass, M. F., Chatterjee, D., Akira, S. & Baaten, B. J. G. (2012) Matrix Metalloprotease 9 Mediates Neutrophil Migration into the Airways in Response to Influenza Virus-Induced Toll-Like Receptor Signaling. *PLOS Pathogens*, 8(4), e1002641.

Brewster, J. L., Martin, S. L., Toms, J., Goss, D., Wang, K., Zachrone, K., Davis, A., Carlson, G., Hood, L. & Coffin, J. D. (2000) Deletion of Dad1 in mice induces an apoptosis-associated embryonic death. *genesis*, 26(4), 271-278.

Briona, L. K. & Dorsky, R. I. (2014) Radial glial progenitors repair the zebrafish spinal cord following transection. *Experimental Neurology*, 256, 81-92.

Briona, L. K., Poulain, F. E., Mosimann, C. & Dorsky, R. I. (2015) Wnt/ß-catenin signaling is required for radial glial neurogenesis following spinal cord injury. *Developmental Biology*, 403(1), 15-21.

Brown, C. H., Bains, J. S., Ludwig, M. & Stern, J. E. (2013) Physiological Regulation of Magnocellular Neurosecretory Cell Activity: Integration of Intrinsic, Local and Afferent Mechanisms. *Journal of Neuroendocrinology*, 25(8), 678-710.

Brownlie, A. & Zon, L. (1999) The Zebrafish as a Model System for the Study of Hematopoiesis: Zebrafish mutants point the way to novel genes involved in the generation of vertebrate blood cells. *BioScience*, 49(5), 382-392.

Brownstein, C., Deora, A. B., Jacovina, A. T., Weintraub, R., Gertler, M., Khan, K. M. F., Falcone, D. J. & Hajjar, K. A. (2004) Annexin II mediates plasminogen-dependent matrix invasion by human monocytes: enhanced expression by macrophages. *Blood*, 103(1), 317-324.

Bruni, J. E. & Anderson, W. A. (1987) Ependyma of the Rat Fourth Ventricle and Central Canal: Response to Injury. *Cells Tissues Organs*, 128(4), 265-273.

Budick, S. A. & O'Malley, D. M. (2000) Locomotor repertoire of the larval zebrafish: swimming, turning and prey capture. *Journal of Experimental Biology*, 203(17), 2565-2579.

Buss, R. R. & Drapeau, P. (2001) Synaptic drive to motoneurons during fictive swimming in the developing zebrafish. *Journal of neurophysiology*, 86(1), 197-210.

Bustin, M. (1999) Regulation of DNA-Dependent Activities by the Functional Motifs of the High-Mobility-Group Chromosomal Proteins. *Molecular and Cellular Biology*, 19(8), 5237-5246.

Butko, E., Distel, M., Pouget, C., Weijts, B., Kobayashi, I., Ng, K., Mosimann, C., Poulain, F. E., McPherson, A., Ni, C.-W., Stachura, D. L., Del Cid, N., Espín-Palazón, R., Lawson, N. D., Dorsky, R., Clements, W. K. & Traver, D. (2015) Gata2b is a restricted early regulator of hemogenic endothelium in the zebrafish embryo. *Development*, 142(6), 1050-1061.

Butler, E. G. & Ward, M. B. (1967) Reconstitution of the spinal cord after ablation in adult Triturus. *Developmental Biology*, 15(5), 464-486.

Butler, T. L. & Pennypacker, K. R. (2005) The transcriptional response to hypoxic insult controlled by FRA-2. *Gene Expr*, 12(2), 61-7.

Calderari, S., Ria, M., Gérard, C., Nogueira, T. C., Villate, O., Collins, S. C., Neil, H., Gervasi, N., Hue, C., Suarez-Zamorano, N., Prado, C., Cnop, M., Bihoreau, M.-T., Kaisaki, P. J., Cazier, J.-B., Julier, C., Lathrop, M., Werner, M., Eizirik, D. L. & Gauguier, D. (2018) Molecular genetics of the transcription factor GLIS3 identifies its dual function in beta cells and neurons. *Genomics*, 110(2), 98-111.

Caldwell, L. J., Davies, N. O., Cavone, L., Mysiak, K. S., Semenova, S. A., Panula, P., Armstrong, J. D., Becker, C. G. & Becker, T. (2019) Regeneration of Dopaminergic Neurons in Adult Zebrafish Depends on Immune System Activation and Differs for Distinct Populations. *The Journal of Neuroscience*, 39(24), 4694-4713.

Callahan, R. A., Roberts, R., Sengupta, M., Kimura, Y., Higashijima, S.-I. & Bagnall, M. W. (2019) Spinal V2b neurons reveal a role for ipsilateral inhibition in speed control. *eLife*, 8, e47837.

Cao, J., Spielmann, M., Qiu, X., Huang, X., Ibrahim, D. M., Hill, A. J., Zhang, F., Mundlos, S., Christiansen, L., Steemers, F. J., Trapnell, C. & Shendure, J. (2019) The single-cell transcriptional landscape of mammalian organogenesis. *Nature*, 566(7745), 496-502.

Cao, Y., Qiu, Y., Tu, G. & Yang, C. (2020) Single-cell RNA Sequencing in Immunology. *Curr Genomics*, 21(8), 564-575.

Carrillo, S. A., Anguita-Salinas, C., Peña, O. A., Morales, R. A., Muñoz-Sánchez, S., Muñoz-Montecinos, C., Paredes-Zúñiga, S., Tapia, K. & Allende, M. L. (2016) Macrophage Recruitment Contributes to Regeneration of Mechanosensory Hair Cells in the Zebrafish Lateral Line. *J Cell Biochem*, 117(8), 1880-9.

Cavone, L., McCann, T., Drake, L. K., Aguzzi, E. A., Oprişoreanu, A. M., Pedersen, E., Sandi, S., Selvarajah, J., Tsarouchas, T. M., Wehner, D., Keatinge, M., Mysiak, K. S., Henderson, B. E. P., Dobie, R., Henderson, N. C., Becker, T. & Becker, C. G. (2021) A unique macrophage subpopulation signals directly to progenitor cells to promote regenerative neurogenesis in the zebrafish spinal cord. *Dev Cell*, 56(11), 1617-1630.e6.

Chan, K. T., Roadcap, D. W., Holoweckyj, N. & Bear, J. E. (2012) Coronin 1C harbours a second actin-binding site that confers co-operative binding to F-actin. *Biochem J*, 444(1), 89-96.

Chang, W., Pedroni, A., Bertuzzi, M., Kizil, C., Simon, A. & Ampatzis, K. (2021) Locomotion dependent neuron-glia interactions control neurogenesis and regeneration in the adult zebrafish spinal cord. *Nature Communications*, 12(1), 4857.

Chapouton, P., Skupien, P., Hesl, B., Coolen, M., Moore, J. C., Madelaine, R., Kremmer, E., Faus-Kessler, T., Blader, P., Lawson, N. D. & Bally-Cuif, L. (2010) Notch activity levels control the balance between quiescence and recruitment of adult neural stem cells. *J Neurosci*, 30(23), 7961-74.

Charité, J., de Graaff, W., Vogels, R., Meijlink, F. & Deschamps, J. (1995) Regulation of the Hoxb-8 Gene: Synergism between Multimerized cis-Acting Elements Increases Responsiveness to Positional Information. *Developmental Biology*, 171(2), 294-305.

Chen, J. & Guan, Z. (2022) Function of Oncogene Mycn in Adult Neurogenesis and Oligodendrogenesis. *Molecular Neurobiology*, 59(1), 77-92.

Chen, J., Leong, S.-Y. & Schachner, M. (2005) Differential expression of cell fate determinants in neurons and glial cells of adult mouse spinal cord after compression injury. *European Journal of Neuroscience*, 22(8), 1895-1906.

Chen, J., Poskanzer, K. E., Freeman, M. R. & Monk, K. R. (2020) Live-imaging of astrocyte morphogenesis and function in zebrafish neural circuits. *Nature Neuroscience*, 23(10), 1297-1306.

Chen, K.-B., Uchida, K., Nakajima, H., Yayama, T., Hirai, T., Watanabe, S., Guerrero, A. R., Kobayashi, S., Ma, W.-Y., Liu, S.-Y. & Baba, H. (2011) Tumor Necrosis Factor-α Antagonist Reduces Apoptosis of Neurons and Oligodendroglia in Rat Spinal Cord Injury. *Spine*, 36(17).

Chen, Z., Shao, X.-y., Wang, C., Hua, M.-h., Wang, C.-n., Wang, X., Wang, Q.-j., Yao, J.-y., Fan, Y.-h. & Qin, Y.-w. (2018) Mycobacterium marinum Infection in

Zebrafish and Microglia Imitates the Early Stage of Tuberculous Meningitis. *Journal of Molecular Neuroscience*, 64(2), 321-330.

Cheriyan, T., Ryan, D. J., Weinreb, J. H., Cheriyan, J., Paul, J. C., Lafage, V., Kirsch, T. & Errico, T. J. (2014) Spinal cord injury models: a review. *Spinal Cord*, 52(8), 588-595.

Cho, S. J., Park, E., Baker, A. & Reid, A. Y. (2020) Age Bias in Zebrafish Models of Epilepsy: What Can We Learn From Old Fish? *Front Cell Dev Biol*, 8, 573303.

Cigliola, V., Becker, C. J. & Poss, K. D. (2020) Building bridges, not walls: spinal cord regeneration in zebrafish. *Disease Models & Mechanisms*, 13(5), dmm044131.

Clovis, Y. M., Seo, S. Y., Kwon, J.-S., Rhee, J. C., Yeo, S., Lee, J. W., Lee, S. & Lee, S.-K. (2016) Chx10 Consolidates V2a Interneuron Identity through Two Distinct Gene Repression Modes. *Cell reports*, 16(6), 1642-1652.

Conedera, F. M., Pousa, A. M. Q., Mercader, N., Tschopp, M. & Enzmann, V. (2019) Retinal microglia signaling affects Müller cell behavior in the zebrafish following laser injury induction. *Glia*, 67(6), 1150-1166.

Conner, C., Ackerman, K. M., Lahne, M., Hobgood, J. S. & Hyde, D. R. (2014) Repressing Notch Signaling and Expressing TNFα Are Sufficient to Mimic Retinal Regeneration by Inducing Müller Glial Proliferation to Generate Committed Progenitor Cells. *The Journal of Neuroscience*, 34(43), 14403-14419.

Conti, P., Reale, M., Barbacane, R. C., Bongrazio, M., Panara, M. R., Fiore, S., Dempsey, R. & Borish, L. (1990) Leukocyte inhibitory factor activates human neutrophils and macrophages to release leukotriene B4 and thromboxanes. *Cytokine*, 2(2), 142-148.

Cosacak, M. I., Bhattarai, P., Reinhardt, S., Petzold, A., Dahl, A., Zhang, Y. & Kizil, C. (2019) Single-Cell Transcriptomics Analyses of Neural Stem Cell Heterogeneity and Contextual Plasticity in a Zebrafish Brain Model of Amyloid Toxicity. *Cell Reports*, 27(4), 1307-1318.e3.

Crowe, M. J., Bresnahan, J. C., Shuman, S. L., Masters, J. N. & Beattie, M. S. (1997) Apoptosis and delayed degeneration after spinal cord injury in rats and monkeys. *Nature Medicine*, 3(1), 73-76.

Da'as, S., Teh, E. M., Dobson, J. T., Nasrallah, G. K., McBride, E. R., Wang, H., Neuberg, D. S., Marshall, J. S., Lin, T.-J. & Berman, J. N. (2011) Zebrafish mast cells possess an FcεRI-like receptor and participate in innate and adaptive immune responses. *Developmental & Comparative Immunology*, 35(1), 125-134.

Dalli, J., Jones, C. P., Cavalcanti, D. M., Farsky, S. H., Perretti, M. & Rankin, S. M. (2012) Annexin A1 regulates neutrophil clearance by macrophages in the mouse bone marrow. *Faseb j*, 26(1), 387-96.

Danilova, N. & Steiner, L. A. (2002) B cells develop in the zebrafish pancreas. *Proc Natl Acad Sci U S A*, 99(21), 13711-6.

Davis, J. M., Clay, H., Lewis, J. L., Ghori, N., Herbomel, P. & Ramakrishnan, L. (2002) Real-time visualization of mycobacterium-macrophage interactions leading to initiation of granuloma formation in zebrafish embryos. *Immunity*, 17(6), 693-702.

de Bakker, D. E. M., Bouwman, M., Dronkers, E., Simões, F. C., Riley, P. R., Goumans, M.-J., Smits, A. M. & Bakkers, J. (2021) Prrx1b restricts fibrosis and promotes Nrg1-dependent cardiomyocyte proliferation during zebrafish heart regeneration. *Development*, 148(19), dev198937.

Deneen, B., Ho, R., Lukaszewicz, A., Hochstim, C. J., Gronostajski, R. M. & Anderson, D. J. (2006) The Transcription Factor NFIA Controls the Onset of Gliogenesis in the Developing Spinal Cord. *Neuron*, 52(6), 953-968.

Deng, Q., Yoo, S. K., Cavnar, P. J., Green, J. M. & Huttenlocher, A. (2011) Dual roles for Rac2 in neutrophil motility and active retention in zebrafish hematopoietic tissue. *Developmental cell*, 21(4), 735-745.

Dervan, A. G. & Roberts, B. L. (2003) Reaction of spinal cord central canal cells to cord transection and their contribution to cord regeneration. *Journal of Comparative Neurology*, 458(3), 293-306.

Devanney, N. A., Stewart, A. N. & Gensel, J. C. (2020) Microglia and macrophage metabolism in CNS injury and disease: The role of immunometabolism in neurodegeneration and neurotrauma. *Experimental Neurology*, 329, 113310.

Dhara, S. P., Rau, A., Flister, M. J., Recka, N. M., Laiosa, M. D., Auer, P. L. & Udvadia, A. J. (2019) Cellular reprogramming for successful CNS axon regeneration is driven by a temporally changing cast of transcription factors. *Scientific Reports*, 9(1), 14198.

Di Giovanni, S., Knoblach, S. M., Brandoli, C., Aden, S. A., Hoffman, E. P. & Faden, A. I. (2003) Gene profiling in spinal cord injury shows role of cell cycle in neuronal death. *Annals of Neurology*, 53(4), 454-468.

Di, Q., Lin, Q., Huang, Z., Chi, Y., Chen, X., Zhang, W. & Zhang, Y. (2017) Zebrafish nephrosin helps host defence against Escherichia coli infection. *Open Biology*, 7(8), 170040.

Dias, T. B., Yang, Y.-J., Ogai, K., Becker, T. & Becker, C. G. (2012) Notch Signaling Controls Generation of Motor Neurons in the Lesioned Spinal Cord of Adult Zebrafish. *The Journal of Neuroscience*, 32(9), 3245-3252.

Ding, Q., Joshi, P. S., Xie, Z. H., Xiang, M. & Gan, L. (2012) BARHL2 transcription factor regulates the ipsilateral/contralateral subtype divergence in postmitotic dI1 neurons of the developing spinal cord. *Proc Natl Acad Sci U S A*, 109(5), 1566-71.

Diotel, N., Vaillant, C., Gueguen, M.-M., Mironov, S., Anglade, I., Servili, A., Pellegrini, E. & Kah, O. (2010) Cxcr4 and Cxcl12 expression in radial glial cells of the brain of adult zebrafish. *Journal of Comparative Neurology*, 518(24), 4855-4876.

Dobson, J. T., Seibert, J., Teh, E. M., Da'as, S., Fraser, R. B., Paw, B. H., Lin, T.-J. & Berman, J. N. (2008) Carboxypeptidase A5 identifies a novel mast cell lineage in

the zebrafish providing new insight into mast cell fate determination. *Blood*, 112(7), 2969-2972.

Dockrell, D. H. & Whyte, M. K. B. (2006) Regulation of phagocyte lifespan in the lung during bacterial infection. *Journal of Leukocyte Biology*, 79(5), 904-908.

Doetsch, F., Caillé, I., Lim, D. A., García-Verdugo, J. M. & Alvarez-Buylla, A. (1999) Subventricular Zone Astrocytes Are Neural Stem Cells in the Adult Mammalian Brain. *Cell*, 97(6), 703-716.

Dovi, J. V., He, L. K. & DiPietro, L. A. (2003) Accelerated wound closure in neutrophil-depleted mice. *J Leukoc Biol*, 73(4), 448-55.

Drake, L. K., Keatinge, M., Tsarouchas, T. M., Becker, C. G., Lyons, D. A. & Becker, T. (2023) Rapid Testing of Gene Function in Axonal Regeneration After Spinal Cord Injury Using Larval Zebrafish. *Methods Mol Biol*, 2636, 263-277.

Dugger, B. N. & Dickson, D. W. (2017) Pathology of Neurodegenerative Diseases. *Cold Spring Harb Perspect Biol*, 9(7).

E. Young, A. & Murphy, G. C. (2009) Employment status after spinal cord injury (1992–2005): a review with implications for interpretation, evaluation, further research, and clinical practice. *International Journal of Rehabilitation Research*, 32(1), 1-11.

Early, J. J., Marshall-Phelps, K. L. H., Williamson, J. M., Swire, M., Kamadurai, H., Muskavitch, M. & Lyons, D. A. (2018) An automated high-resolution in vivo screen in zebrafish to identify chemical regulators of myelination. *eLife*, 7, e35136.

Edwards-Faret, G., González-Pinto, K., Cebrián-Silla, A., Peñailillo, J., García-Verdugo, J. M. & Larraín, J. (2021) Cellular response to spinal cord injury in regenerative and non-regenerative stages in Xenopus laevis. *Neural Development*, 16(1), 2.

Ekdahl, C. T., Claasen, J. H., Bonde, S., Kokaia, Z. & Lindvall, O. (2003) Inflammation is detrimental for neurogenesis in adult brain. *Proc Natl Acad Sci U S A*, 100(23), 13632-7.

El-Daher, F., Drake, L. K., Wehner, D., Westphal, M., Porter, N. J., Becker, C. G. & Becker, T. (in preparation) Microglia accumulation is essential for tissue contraction in wound closure after brain injury in zebrafish larvae.

Ellett, F., Pase, L., Hayman, J. W., Andrianopoulos, A. & Lieschke, G. J. (2011) mpeg1 promoter transgenes direct macrophage-lineage expression in zebrafish. *Blood*, 117(4), e49-e56.

Elsaeidi, F., Bemben, M. A., Zhao, X. F. & Goldman, D. (2014) Jak/Stat signaling stimulates zebrafish optic nerve regeneration and overcomes the inhibitory actions of Socs3 and Sfpq. *J Neurosci*, 34(7), 2632-44.

Emanuele Michael, J., Ciccia, A., Elia Andrew, E. H. & Elledge Stephen, J. (2011) Proliferating cell nuclear antigen (PCNA)-associated KIAA0101/PAF15 protein is a

cell cycle-regulated anaphase-promoting complex/cyclosome substrate. *Proceedings of the National Academy of Sciences*, 108(24), 9845-9850.

Fager, N. & Jaworski, D. M. (2000) Differential spatial distribution and temporal regulation of tissue inhibitor of metalloproteinase mRNA expression during rat central nervous system development. *Mechanisms of Development*, 98(1), 105-109.

Falcone, D. J., Borth, W., Khan, K. M. F. & Hajjar, K. A. (2001) Plasminogen-mediated matrix invasion and degradation by macrophages is dependent on surface expression of annexin II. *Blood*, 97(3), 777-784.

Fan, X., Krahling, S., Smith, D., Williamson, P. & Schlegel, R. A. (2004) Macrophage Surface Expression of Annexins I and II in the Phagocytosis of Apoptotic Lymphocytes. *Molecular Biology of the Cell*, 15(6), 2863-2872.

Fang, P., Pan, H.-C., Lin, S. L., Zhang, W.-Q., Rauvala, H., Schachner, M. & Shen, Y.-Q. (2014) HMGB1 Contributes to Regeneration After Spinal Cord Injury in Adult Zebrafish. *Molecular Neurobiology*, 49(1), 472-483.

Farooque, M., Isaksson, J. & Olsson, Y. (2001) Improved recovery after spinal cord injury in neuronal nitric oxide synthase-deficient mice but not in TNF-alpha-deficient mice. *J Neurotrauma*, 18(1), 105-14.

Fawcett, J. W. (2020) The Struggle to Make CNS Axons Regenerate: Why Has It Been so Difficult? *Neurochemical Research*, 45(1), 144-158.

Fei, J.-F., Schuez, M., Tazaki, A., Taniguchi, Y., Roensch, K. & Tanaka, E. M. (2014) CRISPR-mediated genomic deletion of Sox2 in the axolotl shows a requirement in spinal cord neural stem cell amplification during tail regeneration. *Stem cell reports*, 3(3), 444-459.

Feng, L., Hatten, M. E. & Heintz, N. (1994) Brain lipid-binding protein (BLBP): a novel signaling system in the developing mammalian CNS. *Neuron*, 12(4), 895-908.

Ferrero, G., Gomez, E., lyer, S., Rovira, M., Miserocchi, M., Langenau, D. M., Bertrand, J. Y. & Wittamer, V. (2020) The macrophage-expressed gene (mpeg) 1 identifies a subpopulation of B cells in the adult zebrafish. *Journal of Leukocyte Biology*, 107(3), 431-443.

Flanagan-Steet, H., Fox, M. A., Meyer, D. & Sanes, J. R. (2005) Neuromuscular synapses can form in vivo by incorporation of initially aneural postsynaptic specializations. *Development*, 132(20), 4471-4481.

Franceschini, A., Szklarczyk, D., Frankild, S., Kuhn, M., Simonovic, M., Roth, A., Lin, J., Minguez, P., Bork, P., von Mering, C. & Jensen, L. J. (2013) STRING v9.1: protein-protein interaction networks, with increased coverage and integration. *Nucleic Acids Res*, 41(Database issue), D808-15.

Francius, C., Hidalgo-Figueroa, M., Debrulle, S., Pelosi, B., Rucchin, V., Ronellenfitch, K., Panayiotou, E., Makrides, N., Misra, K., Harris, A., Hassani, H., Schakman, O., Parras, C., Xiang, M., Malas, S., Chow, R. L. & Clotman, F. (2016) Vsx1 Transiently Defines an Early Intermediate V2 Interneuron Precursor Compartment in the Mouse Developing Spinal Cord. *Front Mol Neurosci*, 9, 145.

Franco-Bocanegra, D. K., McAuley, C., Nicoll, J. A. R. & Boche, D. (2019) Molecular Mechanisms of Microglial Motility: Changes in Ageing and Alzheimer's Disease. *Cells*, 8(6).

Fry, E. J., Stolp, H. B., Lane, M. A., Dziegielewska, K. M. & Saunders, N. R. (2003) Regeneration of supraspinal axons after complete transection of the thoracic spinal cord in neonatal opossums (Monodelphis domestica). *Journal of Comparative Neurology*, 466(3), 422-444.

Fukazawa, T., Naora, Y., Kunieda, T. & Kubo, T. (2009) Suppression of the immune response potentiates tadpole tail regeneration during the refractory period. *Development*, 136(14), 2323-2327.

Gadea, A., Schinelli, S. & Gallo, V. (2008) Endothelin-1 regulates astrocyte proliferation and reactive gliosis via a JNK/c-Jun signaling pathway. *J Neurosci*, 28(10), 2394-408.

Gaiddon, C., Loeffler, J. P. & Larmet, Y. (1996) Brain-Derived Neurotrophic Factor Stimulates AP-1 and Cyclic AMP-Responsive Element Dependent Transcriptional Activity in Central Nervous System Neurons. *Journal of Neurochemistry*, 66(6), 2279-2286.

Galloway, J. L. & Zon, L. I. (2003) 3 ontogeny of hematopoiesis: examining the emergence of hematopoietic cells in the vertebrate embryo.

Gao, J., Zhang, C., Yang, B., Sun, L., Zhang, C., Westerfield, M. & Peng, G. (2012) Dcc Regulates Asymmetric Outgrowth of Forebrain Neurons in Zebrafish. *PLOS ONE*, 7(5), e36516.

Gao, K., Wang, C. R., Jiang, F., Wong, A. Y., Su, N., Jiang, J. H., Chai, R. C., Vatcher, G., Teng, J., Chen, J., Jiang, Y. W. & Yu, A. C. (2013) Traumatic scratch injury in astrocytes triggers calcium influx to activate the JNK/c-Jun/AP-1 pathway and switch on GFAP expression. *Glia*, 61(12), 2063-77.

Genovese, T., Mazzon, E., Crisafulli, C., Di Paola, R., Muià, C., Esposito, E., Bramanti, P. & Cuzzocrea, S. (2008) TNF-alpha blockage in a mouse model of SCI: evidence for improved outcome. *Shock*, 29(1), 32-41.

Gerdes, J., Li, L., Schlueter, C., Duchrow, M., Wohlenberg, C., Gerlach, C., Stahmer, I., Kloth, S., Brandt, E. & Flad, H. D. (1991) Immunobiochemical and molecular biologic characterization of the cell proliferation-associated nuclear antigen that is defined by monoclonal antibody Ki-67. *The American journal of pathology*, 138(4), 867-873.

Gerdes, J., Schwab, U., Lemke, H. & Stein, H. (1983) Production of a mouse monoclonal antibody reactive with a human nuclear antigen associated with cell proliferation. *International Journal of Cancer*, 31(1), 13-20.

Godwin, J. W., Pinto, A. R. & Rosenthal, N. A. (2013) Macrophages are required for adult salamander limb regeneration. *Proceedings of the National Academy of Sciences*, 110(23), 9415-9420.

Goldshmit, Y., Sztal, T. E., Jusuf, P. R., Hall, T. E., Nguyen-Chi, M. & Currie, P. D. (2012) Fgf-Dependent Glial Cell Bridges Facilitate Spinal Cord Regeneration in Zebrafish. *The Journal of Neuroscience*, 32(22), 7477-7492.

Goldshmit, Y., Tang, J. K. K. Y., Siegel, A. L., Nguyen, P. D., Kaslin, J., Currie, P. D. & Jusuf, P. R. (2018) Different Fgfs have distinct roles in regulating neurogenesis after spinal cord injury in zebrafish. *Neural Development*, 13(1), 24.

Gómez-Nicola, D., Valle-Argos, B., Pallas-Bazarra, N. & Nieto-Sampedro, M. (2011) Interleukin-15 regulates proliferation and self-renewal of adult neural stem cells. *Molecular biology of the cell*, 22(12), 1960-1970.

Gosselin, D., Skola, D., Coufal, N. G., Holtman, I. R., Schlachetzki, J. C. M., Sajti, E., Jaeger, B. N., O'Connor, C., Fitzpatrick, C., Pasillas, M. P., Pena, M., Adair, A., Gonda, D. D., Levy, M. L., Ransohoff, R. M., Gage, F. H. & Glass, C. K. (2017) An environment-dependent transcriptional network specifies human microglia identity. *Science*, 356(6344).

Graeber, T. G. & Eisenberg, D. (2001) Bioinformatic identification of potential autocrine signaling loops in cancers from gene expression profiles. *Nature Genetics*, 29(3), 295-300.

Graham, A., Maden, M. & Krumlauf, R. (1991) The murine Hox-2 genes display dynamic dorsoventral patterns of expression during central nervous system development. *Development*, 112(1), 255-264.

Gratton, M. O., Torban, E., Jasmin, S. B., Theriault, F. M., German, M. S. & Stifani, S. (2003) Hes6 promotes cortical neurogenesis and inhibits Hes1 transcription repression activity by multiple mechanisms. *Mol Cell Biol*, 23(19), 6922-35.

Grimbaldeston, M. A., Metz, M., Yu, M., Tsai, M. & Galli, S. J. (2006) Effector and potential immunoregulatory roles of mast cells in IgE-associated acquired immune responses. *Current Opinion in Immunology*, 18(6), 751-760.

Guha, A. & Tator, C. H. (1988) Acute cardiovascular effects of experimental spinal cord injury. *The Journal of trauma*, 28(4), 481-490.

Hagen, E. M., Faerestrand, S., Hoff, J. M., Rekand, T. & Gronning, M. (2011) Cardiovascular and urological dysfunction in spinal cord injury. *Acta Neurologica Scandinavica*, 124(s191), 71-78.

Hall, Christopher J., Boyle, Rachel H., Astin, Jonathan W., Flores, Maria V., Oehlers, Stefan H., Sanderson, Leslie E., Ellett, F., Lieschke, Graham J., Crosier, Kathryn E. & Crosier, Philip S. (2013) Immunoresponsive Gene 1 Augments Bactericidal Activity of Macrophage-Lineage Cells by Regulating β-Oxidation-Dependent Mitochondrial ROS Production. *Cell Metabolism*, 18(2), 265-278.

Hanania, R., Sun, H. S., Xu, K., Pustylnik, S., Jeganathan, S. & Harrison, R. E. (2012) Classically activated macrophages use stable microtubules for matrix metalloproteinase-9 (MMP-9) secretion. *J Biol Chem*, 287(11), 8468-83.

Hargrave, M., Karunaratne, A., Cox, L., Wood, S., Koopman, P. & Yamada, T. (2000) The HMG Box Transcription Factor Gene Sox14 Marks a Novel Subset of

Ventral Interneurons and Is Regulated by Sonic Hedgehog. *Developmental Biology*, 219(1), 142-153.

Harris, E. S., Rouiller, I., Hanein, D. & Higgs, H. N. (2006) Mechanistic differences in actin bundling activity of two mammalian formins, FRL1 and mDia2. *J Biol Chem*, 281(20), 14383-92.

Hasan, S. J., Nelson, B. H., Valenzuela, J. I., Keirstead, H. S., Shull, S. E., Ethell, D. W. & Steeves, J. D. (1991) Functional repair of transected spinal cord in embryonic chick. *Restor Neurol Neurosci*, 2(3), 137-54.

Haynes, S. E., Hollopeter, G., Yang, G., Kurpius, D., Dailey, M. E., Gan, W. B. & Julius, D. (2006) The P2Y12 receptor regulates microglial activation by extracellular nucleotides. *Nat Neurosci*, 9(12), 1512-9.

Hellman, N. E., Liu, Y., Merkel, E., Austin, C., Le Corre, S., Beier, D. R., Sun, Z., Sharma, N., Yoder, B. K. & Drummond, I. A. (2010) The zebrafish foxj1a transcription factor regulates cilia function in response to injury and epithelial stretch. *Proc Natl Acad Sci U S A*, 107(43), 18499-504.

Herbomel, P., Thisse, B. & Thisse, C. (1999) Ontogeny and behaviour of early macrophages in the zebrafish embryo. *Development*, 126(17), 3735-45.

Herbomel, P., Thisse, B. & Thisse, C. (2001) Zebrafish Early Macrophages Colonize Cephalic Mesenchyme and Developing Brain, Retina, and Epidermis through a M-CSF Receptor-Dependent Invasive Process. *Developmental Biology*, 238(2), 274-288.

Hicks, S. C., Townes, F. W., Teng, M. & Irizarry, R. A. (2018) Missing data and technical variability in single-cell RNA-sequencing experiments. *Biostatistics*, 19(4), 562-578.

Hirose, K., Rutherford, M. A. & Warchol, M. E. (2017) Two cell populations participate in clearance of damaged hair cells from the sensory epithelia of the inner ear. *Hearing research*, 352, 70-81.

Holder, N., Clarke, J. D. W., Kamalati, T. & Lane, E. B. (1990) Heterogeneity in spinal radial glia demonstrated by intermediate filament expression and HRP labelling. *Journal of Neurocytology*, 19(6), 915-928.

Hu, H., Miao, Y. R., Jia, L. H., Yu, Q. Y., Zhang, Q. & Guo, A. Y. (2019) AnimalTFDB 3.0: a comprehensive resource for annotation and prediction of animal transcription factors. *Nucleic Acids Res*, 47(D1), D33-d38.

Hu, Z., Ma, J., Yue, H., Luo, Y., Li, X., Wang, C., Wang, L., Sun, B., Chen, Z., Wang, L. & Gu, Y. (2022) Involvement of LIN28A in Wnt-dependent regulation of hippocampal neurogenesis in the aging brain. *Stem Cell Reports*, 17(7), 1666-1682.

Hughes, A. N. & Appel, B. (2020) Microglia phagocytose myelin sheaths to modify developmental myelination. *Nature neuroscience*, 23(9), 1055-1066.

Hui, S. P., Dutta, A. & Ghosh, S. (2010) Cellular response after crush injury in adult zebrafish spinal cord. *Developmental Dynamics*, 239(11), 2962-2979.

Hui, S. P., Nag, T. C. & Ghosh, S. (2015) Characterization of Proliferating Neural Progenitors after Spinal Cord Injury in Adult Zebrafish. *PLOS ONE*, 10(12), e0143595.

Hui, S. P., Sengupta, D., Lee, S. G. P., Sen, T., Kundu, S., Mathavan, S. & Ghosh, S. (2014) Genome Wide Expression Profiling during Spinal Cord Regeneration Identifies Comprehensive Cellular Responses in Zebrafish. *PLOS ONE*, 9(1), e84212.

Hui, S. P., Sheng, D. Z., Sugimoto, K., Gonzalez-Rajal, A., Nakagawa, S., Hesselson, D. & Kikuchi, K. (2017) Zebrafish Regulatory T Cells Mediate Organ-Specific Regenerative Programs. *Developmental Cell*, 43(6), 659-672.e5.

Iancu-Rubin, C., Tripodi, J., Najfeld, V. & Atweh, G. F. (2009) The Role of Microtubule Regulatory Protein Stathmin (STMN1) in Megakaryopoiesis. *Blood*, 114(22), 4591-4591.

Iannotti, C. A., Clark, M., Horn, K. P., van Rooijen, N., Silver, J. & Steinmetz, M. P. (2011) A combination immunomodulatory treatment promotes neuroprotection and locomotor recovery after contusion SCI. *Experimental Neurology*, 230(1), 3-15.

Isles, H. M., Loynes, C. A., Alasmari, S., Kon, F. C., Henry, K. M., Kadochnikova, A., Hales, J., Muir, C. F., Keightley, M.-C., Kadirkamanathan, V., Hamilton, N., Lieschke, G. J., Renshaw, S. A. & Elks, P. M. (2021) Pioneer neutrophils release chromatin within in vivo swarms. *eLife*, 10, e68755.

Ito, K., Sportoletti, P., Clohessy, J. G., Silvia, G. & Pandolfi, P. P. (2010) The Role of Nucleophosmin In Hematopoietic Stem Cells and the Pathogenesis of Myelodysplastic Syndrome. *Blood*, 116(21), 95-95.

Iwanami, A., Yamane, J., Katoh, H., Nakamura, M., Momoshima, S., Ishii, H., Tanioka, Y., Tamaoki, N., Nomura, T., Toyama, Y. & Okano, H. (2005) Establishment of graded spinal cord injury model in a nonhuman primate: The common marmoset. *Journal of Neuroscience Research*, 80(2), 172-181.

Jacovina, A. T., Zhong, F., Khazanova, E., Lev, E., Deora, A. B. & Hajjar, K. A. (2001) Neuritogenesis and the nerve growth factor-induced differentiation of PC-12 cells requires annexin II-mediated plasmin generation. *J Biol Chem*, 276(52), 49350-8.

Ji, Z., Zhou, Z.-L., Hao, Q., Zhao, L., Cui, C., Huang, S.-B., Yang, Y.-L. & Shen, Y.-Q. (2021) Activating Transcription Factor 6 Contributes to Functional Recovery After Spinal Cord Injury in Adult Zebrafish. *Journal of Molecular Neuroscience*, 71(4), 734-745.

Jin, K., Mao, X. O., Sun, Y., Xie, L., Jin, L., Nishi, E., Klagsbrun, M. & Greenberg, D. A. (2002) Heparin-Binding Epidermal Growth Factor-Like Growth Factor: Hypoxia-Inducible Expression In Vitro and Stimulation of Neurogenesis In Vitro and In Vivo</em&gt. *The Journal of Neuroscience*, 22(13), 5365.

Jin, K., Sun, Y., Xie, L., Batteur, S., Mao, X. O., Smelick, C., Logvinova, A. & Greenberg, D. A. (2003) Neurogenesis and aging: FGF-2 and HB-EGF restore

neurogenesis in hippocampus and subventricular zone of aged mice. *Aging Cell*, 2(3), 175-83.

Jin, M., Li, J., Hu, R., Xu, B., Huang, G., Huang, W., Chen, B., He, J. & Cao, Y. (2021) Cyclin A2/cyclin-dependent kinase 1-dependent phosphorylation of Top2a is required for S phase entry during retinal development in zebrafish. *J Genet Genomics*, 48(1), 63-74.

Johansson, P., Corripio-Miyar, Y., Wang, T., Collet, B., Secombes, C. J. & Zou, J. (2012) Characterisation and expression analysis of the rainbow trout (Oncorhynchus mykiss) homologue of the human dendritic cell marker CD208/lysosomal associated membrane protein 3. *Developmental & Comparative Immunology*, 37(3), 402-413.

Johansson, S., Price, J. & Modo, M. (2008) Effect of Inflammatory Cytokines on Major Histocompatibility Complex Expression and Differentiation of Human Neural Stem/Progenitor Cells. *Stem Cells*, 26(9), 2444-2454.

Johnson, K., Barragan, J., Bashiruddin, S., Smith, C. J., Tyrrell, C., Parsons, M. J., Doris, R., Kucenas, S., Downes, G. B., Velez, C. M., Schneider, C., Sakai, C., Pathak, N., Anderson, K., Stein, R., Devoto, S. H., Mumm, J. S. & Barresi, M. J. F. (2016) Gfap-positive radial glial cells are an essential progenitor population for later-born neurons and glia in the zebrafish spinal cord. *Glia*, 64(7), 1170-1189.

Jung, S.-H., Kim, S., Chung, A.-Y., Kim, H.-T., So, J.-H., Ryu, J., Park, H.-C. & Kim, C.-H. (2010) Visualization of myelination in GFP-transgenic zebrafish. *Developmental Dynamics*, 239(2), 592-597.

Kakebeen, A. D., Chitsazan, A. D., Williams, M. C., Saunders, L. M. & Wills, A. E. (2020) Chromatin accessibility dynamics and single cell RNA-Seq reveal new regulators of regeneration in neural progenitors. *Elife*, 9.

Kanagaraj, P., Chen, J. Y., Skaggs, K., Qadeer, Y., Connors, M., Cutler, N., Richmond, J., Kommidi, V., Poles, A., Affrunti, D., Powell, C., Goldman, D. & Parent, J. M. (2022) Microglia Stimulate Zebrafish Brain Repair Via a Tumor Necrosis Factor-α-Initiated Inflammatory Cascade. *bioRxiv*, 2020.10.08.330662.

Karunaratne, A., Hargrave, M., Poh, A. & Yamada, T. (2002) GATA Proteins Identify a Novel Ventral Interneuron Subclass in the Developing Chick Spinal Cord. *Developmental Biology*, 249(1), 30-43.

Kaveh, A., Bruton, F. A., Buckley, C., Oremek, M. E. M., Tucker, C. S., Mullins, J. J., Taylor, J. M., Rossi, A. G. & Denvir, M. A. (2020) Live Imaging of Heart Injury in Larval Zebrafish Reveals a Multi-Stage Model of Neutrophil and Macrophage Migration. *Frontiers in Cell and Developmental Biology*, 8.

Kawakami, A., Fukazawa, T. & Takeda, H. (2004) Early fin primordia of zebrafish larvae regenerate by a similar growth control mechanism with adult regeneration. *Developmental Dynamics*, 231(4), 693-699.

Keatinge, M., Tsarouchas, T. M., Munir, T., Porter, N. J., Larraz, J., Gianni, D., Tsai, H.-H., Becker, C. G., Lyons, D. A. & Becker, T. (2021) CRISPR gRNA phenotypic screening in zebrafish reveals pro-regenerative genes in spinal cord injury. *PLOS Genetics*, 17(4), e1009515.

Keshava Prasad, T. S., Goel, R., Kandasamy, K., Keerthikumar, S., Kumar, S., Mathivanan, S., Telikicherla, D., Raju, R., Shafreen, B., Venugopal, A., Balakrishnan, L., Marimuthu, A., Banerjee, S., Somanathan, D. S., Sebastian, A., Rani, S., Ray, S., Harrys Kishore, C. J., Kanth, S., Ahmed, M., Kashyap, M. K., Mohmood, R., Ramachandra, Y. L., Krishna, V., Rahiman, B. A., Mohan, S., Ranganathan, P., Ramabadran, S., Chaerkady, R. & Pandey, A. (2009) Human Protein Reference Database--2009 update. *Nucleic Acids Res*, 37(Database issue), D767-72.

Kettenmann, H., Hanisch, U.-K., Noda, M. & Verkhratsky, A. (2011) Physiology of Microglia. *Physiological Reviews*, 91(2), 461-553.

Kharchenko, P. V., Silberstein, L. & Scadden, D. T. (2014) Bayesian approach to single-cell differential expression analysis. *Nature Methods*, 11(7), 740-742.

Kigerl, K. A., Gensel, J. C., Ankeny, D. P., Alexander, J. K., Donnelly, D. J. & Popovich, P. G. (2009) Identification of two distinct macrophage subsets with divergent effects causing either neurotoxicity or regeneration in the injured mouse spinal cord. *J Neurosci*, 29(43), 13435-44.

Kim, S. H., Oh, J., Choi, J. Y., Jang, J. Y., Kang, M. W. & Lee, C. E. (2008) Identification of human thioredoxin as a novel IFN-gamma-induced factor: mechanism of induction and its role in cytokine production. *BMC Immunol*, 9, 64.

Kimmel, C. B., Ballard, W. W., Kimmel, S. R., Ullmann, B. & Schilling, T. F. (1995) Stages of embryonic development of the zebrafish. *Dev Dyn*, 203(3), 253-310.

Kimura, Y., Okamura, Y. & Higashijima, S.-i. (2006) alx, a Zebrafish Homolog of Chx10, Marks Ipsilateral Descending Excitatory Interneurons That Participate in the Regulation of Spinal Locomotor Circuits. *The Journal of Neuroscience*, 26(21), 5684.

Kinsella, R. J., Kähäri, A., Haider, S., Zamora, J., Proctor, G., Spudich, G., Almeida-King, J., Staines, D., Derwent, P., Kerhornou, A., Kersey, P. & Flicek, P. (2011) Ensembl BioMarts: a hub for data retrieval across taxonomic space. *Database (Oxford)*, 2011, bar030.

Kirby, B. B., Takada, N., Latimer, A. J., Shin, J., Carney, T. J., Kelsh, R. N. & Appel, B. (2006) In vivo time-lapse imaging shows dynamic oligodendrocyte progenitor behavior during zebrafish development. *Nature Neuroscience*, 9(12), 1506-1511.

Kirkham, M., Hameed, L. S., Berg, Daniel A., Wang, H. & Simon, A. (2014) Progenitor Cell Dynamics in the Newt Telencephalon during Homeostasis and Neuronal Regeneration. *Stem Cell Reports*, 2(4), 507-519.

Kishimoto, N., Alfaro-Cervello, C., Shimizu, K., Asakawa, K., Urasaki, A., Nonaka, S., Kawakami, K., Garcia-Verdugo, J. M. & Sawamoto, K. (2011) Migration of neuronal precursors from the telencephalic ventricular zone into the olfactory bulb in adult zebrafish. *Journal of Comparative Neurology*, 519(17), 3549-3565.

Kizil, C., Dudczig, S., Kyritsis, N., Machate, A., Blaesche, J., Kroehne, V. & Brand, M. (2012a) The chemokine receptor cxcr5 regulates the regenerative neurogenesis response in the adult zebrafish brain. *Neural Development*, 7(1), 27.

Kizil, C., Kyritsis, N., Dudczig, S., Kroehne, V., Freudenreich, D., Kaslin, J. & Brand, M. (2012b) Regenerative Neurogenesis from Neural Progenitor Cells Requires Injury-Induced Expression of Gata3. *Developmental Cell*, 23(6), 1230-1237.

Klatt Shaw, D. & Mokalled, M. H. (2021) Efficient CRISPR/Cas9 mutagenesis for neurobehavioral screening in adult zebrafish. *G3 Genes|Genomes|Genetics*, 11(8), jkab089.

Klatt Shaw, D., Saraswathy, V. M., Zhou, L., McAdow, A. R., Burris, B., Butka, E., Morris, S. A., Dietmann, S. & Mokalled, M. H. (2021) Localized EMT reprograms glial progenitors to promote spinal cord repair. *Dev Cell*, 56(5), 613-626.e7.

Kopacek, J., Sakaguchi, S., Shigematsu, K., Nishida, N., Atarashi, R., Nakaoke, R., Moriuchi, R., Niwa, M. & Katamine, S. (2000) Upregulation of the Genes Encoding Lysosomal Hydrolases, a Perforin-Like Protein, and Peroxidases in the Brains of Mice Affected with an Experimental Prion Disease. *Journal of Virology*, 74(1), 411-417.

Kornblum, H. I., Zurcher, S. D., Werb, Z., Derynck, R. & Seroogy, K. B. (1999) Multiple trophic actions of heparin-binding epidermal growth factor (HB-EGF) in the central nervous system. *Eur J Neurosci*, 11(9), 3236-46.

Koyano-Nakagawa, N., Kim, J., Anderson, D. & Kintner, C. (2000) Hes6 acts in a positive feedback loop with the neurogenins to promote neuronal differentiation. *Development*, 127(19), 4203-4216.

Kroehne, V., Freudenreich, D., Hans, S., Kaslin, J. & Brand, M. (2011) Regeneration of the adult zebrafish brain from neurogenic radial glia-type progenitors. *Development*, 138(22), 4831-41.

Kroll, F., Powell, G. T., Ghosh, M., Gestri, G., Antinucci, P., Hearn, T. J., Tunbak, H., Lim, S., Dennis, H. W., Fernandez, J. M., Whitmore, D., Dreosti, E., Wilson, S. W., Hoffman, E. J. & Rihel, J. (2021) A simple and effective F0 knockout method for rapid screening of behaviour and other complex phenotypes. *eLife*, 10, e59683.

Krzyszczyk, P., Schloss, R., Palmer, A. & Berthiaume, F. (2018) The role of macrophages in acute and chronic wound healing and interventions to promote pro-wound healing phenotypes. *Frontiers in physiology*, 9, 419.

Kucenas, S., Snell, H. & Appel, B. (2008a) nkx2.2a promotes specification and differentiation of a myelinating subset of oligodendrocyte lineage cells in zebrafish. *Neuron Glia Biol*, 4(2), 71-81.

Kucenas, S., Takada, N., Park, H.-C., Woodruff, E., Broadie, K. & Appel, B. (2008b) CNS-derived glia ensheath peripheral nerves and mediate motor root development. *Nature Neuroscience*, 11(2), 143-151.

Kudoh, T., Wilson, S. W. & Dawid, I. B. (2002) Distinct roles for Fgf, Wnt and retinoic acid in posteriorizing the neural ectoderm. *Development*, 129(18), 4335-4346.

Kurtz, A., Zimmer, A., Schnütgen, F., Brüning, G., Spener, F. & Müller, T. (1994) The expression pattern of a novel gene encoding brain-fatty acid binding protein correlates with neuronal and glial cell development. *Development*, 120(9), 2637-49.

Kuscha, V., Barreiro-Iglesias, A., Becker, C. G. & Becker, T. (2012a) Plasticity of tyrosine hydroxylase and serotonergic systems in the regenerating spinal cord of adult zebrafish. *J Comp Neurol*, 520(5), 933-51.

Kuscha, V., Frazer, S. L., Dias, T. B., Hibi, M., Becker, T. & Becker, C. G. (2012b) Lesion-induced generation of interneuron cell types in specific dorsoventral domains in the spinal cord of adult zebrafish. *Journal of Comparative Neurology*, 520(16), 3604-3616.

Kyriakis, J. M. (1999) Activation of the AP-1 transcription factor by inflammatory cytokines of the TNF family. *Gene Expr*, 7(4-6), 217-31.

Kyritsis, N., Kizil, C., Zocher, S., Kroehne, V., Kaslin, J., Freudenreich, D., Iltzsche, A. & Brand, M. (2012) Acute Inflammation Initiates the Regenerative Response in the Adult Zebrafish Brain. *Science*, 338(6112), 1353-1356.

Lai, S.-L., Marín-Juez, R., Moura, P. L., Kuenne, C., Lai, J. K. H., Tsedeke, A. T., Guenther, S., Looso, M. & Stainier, D. Y. R. (2017) Reciprocal analyses in zebrafish and medaka reveal that harnessing the immune response promotes cardiac regeneration. *eLife*, 6, e25605.

Lam, S. H., Chua, H. L., Gong, Z., Lam, T. J. & Sin, Y. M. (2004) Development and maturation of the immune system in zebrafish, Danio rerio: a gene expression profiling, in situ hybridization and immunological study. *Dev Comp Immunol*, 28(1), 9-28.

Lange, C., Rost, F., Machate, A., Reinhardt, S., Lesche, M., Weber, A., Kuscha, V., Dahl, A., Rulands, S. & Brand, M. (2020) Single cell sequencing of radial glia progeny reveals the diversity of newborn neurons in the adult zebrafish brain. *Development*, 147(1).

Lau, Eunice Yuen T., Lo, J., Cheng, Bowie Yik L., Ma, Mark Kin F., Lee, Joyce Man F., Ng, Johnson Kai Y., Chai, S., Lin, Chi H., Tsang, Suk Y., Ma, S., Ng, Irene Oi L. & Lee, Terence Kin W. (2016) Cancer-Associated Fibroblasts Regulate Tumor-Initiating Cell Plasticity in Hepatocellular Carcinoma through c-Met/FRA1/HEY1 Signaling. *Cell Reports*, 15(6), 1175-1189.

Le Dréau, G. & Martí, E. (2012) Dorsal–ventral patterning of the neural tube: A tale of three signals. *Developmental Neurobiology*, 72(12), 1471-1481.

Le Guyader, D., Redd, M. J., Colucci-Guyon, E., Murayama, E., Kissa, K., Briolat, V., Mordelet, E., Zapata, A., Shinomiya, H. & Herbomel, P. (2008) Origins and unconventional behavior of neutrophils in developing zebrafish. *Blood*, 111(1), 132-141.

Lee-Liu, D., Moreno, M., Almonacid, L. I., Tapia, V. S., Muñoz, R., von Marées, J., Gaete, M., Melo, F. & Larraín, J. (2014) Genome-wide expression profile of the response to spinal cord injury in Xenopus laevis reveals extensive differences between regenerative and non-regenerative stages. *Neural Development*, 9(1), 12.

Lee, H. J., Hou, Y., Chen, Y., Dailey, Z. Z., Riddihough, A., Jang, H. S., Wang, T. & Johnson, S. L. (2020) Regenerating zebrafish fin epigenome is characterized by

stable lineage-specific DNA methylation and dynamic chromatin accessibility. *Genome Biology*, 21(1), 52.

Lee, S., Amici, S., Tavori, H., Zeng, W. M., Freeland, S., Fazio, S. & Notterpek, L. (2014) PMP22 Is Critical for Actin-Mediated Cellular Functions and for Establishing Lipid Rafts. *The Journal of Neuroscience*, 34(48), 16140.

Leu, J. I., Crissey, M. A., Leu, J. P., Ciliberto, G. & Taub, R. (2001) Interleukin-6-induced STAT3 and AP-1 amplify hepatocyte nuclear factor 1-mediated transactivation of hepatic genes, an adaptive response to liver injury. *Mol Cell Biol*, 21(2), 414-24.

Lewis, K. L., Del Cid, N. & Traver, D. (2014) Perspectives on antigen presenting cells in zebrafish. *Developmental and comparative immunology*, 46(1), 63-73.

Li, L., Yan, B., Shi, Y.-Q., Zhang, W.-Q. & Wen, Z.-L. (2012a) Live Imaging Reveals Differing Roles of Macrophages and Neutrophils during Zebrafish Tail Fin Regeneration *. *Journal of Biological Chemistry*, 287(30), 25353-25360.

Li, R., Sahu, S. & Schachner, M. (2018) Phenelzine, a cell adhesion molecule L1 mimetic small organic compound, promotes functional recovery and axonal regrowth in spinal cord-injured zebrafish. *Pharmacology Biochemistry and Behavior*, 171, 30-38.

Li, X., Pontén, A., Aase, K., Karlsson, L., Abramsson, A., Uutela, M., Bäckström, G., Hellström, M., Boström, H., Li, H., Soriano, P., Betsholtz, C., Heldin, C.-H., Alitalo, K., Östman, A. & Eriksson, U. (2000) PDGF-C is a new protease-activated ligand for the PDGF α-receptor. *Nature Cell Biology*, 2(5), 302-309.

Li, Y., Du, X. F., Liu, C. S., Wen, Z. L. & Du, J. L. (2012b) Reciprocal regulation between resting microglial dynamics and neuronal activity in vivo. *Dev Cell*, 23(6), 1189-202.

Li, Y., He, X., Kawaguchi, R., Zhang, Y., Wang, Q., Monavarfeshani, A., Yang, Z., Chen, B., Shi, Z., Meng, H., Zhou, S., Zhu, J., Jacobi, A., Swarup, V., Popovich, P. G., Geschwind, D. H. & He, Z. (2020) Microglia-organized scar-free spinal cord repair in neonatal mice. *Nature*, 587(7835), 613-618.

Lidal, I. B., Snekkevik, H., Aamodt, G., Hjeltnes, N., Biering-Sørensen, F. & Stanghelle, J. K. (2007) Mortality after spinal cord injury in Norway. *J Rehabil Med*, 39(2), 145-51.

Lieschke, G. J., Oates, A. C., Crowhurst, M. O., Ward, A. C. & Layton, J. E. (2001) Morphologic and functional characterization of granulocytes and macrophages in embryonic and adult zebrafish. *Blood*, 98(10), 3087-3096.

Lillesaar, C., Tannhäuser, B., Stigloher, C., Kremmer, E. & Bally-Cuif, L. (2007) The serotonergic phenotype is acquired by converging genetic mechanisms within the zebrafish central nervous system. *Developmental Dynamics*, 236(4), 1072-1084.

Liu, K., Petree, C., Requena, T., Varshney, P. & Varshney, G. K. (2019) Expanding the CRISPR Toolbox in Zebrafish for Studying Development and Disease. *Frontiers in Cell and Developmental Biology*, 7.

Liu, L., Zhang, X., Nan, C., Zhao, Z., Ma, S., Li, W., Hu, H. & Liang, Z. (2017) MicroRNA-182 targets protein phosphatase 1 regulatory inhibitor subunit 1C in glioblastoma. *Oncotarget*, 8(70), 114677-114684.

Llorens-Bobadilla, E., Chell, J. M., Le Merre, P., Wu, Y., Zamboni, M., Bergenstråhle, J., Stenudd, M., Sopova, E., Lundeberg, J., Shupliakov, O., Carlén, M. & Frisén, J. (2020) A latent lineage potential in resident neural stem cells enables spinal cord repair. *Science*, 370(6512), eabb8795.

Loynes, C. A., Lee, J. A., Robertson, A. L., Steel, M. J., Ellett, F., Feng, Y., Levy, B. D., Whyte, M. K. B. & Renshaw, S. A. (2018) PGE₂ production at sites of tissue injury promotes an anti-inflammatory neutrophil phenotype and determines the outcome of inflammation resolution in vivo. *Science Advances*, 4(9), eaar8320.

Luecken, M. D. & Theis, F. J. (2019) Current best practices in single-cell RNA-seq analysis: a tutorial. *Molecular Systems Biology*, 15(6), e8746.

Lugo-Villarino, G., Balla Keir, M., Stachura David, L., Bañuelos, K., Werneck Miriam, B. F. & Traver, D. (2010) Identification of dendritic antigen-presenting cells in the zebrafish. *Proceedings of the National Academy of Sciences*, 107(36), 15850-15855.

Lund, M. C., Ellman, D. G., Nissen, M., Nielsen, P. S., Nielsen, P. V., Jørgensen, C., Andersen, D. C., Gao, H., Brambilla, R., Degn, M., Clausen, B. H. & Lambertsen, K. L. (2022) The Inflammatory Response after Moderate Contusion Spinal Cord Injury: A Time Study. *Biology*, 11(6). Available online: [Accessed.

Machado-Neto, J. A., Saad, S. T. & Traina, F. (2014) Stathmin 1 in normal and malignant hematopoiesis. *BMB Rep*, 47(12), 660-5.

Mahony, C. B., Noyvert, B., Vrljicak, P., Ott, S., Higgs, M. & Monteiro, R. (2021) Gata2a maintains cebpa and npm1a in haematopoietic stem cells to sustain lineage differentiation and genome stability. *bioRxiv*, 2021.07.19.452890.

Makowski, L., Brittingham, K. C., Reynolds, J. M., Suttles, J. & Hotamisligil, G. S. (2005) The fatty acid-binding protein, aP2, coordinates macrophage cholesterol trafficking and inflammatory activity. Macrophage expression of aP2 impacts peroxisome proliferator-activated receptor gamma and IkappaB kinase activities. *J Biol Chem*, 280(13), 12888-95.

Malatesta, P., Appolloni, I. & Calzolari, F. (2008) Radial glia and neural stem cells. *Cell and Tissue Research*, 331(1), 165-178.

Malatesta, P., Hartfuss, E. & Gotz, M. (2000) Isolation of radial glial cells by fluorescent-activated cell sorting reveals a neuronal lineage. *Development*, 127(24), 5253-5263.

Malinin, N. L., Plow, E. F. & Byzova, T. V. (2010) Kindlins in FERM adhesion. *Blood*, 115(20), 4011-7.

Mardakheh, F. K., Self, A. & Marshall, C. J. (2016) RHO binding to FAM65A regulates Golgi reorientation during cell migration. *J Cell Sci*, 129(24), 4466-4479.

Martin, P. & Feng, Y. (2009) Wound healing in zebrafish. *Nature*, 459(7249), 921-923.

Masud, S., Torraca, V. & Meijer, A. H. (2017) Chapter Eight - Modeling Infectious Diseases in the Context of a Developing Immune System, in Sadler, K. C. (ed), *Current Topics in Developmental Biology*Academic Press, 277-329.

Masutani, H., Bai, J., Kim, Y. C. & Yodoi, J. (2004) Thioredoxin as a neurotrophic cofactor and an important regulator of neuroprotection. *Mol Neurobiol*, 29(3), 229-42.

Mathias, J. R., Dodd, M. E., Walters, K. B., Yoo, S. K., Ranheim, E. A. & Huttenlocher, A. (2009) Characterization of zebrafish larval inflammatory macrophages. *Developmental & Comparative Immunology*, 33(11), 1212-1217.

Mathias, J. R., Perrin, B. J., Liu, T.-X., Kanki, J., Look, A. T. & Huttenlocher, A. (2006) Resolution of inflammation by retrograde chemotaxis of neutrophils in transgenic zebrafish. *Journal of Leukocyte Biology*, 80(6), 1281-1288.

Maurer, P., Rorive, S., de Kerchove d'Exaerde, A., Schiffmann, S. N., Salmon, I. & de Launoit, Y. (2004) The Ets transcription factor Fev is specifically expressed in the human central serotonergic neurons. *Neurosci Lett*, 357(3), 215-8.

Mazaheri, F., Breus, O., Durdu, S., Haas, P., Wittbrodt, J., Gilmour, D. & Peri, F. (2014) Distinct roles for BAI1 and TIM-4 in the engulfment of dying neurons by microglia. *Nature Communications*, 5(1), 4046.

Mazzolini, J., Le Clerc, S., Morisse, G., Coulonges, C., Kuil, L. E., van Ham, T. J., Zagury, J.-F. & Sieger, D. (2020) Gene expression profiling reveals a conserved microglia signature in larval zebrafish. *Glia*, 68(2), 298-315.

McArthur, S., Gobbetti, T., Kusters, D. H., Reutelingsperger, C. P., Flower, R. J. & Perretti, M. (2015) Definition of a Novel Pathway Centered on Lysophosphatidic Acid To Recruit Monocytes during the Resolution Phase of Tissue Inflammation. *J Immunol*, 195(3), 1139-51.

McCormack, R., de Armas, L. R., Shiratsuchi, M., Ramos, J. E. & Podack, E. R. (2013) Inhibition of Intracellular Bacterial Replication in Fibroblasts Is Dependent on the Perforin-Like Protein (Perforin-2) Encoded by Macrophage-Expressed Gene 1. *Journal of Innate Immunity*, 5(2), 185-194.

McCormack, R. M., de Armas, L. R., Shiratsuchi, M., Fiorentino, D. G., Olsson, M. L., Lichtenheld, M. G., Morales, A., Lyapichev, K., Gonzalez, L. E., Strbo, N., Sukumar, N., Stojadinovic, O., Plano, G. V., Munson, G. P., Tomic-Canic, M., Kirsner, R. S., Russell, D. G. & Podack, E. R. (2015) Perforin-2 is essential for intracellular defense of parenchymal cells and phagocytes against pathogenic bacteria. *Elife*, 4.

McDonald, J. W. & Sadowsky, C. (2002) Spinal-cord injury. *The Lancet*, 359(9304), 417-425.

McKerracher, L. a., David, S., Jackson, D., Kottis, V., Dunn, R. & Braun, P. (1994) Identification of myelin-associated glycoprotein as a major myelin-derived inhibitor of neurite growth. *Neuron*, 13(4), 805-811.

Meijer, A. H., van der Sar, A. M., Cunha, C., Lamers, G. E. M., Laplante, M. A., Kikuta, H., Bitter, W., Becker, T. S. & Spaink, H. P. (2008) Identification and real-time imaging of a myc-expressing neutrophil population involved in inflammation and mycobacterial granuloma formation in zebrafish. *Developmental & Comparative Immunology*, 32(1), 36-49.

Meletis, K., Barnabé-Heider, F., Carlén, M., Evergren, E., Tomilin, N., Shupliakov, O. & Frisén, J. (2008) Spinal Cord Injury Reveals Multilineage Differentiation of Ependymal Cells. *PLOS Biology*, 6(7), e182.

Meller, J., Chen, Z., Dudiki, T., Cull, R. M., Murtazina, R., Bal, S. K., Pluskota, E., Stefl, S., Plow, E. F., Trapp, B. D. & Byzova, T. V. (2017) Integrin-Kindlin3 requirements for microglial motility in vivo are distinct from those for macrophages. *JCI Insight*, 2(11).

Mojzesz, M., Widziolek, M., Adamek, M., Orzechowska, U., Podlasz, P., Prajsnar, T. K., Pooranachandran, N., Pecio, A., Michalik, A., Surachetpong, W., Chadzinska, M. & Rakus, K. (2021) Tilapia Lake Virus-Induced Neuroinflammation in Zebrafish: Microglia Activation and Sickness Behavior. *Frontiers in immunology*, 12, 760882-760882.

Mokalled, M. H., Patra, C., Dickson, A. L., Endo, T., Stainier, D. Y. R. & Poss, K. D. (2016) Injury-induced ctgfa directs glial bridging and spinal cord regeneration in zebrafish. *Science*, 354(6312), 630-634.

Mondal, B., Jin, H., Kallappagoudar, S., Sedkov, Y., Martinez, T., Sentmanat, M. F., Poet, G. J., Li, C., Fan, Y., Pruett-Miller, S. M. & Herz, H. M. (2020) The histone deacetylase complex MiDAC regulates a neurodevelopmental gene expression program to control neurite outgrowth. *Elife*, 9.

Monje, M. L., Toda, H. & Palmer, T. D. (2003a) Inflammatory blockade restores adult hippocampal neurogenesis. *Science*, 302(5651), 1760-5.

Monje, P., Marinissen, M. J. & Gutkind, J. S. (2003b) Phosphorylation of the carboxyl-terminal transactivation domain of c-Fos by extracellular signal-regulated kinase mediates the transcriptional activation of AP-1 and cellular transformation induced by platelet-derived growth factor. *Mol Cell Biol*, 23(19), 7030-43.

Moraes, L. A., Kar, S., Foo, S. L., Gu, T., Toh, Y. Q., Ampomah, P. B., Sachaphibulkij, K., Yap, G., Zharkova, O., Lukman, H. M., Fairhurst, A.-M., Kumar, A. P. & Lim, L. H. K. (2017) Annexin-A1 enhances breast cancer growth and migration by promoting alternative macrophage polarization in the tumour microenvironment. *Scientific Reports*, 7(1), 17925.

Moran-Rivard, L., Kagawa, T., Saueressig, H., Gross, M. K., Burrill, J. & Goulding, M. (2001) Evx1 is a postmitotic determinant of v0 interneuron identity in the spinal cord. *Neuron*, 29(2), 385-99.

Moreno-Manzano, V., Rodríguez-Jiménez, F. J., García-Roselló, M., Laínez, S., Erceg, S., Calvo, M. T., Ronaghi, M., Lloret, M., Planells-Cases, R., Sánchez-Puelles, J. M. & Stojkovic, M. (2009) Activated Spinal Cord Ependymal Stem Cells Rescue Neurological Function. *Stem Cells*, 27(3), 733-743.

Mori, T., Buffo, A. & Götz, M. (2005) The Novel Roles of Glial Cells Revisited: The Contribution of Radial Glia and Astrocytes to Neurogenesis, *Current Topics in Developmental Biology*Academic Press, 67-99.

Morita, H., Ishibashi, T. & Yamashita, S. (1961) Synaptic Transmission in Neurosecretory Cells. *Nature*, 191(4784), 183-183.

Morsch, M., Radford, R., Lee, A., Don, E. K., Badrock, A. P., Hall, T. E., Cole, N. J. & Chung, R. (2015) In vivo characterization of microglial engulfment of dying neurons in the zebrafish spinal cord. *Frontiers in cellular neuroscience*, 9, 321-321.

Moyse, B. R. & Richardson, R. J. (2020) A Population of Injury-Responsive Lymphoid Cells Expresses mpeg1.1 in the Adult Zebrafish Heart. *Immunohorizons*, 4(8), 464-474.

Muire, P. J., Hanson, L., Yoder, J. & Petrie-Hanson, L. (2016) Transcript analysis of natural killer (NK) cell specific genes in the liver, kidney and spleen tissues of rag1^{−/−} mutant zebrafish in response to in vivo administration of TLR ligands. *The Journal of Immunology*, 196(1 Supplement), 216.4.

Muñoz, R., Edwards-Faret, G., Moreno, M., Zuñiga, N., Cline, H. & Larraín, J. (2015) Regeneration of Xenopus laevis spinal cord requires Sox2/3 expressing cells. *Developmental biology*, 408(2), 229-243.

Myers, P. Z., Eisen, J. S. & Westerfield, M. (1986) Development and axonal outgrowth of identified motoneurons in the zebrafish. *The Journal of Neuroscience*, 6(8), 2278.

Nakagawa, T., Sasahara, M., Hayase, Y., Haneda, M., Yasuda, H., Kikkawa, R., Higashiyama, S. & Hazama, F. (1998) Neuronal and glial expression of heparin-binding EGF-like growth factor in central nervous system of prenatal and early postnatal rat. *Developmental Brain Research*, 108(1), 263-272.

Nelson, C. M., Ackerman, K. M., Hayer, P., Bailey, T. J., Gorsuch, R. A. & Hyde, D. R. (2013) Tumor Necrosis Factor-Alpha Is Produced by Dying Retinal Neurons and Is Required for Müller Glia Proliferation during Zebrafish Retinal Regeneration. *The Journal of Neuroscience*, 33(15), 6524.

New, M., Van Acker, T., Sakamaki, J. I., Jiang, M., Saunders, R. E., Long, J., Wang, V. M., Behrens, A., Cerveira, J., Sudhakar, P., Korcsmaros, T., Jefferies, H. B. J., Ryan, K. M., Howell, M. & Tooze, S. A. (2019) MDH1 and MPP7 Regulate Autophagy in Pancreatic Ductal Adenocarcinoma. *Cancer Res*, 79(8), 1884-1898.

Nguyen-Chi, M., Laplace-Builhé, B., Travnickova, J., Luz-Crawford, P., Tejedor, G., Lutfalla, G., Kissa, K., Jorgensen, C. & Djouad, F. (2017) TNF signaling and macrophages govern fin regeneration in zebrafish larvae. *Cell Death Dis*, 8(8), e2979.

Nguyen-Chi, M., Laplace-Builhe, B., Travnickova, J., Luz-Crawford, P., Tejedor, G., Phan, Q. T., Duroux-Richard, I., Levraud, J.-P., Kissa, K., Lutfalla, G., Jorgensen, C. & Djouad, F. (2015) Identification of polarized macrophage subsets in zebrafish. *eLife*, 4, e07288.

Nguyen-Chi, M., Phan, Q. T., Gonzalez, C., Dubremetz, J. F., Levraud, J. P. & Lutfalla, G. (2014) Transient infection of the zebrafish notochord with E. coli induces chronic inflammation. *Dis Model Mech*, 7(7), 871-82.

Nogueira-Rodrigues, J., Leite, S. C., Pinto-Costa, R., Sousa, S. C., Luz, L. L., Sintra, M. A., Oliveira, R., Monteiro, A. C., Pinheiro, G. G., Vitorino, M., Silva, J. A., Simão, S., Fernandes, V. E., Provazník, J., Benes, V., Cruz, C. D., Safronov, B. V., Magalhães, A., Reis, C. A., Vieira, J., Vieira, C. P., Tiscórnia, G., Araújo, I. M. & Sousa, M. M. (2021) Rewired glycosylation activity promotes scarless regeneration and functional recovery in spiny mice after complete spinal cord transection. *Developmental Cell*.

Norrby, K. (2002) Mast cells and angiogenesis. *APMIS*, 110(5), 355-371.

O'Malley, D. M., Kao, Y.-H. & Fetcho, J. R. (1996) Imaging the Functional Organization of Zebrafish Hindbrain Segments during Escape Behaviors. *Neuron*, 17(6), 1145-1155.

Odenthal, J. & Nüsslein-Volhard, C. (1998) fork head domain genes in zebrafish. *Development Genes and Evolution*, 208(5), 245-258.

Odenthal, J., van Eeden, F. J. M., Haffter, P., Ingham, P. W. & Nüsslein-Volhard, C. (2000) Two Distinct Cell Populations in the Floor Plate of the Zebrafish Are Induced by Different Pathways. *Developmental Biology*, 219(2), 350-363.

Ogai, K., Kuwana, A., Hisano, S., Nagashima, M., Koriyama, Y., Sugitani, K., Mawatari, K., Nakashima, H. & Kato, S. (2014) Upregulation of Leukemia Inhibitory Factor (LIF) during the Early Stage of Optic Nerve Regeneration in Zebrafish. *PLOS ONE*, 9(8), e106010.

Ohnmacht, J., Yang, Y., Maurer, G. W., Barreiro-Iglesias, A., Tsarouchas, T. M., Wehner, D., Sieger, D., Becker, C. G. & Becker, T. (2016) Spinal motor neurons are regenerated after mechanical lesion and genetic ablation in larval zebrafish. *Development*, 143(9), 1464-1474.

Ohri, S. S., Maddie, M. A., Zhao, Y., Qiu, M. S., Hetman, M. & Whittemore, S. R. (2011) Attenuating the endoplasmic reticulum stress response improves functional recovery after spinal cord injury. *Glia*, 59(10), 1489-1502.

Oosterhof, N., Holtman, I. R., Kuil, L. E., van der Linde, H. C., Boddeke, E. W. G. M., Eggen, B. J. L. & van Ham, T. J. (2017) Identification of a conserved and acute neurodegeneration-specific microglial transcriptome in the zebrafish. *Glia*, 65(1), 138-149.

Oosterhof, N., Kuil, L. E., van der Linde, H. C., Burm, S. M., Berdowski, W., van Ijcken, W. F. J., van Swieten, J. C., Hol, E. M., Verheijen, M. H. G. & van Ham, T. J. (2018) Colony-Stimulating Factor 1 Receptor (CSF1R) Regulates Microglia Density

and Distribution, but Not Microglia Differentiation In Vivo. *Cell Reports*, 24(5), 1203-1217.e6.

Osorio, D. & Cai, J. J. (2020) Systematic determination of the mitochondrial proportion in human and mice tissues for single-cell RNA-sequencing data quality control. *Bioinformatics*, 37(7), 963-967.

Ouyang, B., Pan, H., Lu, L., Li, J., Stambrook, P., Li, B. & Dai, W. (1997) Human Prk Is a Conserved Protein Serine/Threonine Kinase Involved in Regulating M Phase Functions *. *Journal of Biological Chemistry*, 272(45), 28646-28651.

Palić, D., Andreasen, C. B., Ostojić, J., Tell, R. M. & Roth, J. A. (2007) Zebrafish (Danio rerio) whole kidney assays to measure neutrophil extracellular trap release and degranulation of primary granules. *J Immunol Methods*, 319(1-2), 87-97.

Paredes, R., Ishibashi, S., Borrill, R., Robert, J. & Amaya, E. (2015) Xenopus: An in vivo model for imaging the inflammatory response following injury and bacterial infection. *Dev Biol*, 408(2), 213-28.

Park, D., Han, C. Z., Elliott, M. R., Kinchen, J. M., Trampont, P. C., Das, S., Collins, S., Lysiak, J. J., Hoehn, K. L. & Ravichandran, K. S. (2011) Continued clearance of apoptotic cells critically depends on the phagocyte Ucp2 protein. *Nature*, 477(7363), 220-224.

Park, H.-C., Mehta, A., Richardson, J. S. & Appel, B. (2002) olig2 is required for zebrafish primary motor neuron and oligodendrocyte development. *Developmental biology*, 248(2), 356-368.

Park, H.-C., Shin, J., Roberts, R. K. & Appel, B. (2007) An olig2 reporter gene marks oligodendrocyte precursors in the postembryonic spinal cord of zebrafish. *Developmental Dynamics*, 236(12), 3402-3407.

Parmentier, C., Taxi, J., Balment, R., Nicolas, G. & Calas, A. (2006) Caudal neurosecretory system of the zebrafish: ultrastructural organization and immunocytochemical detection of urotensins. *Cell Tissue Res*, 325(1), 111-24.

Patton, E. E. & Tobin, D. M. (2019) Spotlight on zebrafish: the next wave of translational research. *Dis Model Mech*, 12(3).

Pelzer, D., Phipps, L. S., Thuret, R., Gallardo-Dodd, C. J., Baker, S. M. & Dorey, K. (2021) Foxm1 regulates neural progenitor fate during spinal cord regeneration. *EMBO Rep*, 22(9), e50932.

Penas, C., Guzmán, M.-S., Verdú, E., Forés, J., Navarro, X. & Casas, C. (2007) Spinal cord injury induces endoplasmic reticulum stress with different cell-type dependent response. *Journal of Neurochemistry*, 102(4), 1242-1255.

Peng, S.-x., Yao, L., Cui, C., Zhao, H.-d., Liu, C.-j., Li, Y.-h., Wang, L.-f., Huang, S.-b. & Shen, Y.-q. (2017) Semaphorin4D promotes axon regrowth and swimming ability during recovery following zebrafish spinal cord injury. *Neuroscience*, 351, 36-46.

Pérez-Martínez, L. & Jaworski, D. M. (2005) Tissue inhibitor of metalloproteinase-2 promotes neuronal differentiation by acting as an anti-mitogenic signal. *J Neurosci*, 25(20), 4917-29.

Peri, F. & Nüsslein-Volhard, C. (2008) Live Imaging of Neuronal Degradation by Microglia Reveals a Role for v0-ATPase a1 in Phagosomal Fusion In Vivo. *Cell*, 133(5), 916-927.

Persson, E., Voznesensky, O. S., Huang, Y. F. & Lerner, U. H. (2005) Increased expression of interleukin-6 by vasoactive intestinal peptide is associated with regulation of CREB, AP-1 and C/EBP, but not NF-kappaB, in mouse calvarial osteoblasts. *Bone*, 37(4), 513-29.

Petersen, A., Soderstrom, M., Saha, B. & Sharma, P. (2021) Animal models of traumatic brain injury: a review of pathophysiology to biomarkers and treatments. *Experimental Brain Research*, 239(10), 2939-2950.

Phipps, L. S., Marshall, L., Dorey, K. & Amaya, E. (2020) Model systems for regeneration: Xenopus. *Development*, 147(6), dev180844.

Picelli, S., Faridani, O. R., Björklund, Å. K., Winberg, G., Sagasser, S. & Sandberg, R. (2014) Full-length RNA-seq from single cells using Smart-seq2. *Nature Protocols*, 9(1), 171-181.

Picker, A., Scholpp, S., Böhli, H., Takeda, H. & Brand, M. (2002) A novel positive transcriptional feedback loop in midbrain-hindbrain boundary development is revealed through analysis of the zebrafish pax2.1 promoter in transgenic lines. *Development*, 129(13), 3227-39.

Pierfelice, T., Alberi, L. & Gaiano, N. (2011) Notch in the Vertebrate Nervous System: An Old Dog with New Tricks. *Neuron*, 69(5), 840-855.

Pillai, A., Mansouri, A., Behringer, R., Westphal, H. & Goulding, M. (2007) Lhx1 and Lhx5 maintain the inhibitory-neurotransmitter status of interneurons in the dorsal spinal cord. *Development*, 134(2), 357-366.

Popovich, P. G., Guan, Z., Wei, P., Huitinga, I., van Rooijen, N. & Stokes, B. T. (1999) Depletion of hematogenous macrophages promotes partial hindlimb recovery and neuroanatomical repair after experimental spinal cord injury. *Experimental neurology*, 158(2), 351-365.

Post, M. W. & van Leeuwen, C. M. (2012) Psychosocial issues in spinal cord injury: a review. *Spinal Cord*, 50(5), 382-9.

Powner, D., Kopp, P. M., Monkley, S. J., Critchley, D. R. & Berditchevski, F. (2011) Tetraspanin CD9 in cell migration. *Biochem Soc Trans*, 39(2), 563-7.

Prame Kumar, K., Nicholls, A. J. & Wong, C. H. Y. (2018) Partners in crime: neutrophils and monocytes/macrophages in inflammation and disease. *Cell Tissue Res*, 371(3), 551-565.

Prinz, M., Erny, D. & Hagemeyer, N. (2017) Ontogeny and homeostasis of CNS myeloid cells. *Nature Immunology*, 18(4), 385-392.

Puls, B., Ding, Y., Zhang, F., Pan, M., Lei, Z., Pei, Z., Jiang, M., Bai, Y., Forsyth, C., Metzger, M., Rana, T., Zhang, L., Ding, X., Keefe, M., Cai, A., Redilla, A., Lai, M., He, K., Li, H. & Chen, G. (2020) Regeneration of Functional Neurons After Spinal Cord Injury via in situ NeuroD1-Mediated Astrocyte-to-Neuron Conversion. *Frontiers in Cell and Developmental Biology*, 8.

Qi, Y., Andolfi, L., Frattini, F., Mayer, F., Lazzarino, M. & Hu, J. (2015) Membrane stiffening by STOML3 facilitates mechanosensation in sensory neurons. *Nat Commun*, 6, 8512.

Raj, B., Wagner, D. E., McKenna, A., Pandey, S., Klein, A. M., Shendure, J., Gagnon, J. A. & Schier, A. F. (2018) Simultaneous single-cell profiling of lineages and cell types in the vertebrate brain. *Nat Biotechnol*, 36(5), 442-450.

Ramer, L. M., Ramer, M. S. & Bradbury, E. J. (2014) Restoring function after spinal cord injury: towards clinical translation of experimental strategies. *The Lancet Neurology*, 13(12), 1241-1256.

Ramilowski, J. A., Goldberg, T., Harshbarger, J., Kloppmann, E., Lizio, M., Satagopam, V. P., Itoh, M., Kawaji, H., Carninci, P., Rost, B. & Forrest, A. R. (2015) A draft network of ligand-receptor-mediated multicellular signalling in human. *Nat Commun*, 6, 7866.

Ravanelli, A. M. & Appel, B. (2015) Motor neurons and oligodendrocytes arise from distinct cell lineages by progenitor recruitment. *Genes & Development*, 29(23), 2504-2515.

Reade, A., Motta-Mena, L. B., Gardner, K. H., Stainier, D. Y., Weiner, O. D. & Woo, S. (2017) TAEL: a zebrafish-optimized optogenetic gene expression system with fine spatial and temporal control. *Development*, 144(2), 345-355.

Recalcati, S., Invernizzi, P., Arosio, P. & Cairo, G. (2008) New functions for an iron storage protein: The role of ferritin in immunity and autoimmunity. *Journal of Autoimmunity*, 30(1), 84-89.

Reimer, M. M., Kuscha, V., Wyatt, C., Sörensen, I., Frank, R. E., Knüwer, M., Becker, T. & Becker, C. G. (2009) Sonic Hedgehog Is a Polarized Signal for Motor Neuron Regeneration in Adult Zebrafish. *The Journal of Neuroscience*, 29(48), 15073-15082.

Reimer, Michell M., Norris, A., Ohnmacht, J., Patani, R., Zhong, Z., Dias, Tatyana B., Kuscha, V., Scott, Angela L., Chen, Y.-C., Rozov, S., Frazer, Sarah L., Wyatt, C., Higashijima, S.-i., Patton, E. E., Panula, P., Chandran, S., Becker, T. & Becker, Catherina G. (2013) Dopamine from the Brain Promotes Spinal Motor Neuron Generation during Development and Adult Regeneration. *Developmental Cell*, 25(5), 478-491.

Reimer, M. M., Sörensen, I., Kuscha, V., Frank, R. E., Liu, C., Becker, C. G. & Becker, T. (2008) Motor Neuron Regeneration in Adult Zebrafish. *The Journal of Neuroscience*, 28(34), 8510-8516.

Reitz, A., Tobe, V., Knapp, P. A. & Schurch, B. (2004) Impact of spinal cord injury on sexual health and quality of life. *International Journal of Impotence Research*, 16(2), 167-174.

Ren, Y., Ao, Y., O'Shea, T. M., Burda, J. E., Bernstein, A. M., Brumm, A. J., Muthusamy, N., Ghashghaei, H. T., Carmichael, S. T., Cheng, L. & Sofroniew, M. V. (2017) Ependymal cell contribution to scar formation after spinal cord injury is minimal, local and dependent on direct ependymal injury. *Scientific Reports*, 7(1), 41122.

Renault, T., Faury, N., Barbosa-Solomieu, V. & Moreau, K. (2011) Suppression substractive hybridisation (SSH) and real time PCR reveal differential gene expression in the Pacific cupped oyster, Crassostrea gigas, challenged with Ostreid herpesvirus 1. *Developmental & Comparative Immunology*, 35(7), 725-735.

Renshaw, S. A. & Trede, N. S. (2012) A model 450 million years in the making: zebrafish and vertebrate immunity. *Disease Models & Mechanisms*, 5(1), 38-47.

Rose-John, S. (2018) Interleukin-6 Family Cytokines. *Cold Spring Harb Perspect Biol*, 10(2).

Rossi, F., Casano, Alessandra M., Henke, K., Richter, K. & Peri, F. (2015) The SLC7A7 Transporter Identifies Microglial Precursors prior to Entry into the Brain. *Cell Reports*, 11(7), 1008-1017.

Rothenaigner, I., Krecsmarik, M., Hayes, J. A., Bahn, B., Lepier, A., Fortin, G., Götz, M., Jagasia, R. & Bally-Cuif, L. (2011) Clonal analysis by distinct viral vectors identifies bona fide neural stem cells in the adult zebrafish telencephalon and characterizes their division properties and fate. *Development*, 138(8), 1459-1469.

Rougeot, J., Torraca, V., Zakrzewska, A., Kanwal, Z., Jansen, H. J., Sommer, F., Spaink, H. P. & Meijer, A. H. (2019) RNAseq Profiling of Leukocyte Populations in Zebrafish Larvae Reveals a cxcl11 Chemokine Gene as a Marker of Macrophage Polarization During Mycobacterial Infection. *Front Immunol*, 10, 832.

Sabin, K., Santos-Ferreira, T., Essig, J., Rudasill, S. & Echeverri, K. (2015) Dynamic membrane depolarization is an early regulator of ependymoglial cell response to spinal cord injury in axolotl. *Developmental Biology*, 408(1), 14-25.

Saito, A., Kanemoto, S., Kawasaki, N., Asada, R., Iwamoto, H., Oki, M., Miyagi, H., Izumi, S., Sanosaka, T., Nakashima, K. & Imaizumi, K. (2012) Unfolded protein response, activated by OASIS family transcription factors, promotes astrocyte differentiation. *Nature Communications*, 3(1), 967.

Saleh, A., Smith, D. R., Balakrishnan, S., Dunn, L., Martens, C., Tweed, C. W. & Fernyhough, P. (2011) Tumor necrosis factor-α elevates neurite outgrowth through an NF-κB-dependent pathway in cultured adult sensory neurons: Diminished expression in diabetes may contribute to sensory neuropathy. *Brain Res*, 1423, 87-95.

Sanderson, L. E., Lanko, K., Alsagob, M., Almass, R., Al-Ahmadi, N., Najafi, M., Al-Muhaizea, M. A., Alzaidan, H., AlDhalaan, H., Perenthaler, E., van der Linde, H. C., Nikoncuk, A., Kühn, N. A., Antony, D., Owaidah, T. M., Raskin, S., Vieira, L. G. D.

R., Mombach, R., Ahangari, N., Silveira, T. R. D., Ameziane, N., Rolfs, A., Alharbi, A., Sabbagh, R. M., AlAhmadi, K., Alawam, B., Ghebeh, H., AlHargan, A., Albader, A. A., Binhumaid, F. S., Goljan, E., Monies, D., Mustafa, O. M., Aldosary, M., AlBakheet, A., Alyounes, B., Almutairi, F., Al-Odaib, A., Aksoy, D. B., Basak, A. N., Palvadeau, R., Trabzuni, D., Rosenfeld, J. A., Karimiani, E. G., Meyer, B. F., Karakas, B., Al-Mohanna, F., Arold, S. T., Colak, D., Maroofian, R., Houlden, H., Bertoli-Avella, A. M., Schmidts, M., Barakat, T. S., van Ham, T. J. & Kaya, N. (2021) Bi-allelic variants in HOPS complex subunit VPS41 cause cerebellar ataxia and abnormal membrane trafficking. *Brain*, 144(3), 769-780.

Sanz-Morejón, A., García-Redondo, A. B., Reuter, H., Marques, I. J., Bates, T., Galardi-Castilla, M., Große, A., Manig, S., Langa, X., Ernst, A., Piragyte, I., Botos, M.-A., González-Rosa, J. M., Ruiz-Ortega, M., Briones, A. M., Salaices, M., Englert, C. & Mercader, N. (2019) Wilms Tumor 1b Expression Defines a Pro-regenerative Macrophage Subtype and Is Required for Organ Regeneration in the Zebrafish. *Cell Reports*, 28(5), 1296-1306.e6.

Schainberg, H., Borish, L., King, M., Rocklin, R. E. & Rosenwasser, L. J. (1988) Leukocyte inhibitory factor stimulates neutrophil-endothelial cell adhesion. *J Immunol*, 141(9), 3055-60.

Schier, A. F. & Talbot, W. S. (2005) Molecular Genetics of Axis Formation in Zebrafish. *Annual Review of Genetics*, 39(1), 561-613.

Schmidt, R., Strähle, U. & Scholpp, S. (2013) Neurogenesis in zebrafish – from embryo to adult. *Neural Development*, 8(1), 3.

Schmitz, B., Papan, C. & Campos-Ortega, J. A. (1993) Neurulation in the anterior trunk region of the zebrafish Brachydanio rerio. *Roux's archives of developmental biology*, 202(5), 250-259.

Scholtens, D. & von Heydebreck, A. (2005) Analysis of Differential Gene Expression Studies, in Gentleman, R., Carey, V. J., Huber, W., Irizarry, R. A. & Dudoit, S. (eds), *Bioinformatics and Computational Biology Solutions Using R and Bioconductor*. New York, NY: Springer New York, 229-248.

Schwab, J. M., Zhang, Y., Kopp, M. A., Brommer, B. & Popovich, P. G. (2014) The paradox of chronic neuroinflammation, systemic immune suppression, autoimmunity after traumatic chronic spinal cord injury. *Experimental neurology*, 258, 121-129.

Schwartz, M., Solomon, A., Lavie, V., Ben-Bassat, S., Belkin, M. & Cohen, A. (1991) Tumor necrosis factor facilitates regeneration of injured central nervous system axons. *Brain Research*, 545(1), 334-338.

See, P., Dutertre, C.-A., Chen, J., Günther, P., McGovern, N., Irac Sergio, E., Gunawan, M., Beyer, M., Händler, K., Duan, K., Sumatoh Hermi Rizal, B., Ruffin, N., Jouve, M., Gea-Mallorquí, E., Hennekam Raoul, C. M., Lim, T., Yip Chan, C., Wen, M., Malleret, B., Low, I., Shadan Nurhidaya, B., Fen Charlene Foong, S., Tay, A., Lum, J., Zolezzi, F., Larbi, A., Poidinger, M., Chan Jerry, K. Y., Chen, Q., Rénia, L., Haniffa, M., Benaroch, P., Schlitzer, A., Schultze Joachim, L., Newell Evan, W. & Ginhoux, F. (2017) Mapping the human DC lineage through the integration of high-dimensional techniques. *Science*, 356(6342), eaag3009.

Sharma, H. S., Winkler, T., Stålberg, E., Gordh, T., Alm, P. & Westman, J. (2003) Topical application of TNF-α antiserum attenuates spinal cord trauma induced edema formation, microvascular permeability disturbances and cell injury in the rat, *Brain Edema XII*. Vienna, 2003//. Springer Vienna.

Sharma, K., Sheng, H. Z., Lettieri, K., Li, H., Karavanov, A., Potter, S., Westphal, H. & Pfaff, S. L. (1998) LIM homeodomain factors Lhx3 and Lhx4 assign subtype identities for motor neurons. *Cell*, 95(6), 817-28.

Sharman, J. L., Benson, H. E., Pawson, A. J., Lukito, V., Mpamhanga, C. P., Bombail, V., Davenport, A. P., Peters, J. A., Spedding, M., Harmar, A. J. & Nc, I. (2013) IUPHAR-DB: updated database content and new features. *Nucleic Acids Research*, 41(D1), D1083-D1088.

Shaulian, E. & Karin, M. (2001) AP-1 in cell proliferation and survival. *Oncogene*, 20(19), 2390-400.

Shihabuddin, L. S., Horner, P. J., Ray, J. & Gage, F. H. (2000) Adult Spinal Cord Stem Cells Generate Neurons after Transplantation in the Adult Dentate Gyrus. *The Journal of Neuroscience*, 20(23), 8727.

Shin, J., Park, H.-C., Topczewska, J. M., Mawdsley, D. J. & Appel, B. (2003) Neural cell fate analysis in zebrafish using olig2 BAC transgenics. *Methods in Cell Science*, 25(1), 7-14.

Sieger, D., Moritz, C., Ziegenhals, T., Prykhozhij, S. & Peri, F. (2012) Long-Range Ca2+ Waves Transmit Brain-Damage Signals to Microglia. *Developmental Cell*, 22(6), 1138-1148.

Silva, N. J., Dorman, L. C., Vainchtein, I. D., Horneck, N. C. & Molofsky, A. V. (2021) In situ and transcriptomic identification of microglia in synapse-rich regions of the developing zebrafish brain. *Nature communications*, 12(1), 5916-5916.

Simkin, J., Gawriluk, T. R., Gensel, J. C. & Seifert, A. W. (2017) Macrophages are necessary for epimorphic regeneration in African spiny mice. *eLife*, 6, e24623.

Slanchev, K., Carney, T. J., Stemmler, M. P., Koschorz, B., Amsterdam, A., Schwarz, H. & Hammerschmidt, M. (2009) The Epithelial Cell Adhesion Molecule EpCAM Is Required for Epithelial Morphogenesis and Integrity during Zebrafish Epiboly and Skin Development. *PLOS Genetics*, 5(7), e1000563.

Sofroniew, M. V. (2018) Dissecting spinal cord regeneration. *Nature*, 557(7705), 343-350.

Soneson, C. & Robinson, M. D. (2018) Bias, robustness and scalability in single-cell differential expression analysis. *Nature Methods*, 15(4), 255-261.

Song, H.-D., Sun, X.-J., Deng, M., Zhang, G.-W., Zhou, Y., Wu, X.-Y., Sheng, Y., Chen, Y., Ruan, Z., Jiang, C.-L., Fan, H.-Y., Zon Leonard, I., Kanki John, P., Liu Ting, X., Look, A. T. & Chen, Z. (2004) Hematopoietic gene expression profile in zebrafish kidney marrow. *Proceedings of the National Academy of Sciences*, 101(46), 16240-16245.

Soza-Ried, C., Hess, I., Netuschil, N., Schorpp, M. & Boehm, T. (2010) Essential role of c-myb in definitive hematopoiesis is evolutionarily conserved. *Proceedings of the National Academy of Sciences*, 107(40), 17304-17308.

Spilsbury, K., O'Mara, M.-A., Wu, W. M., Rowe, P. B., Symonds, G. & Takayama, Y. (1995) Isolation of a Novel Macrophage-Specific Gene by Differential cDNA Analysis. *Blood*, 85(6), 1620-1629.

Squair, J. W., Gautier, M., Kathe, C., Anderson, M. A., James, N. D., Hutson, T. H., Hudelle, R., Qaiser, T., Matson, K. J. E., Barraud, Q., Levine, A. J., La Manno, G., Skinnider, M. A. & Courtine, G. (2021) Confronting false discoveries in single-cell differential expression. *Nature Communications*, 12(1), 5692.

Stachura, D. L. & Traver, D. (2011) Chapter 4 - Cellular Dissection of Zebrafish Hematopoiesis, in Detrich, H. W., Westerfield, M. & Zon, L. I. (eds), *Methods in Cell Biology*Academic Press, 75-110.

Stanton, S. E., McReynolds, L. J., Evans, T. & Schreiber-Agus, N. (2006) Yaf2 Inhibits Caspase 8-mediated Apoptosis and Regulates Cell Survival during Zebrafish Embryogenesis*. *Journal of Biological Chemistry*, 281(39), 28782-28793.

Stenudd, M., Sabelström, H., Llorens-Bobadilla, E., Zamboni, M., Blom, H., Brismar, H., Zhang, S., Basak, O., Clevers, H., Göritz, C., Barnabé-Heider, F. & Frisén, J. (2022) Identification of a discrete subpopulation of spinal cord ependymal cells with neural stem cell properties. *Cell Rep*, 38(9), 110440.

Stirling, D. P., Liu, S., Kubes, P. & Yong, V. W. (2009) Depletion of Ly6G/Gr-1 leukocytes after spinal cord injury in mice alters wound healing and worsens neurological outcome. *J Neurosci*, 29(3), 753-64.

Stolt, C. C., Rehberg, S., Ader, M., Lommes, P., Riethmacher, D., Schachner, M., Bartsch, U. & Wegner, M. (2002) Terminal differentiation of myelin-forming oligodendrocytes depends on the transcription factor Sox10. *Genes & development*, 16(2), 165-170.

Streeter, K. A., Sunshine, M. D., Brant, J. O., Sandoval, A. G. W., Maden, M. & Fuller, D. D. (2020) Molecular and histologic outcomes following spinal cord injury in spiny mice, Acomys cahirinus. *Journal of Comparative Neurology*, 528(9), 1535-1547.

Stuart, T., Butler, A., Hoffman, P., Hafemeister, C., Papalexi, E., Mauck, W. M., III, Hao, Y., Stoeckius, M., Smibert, P. & Satija, R. (2019) Comprehensive Integration of Single-Cell Data. *Cell*, 177(7), 1888-1902.e21.

Su, Z., Niu, W., Liu, M.-L., Zou, Y. & Zhang, C.-L. (2014) In vivo conversion of astrocytes to neurons in the injured adult spinal cord. *Nature Communications*, 5(1), 3338.

Sun, N., Petiwala, S., Wang, R., Lu, C., Hu, M., Ghosh, S., Hao, Y., Miller, C. P. & Chung, N. (2019) Development of drug-inducible CRISPR-Cas9 systems for large-scale functional screening. *BMC Genomics*, 20(1), 225.

Sundqvist, A., Vasilaki, E., Voytyuk, O., Bai, Y., Morikawa, M., Moustakas, A., Miyazono, K., Heldin, C.-H., ten Dijke, P. & van Dam, H. (2020) TGFβ and EGF signaling orchestrates the AP-1- and p63 transcriptional regulation of breast cancer invasiveness. *Oncogene*, 39(22), 4436-4449.

Suzuki, M., Tachibana, I., Takeda, Y., He, P., Minami, S., Iwasaki, T., Kida, H., Goya, S., Kijima, T., Yoshida, M., Kumagai, T., Osaki, T. & Kawase, I. (2009) Tetraspanin CD9 Negatively Regulates Lipopolysaccharide-Induced Macrophage Activation and Lung Inflammation. *The Journal of Immunology*, 182(10), 6485.

Svahn, A. J., Graeber, M. B., Ellett, F., Lieschke, G. J., Rinkwitz, S., Bennett, M. R. & Becker, T. S. (2013) Development of ramified microglia from early macrophages in the zebrafish optic tectum. *Developmental Neurobiology*, 73(1), 60-71.

Tannenbaum, J. & Bennett, B. T. (2015) Russell and Burch's 3Rs then and now: the need for clarity in definition and purpose. *J Am Assoc Lab Anim Sci*, 54(2), 120-32.

Tao, Y., Ruan, H., Guo, X., Li, L. & Shen, W. (2015) HDAC1 Regulates the Proliferation of Radial Glial Cells in the Developing Xenopus Tectum. *PLOS ONE*, 10(3), e0120118.

Tauzin, S., Starnes, T. W., Becker, F. B., Lam, P.-y. & Huttenlocher, A. (2014) Redox and Src family kinase signaling control leukocyte wound attraction and neutrophil reverse migration. *Journal of Cell Biology*, 207(5), 589-598.

Terman, J. R., Wang, X. M. & Martin, G. F. (1996) Growth of dorsal spinocerebellar axons through a lesion of their spinal pathway during early development in the North American opossum, Didelphis virginiana. *Developmental Brain Research*, 93(1), 33-48.

Thiel, W. A., Esposito, E. J., Findley, A. P., Blume, Z. I. & Mitchell, D. M. (2022) Modulation of retinoid-X-receptors differentially regulates expression of apolipoprotein genes apoc1 and apoeb by zebrafish microglia. *Biol Open*, 11(1).

Thomas, M. L. (1989) The Leukocyte Common Antigen Family. *Annual Review of Immunology*, 7(1), 339-369.

Thor, S., Andersson, S. G., Tomlinson, A. & Thomas, J. B. (1999) A LIM-homeodomain combinatorial code for motor-neuron pathway selection. *Nature*, 397(6714), 76-80.

Torraca, V., Otto, N. A., Tavakoli-Tameh, A. & Meijer, A. H. (2017) The inflammatory chemokine Cxcl18b exerts neutrophil-specific chemotaxis via the promiscuous chemokine receptor Cxcr2 in zebrafish. *Developmental & Comparative Immunology*, 67, 57-65.

Torti, F. M. & Torti, S. V. (2002) Regulation of ferritin genes and protein. *Blood*, 99(10), 3505-3516.

Tran, H. T. N., Ang, K. S., Chevrier, M., Zhang, X., Lee, N. Y. S., Goh, M. & Chen, J. (2020) A benchmark of batch-effect correction methods for single-cell RNA sequencing data. *Genome Biology*, 21(1), 12.

Tsarouchas, T. M., Wehner, D., Cavone, L., Munir, T., Keatinge, M., Lambertus, M., Underhill, A., Barrett, T., Kassapis, E., Ogryzko, N., Feng, Y., van Ham, T. J., Becker, T. & Becker, C. G. (2018) Dynamic control of proinflammatory cytokines Il-1β and Tnf-α by macrophages in zebrafish spinal cord regeneration. *Nature Communications*, 9(1), 4670.

Tsujioka, H., Kunieda, T., Katou, Y., Shirahige, K., Fukazawa, T. & Kubo, T. (2017) interleukin-11 induces and maintains progenitors of different cell lineages during Xenopus tadpole tail regeneration. *Nature Communications*, 8(1), 495.

Turner, K. J., Hawkins, T. A., Yáñez, J., Anadón, R., Wilson, S. W. & Folgueira, M. (2016) Afferent Connectivity of the Zebrafish Habenulae. *Frontiers in Neural Circuits*, 10.

Untergasser, A., Cutcutache, I., Koressaar, T., Ye, J., Faircloth, B. C., Remm, M. & Rozen, S. G. (2012) Primer3--new capabilities and interfaces. *Nucleic Acids Res*, 40(15), e115.

Vallejos, C. A., Risso, D., Scialdone, A., Dudoit, S. & Marioni, J. C. (2017) Normalizing single-cell RNA sequencing data: challenges and opportunities. *Nature Methods*, 14(6), 565-571.

van Leeuwen, L. M., van der Kuip, M., Youssef, S. A., de Bruin, A., Bitter, W., van Furth, A. M. & van der Sar, A. M. (2014) Modeling tuberculous meningitis in zebrafish using Mycobacterium marinum. *Disease Models & Mechanisms*, 7(9), 1111-1122.

van Raamsdonk, W., Maslam, S., de Jong, D. H., Smit-Onel, M. J. & Velzing, E. (1998) Long term effects of spinal cord transection in zebrafish: swimming performances, and metabolic properties of the neuromuscular system. *Acta Histochem*, 100, 117-31.

Varshney, G. K., Pei, W., LaFave, M. C., Idol, J., Xu, L., Gallardo, V., Carrington, B., Bishop, K., Jones, M., Li, M., Harper, U., Huang, S. C., Prakash, A., Chen, W., Sood, R., Ledin, J. & Burgess, S. M. (2015) High-throughput gene targeting and phenotyping in zebrafish using CRISPR/Cas9. *Genome Res*, 25(7), 1030-42.

Vassalli, P. (1992) The pathophysiology of tumor necrosis factors. *Annu Rev Immunol*, 10, 411-52.

Vasudevan, D., Liu, Y. C., Barrios, J. P., Wheeler, M. K., Douglass, A. D. & Dorsky, R. I. (2021) Regenerated interneurons integrate into locomotor circuitry following spinal cord injury. *Exp Neurol*, 342, 113737.

Vidak, E., Javoršek, U., Vizovišek, M. & Turk, B. (2019) Cysteine Cathepsins and their Extracellular Roles: Shaping the Microenvironment. *Cells*, 8(3).

Voigt, T. (1989) Development of glial cells in the cerebral wall of ferrets: direct tracing of their transformation from radial glia into astrocytes. *J Comp Neurol*, 289(1), 74-88.

Wajant, H. & Scheurich, P. (2011) TNFR1-induced activation of the classical NF-κB pathway. *The FEBS Journal*, 278(6), 862-876.

Wan, J., Ramachandran, R. & Goldman, D. (2012) HB-EGF is necessary and sufficient for Müller glia dedifferentiation and retina regeneration. *Dev Cell*, 22(2), 334-47.

Wan, Q., Kuang, E., Dong, W., Zhou, S., Xu, H., Qi, Y. & Liu, Y. (2007) Reticulon 3 mediates Bcl-2 accumulation in mitochondria in response to endoplasmic reticulum stress. *Apoptosis*, 12(2), 319-28.

Wang, F., Tidei Joseph, J., Polich Eric, D., Gao, Y., Zhao, H., Perrone-Bizzozero Nora, I., Guo, W. & Zhao, X. (2015) Positive feedback between RNA-binding protein HuD and transcription factor SATB1 promotes neurogenesis. *Proceedings of the National Academy of Sciences*, 112(36), E4995-E5004.

Wang, L.-F., Huang, S.-B., Zhao, H.-D., Liu, C.-J., Yao, L. & Shen, Y.-Q. (2017a) Activating transcription factor 3 promotes spinal cord regeneration of adult zebrafish. *Biochemical and Biophysical Research Communications*, 488(3), 522-527.

Wang, P., Chen, X., Wang, Y., Jia, C., Liu, X., Wang, Y., Wu, H., Cai, H., Shen, H.-M. & Le, W. (2021a) Essential role for autophagy protein VMP1 in maintaining neuronal homeostasis and preventing axonal degeneration. *Cell Death & Disease*, 12(1), 116.

Wang, X., He, Y., Zhang, Q., Ren, X. & Zhang, Z. (2021b) Direct Comparative Analyses of 10X Genomics Chromium and Smart-seq2. *Genomics, Proteomics & Bioinformatics*, 19(2), 253-266.

Wang, Y., Subramanian, M., Yurdagul, A., Barbosa-Lorenzi, V. C., Cai, B., de Juan-Sanz, J., Ryan, T. A., Nomura, M., Maxfield, F. R. & Tabas, I. (2017b) Mitochondrial Fission Promotes the Continued Clearance of Apoptotic Cells by Macrophages. *Cell*, 171(2), 331-345.e22.

Wang, Z., He, X. & Fan, X. (2018) Postnatal administration of memantine rescues TNF-α-induced decreased hippocampal precursor proliferation. *Neuroscience Letters*, 662, 173-180.

Wehner, D., Tsarouchas, T. M., Michael, A., Haase, C., Weidinger, G., Reimer, M. M., Becker, T. & Becker, C. G. (2017a) Wnt signaling controls pro-regenerative Collagen XII in functional spinal cord regeneration in zebrafish. *Nature Communications*, 8(1), 126.

Wehner, D., Tsarouchas, T. M., Michael, A., Haase, C., Weidinger, G., Reimer, M. M., Becker, T. & Becker, C. G. (2017b) Wnt signaling controls pro-regenerative Collagen XII in functional spinal cord regeneration in zebrafish. *Nat Commun*, 8(1), 126.

Wei, X., Fu, S., Li, H., Liu, Y., Wang, S., Feng, W., Yang, Y., Liu, X., Zeng, Y.-Y., Cheng, M., Lai, Y., Qiu, X., Wu, L., Zhang, N., Jiang, Y., Xu, J., Su, X., Peng, C., Han, L., Lou, W. P.-K., Liu, C., Yuan, Y., Ma, K., Yang, T., Pan, X., Gao, S., Chen, A., Esteban, M. A., Yang, H., Wang, J., Fan, G., Liu, L., Chen, L., Xu, X., Fei, J.-F. & Gu, Y. (2021) Spatiotemporal transcriptome at single-cell resolution reveals key radial glial cell population in axolotl telencephalon development and regeneration. *bioRxiv*, 2021.10.23.465550.

Weiss, S., Dunne, C., Hewson, J., Wohl, C., Wheatley, M., Peterson, A. C. & Reynolds, B. A. (1996) Multipotent CNS Stem Cells Are Present in the Adult Mammalian Spinal Cord and Ventricular Neuroaxis. *The Journal of Neuroscience*, 16(23), 7599.

Werb, Z., Chin, J. R., Takemura, R., Oropeza, R. L., Bainton, D. F., Stenberg, P., Taylor, J. M. & Reardon, C. (1986) The Cell and Molecular Biology of Apolipoprotein E Synthesis by Macro Phages, *Ciba Foundation Symposium 118 - Biochemistry of Macrophages*, 155-171.

Westerfield, M. (2007) *The Zebrafish Book. A Guide for the Laboratory Use of Zebrafish (Danio rerio)*, 5 edition. Eugene: University of Oregon Press.

WHO (2013) Internation perspectives on Spinal Cord Injury.

Wiens, M., Korzhev, M., Krasko, A., Thakur, N. L., Perović-Ottstadt, S., Breter, H. J., Ushijima, H., Diehl-Seifert, B., Müller, I. M. & Müller, W. E. (2005) Innate immune defense of the sponge Suberites domuncula against bacteria involves a MyD88-dependent signaling pathway. Induction of a perforin-like molecule. *J Biol Chem*, 280(30), 27949-59.

Willett, C. E., Cortes, A., Zuasti, A. & Zapata, A. G. (1999) Early hematopoiesis and developing lymphoid organs in the zebrafish. *Developmental Dynamics*, 214(4), 323-336.

Wilson, M. A., Gaze, R. M., Goodbrand, I. A. & Taylor, J. S. (1992) Regeneration in the Xenopus tadpole optic nerve is preceded by a massive macrophage/microglial response. *Anat Embryol (Berl)*, 186(1), 75-89.

Wilson, S. W., Ross, L. S., Parrett, T. & Easter, S. S. (1990) The development of a simple scaffold of axon tracts in the brain of the embryonic zebrafish, Brachydanio rerio. *Development*, 108(1), 121-145.

Wittamer, V., Bertrand, J. Y., Gutschow, P. W. & Traver, D. (2011) Characterization of the mononuclear phagocyte system in zebrafish. *Blood*, 117(26), 7126-7135.

Wu, C., Keivens, V. M., O'Toole, T. E., McDonald, J. A. & Ginsberg, M. H. (1995) Integrin activation and cytoskeletal interaction are essential for the assembly of a fibronectin matrix. *Cell*, 83(5), 715-24.

Wu, S., Nguyen, L. T. M., Pan, H., Hassan, S., Dai, Y., Xu, J. & Wen, Z. (2020) Two phenotypically and functionally distinct microglial populations in adult zebrafish. *Sci Adv*, 6(47).

Wulf, P., Bernhardt, R. R. & Suter, U. (1999) Characterization of peripheral myelin protein 22 in zebrafish (zPMP22) suggests an early role in the development of the peripheral nervous system. *J Neurosci Res*, 57(4), 467-78.

Wullimann, M. F. & Puelles, L. (1999) Postembryonic neural proliferation in the zebrafish forebrain and its relationship to prosomeric domains. *Anat Embryol (Berl)*, 199(4), 329-48.

Xiong, F., Tentner, Andrea R., Huang, P., Gelas, A., Mosaliganti, Kishore R., Souhait, L., Rannou, N., Swinburne, Ian A., Obholzer, Nikolaus D., Cowgill, Paul D., Schier, Alexander F. & Megason, Sean G. (2013) Specified Neural Progenitors Sort to Form Sharp Domains after Noisy Shh Signaling. *Cell*, 153(3), 550-561.

Yamamoto, S.-i., Nagao, M., Sugimori, M., Kosako, H., Nakatomi, H., Yamamoto, N., Takebayashi, H., Nabeshima, Y.-i., Kitamura, T., Weinmaster, G., Nakamura, K. & Nakafuku, M. (2001) Transcription Factor Expression and Notch-Dependent Regulation of Neural Progenitors in the Adult Rat Spinal Cord. *The Journal of Neuroscience*, 21(24), 9814.

Yang, C.-T., Cambier, C. J., Davis, J. M., Hall, Christopher J., Crosier, Philip S. & Ramakrishnan, L. (2012) Neutrophils Exert Protection in the Early Tuberculous Granuloma by Oxidative Killing of Mycobacteria Phagocytosed from Infected Macrophages. *Cell Host & Microbe*, 12(3), 301-312.

Yang, T., Buchan, H. L., Townsend, K. J. & Craig, R. W. (1996) MCL-1, a member of the BLC-2 family, is induced rapidly in response to signals for cell differentiation or death, but not to signals for cell proliferation. *J Cell Physiol*, 166(3), 523-36.

Ye, N., Ding, Y., Wild, C., Shen, Q. & Zhou, J. (2014) Small Molecule Inhibitors Targeting Activator Protein 1 (AP-1). *Journal of Medicinal Chemistry*, 57(16), 6930-6948.

Yeo, S.-Y., Kim, M., Kim, H.-S., Huh, T.-L. & Chitnis, A. B. (2007) Fluorescent protein expression driven by her4 regulatory elements reveals the spatiotemporal pattern of Notch signaling in the nervous system of zebrafish embryos. *Developmental Biology*, 301(2), 555-567.

Ying, Z., Misra, V. & Verge, V. M. K. (2014) Sensing nerve injury at the axonal ER: Activated Luman/CREB3 serves as a novel axonally synthesized retrograde regeneration signal. *Proceedings of the National Academy of Sciences*, 111(45), 16142-16147.

Yoon, J., Kim, J. H., Lee, O. J., Lee, S. Y., Lee, S. H., Park, J. B., Lee, J. Y., Kim, S. C. & Kim, J. (2013) AP-1(c-Jun/FosB) mediates xFoxD5b expression in Xenopus early developmental neurogenesis. *Int J Dev Biol*, 57(11-12), 865-72.

Yu, Y. & Schachner, M. (2013) Syntenin-a promotes spinal cord regeneration following injury in adult zebrafish. *European Journal of Neuroscience*, 38(2), 2280-2289.

Yuizumi, N., Harada, Y., Kuniya, T., Sunabori, T., Koike, M., Wakabayashi, M., Ishihama, Y., Suzuki, Y., Kawaguchi, D. & Gotoh, Y. (2021) Maintenance of neural stem-progenitor cells by the lysosomal biosynthesis regulators TFEB and TFE3 in the embryonic mouse telencephalon. *Stem Cells*, 39(7), 929-944.

Zainolabidin, N., Kamath, S. P., Thanawalla, A. R. & Chen, A. I. (2017) Distinct Activities of Tfap2A and Tfap2B in the Specification of GABAergic Interneurons in the Developing Cerebellum. *Frontiers in Molecular Neuroscience*, 10.

Zakrzewska, A., Cui, C., Stockhammer, O. W., Benard, E. L., Spaink, H. P. & Meijer, A. H. (2010) Macrophage-specific gene functions in Spi1-directed innate immunity. *Blood, The Journal of the American Society of Hematology*, 116(3), e1-e11.

Zammit, P. S., Clarke, J. D. W., Golding, J. P., Goodbrand, I. A. & Tonge, D. A. (1993) Macrophage response during axonal regeneration in the axolotl central and peripheral nervous system. *Neuroscience*, 54(3), 781-789.

Zappia, L. & Theis, F. J. (2021) Over 1000 tools reveal trends in the single-cell RNA-seq analysis landscape. *Genome Biology*, 22(1), 301.

Zeng, Q., McCauley, L. K. & Wang, C. Y. (2002) Hepatocyte growth factor inhibits anoikis by induction of activator protein 1-dependent cyclooxygenase-2. Implication in head and neck squamous cell carcinoma progression. *J Biol Chem*, 277(51), 50137-42.

Zhang, G., Ferg, M., Lübke, L., Takamiya, M., Beil, T., Gourain, V., Diotel, N., Strähle, U. & Rastegar, S. (2020a) Bone morphogenetic protein signaling regulates Id1-mediated neural stem cell quiescence in the adult zebrafish brain via a phylogenetically conserved enhancer module. *STEM CELLS*, 38(7), 875-889.

Zhang, G., Lübke, L., Chen, F., Beil, T., Takamiya, M., Diotel, N., Strähle, U. & Rastegar, S. (2021) Neuron-Radial Glial Cell Communication via BMP/Id1 Signaling Is Key to Long-Term Maintenance of the Regenerative Capacity of the Adult Zebrafish Telencephalon. *Cells*, 10(10). Available online: [Accessed.

Zhang, R., Liu, X., Li, Y., Wang, M., Chen, L. & Hu, B. (2020b) Suppression of inflammation delays hair cell regeneration and functional recovery following lateral line damage in zebrafish larvae. *Biomolecules*, 10(10), 1451.

Zheng, J., Song, C. & Zhang, C. C. (2011) A new chapter: hematopoietic stem cells are direct players in immunity. *Cell & Bioscience*, 1(1), 33.

Zhou, Y. & Besner, G. E. (2010) Heparin-binding epidermal growth factor-like growth factor is a potent neurotrophic factor for PC12 cells. *Neurosignals*, 18(3), 141-51.

Zhou, Y., Zhou, B., Pache, L., Chang, M., Khodabakhshi, A. H., Tanaseichuk, O., Benner, C. & Chanda, S. K. (2019) Metascape provides a biologist-oriented resource for the analysis of systems-level datasets. *Nature Communications*, 10(1), 1523.

Publication

Article

Developmental Cell

A unique macrophage subpopulation signals directly to progenitor cells to promote regenerative neurogenesis in the zebrafish spinal cord

Graphical abstract

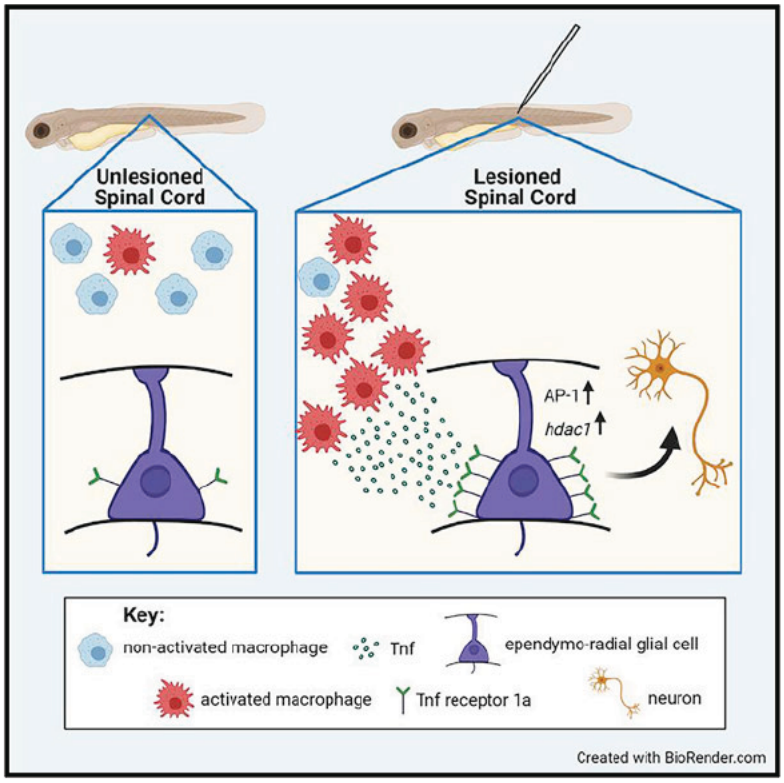

Highlights

- A direct signaling axis from injury to regenerated neurons is established
- scRNA-seq reveals a pro-regenerative macrophage
- Spinal progenitors directly react to human TNF with enhanced neurogenesis
- *hdac1* in spinal progenitors promotes regenerative neurogenesis *in vivo*

Authors

Leonardo Cavone, Tess McCann, Louisa K. Drake, ..., Neil C. Henderson, Thomas Becker, Catherina G. Becker

Correspondence

thomas.becker@ed.ac.uk (T.B.), catherina.becker@ed.ac.uk (C.G.B.)

In brief

Cavone et al. show that after a spinal injury, neural progenitor cells read TNF, a cytokine derived from specific infiltrating macrophages, to promote regeneration of destroyed neurons in larval zebrafish. This mechanism of regenerative neurogenesis, not seen in spinal development, could provide therapeutic targets for non-regenerating vertebrates.

Cavone et al., 2021, Developmental Cell *56*, 1617–1630
June 7, 2021
https://doi.org/10.1016/j.devcel.2021.04.031

CellPress

Developmental Cell

CellPress

Article

A unique macrophage subpopulation signals directly to progenitor cells to promote regenerative neurogenesis in the zebrafish spinal cord

Leonardo Cavone,[1,7] Tess McCann,[1,7] Louisa K. Drake,[1,7] Erika A. Aguzzi,[1] Ana-Maria Oprişoreanu,[1] Elisa Pedersen,[1] Soe Sandi,[1] Jathurshan Selvarajah,[1] Themistoklis M. Tsarouchas,[1] Daniel Wehner,[1,5,6] Marcus Keatinge,[1] Karolina S. Mysiak,[1] Beth E.P. Henderson,[2] Ross Dobie,[2] Neil C. Henderson,[2,3] Thomas Becker,[1,8,*] and Catherina G. Becker[1,4,*]

[1]Centre for Discovery Brain Sciences, University of Edinburgh, The Chancellor's Building, 49 Little France Crescent, Edinburgh EH16 4SB, UK
[2]Centre for Inflammation Research, The Queen's Medical Research Institute, University of Edinburgh, Edinburgh, UK
[3]MRC Human Genetics Unit, Institute of Genetics and Molecular Medicine, University of Edinburgh, Edinburgh, UK
[4]Euan MacDonald Centre for Motor Neurone Disease Research University of Edinburgh, Edinburgh, UK
[5]Max Planck Institute for the Science of Light, Staudtstraße 2, Erlangen 91058, Germany
[6]Max-Planck-Zentrum fur Physik und Medizin, Staudtstraße 2, Erlangen 91058, Germany
[7]These authors contributed equally
[8]Lead contact
*Correspondence: thomas.becker@ed.ac.uk (T.B.), catherina.becker@ed.ac.uk (C.G.B.)
https://doi.org/10.1016/j.devcel.2021.04.031

SUMMARY

Central nervous system injury re-initiates neurogenesis in anamniotes (amphibians and fishes), but not in mammals. Activation of the innate immune system promotes regenerative neurogenesis, but it is fundamentally unknown whether this is indirect through the activation of known developmental signaling pathways or whether immune cells directly signal to progenitor cells using mechanisms that are unique to regeneration. Using single-cell RNA-seq of progenitor cells and macrophages, as well as cell-type-specific manipulations, we provide evidence for a direct signaling axis from specific lesion-activated macrophages to spinal progenitor cells to promote regenerative neurogenesis in zebrafish. Mechanistically, TNFa from pro-regenerative macrophages induces Tnfrsf1a-mediated AP-1 activity in progenitors to increase regeneration-promoting expression of *hdac1* and neurogenesis. This establishes the principle that macrophages directly communicate to spinal progenitor cells via non-developmental signals after injury, providing potential targets for future interventions in the regeneration-deficient spinal cord of mammals.

INTRODUCTION

Tissue damage to the spinal cord after injury severs long axonal connections of surviving neurons and leads to extensive local loss of neurons. To repair these distinct types of damage, different types of cells need to react to injury; surviving neurons need to re-initiate axon growth and local progenitor cells need to re-initiate neurogenesis. Anamniotes, in contrast to mammals, are capable of axon regrowth and re-initiate neurogenesis from progenitor cells after injury of the spinal cord (Becker and Becker, 2015; Stenudd et al., 2015). Here, we focus on the mechanisms of neuronal replacement from spinal progenitor cells in zebrafish, to address the fundamental question whether regenerative neurogenesis recapitulates developmental neurogenesis or is driven by regeneration-specific signals (Becker and Becker, 2015; Hunyara and Kolodkin, 2020). Answering this question may have important implications for interventions in mammals using transplantation of neural stem cells for repair (Lu et al., 2014) and those trying to restore neurogenic function of endogenous progenitor cells in the spinal cord. Endogenous spinal progenitors in mammals have stem cell potential (Shihabuddin et al., 2000) and are induced to proliferate after injury but produce mainly scar-related astrocytes (Meletis et al., 2008). However, spinal progenitor cells in mice can be re-programmed to produce substantial numbers of oligodendrocytes *in vivo* following injury, but neurogenesis has not been achieved. There is evidence to suggest presence of spinal progenitor cells also in humans (Becker et al., 2018).

The immune response after injury is an obvious source for non-developmental signals and positive effects of macrophages have been demonstrated during regenerative neurogenesis in zebrafish (Hui et al., 2017; Kyritsis et al., 2012; Ohnmacht et al., 2016). However, determining whether and how macrophages act on progenitor cells to allow them to revert to neurogenesis has been hampered by the fact that immune cells interact with themselves and other cell types via the same signaling molecules, e.g., cytokines and chemokines (Becker and Becker, 2020; Greenhalgh et al., 2020). Hence, macrophage

effects could be indirect by inducing the re-expression of developmental signals from the environment. Indeed, developmental signals, such as Wnt, Fgf, Shh, and dopamine are re-expressed after spinal injury in zebrafish and promote regenerative neurogenesis from ependymo-radial glia (ERG) progenitor cells (Briona et al., 2015; Goldshmit et al., 2018; Reimer et al., 2009, 2013). Macrophages initially drive inflammation and may have a more reparative phenotype later on, but the identity of pro-regenerative macrophages after spinal injury is unknown. Subtypes of macrophages with different, so-called M1 and M2 polarization states may be present that produce different signals (Wentzel et al., 2020). Here, we test the hypothesis that specific pro-regenerative macrophages signal directly to progenitor cells, leading to re-initiation of neurogenesis by non-developmental pathways.

The cytokine tumor necrosis factor (Tnf; also known as Tnf-α) is a candidate for a regeneration-specific signal that could directly regulate gene activity in spinal ERGs, as *tnfa*, the major ortholog of the *TNF* gene in zebrafish, is mainly expressed by macrophages in the spinal injury site in larval zebrafish (Tsarouchas et al., 2018). We have previously shown that Tnf signaling in zebrafish promotes regrowth of axons from pre-existing injured neurons, but a potential role in regenerative neurogenesis from spinal ERG progenitors is unknown (Tsarouchas et al., 2018). The role of TNF signaling may be highly context dependent, as positive (Bernardino et al., 2008; Chen et al., 2017; Nelson et al., 2013; Zhang et al., 2012) and negative (Johansson et al., 2008; Lan et al., 2012; Wang et al., 2018) functions for neurogenesis have been reported. After spinal injury, Tnf signaling may exacerbate overall outcome in mammals (Esposito and Cuzzocrea, 2011; Ferguson et al., 2008; Kroner et al., 2014), but specific actions on spinal progenitor cells are not known.

After spinal injury in larval and adult zebrafish, spinal ERG progenitor cells switch from their late developmental role in generating oligodendrocytes to generating neurons, akin to their earlier developmental state (Mokalled et al., 2016; Ohnmacht et al., 2016; Reimer et al., 2008). For example, low levels of motor neuron generation are increased by 400% close to a spinal injury site (Ohnmacht et al., 2016). For such a switch, concerted changes in the expression of several genes are needed, which are likely to involve epigenetic changes, such as histone deacetylation (Goldman and Poss, 2020). Indeed, activity of histone deacetylase 1 (Hdac1) regulates neural differentiation (Janssens et al., 2017; Montgomery et al., 2009; Olivera-Martinez et al., 2014; Tang et al., 2019; Yamaguchi et al., 2005) and is a decisive factor in developmental motor neuron generation in zebrafish (Cunliffe, 2004).

Here, we demonstrate that Tnf, derived from a pro-regenerative subset of macrophages, acts directly on spinal ERG progenitor cells in zebrafish via AP-1 activity to increase expression of *hdac1*, which in turn promotes neurogenesis after spinal cord injury.

RESULTS

Single-cell expression profiling indicates Tnf pathway activity in ventricular progenitor cells after injury

To analyze lesion-induced gene regulation in progenitor cells at single-cell resolution, we performed single-cell RNA-seq (scRNA-seq) on FACS-isolated *her4.3*:GFP ERG progenitors at 24 h after spinal injury (hours post-lesion; hpl) at 3 days post-fertilization (dpf), compared with age-matched uninjured animals. At this post-injury time point, spinal progenitor cells show increased lesion-induced proliferation (Ohnmacht et al., 2016). Increased numbers of new neurons, of which the majority are new motor neurons, are observed at 48 hpl (Ohnmacht et al., 2016). We pooled cells from 600 larvae per condition for injured and uninjured samples, yielding 2,477 cell profiles for the unlesioned and 1,203 cell profiles for the lesioned samples after quality control (Figure S1A; STAR methods).

Unsupervised clustering revealed 16 distinct clusters mostly including subpopulations of neural cells, such as ERG progenitor cells, identified by specific marker genes (Figure 1A; Table S1; Data S1). Cell clusters were similar for unlesioned and lesioned samples, with a visible over-representation of neuroblasts after injury (Figure 1B). ERG progenitors, including proliferating ERG progenitors, were identified by high levels of endogenous *her4.3* expression, which overlaps with expression of *sox2* and *foxj1a*, markers for spinal ventricular progenitor cells across vertebrates (Becker et al., 2018). Only these populations of cells contained proliferating cells, indicated by high levels of *mki67* and *ccnd1* (Lange et al., 2020) expression. This underscores their likely progenitor cell identity (Figure 1C). Undifferentiated and differentiated neurons and oligodendrocytes that did not detectably express *her4.3* were also included in the FACS-isolated *her4.3*:GFP population of cells. That is likely caused by the relative stability of the GFP protein, which remained in the progeny of GFP-expressing *her4.3*$^{+}$ ERG progenitor cells, effectively acting as a short-term cell lineage tracer (Lange et al., 2020). This allowed us to compare representation of cell types in our samples. We found a 480% relative increase in neuroblast (69 neuroblasts relative to 328 progenitor cells in the uninjured profile and 281 neuroblasts relative to 148 progenitor cells in the lesioned sample) and a 23% reduction in oligodendrocyte production (348 oligodendrocytes relative to 328 progenitor cells in the uninjured profile and 122 oligodendrocytes relative to 148 progenitor cells in the lesioned profile) after injury (Table S2). Similarly, global comparisons indicated increases in expression of neuroblast-related genes, such as *gap43* (6.9-fold, $p < 0.001$), *sox11b* (2.1-fold, $p < 0.001$), and *atf3* (4.4-fold, $p < 0.001$), and downregulation of oligodendrocyte-related genes, such as *plp1b* (3.2-fold, $p < 0.001$), *mbpa* (3.0-fold, $p < 0.001$), and *mag* (1.9-fold, $p = 0.02$; Table S3). This confirmed a switch from oligodendrogenesis to neurogenesis after injury, as previously reported (Ohnmacht et al., 2016).

In progenitor cells (ERG progenitors plus proliferating ERG progenitors in Figure 1A), genes related to Tnf signaling were strongly upregulated after injury. This comprised *fosl2* (Jahangiri et al., 2016) (2.8-fold, $p < 0.001$, rank 8) and *junbb* (Mechta-Grigoriou et al., 2001) (2.2-fold, p value < 0.001, rank 17), components of the AP-1 transcriptional regulator complex that is activated by Tnf (Kyriakis, 1999). *nfkb1*, another major signal transducer of Tnf, was not detectably expressed (Hayden and Ghosh, 2014). Expression of *tnfaip2b*, a Tnf-regulated gene (Wolf et al., 1994), was increased after injury (1.8-fold, $p < 0.001$, rank 37; Table S4). The principal Tnf receptor, *tnfrsf1a*, was also upregulated 1.4-fold ($p < 0.001$; Data S2). The proportion of *tnfrsf1a*-expressing progenitor cells increased from 18%

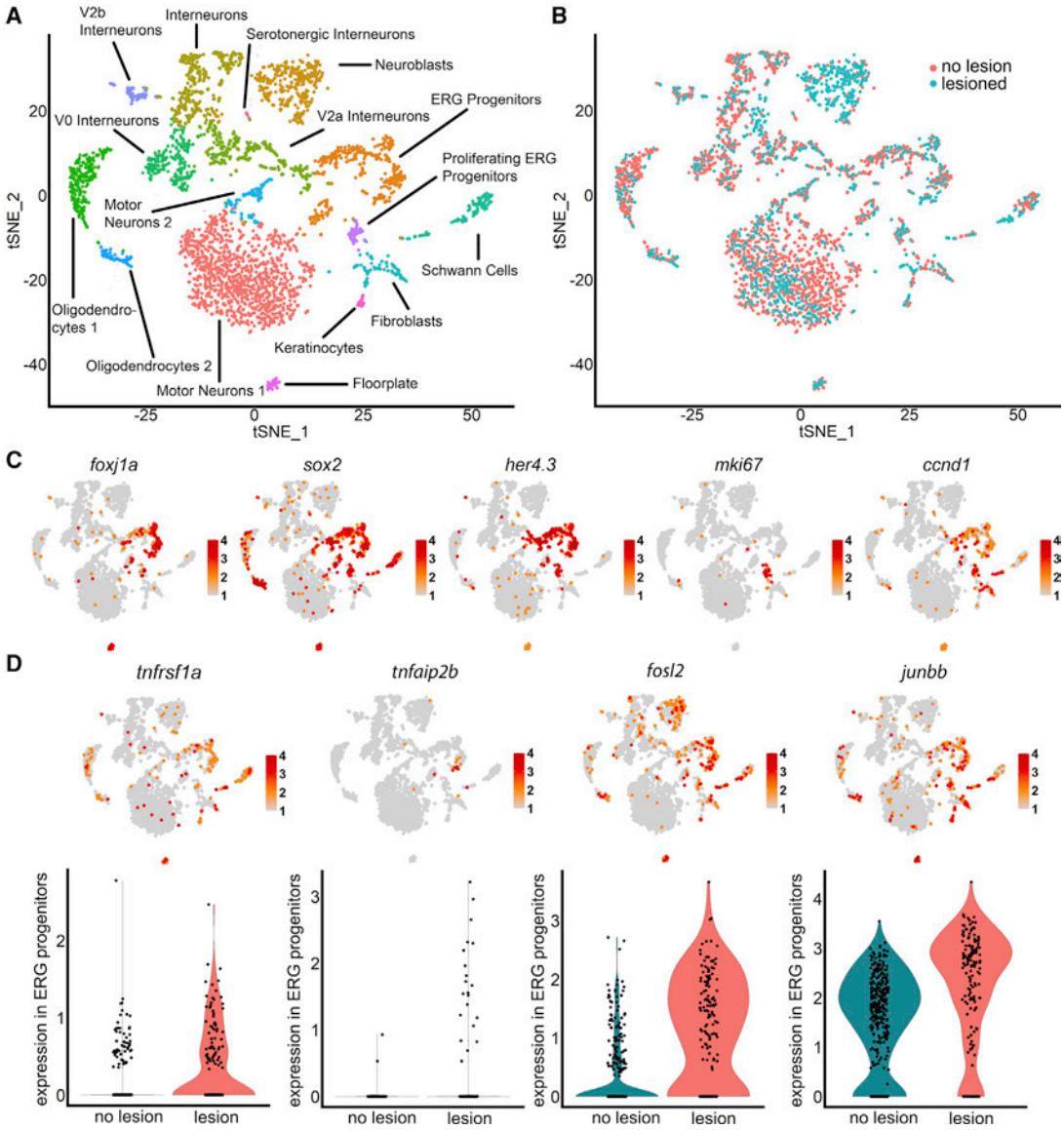

Figure 1. scRNA seq indicates importance of TNF signaling in progenitor cells

(A) Unsupervised clustering of *her4.3*:GFP$^+$ cells identifies progenitor and other neural clusters.

(B) Cells from lesioned and unlesioned samples contribute to cell clusters with a disproportionally high contribution of the lesioned sample to "neuroblasts."

(C) Marker gene distribution identifies proliferating ERG progenitor cell clusters.

(D) TNF receptor (*tnfrsf1a*), downstream gene (*tnfaip2b*), and components of AP 1 signal transducing complex (*fosl2*, *junbb*) are enriched in ERG progenitor cells (tSNE plots), and expression is increased after injury (violin plots). For clarity, only cells with expression of > 2 are indicated in the feature plot of *junbb*. Color codes indicate expression levels from low (gray) to high (red) (see also Figure S1; Table S1).

(59/328 progenitor cells) in the unlesioned sample to 45% (66/148) after injury. Transcripts for the *tnfa/b* ligands were not noticeably expressed in our profiles, suggesting absence of auto- or paracrine signaling from progenitors or their progeny. Notably, all of the above transcripts were enriched in progenitor cells, compared with most other cell clusters (Figure 1D). Other receptors that could activate the AP-1 complex were also enriched in progenitor cells (*egfra, il4r.1, met, tgfbr1a*; Figure S1B). Of these, *met* showed a moderate upregulation after injury (1.18-fold, $p < 0.0001$; Table S5). Overall, this profile suggests *tnfrsf1a*-mediated sensitivity to exogenous Tnf and activation of the Tnf downstream signaling complex AP-1 in spinal progenitor cells after injury.

tnfa-expressing macrophages have a unique activation state

Reactive macrophages in the injury site are the principal source of Tnf (Tsarouchas et al., 2018). To characterize the subtype of Tnf-producing macrophage, we used scRNA-seq of FACS sorted *mpeg1*:GFP$^+$ cells from the injury site of lesioned larvae and

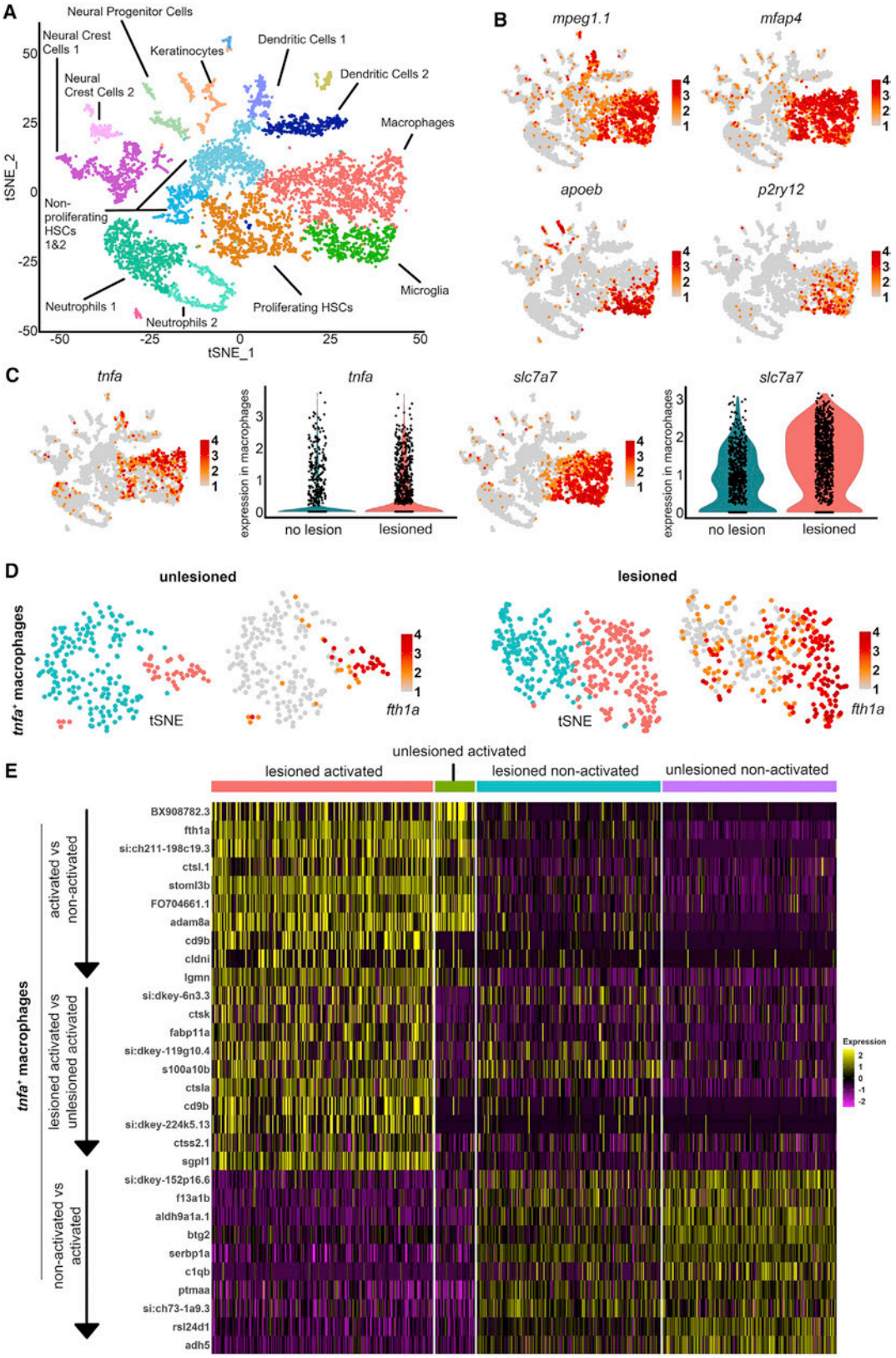

(legend on next page)

from corresponding control tissue of age-matched unlesioned controls at the same time point as for the spinal progenitor cells (24 hpl). The transgene is widely used to label macrophages in zebrafish. However, *mpeg1* (also known as *perforin2*) is also expressed in other immune and non-immune cells (Ferrero et al., 2020; McCormack et al., 2015). We obtained 3,767 cells from 1,800 unlesioned and 4,579 cells from 1,800 lesioned animals after quality control (Figure S1**C**). Unsupervised clustering revealed 16 clusters, with *tnfa* mainly expressed in a cluster of non-proliferating cells that expressed high levels of macrophage markers *mpeg1* and *mfap4*. Interestingly, an adjacent cluster shared expression of *mpeg1, mfap4*, but showed much higher expression of microglia markers, such as *apoeb* and *p2ry12* (Mazzolini et al., 2020) and only low levels of *tnfa* expression, suggesting a microglia identity (Figures 2A–2C; Table S6; Data S3). *Tnfa* was slightly upregulated in the macrophage cluster (1.12-fold; p value = 0.01) after injury, underscoring potentially different roles of microglia and blood-derived macrophages after spinal injury. After injury, cells in the macrophage cluster exhibited a 1.7-fold increase in expression of *slc7a7*, which is essential for macrophage phagocytosis (Demy et al., 2020) (Figure 2C). Hence, *tnfa* was mainly expressed in blood-derived macrophages that engaged in phagocytosis, consistent with their role in debris removal (Tsarouchas et al., 2018).

To determine lesion-induced subtypes of *tnfa*$^+$ macrophages, we performed unsupervised clustering of only these cells for unlesioned and lesioned samples and found two clusters for each sample. Overlaying expression of the activation marker *fth1a* (Torti and Torti, 2002) identified one of the two subpopulations in each sample. This subpopulation was much larger after injury (control: 19%, 40 of 215 cells; injured: 55%, 223 of 408 cells). This is consistent with few macrophages in unlesioned animals that may be activated by naturally occurring cell death and many more macrophages that are activated by extensive cell death after an injury (Tsarouchas et al., 2018) (Figure 2D). We designated these *fth1a*$^+$ subpopulations as "unlesioned activated" and "lesioned activated" *tnfa*$^+$ macrophages, respectively. Lesioned activated *tnfa*$^+$ macrophages were most similar to unlesioned activated *tnfa*$^+$ macrophages in their expression profile (Figure 2E) but showed strongly increased expression of cathepsins *ctsk*, *ctsla*, and *ctss2.1* among the 9 most differentially expressed genes, compared with unlesioned activated *tnfa*$^+$ cells (Table S7). Cathepsin expression is indicative of lesion-induced activation of macrophages (Patel et al., 2018). This supports that we have isolated *tnfa*$^+$ macrophages that are activated by the injury.

To characterize the expression profile of lesioned activated *tnfa*$^+$ cells, we compared these with all cells in the macrophage cluster from unlesioned larvae. This indicated a mixture of upregulated M1 and M2 markers found after classical or alternative activation of macrophages in carp (Wentzel et al., 2020) (Table S8). In addition, lesioned activated *tnfa*$^+$ macrophages expressed high levels of M2 markers *CD9b* (Suzuki et al., 2009) and *IL1R2* (Peters et al., 2013) (Table S8). This characterizes a specific subtype of lesion-activated macrophages as a source cell of Tnf after injury.

ERGs are exposed to macrophage-derived Tnf after injury

To determine whether following spinal injury progenitor cells came into close proximity with lesion-site macrophages and Tnf *in vivo*, we used triple-labeling of Tnf (antibody), macrophages (*mpeg1*:GFP transgene), and motor neuron progenitor ERGs (*olig2*:DsRed transgene) in whole-mounted larvae at 20 hpl. Motor neurons are the most frequently generated cell type in response to injury and a band of *olig2*-expressing ERGs in the ventral spinal cord give rise to these after injury (Ohnmacht et al., 2016).

We frequently found more than 20 *mpeg1*:GFP$^+$ macrophages per larva no more than 20 μm away from *olig2*:DsRed$^+$ ERGs after injury but less than one in the corresponding area in uninjured larvae (Figures S2A and S2B). Antibody labeling showed gradients of specific (Tsarouchas et al., 2018) granular Tnf protein labeling close to macrophages in the injury site that reached into the *olig2*:DsRed$^+$ cell layer (Figures 3A and S2A). This shows that ERGs close to the injury site are exposed to Tnf.

Tnf levels correlate with magnitude of regenerative neurogenesis

To determine the importance of Tnf for neuronal regeneration, we altered its abundance by manipulating the immune response *in vivo*. Dexamethasone, an artificial glucocorticoid with effective immuno-suppressive features (Juszczak and Stankiewicz, 2018; Ronchetti et al., 2018), and bacterial lipopolysaccharides (LPS), which augment the immune response after injury (Novoa et al., 2009), were used. Dexamethasone decreased and LPS increased the numbers of macrophages in the injury site, indicating effective treatment (Figures S2C and S2D). Similarly, injury-induced upregulation of *tnfa* expression was reduced by dexamethasone treatment to uninjured control levels, while LPS treatment increased *tnfa* levels 4.78-fold (compared with lesioned vehicle-treated), as determined by qRT-PCR of isolated injury site tissue at 24 hpl (Figure 3B).

As readouts for regenerative neurogenesis, we determined expression levels of *hdac1*, an epigenetic regulator of motor neuron generation (Cunliffe, 2004), in FACS-isolated *her4.3*:GFP$^+$ ERG progenitor cells from the injured spinal cord. We considered increased *hdac1* expression to indicate increased neurogenic activity of progenitor cells. In addition, we determined numbers of proliferating *olig2*:GFP$^+$/EdU$^+$ motor neuron progenitor ERGs and of *mnx1*:GFP$^+$/EdU$^+$ newly

Figure 2. *tnfa*$^+$ macrophages have a unique signature after injury

(A) Unsupervised clustering of *mpeg1*:GFP$^+$ cells at 1 dpl shows multiple clusters of cell identities.

(B) Macrophages and microglia express *mpeg1* and *mfap4*, but macrophages express lower levels of *apoeb* and *p2ry12* than microglia.

(C) *tnfa* is mainly expressed in macrophages. *tnfa* and *slc7a7* are upregulated in macrophages after injury.

(D) Unsupervised clustering of *tnfa*$^+$ macrophages identifies two clusters in unlesioned and lesioned samples. Expression of *fth1a* identifies clusters of "activated macrophages." For clarity, only cells with expression of > 1 are indicated in feature plot of *fth1a*.

(E) Heatmaps of differentially expressed genes between *tnfa*$^+$ macrophages. Top 10 genes shown for the indicated categories (see also Figure S1; Tables S1–S5).

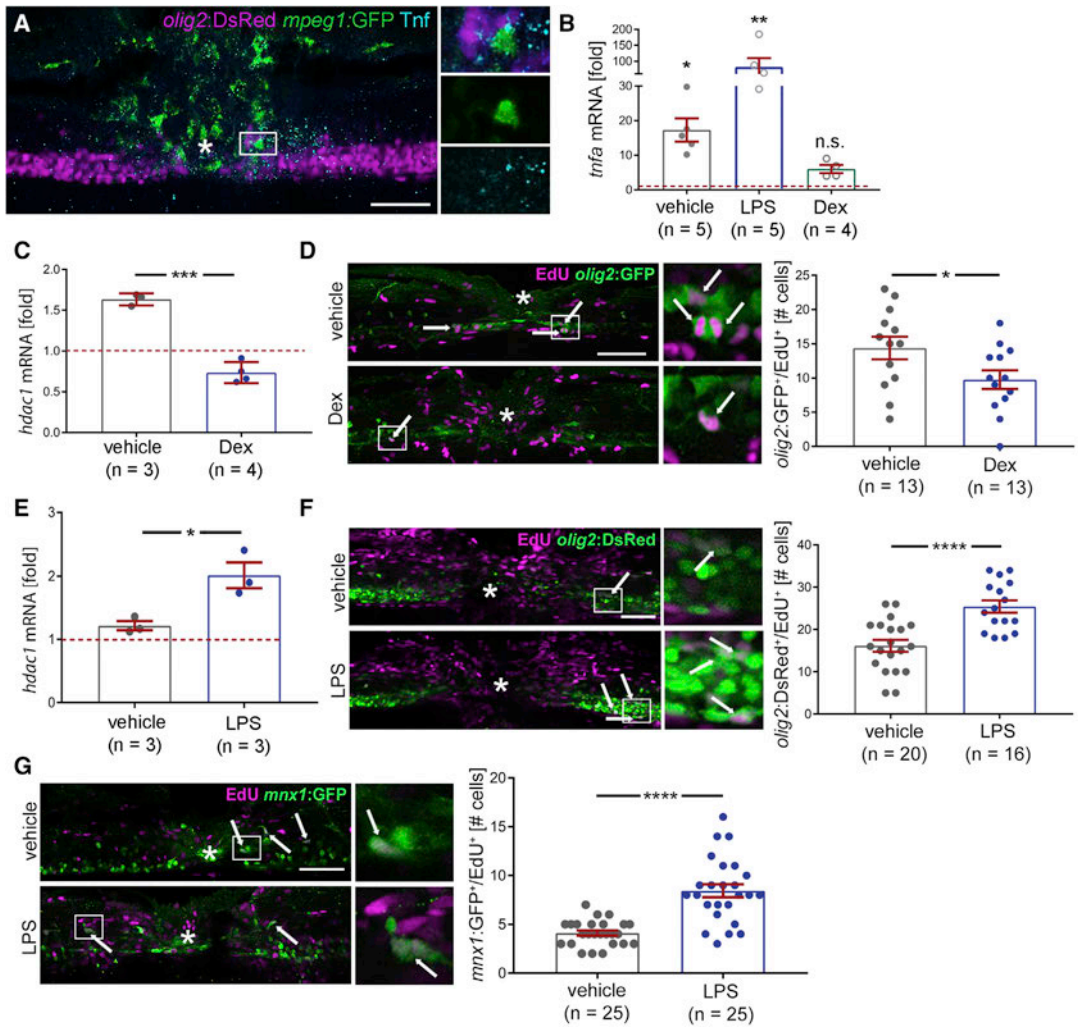

Figure 3. Tnf levels correlate with immune system induced regenerative neurogenesis

All photomicrographs are lateral views at 48 hpl (except A); asterisk indicates injury site; boxed areas are shown in higher magnification on the right. All qRT PCR results are relative to unlesioned control, set to 1 and indicated by dashed red line; each dot represents one experiment.

(A) Macrophages (*mpeg1*:GFP$^+$) and Tnf protein are concentrated in the spinal injury site and close to (within 20 μm) motor neuron progenitor cells (*olig2*:DsRed$^+$). A 4 dpf larva is shown at 22 hpl (top: merge of all channels; middle: *mpeg1*:GFP; bottom: Tnf). See Figure S2A for separate channels and S2B for quantification.

(B) qRT PCR shows LPS increases and dexamethasone decreases *tnfa* expression (Incubation: −6 to 24 hpl for dexamethasone and 0 to 24 hpl for LPS; analysis at 24 hpl; Kruskal Wallis test p = 0.0007; Dunn's post test: *p = 0.027; ***p = 0.0003; n.s.: p = 0.687.

(C) Dexamethasone decreases *hdac1* mRNA expression after injury (incubation: −6 to 24 hpl; t test: ****p = 0.0001).

(D) Dexamethasone treatment reduces the number of proliferating motor neuron progenitor ERGs (*olig2*:GFP$^+$/EdU$^+$; incubation: dexamethasone: −6 to 48 hpl; EdU 0 to 48 hpl; t test: *p = 0.040).

(E) LPS treatment increases *hdac1* mRNA expression after injury (incubation: 0 to 24 hpl; t test: *p = 0.023).

(F and G) LPS treatment increases the number of proliferating motor neuron progenitor ERGs (*olig2*:GFP$^+$/EdU$^+$) (F; t test, ****p < 0.0001) and number of new motor neurons (G; *mnx1*:GFP$^+$/EdU$^+$; t test, ****p < 0.0001); incubation: LPS: 0 to 48 hpl; EdU 0 to 48 hpl). Scale bars: 50 μm; 10 μm for insets. Data are rep resented as mean ± SEM (see also Figure S2; Tables S6 S8).

generated motor neurons after exposure to EdU for 48 hpl (Ohnmacht et al., 2016).

After dexamethasone treatment, *hdac1* expression was reduced by 55% in purified *her4.3*:GFP$^+$ cells (> 94%; Figure S2G), indicating that progenitor cells expressed lower levels of *hdac1* after the treatment (Figure 3C). In whole-mount preparations, we found that the number of EdU incorporating *olig2*:GFP$^+$ motor neuron progenitor ERGs was reduced by 32% (Figure 3D), demonstrating that proliferation of progenitor cells was reduced by the dexamethasone treatment. Numbers of motor neurons were similarly reduced in this experimental paradigm (Ohnmacht et al., 2016), showing that reduced proliferation of progenitor cells led to decreased neurogenesis. Dexamethasone treatment also reduced developmental neurogenesis in unlesioned larvae (Figure S2E). This confirms that dexamethasone also directly influences neurogenesis in addition to dampening the immune response (Nelson et al., 2019).

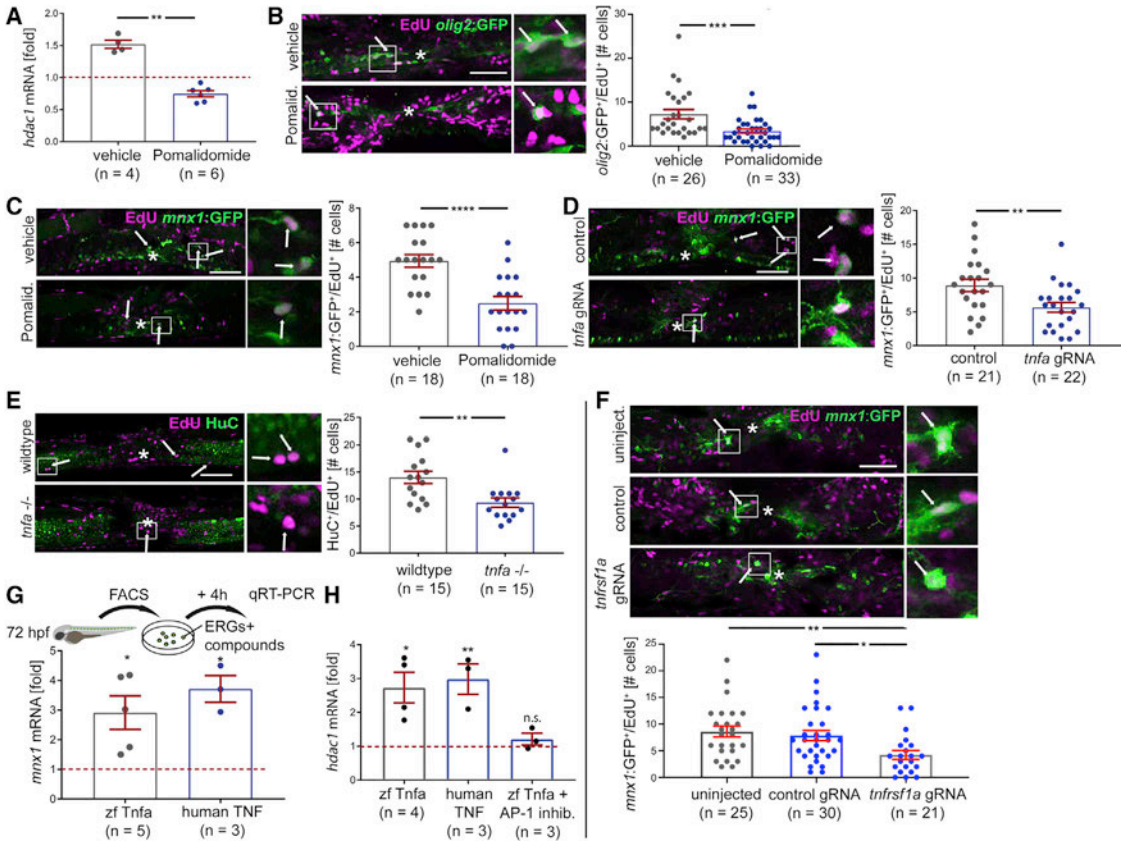

Figure 4. Tnf signaling promotes regenerative neurogenesis from progenitors

Lateral views at 48 hpl are shown in photomicrographs; asterisks indicate the injury site; arrows indicate double labeled cells; boxed areas are shown in higher magnification on the right. All qRT PCR results are relative to unlesioned control, set to 1 and indicated by dashed red line; each dot represents one experiment.

(A) Pomalidomide incubation reduces *hdac1* mRNA levels in qRT PCR of purified ERG progenitor cells (incubation: 0 to 24 hpl; Mann Whitney U test: **p = 0.0095).

(B and C) Pomalidomide treatment reduces the number of newly formed motor neuron progenitor cells (*olig2*:GFP$^+$/EdU$^+$; t test, ***p = 0.0008; B) and motor neurons (*mnx1*:GFP$^+$/EdU$^+$; t test, ****p < 0.0001; C) after spinal injury (incubation −2 to 48 hpl).

(D) Acute *tnfa* gRNA perturbation reduces the number of newly formed motor neurons (*mnx1*:GFP$^+$/EdU$^+$) after spinal injury (EdU incubation 0 to 48 hpl; t test, **p = 0.0077).

(E) Homozygous mutants for *tnfa* show reduced lesion induced generation of neurons (HuC$^+$/EdU$^+$; EdU incubation: 0 to 48 hpl; t test, **p = 0.0026).

(F) Acute injection of *tnfrsf1a* gRNA attenuates lesion induced motor neuron (*mnx1*:GFP$^+$/EdU$^+$; ANOVA and Tukey's post test, **p = 0.0085, *p = 0.026) generation.

(G and H) *Ex vivo* incubation of ERG progenitors with recombinant zebrafish (zf) Tnf α and human TNF proteins for 4 h increases *mnx1* mRNA expression levels, normalized to controls (G; Kruskall Wallis test p = 0.0017; Dunn's post test *p = 0.0244 for zf Tnf α, *p = 0.0160 for human Tnf). *hdac1* mRNA expression (F) is also increased by both proteins compared with controls (one way ANOVA p = 0.0029; Tukey's post test: *p = 0.0127; **p = 0.0085), but not in the presence of the AP 1 inhibitor S11302 (n.s. p = 0.9695). Scale bars, 50; 10 μm for insets. Data are represented as mean ± SEM. (see also Figure S3)

Conversely, LPS treatment increased *hdac1* expression (1.7-fold; Figure 3E), as well as the numbers of newly formed motor neuron progenitor cells (*olig2*:GFP$^+$/EdU$^+$; by 57.5%; Figure 3F) and motor neurons (*mnx1*:GFP$^+$/EdU$^+$; by 104%; Figure 3G). In unlesioned animals, the number of newly formed motor neuron progenitor cells (*olig2*:GFP$^+$/EdU$^+$; Figure S2F) was not altered by LPS treatment. Hence, systemic stimulation of the immune system alone was insufficient to augment constitutive neurogenesis, similar to other CNS regions (Caldwell et al., 2019). Overall, these findings show that regenerative neurogenesis in the spinal cord is regulated by the immune response at the level of gene expression and proliferation of ERG progenitor cells and positively correlates with levels of *tnfa* expression in the injury site.

Tnf and Tnfrsf1a are necessary for regenerative neurogenesis

To directly test the relevance of Tnf signaling for regenerative neurogenesis, we used three approaches *in vivo*, the drug pomalidomide that inhibits Tnf release (Muller et al., 1999), a highly effective *tnfa* gRNA (Tsarouchas et al., 2018) that acutely mutates the gene after injection into zygotes, and a stable *tnfa* mutant line (Keatinge et al., 2021).

Pomalidomide reduced the levels of *hdac1* mRNA expression detected by qRT-PCR in FACS-purified *her4.3*:GFP$^+$ progenitor cells by 51.7% at 24 hpl (Figure 4A), indicating that Tnf signaling promotes *hdac1* expression in progenitor cells. The number of newly generated motor neuron progenitor cells

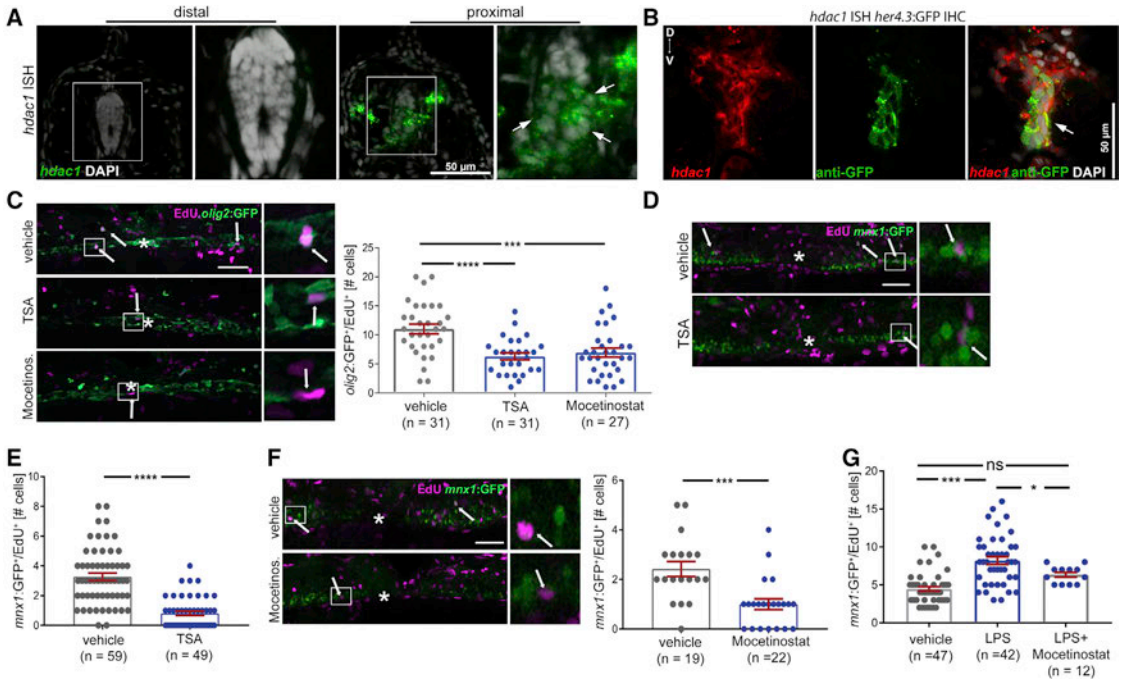

Figure 5. Hdac1 function is necessary for regenerative neurogenesis downstream of immune system activity

Cross sections for (A and B) at 24 hpl; lateral views for (C, D, and F) at 48 hpl are shown; asterisks indicate the injury site; arrows indicate double labeled cells; boxed areas are shown in higher magnification on the right. All incubations were from 0 to 48 hpl.

(A and B) The fluorescent *in situ* hybridization (ISH) signal for *hdac1* is stronger in the spinal cord proximal to the injury site than distal to it (arrows in A). Proximal to the injury site, the *hdac1* ISH signal overlaps with GFP immunohistochemistry (IHC), detecting the *her4.3*:GFP transgene.

(C) TSA and mocetinostat reduce the number of newly generated motor neuron progenitor ERGs (*olig2*:GFP$^+$/EdU$^+$); example images and quantification are shown (one way ANOVA; $p < 0.0001$; Tukey's post test: ***$p = 0.0005$; ****$p < 0.0001$).

(D and E) TSA reduces the number of newly generated motor neurons (*mnx1*:GFP$^+$/EdU$^+$) after spinal injury; example images in (D), quantification in (E) (t test ****$p < 0.0001$).

(F) Mocetinostat treatment reduces the number of newly generated motor neurons after injury (Mann Whitney U test ***$p = 0.0002$).

(G) Mocetinostat co application partially suppresses LPS induced increase in motor neuron generation after injury (one way ANOVA $p < 0.0001$; Holm Sidak's post test ****$p < 0.0001$; *$p = 0.0463$; ns, $p = 0.0643$). Scale bars: (A and B): 50 µm, inset 25 µm; (C, D, and F): 50 µm, insets: 10 µm. Data are represented as mean ± SEM (see also Figure S4).

(*olig2:*GFP$^+$/EdU$^+$) in whole-mounted larvae was reduced by 53% at 48 hpl (Figure 4B), showing that Tnf signaling affects progenitor cell proliferation. Moreover, Pomalidomide treatment reduced the number of new motor neurons by 49% at 48 hpl (Figure 4C), similar to the reduction in the number of proliferating progenitor cells. This suggests that Tnf signaling acts mainly at the level of gene regulation and proliferation of progenitor cells to enhance lesion-induced neurogenesis.

Acute injection of *tnfa* gRNA and Cas9 protein for efficient *tnfa* gene editing reduced the number of newly generated motor neurons (*mnx1*:GFP$^+$/EdU$^+$) by 36.2% at 48 hpl (Figure 4D). Finally, we utilized a stable *tnfa* germ-line mutant to analyze the overall level of neurogenesis using an antibody against HuC/HuD (abbreviated as HuC), as a pan-neuronal marker, in combination with EdU labeling. This indicated a 33.4% reduction in the number of HuC$^+$/EdU$^+$ neurons compared with wild-type animals at 48 hpl (Figure 4E). Hence, Tnf signaling promotes regenerative neurogenesis.

Gene expression profiling indicated increased expression of the Tnf receptor gene *tnfrsf1a* in ERG progenitor cells after injury. To elucidate the functional importance of this receptor for regenerative neurogenesis, we designed efficient gRNAs targeting exons 4 and 5 of *tnfrsf1a* (Figure S3A). Acute injection caused reduced number of newly generated motor neurons (*mnx1*:GFP$^+$/EdU$^+$) compared with uninjected (by 51%) and control gRNA-injected larvae (by 46%) at 48 hpl (Figure 4F). In contrast, ongoing neurogenesis of motor neurons in uninjured larvae was not affected by *tnfrsf1a* gRNA injections (Figure S3B). This shows that the receptor is dispensable for developmental neurogenesis. Together these data show that both *tnfa* and *tnfrsf1a* are necessary for lesion-induced regenerative neurogenesis.

Tnf directly promotes expression of regeneration-associated genes in ERGs

Disruption of *tnfa* does not alter kinetics of macrophage invasion but leads to transiently increased neutrophil counts in the injury site at 24 hpl (Tsarouchas et al., 2018). This could mean that lack of Tnf signaling affects regenerative neurogenesis indirectly. To determine whether Tnf signaling stimulated spinal progenitor cells directly, we established an *ex vivo* paradigm, in which FACS-purified progenitor cells (4 dpf, *her4.3*:GFP$^+$) were

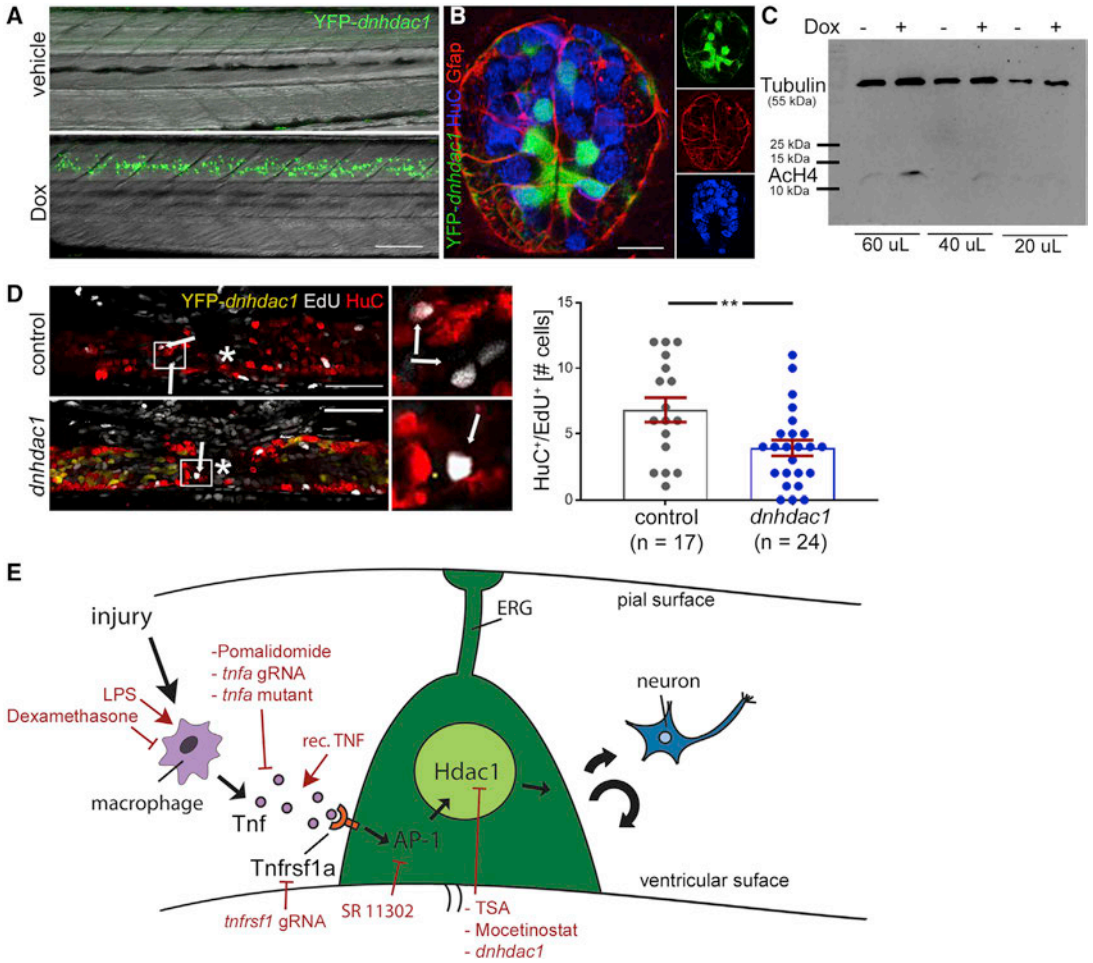

Figure 6. Hdac1 function in ERG progenitor cells is necessary for regenerative neurogenesis

(A) Doxycycline (Dox) exposure leads to strong detectability of YFP in *tg(her4.3:TetA; TetRE:YFP dnhdac1)* transgenic animals at 24 h post induction; lateral views are shown (rostral left; dorsal up).

(B) A cross section (dorsal up) through the spinal cord of a *tg(her4.3:TetA; TetRE:YFP dnhdac1)* larva shows labeling in ventricular ERG progenitors, some of which are glial fibrillary acidic protein (Gfap) immune positive. Peripheral HuC immuno labeled neurons are rarely labeled by the trasngene.

(C) Western blot shows a doxycycline induced increase in histone acetylation levels (AcH4) in FACS purified ERGs. Anti tubulin labeling was used as a standard.

(D) Activation of transgene expression reduces the number of newly generated neurons (HuC+/EdU+, t test: **p = 0.009; incubation time for doxycycline and EdU: 0 to 48 hpl). Control is doxycycline treated non transgenic siblings.

(E) Graphical summary of immune system mediated regenerative neurogenesis with experimental interventions indicated in red. Scale bars: 50 μm. Data are represented as mean ± SEM.

exposed to recombinant zebrafish Tnf-α and human TNF proteins for 4 h. Isolated ERGs were still viable after 4 h *ex vivo* (Figure S3C). To determine whether Tnf proteins could drive ERGs in this preparation toward neurogenesis, we determined expression levels of *mnx1* (Seredick et al., 2012), as a proxy for motor neuron differentiation, by qRT-PCR. Treatments with both zebrafish Tnf-α (2.9-fold) and human Tnf (3.7-fold) led to upregulation of *mnx1* (Figure 4G). This indicates that isolated ERGs are sensitive to Tnf signaling and that Tnf signaling drives progenitor cells toward motor neuron differentiation.

Next, we tested effects of Tnf on *hdac1* expression in this *ex vivo* system. As *in vivo*, *hdac1* mRNA expression was increased by recombinant zebrafish Tnf-α (2.7-fold) and human Tnf (3.0-fold; Figure 4H). Since AP-1 components were upregulated in the scRNA-seq datasets after injury, we hypothesized that *hdac1* expression could be upregulated through AP-1 activity downstream of Tnf signaling. Indeed, the pharmacological AP-1 inhibitor SR 11302 (Ye et al., 2014) fully abolished Tnf-α-mediated upregulation of *hdac1* in ERGs *ex vivo* (Figure 4H). This provides evidence for an AP-1-dependent mechanism of direct Tnf signaling to ERG progenitors in regenerative neurogenesis.

hdac1 upregulation in progenitor cells is necessary for regenerative neurogenesis

Next, we aimed to determine whether Tnf-dependent *hdac1* expression was functionally important for neuronal regeneration, rather than merely correlated with it. First, we used *in situ*

hybridization to determine expression of *hdac1* in ventricular progenitor cells. At 24 hpl, *hdac1* transcripts were detectable in the spinal cord proximal to the injury site, but not at a distance to it, in agreement with the proximodistal gradient of lesion-induced neurogenesis in this system (Ohnmacht et al., 2016) (Figures 5A and S4A). Double labeling with anti-GFP in the *her4.3*:GFP transgenic line demonstrated that *hdac1* expression occurred in ERG progenitor cells, but also other non-progenitor cells (Figures 5A and 5B). Hence, *in situ* hybridization confirmed increased endogenous *hdac1* expression in ERGs that correlated with regenerative neurogenesis after injury.

To establish whether Hdac1 function was necessary for regenerative neurogenesis, we used the pharmacological pan-Hdac inhibitor trichostatin A (Yoshida et al., 1995) (TSA, 200 nM) and the more Hdac1-selective inhibitor mocetinostat (Fournel et al., 2008) (1 μM). Both compounds reduced lesion-induced proliferation of *olig2*:GFP$^+$/EdU$^+$ progenitor cells (TSA: by 42.92%; mocetinostat: by 36.83%; Figure 5C) and the number of newly generated *mnx1*:GFP$^+$/EdU$^+$ motor neurons (TSA: by 75%; mocetinostat: by 59%; Figures 5D–5F). Moreover, inhibition of Hdac1 function by mocetinostat abolished the promoting effect of LPS on lesion-induced generation of *mnx1*:GFP$^+$/EdU$^+$ motor neurons (Figure 5G). However, LPS compensated for some of the inhibitory effect of mocetinostat on neurogenesis (compare Figures 5F and 5G), indicating that LPS did not act through the Tnf/Hdac1 axis alone. This indicates that Hdac1 partially mediates immune system-induced regenerative neurogenesis.

In addition to spinal progenitor cells, other cell types surrounding the injury site increased expression of *hdac1*. Therefore, effects of inhibiting *hdac1* could, at least in part, be indirect through other cells, such as immune cells. To determine the functional importance of Hdac1 specifically in progenitor cells after injury, we spatiotemporally conditionally inhibited Hdac1 function only in ERG progenitors. To this end we used the TetON system for conditional cell-type-specific gene expression (Knopf et al., 2010). We generated a double-transgenic line, in which the regulatory sequences of the ERG progenitor gene *her4.3* drove expression of the doxycycline (DOX)-inducible Tet-activator protein (Wehner et al., 2014) and a Tet-responder line, in which a dominant-negative form of *hdac1*, fused to a YFP fluorescent reporter, was expressed. To obtain a dominant-negative form of *hdac1*, we introduced a point mutation causing a shift from histidine to alanine in position 142 in the deacetylase active domain to produce a deacetylase domain-dead version of the protein. This approach was equivalent to dominant-negative approaches to the highly conserved sequence of the domain in the human gene (Hassig et al., 1998; Pinho et al., 2016). The line was designated Tg (*her4.3*:-TetA;*TetRe*:YFP-dnhdac1). Upon DOX treatment, the *YFP-dnhdac1* transgene was expressed in ventricular progenitor cells to a much higher level than without induction or in other cell types after induction, indicating spatiotemporally controlled expression (Figures 6A and 6B). The construct was functional, as shown by ~4-fold higher acetylation levels of histones in ERG progenitor cells, compared with uninduced controls (Figure 6C).

Using this double-transgenic line to selectively target *dnhdac1* to progenitor cells reduced the number of newly generated HuC$^+$/EdU$^+$ neurons by 42.7% after injury (Figure 6D). In uninjured animals, ongoing neurogenesis was also reduced by overexpression of *dnhdac1* in progenitor cells (Figure S4B), confirming that *hdac1* is important for developmental neurogenesis. This shows that *hdac1*, specifically in progenitor cells, is a functional link in the chain of events of immune-system-activated regenerative neurogenesis (summarized in Figure 6E).

In adult fish, a rapid invasion of the injured spinal cord by macrophages occurs within days (Hui et al., 2010) and lesion-activated macrophages produce Tnf. *In situ* hybridization for *hdac1* at 2 weeks post-lesion, the peak of regenerative neurogenesis (Reimer et al., 2008), indicated a strong increase in expression selectively in the ventricular layer (Figure S4C). This included *olig2*:GFP$^+$ motor neuron progenitor cells (Figure S4D). These observations support that macrophage to spinal ERG progenitor cell signaling in spinal cord regeneration is likely conserved across developmental stages.

DISCUSSION

We provide evidence for direct communication from a subset of pro-regenerative macrophages to spinal progenitor cells via Tnf to promote injury-induced neurogenesis.

Do activated *tnfa*$^+$ macrophages represent pro-regenerative macrophages?

Similar to mammals, activated *tnfa*$^+$ macrophages show high levels of cathepsin expression after injury, identifying them as reactive macrophages (Bühling et al., 2001). Tnf is seen as a marker for pro-inflammatory M1-like differentiated macrophages, also in zebrafish, but it is now recognized that M1 versus M2 polarization signifies a spectrum of differentiation stages (Nguyen-Chi et al., 2015). Using scRNA-seq, we can now fully dissect the expression profile of specific subtypes of macrophages. For example, lesion-activated *tnfa*$^+$ macrophages express a mixture of M1 and M2 markers, including *hbegf*, an M2 marker with likely additional pro-regenerative properties (Wan et al., 2012). By virtue of the direct pro-regenerative action of *tnfa* on spinal neurogenesis, we identify lesion-activated *tnfa*$^+$ macrophages as a pro-regenerative subtype in CNS regeneration.

Experimental inhibition of Tnf signaling reduces neurogenesis by around 50% but does not completely abolish it. That is likely because reactivated developmental neurogenic signals, such as growth factors and neurotransmitters (Briona et al., 2015; Goldshmit et al., 2012, 2018; Mokalled et al., 2016; Reimer et al., 2009, 2013) contribute to regeneration.

Since Tnf also promotes axon regrowth after spinal injury in zebrafish, the same macrophage subtype could also act on axotomized neurons to promote axon growth (Tsarouchas et al., 2018). However, Tnf could also act via stimulation of ERGs and other cells to secrete growth factors that act on axon growth (Mokalled et al., 2016; Tsata et al., 2021; Wehner et al., 2017). Other pro-regenerative macrophages have been described in other organs, for example Nampt-secreting macrophages in skeletal muscle regeneration (Ratnayake et al., 2021) or *wt1b*-expressing macrophages found in heart and fin regeneration (Sanz-Morejón et al., 2019).

Do pro-regenerative macrophages act on spinal progenitor cells directly?

Crucially, *ex vivo* exposure of purified ERGs to both zebrafish and human Tnf showed direct action on ERGs by upregulating

critical genes for neurogenesis, *hdac1* and *mnx1*. *hdac1* regulation in ERGs also correlated with manipulations of the immune system and Tnf levels *in vivo*, further supporting direct action of the mainly macrophage-derived cytokine Tnf (Tsarouchas et al., 2018). Similar to our acute incubation, exposure of mouse neurospheres to Tnf increases neurogenesis via Tnfrsf1a (Bernardino et al., 2008). However, Tnf exposure inhibits proliferation in rat neurospheres (Ben-Hur et al., 2003). While our cell-type-specific manipulations support direct positive action of Tnf on ERGs, the immune response in the injury site is highly dynamic and interactive. For example, inhibiting *tnfa* expression increases neutrophil numbers and *il-1β* expression in the injury site (Tsarouchas et al., 2018). Hence, Tnf from pro-regenerative macrophages may also indirectly affect spinal neurogenesis via other cell types and signals in the injury site, in addition to its direct action.

Is Tnf a regeneration-specific signal?

Tnf signaling may not be relevant for developmental neurogenesis in the spinal cord. The main source of Tnf are reactive macrophages, only present after an injury (Tsarouchas et al., 2018) and expression of *tnfrsf1a* is dispensable for developmental neurogenesis in unlesioned animals, but not for regenerative neurogenesis, as we show here. In addition, our *tnfa* mutants show apparently normal development. Moreover, during earlier development overall expression levels of *tnfa* are low until at least 2 dpf, after the first wave of motor neuron generation is over. Knockdown experiments of *tnfa* showed that the retina, as part of the central nervous system, also developed normally (Lei et al., 2016). Similarly, *mecp2* mutant zebrafish show reduced levels of *tnfa* expression throughout development but develop to normal body length at least up to 7 dpf (van der Vaart et al., 2017). These observations support the notion of unique Tnf signaling mechanisms during regenerative neurogenesis.

What are the downstream effectors of Tnf?

scRNA-seq highlighted the AP-1 complex as signal transducer, and our pharmacological inhibition of AP-1 confirmed this action in ERGs *ex vivo*. In salamanders, upregulation of AP-1 components *c-fos* and *junb* in spinal ERGs after injury has been linked to a pro-regenerative response. Similarly, Tnf-induced neurogenesis in mouse SVZ neurospheres coincides with increased expression of *c-jun*, also a component of AP-1 (Bernardino et al., 2008). Moreover, *c-jun* abundance in cortical progenitor cells diminishes with age, correlated with reduced neurogenesis, supporting a role for AP-1 in neurogenesis. Notably, our scRNA-seq analysis indicates additional signals that may act via AP-1. Another major signal transducer of Tnf, NF-κB1, forces differentiation of progenitor cells in the developing mammalian cortex (Methot et al., 2013; Yamanishi et al., 2015). We observed only very low levels of *nfkb1* in our scRNA-seq. We speculate that the balance between Nfkb1 and AP-1 signaling in ERGs may determine efficient regenerative neurogenesis.

If Tnf is a signal that acts on ERGs by regeneration-specific mechanisms, these need to eventually converge on generic mechanisms of neurogenesis. Indeed, Tnf signaling increased expression of *mnx1*, a bona fide motor neuron differentiation factor (Seredick et al., 2012), suggesting that at least part of the developmental program for neurogenesis and differentiation is re-initiated by Tnf. *hdac1*, which is similarly increased in expression by Tnf, may function in reprogramming ERGs for neurogenesis (Goldman and Poss, 2020; Mitra et al., 2018). However, using our cell-type-specific inhibition of *hdac1* function in ERGs, we confirm that *hdac1* is required for both regenerative and developmental neurogenesis in zebrafish. Therefore, its upregulation after injury could be also be a part of the reactivated developmental program for neurogenesis. Knowing that *hdac1* and *mnx1* are upregulated during the switch from oligodendrogenesis to neurogenesis in ERG progenitor cells downstream of immune system activation provides a framework to understanding intracellular signaling in spinal progenitor cells after injury. This will be useful for translational approaches, given that simply enhancing extracellular Tnf signaling may negatively affect other aspects of spinal repair.

Limitations of the study

While we show a signaling axis from Tnf via AP-1 and Hdac1 for neurogenesis, there are likely to be additional signals from macrophages that promote regenerative neurogenesis. Further candidates for functional tests can be gleaned from our present scRNA-seq analyses. Moreover, there are likely to be additional or alternative intracellular signaling pathways to promote neurogenesis in ERG cells. For example, even when Hdac1 function was blocked, LPS could partially overcome this block to allow limited neurogenesis. Further scRNA-seq analyses under these experimental conditions, as well as direct binding assays of transcriptional regulators are required to comprehensively unravel the dynamics of intracellular signaling in ERGs in regenerative neurogenesis.

Conclusion

In conclusion, we have provided evidence in a three-dimensional *in vivo* context for direct communication between activated macrophages and spinal progenitor cells after an injury that is specific to a regeneration context and we identify pivotal signals and downstream gene activation. This increases our fundamental understanding of lesion-induced neurogenesis in the spinal cord and provides potential molecular targets for intervention in non-regenerating systems.

STAR★METHODS

Detailed methods are provided in the online version of this paper and include the following:

- KEY RESOURCES TABLE
- RESOURCES AVAILABILITY
  - Lead contact
  - Materials availability
  - Data and code availability
- EXPERIMENTAL MODEL AND SUBJECT DETAILS
  - Animals
- METHOD DETAILS
  - Spinal cord injuries
  - Generation of TetRE:YFP-dnhdac1 line:
  - gRNA injections
  - RFLP analysis of gRNA efficiency
  - Drug treatment of whole larvae

- Ex vivo incubations
- Immunohistochemistry
- In situ hybridisation
- FACS isolation
- qRT-PCR
- Western blot
- scRNAseq
- Cell counting in whole-mounted larvae

● QUANTIFICATION AND STATISTICAL ANALYSIS

SUPPLEMENTAL INFORMATION

Supplemental information can be found online at https://doi.org/10.1016/j.devcel.2021.04.031.

ACKNOWLEDGMENTS

We thank the SuRF facility at Edinburgh Bioquarter for expertly facilitating FACS sorting. Funded by the EU Cofund ERANET NEURON consortium NEURONICHE with contributions from MRC (MR/R001049/1), Spinal Research, and Wings for Life to C.G.B., a project grant from the BBSRC (BB/R003742/1) to T.B. and a Wellcome Trust Senior Research Fellowship in Clinical Science (ref. 219542/Z/19/Z) to N.C.H.; T.M. held a Tissue Repair PhD studentship (MRC), L.K.D. was funded by a BBSRC Eastbio PhD studentship, D.W. was funded by the Deutsche Forschungsgemeinschaft (Forschungsstipendium WE5736/1 1).

AUTHOR CONTRIBUTIONS

Conceptualization, L.C., T.B., and C.G.B.; methodology, L.C., T.M., and L.K.D.; investigation, L.C., T.M., L.K.D., E.A.A., A. M.O., E.P., J.S., T.M.T., M.K., and D.W.; resources: B.E.P.H., R.D., and N.C.H.; writing original draft, L.C., T.B., and C.G.B.; writing review & editing, L.C., T.B., and C.G.B.; funding acquisition, T.B. and C.G.B.; supervision, L.C., D.W., T.B., and C.G.B.

DECLARATION OF INTERESTS

The authors declare no competing interests.

INCLUSION AND DIVERSITY

One or more of the authors of this paper self identifies as a member of the LGBTQ+ community.

Received: October 10, 2020
Revised: March 15, 2021
Accepted: April 28, 2021
Published: May 24, 2021

REFERENCES

Becker, C.G., and Becker, T. (2015). Neuronal regeneration from ependymo radial glial cells: cook, little pot, cook! Dev. Cell *32*, 516 527.

Becker, C.G., Becker, T., and Hugnot, J.P. (2018). The spinal ependymal zone as a source of endogenous repair cells across vertebrates. Prog. Neurobiol. *170*, 67 80.

Becker, T., and Becker, C.G. (2020). Dynamic cell interactions allow spinal cord regeneration in zebrafish. Curr. Opin. Physiol. *14*, 64 69. https://doi.org/10.1016/j.cophys.2020.01.009.

Ben Hur, T., Ben Menachem, O., Furer, V., Einstein, O., Mizrachi Kol, R., and Grigoriadis, N. (2003). Effects of proinflammatory cytokines on the growth, fate, and motility of multipotential neural precursor cells. Mol. Cell. Neurosci. *24*, 623 631.

Bernardino, L., Agasse, F., Silva, B., Ferreira, R., Grade, S., and Malva, J.O. (2008). Tumor necrosis factor alpha modulates survival, proliferation, and neuronal differentiation in neonatal subventricular zone cell cultures. Stem Cells *26*, 2361 2371.

Briona, L.K., Poulain, F.E., Mosimann, C., and Dorsky, R.I. (2015). Wnt/β catenin signaling is required for radial glial neurogenesis following spinal cord injury. Dev. Biol. *403*, 15 21.

Bühling, F., Reisenauer, A., Gerber, A., Krüger, S., Weber, E., Brömme, D., Roessner, A., Ansorge, S., Welte, T., and Röcken, C. (2001). Cathepsin K a marker of macrophage differentiation? J. Pathol. *195*, 375 382.

Caldwell, L.J., Davies, N.O., Cavone, L., Mysiak, K.S., Semenova, S.A., Panula, P., Armstrong, J.D., Becker, C.G., and Becker, T. (2019). Regeneration of dopaminergic neurons in adult zebrafish depends on immune system activation and differs for distinct populations. J. Neurosci. *39*, 4694 4713.

Chen, M., Reed, R.R., and Lane, A.P. (2017). Acute inflammation regulates neuroregeneration through the NF κB pathway in olfactory epithelium. Proc. Natl. Acad. Sci. USA *114*, 8089 8094.

Cunliffe, V.T. (2004). Histone deacetylase 1 is required to repress Notch target gene expression during zebrafish neurogenesis and to maintain the production of motoneurones in response to hedgehog signalling. Development *131*, 2983 2995.

Demy, D.L., Carrère, M., Noche, R., Tauzin, M., Le Bris, M., Baek, C., Leshchiner, I., Goessling, W., and Herbomel, P. (2020). The cationic amino acid exporter Slc7a7 is induced and vital in zebrafish tissue macrophages with sustained efferocytic activity. J. Cell Sci. *133*. https://doi.org/10.1242/jcs.249037.

Ellett, F., Pase, L., Hayman, J.W., Andrianopoulos, A., and Lieschke, G.J. (2011). mpeg1 promoter transgenes direct macrophage lineage expression in zebrafish. Blood *117*, e49 e56.

Esposito, E., and Cuzzocrea, S. (2011). Anti TNF therapy in the injured spinal cord. Trends Pharmacol. Sci. *32*, 107 115.

Faul, F., Erdfelder, E., Buchner, A., and Lang, A.G. (2009). Statistical power analyses using G*Power 3.1: tests for correlation and regression analyses. Behav. Res. Methods *41*, 1149 1160.

Ferguson, A.R., Christensen, R.N., Gensel, J.C., Miller, B.A., Sun, F., Beattie, E.C., Bresnahan, J.C., and Beattie, M.S. (2008). Cell death after spinal cord injury is exacerbated by rapid TNF alpha induced trafficking of GluR2 lacking AMPARs to the plasma membrane. J. Neurosci. *28*, 11391 11400.

Ferrero, G., Gomez, E., Lyer, S., Rovira, M., Miserocchi, M., Langenau, D.M., Bertrand, J.Y., and Wittamer, V. (2020). The macrophage expressed gene (mpeg) 1 identifies a subpopulation of B cells in the adult zebrafish. J. Leukoc. Biol. *107*, 431 443.

Flanagan Steet, H., Fox, M.A., Meyer, D., and Sanes, J.R. (2005). Neuromuscular synapses can form in vivo by incorporation of initially aneural postsynaptic specializations. Development *132*, 4471 4481.

Fournel, M., Bonfils, C., Hou, Y., Yan, P.T., Trachy Bourget, M. C., Kalita, A., Liu, J., Lu, A. H., Zhou, N.Z., Robert, M. F., et al. (2008). MGCD0103, a novel isotype selective histone deacetylase inhibitor, has broad spectrum antitumor activity in vitro and in vivo. Mol. Cancer Ther. *7*, 759 768.

Goldman, J.A., and Poss, K.D. (2020). Gene regulatory programmes of tissue regeneration. Nat. Rev. Genet. *21*, 511 525.

Goldshmit, Y., Sztal, T.E., Jusuf, P.R., Hall, T.E., Nguyen Chi, M., and Currie, P.D. (2012). Fgf dependent glial cell bridges facilitate spinal cord regeneration in zebrafish. J. Neurosci. *32*, 7477 7492.

Goldshmit, Y., Tang, J.K.K.Y., Siegel, A.L., Nguyen, P.D., Kaslin, J., Currie, P.D., and Jusuf, P.R. (2018). Different Fgfs have distinct roles in regulating neurogenesis after spinal cord injury in zebrafish. Neural Dev *13*, 24.

Greenhalgh, A.D., David, S., and Bennett, F.C. (2020). Immune cell regulation of glia during CNS injury and disease. Nat. Rev. Neurosci. *21*, 139 152.

Hassig, C.A., Tong, J.K., Fleischer, T.C., Owa, T., Grable, P.G., Ayer, D.E., and Schreiber, S.L. (1998). A role for histone deacetylase activity in HDAC1 mediated transcriptional repression. Proc. Natl. Acad. Sci. USA *95*, 3519 3524.

Hayden, M.S., and Ghosh, S. (2014). Regulation of NF κB by TNF family cytokines. Semin. Immunol. *26*, 253 266.

Hui, S.P., Dutta, A., and Ghosh, S. (2010). Cellular response after crush injury in adult zebrafish spinal cord. Dev. Dyn. *239*, 2962 2979.

Hui, S.P., Sheng, D.Z., Sugimoto, K., Gonzalez Rajal, A., Nakagawa, S., Hesselson, D., and Kikuchi, K. (2017). Zebrafish regulatory T cells mediate Organ specific regenerative programs. Dev. Cell *43*, 659 672.e5.

Hunyara, J.L., and Kolodkin, A.L. (2020). Repurposing developmental mecha nisms in the adult nervous system. Curr. Opin. Genet. Dev. *65*, 14 21.

Jahangiri, L., Sharpe, M., Novikov, N., González Rosa, J.M., Borikova, A., Nevis, K., Paffett Lugassy, N., Zhao, L., Adams, M., Guner Ataman, B., et al. (2016). The AP 1 transcription factor component Fosl2 potentiates the rate of myocardial differentiation from the zebrafish second heart field. Development *143*, 113 122.

Janssens, D.H., Hamm, D.C., Anhezini, L., Xiao, Q., Siller, K.H., Siegrist, S.E., Harrison, M.M., and Lee, C.Y. (2017). An Hdac1/Rpd3 poised circuit balances continual self renewal and rapid restriction of developmental potential during asymmetric stem cell division. Dev. Cell *40*, 367 380.e7.

Johansson, S., Price, J., and Modo, M. (2008). Effect of inflammatory cyto kines on major histocompatibility complex expression and differentiation of human neural stem/progenitor cells. Stem Cells *26*, 2444 2454.

Juszczak, G.R., and Stankiewicz, A.M. (2018). Glucocorticoids, genes and brain function. Prog. Neuropsychopharmacol. Biol. Psychiatry *82*, 136 168.

Keatinge, M., Tsarouchas, T.M., Munir, T., Porter, N.J., Larraz, J., Gianni, D., Tsai, H.H., Becker, C.G., Lyons, D.A., and Becker, T. (2021). CRISPR gRNA phenotypic screening in zebrafish reveals pro regenerative genes in spinal cord injury. PLoS Genet *17*, e1009515.

Knopf, F., Schnabel, K., Haase, C., Pfeifer, K., Anastassiadis, K., and Weidinger, G. (2010). Dually inducible TetON systems for tissue specific con ditional gene expression in zebrafish. Proc. Natl. Acad. Sci. USA *107*, 19933 19938.

Kroner, A., Greenhalgh, A.D., Zarruk, J.G., Passos Dos Santos, R., Gaestel, M., and David, S. (2014). TNF and increased intracellular iron alter macrophage polarization to a detrimental M1 phenotype in the injured spinal cord. Neuron *83*, 1098 1116.

Kucenas, S., Takada, N., Park, H.C., Woodruff, E., Broadie, K., and Appel, B. (2008). CNS derived glia ensheath peripheral nerves and mediate motor root development. Nat. Neurosci. *11*, 143 151.

Kyriakis, J.M. (1999). Activation of the AP 1 transcription factor by inflamma tory cytokines of the TNF family. Gene Expr *7*, 217 231.

Kyritsis, N., Kizil, C., Zocher, S., Kroehne, V., Kaslin, J., Freudenreich, D., Iltzsche, A., and Brand, M. (2012). Acute inflammation initiates the regenerative response in the adult zebrafish brain. Science *338*, 1353 1356.

Lan, X., Chen, Q., Wang, Y., Jia, B., Sun, L., Zheng, J., and Peng, H. (2012). TNF alpha affects human cortical neural progenitor cell differentiation through the autocrine secretion of leukemia inhibitory factor. PLoS One *7*, e50783.

Lange, C., Rost, F., Machate, A., Reinhardt, S., Lesche, M., Weber, A., Kuscha, V., Dahl, A., Rulands, S., and Brand, M. (2020). Single cell sequencing of radial glia progeny reveals the diversity of newborn neurons in the adult zebrafish brain. Development *147*, dev185595.

Lei, X.D., Sun, Y., Cai, S.J., Fang, Y.W., Cui, J.L., and Li, Y.H. (2016). Role of tumor necrosis factor alpha in zebrafish retinal neurogenesis and myelination. Int. J. Ophthalmol. *9*, 831 837.

Lu, P., Kadoya, K., and Tuszynski, M.H. (2014). Axonal growth and connectiv ity from neural stem cell grafts in models of spinal cord injury. Curr. Opin. Neurobiol. *27*, 103 109.

Mazzolini, J., Le Clerc, S., Morisse, G., Coulonges, C., Kuil, L.E., van Ham, T.J., Zagury, J.F., and Sieger, D. (2020). Gene expression profiling reveals a conserved microglia signature in larval zebrafish. Glia *68*, 298 315.

McCormack, R.M., de Armas, L.R., Shiratsuchi, M., Fiorentino, D.G., Olsson, M.L., Lichtenheld, M.G., Morales, A., Lyapichev, K., Gonzalez, L.E., Strbo, N., et al. (2015). Perforin 2 is essential for intracellular defense of parenchymal cells and phagocytes against pathogenic bacteria. eLife *4*, e06508. https://doi.org/10.7554/eLife.06508.

Mechta Grigoriou, F., Gerald, D., and Yaniv, M. (2001). The mammalian Jun proteins: redundancy and specificity. Oncogene *20*, 2378 2389.

Meletis, K., Barnabé Heider, F., Carlén, M., Evergren, E., Tomilin, N., Shupliakov, O., and Frisén, J. (2008). Spinal cord injury reveals multilineage dif ferentiation of ependymal cells. PLoS Biol *6*, e182.

Methot, L., Hermann, R., Tang, Y., Lo, R., Al Jehani, H., Jhas, S., Svoboda, D., Slack, R.S., Barker, P.A., and Stifani, S. (2013). Interaction and antagonistic roles of NF κB and Hes6 in the regulation of cortical neurogenesis. Mol. Cell. Biol. *33*, 2797 2808.

Mitra, S., Sharma, P., Kaur, S., Khursheed, M.A., Gupta, S., Ahuja, R., Kurup, A.J., Chaudhary, M., and Ramachandran, R. (2018). Histone deacetylase mediated Müller glia reprogramming through Her4.1 Lin28a axis is essential for retina regeneration in zebrafish. iScience *7*, 68 84.

Mokalled, M.H., Patra, C., Dickson, A.L., Endo, T., Stainier, D.Y., and Poss, K.D. (2016). Injury induced ctgfa directs glial bridging and spinal cord regener ation in zebrafish. Science *354*, 630 634.

Montgomery, R.L., Hsieh, J., Barbosa, A.C., Richardson, J.A., and Olson, E.N. (2009). Histone deacetylases 1 and 2 control the progression of neural precur sors to neurons during brain development. Proc. Natl. Acad. Sci. USA *106*, 7876 7881.

Muller, G.W., Chen, R., Huang, S.Y., Corral, L.G., Wong, L.M., Patterson, R.T., Chen, Y., Kaplan, G., and Stirling, D.I. (1999). Amino substituted thalidomide analogs: potent inhibitors of TNF alpha production. Bioorg. Med. Chem. Lett. *9*, 1625 1630.

Nelson, C.M., Ackerman, K.M., O'Hayer, P., Bailey, T.J., Gorsuch, R.A., and Hyde, D.R. (2013). Tumor necrosis factor alpha is produced by dying retinal neurons and is required for Muller glia proliferation during zebrafish retinal regeneration. J. Neurosci. *33*, 6524 6539.

Nelson, C.M., Lennon, V.A., Lee, H., Krug, R.G., 2nd, Kamalova, A., Madigan, N.N., Clark, K.J., Windebank, A.J., and Henley, J.R. (2019). Glucocorticoids target ependymal glia and inhibit repair of the injured spinal cord. Front. Cell Dev. Biol. *7*, 56.

Nguyen Chi, M., Laplace Builhe, B., Travnickova, J., Luz Crawford, P., Tejedor, G., Phan, Q.T., Duroux Richard, I., Levraud, J. P., Kissa, K., Lutfalla, G., et al. (2015). Identification of polarized macrophage subsets in ze brafish. eLife *4*, e07288.

Novoa, B., Bowman, T.V., Zon, L., and Figueras, A. (2009). LPS response and tolerance in the zebrafish (Danio rerio). Fish Shellfish Immunol *26*, 326 331.

Ohnmacht, J., Yang, Y., Maurer, G.W., Barreiro Iglesias, A., Tsarouchas, T.M., Wehner, D., Sieger, D., Becker, C.G., and Becker, T. (2016). Spinal motor neu rons are regenerated after mechanical lesion and genetic ablation in larval ze brafish. Development *143*, 1464 1474.

Olivera Martinez, I., Schurch, N., Li, R.A., Song, J., Halley, P.A., Das, R.M., Burt, D.W., Barton, G.J., and Storey, K.G. (2014). Major transcriptome re orga nisation and abrupt changes in signalling, cell cycle and chromatin regulation at neural differentiation in vivo. Development *141*, 3266 3276.

Patel, S., Homaei, A., El Seedi, H.R., and Akhtar, N. (2018). Cathepsins: pro teases that are vital for survival but can also be fatal. Biomed. Pharmacother. *105*, 526 532.

Peters, V.A., Joesting, J.J., and Freund, G.G. (2013). IL 1 receptor 2 (IL 1R2) and its role in immune regulation. Brain Behav. Immun. *32*, 1 8.

Pinho, B.R., Reis, S.D., Guedes Dias, P., Leitão Rocha, A., Quintas, C., Valentão, P., Andrade, P.B., Santos, M.M., and Oliveira, J.M. (2016). Pharmacological modulation of HDAC1 and HDAC6 in vivo in a zebrafish model: therapeutic implications for Parkinson's disease. Pharmacol. Res. *103*, 328 339.

Ratnayake, D., Nguyen, P.D., Rossello, F.J., Wimmer, V.C., Tan, J.L., Galvis, L.A., Julier, Z., Wood, A.J., Boudier, T., Isiaku, A.I., et al. (2021). Macrophages provide a transient muscle stem cell niche via NAMPT secretion. Nature *591*, 281 287.

Reimer, M.M., Kuscha, V., Wyatt, C., Sörensen, I., Frank, R.E., Knüwer, M., Becker, T., and Becker, C.G. (2009). Sonic hedgehog is a polarized signal for motor neuron regeneration in adult zebrafish. J. Neurosci. *29*, 15073 15082.

Reimer, M.M., Norris, A., Ohnmacht, J., Patani, R., Zhong, Z., Dias, T.B., Kuscha, V., Scott, A.L., Chen, Y. C., Rozov, S., et al. (2013). Dopamine from

the brain promotes spinal motor neuron generation during development and adult regeneration. Dev. Cell *25*, 478 491.

Reimer, M.M., Sörensen, I., Kuscha, V., Frank, R.E., Liu, C., Becker, C.G., and Becker, T. (2008). Motor neuron regeneration in adult zebrafish. J. Neurosci. *28*, 8510 8516.

Renshaw, S.A., Loynes, C.A., Trushell, D.M., Elworthy, S., Ingham, P.W., and Whyte, M.K. (2006). A transgenic zebrafish model of neutrophilic inflammation. Blood *108*, 3976 3978.

Ronchetti, S., Migliorati, G., Bruscoli, S., and Riccardi, C. (2018). Defining the role of glucocorticoids in inflammation. Clin. Sci. (Lond) *132*, 1529 1543.

Sanz Morejón, A., García Redondo, A.B., Reuter, H., Marques, I.J., Bates, T., Galardi Castilla, M., Große, A., Manig, S., Langa, X., Ernst, A., et al. (2019). Wilms tumor 1b expression defines a pro regenerative macrophage subtype and is required for organ regeneration in the zebrafish. Cell Rep *28*, 1296 1306.e6.

Schneider, C.A., Rasband, W.S., and Eliceiri, K.W. (2012). NIH Image to ImageJ: 25 years of image analysis. Nat. Methods *9*, 671 675.

Seredick, S.D., Van Ryswyk, L., Hutchinson, S.A., and Eisen, J.S. (2012). Zebrafish Mnx proteins specify one motoneuron subtype and suppress acqui sition of interneuron characteristics. Neural Dev *7*, 35.

Shihabuddin, L.S., Horner, P.J., Ray, J., and Gage, F.H. (2000). Adult spinal cord stem cells generate neurons after transplantation in the adult dentate gy rus. J. Neurosci. *20*, 8727 8735.

Shin, J., Park, H.C., Topczewska, J.M., Mawdsley, D.J., and Appel, B. (2003). Neural cell fate analysis in zebrafish using olig2 BAC transgenics. Methods Cell Sci *25*, 7 14.

Stenudd, M., Sabelström, H., and Frisén, J. (2015). Role of endogenous neural stem cells in spinal cord injury and repair. JAMA Neurol *72*, 235 237.

Stuart, T., Butler, A., Hoffman, P., Hafemeister, C., Papalexi, E., Mauck, W.M., 3rd, Hao, Y., Stoeckius, M., Smibert, P., and Satija, R. (2019). Comprehensive integration of single cell data. Cell *177*, 1888 1902.e21.

Suzuki, M., Tachibana, I., Takeda, Y., He, P., Minami, S., Iwasaki, T., Kida, H., Goya, S., Kijima, T., Yoshida, M., et al. (2009). Tetraspanin CD9 negatively reg ulates lipopolysaccharide induced macrophage activation and lung inflamma tion. J. Immunol. *182*, 6485 6493.

Tang, T., Zhang, Y., Wang, Y., Cai, Z., Lu, Z., Li, L., Huang, R., Hagelkruys, A., Matthias, P., Zhang, H., et al. (2019). HDAC1 and HDAC2 regulate intermediate progenitor positioning to safeguard neocortical development. Neuron *101*, 1117 1133.e5.

Torti, F.M., and Torti, S.V. (2002). Regulation of ferritin genes and protein. Blood *99*, 3505 3516.

Tsarouchas, T.M., Wehner, D., Cavone, L., Munir, T., Keatinge, M., Lambertus, M., Underhill, A., Barrett, T., Kassapis, E., Ogryzko, N., et al. (2018). Dynamic control of proinflammatory cytokines IL 1beta and Tnf alpha by macrophages in zebrafish spinal cord regeneration. Nat. Commun. *9*, 4670.

Tsata, V., Möllmert, S., Schweitzer, C., Kolb, J., Möckel, C., Böhm, B., Rosso, G., Lange, C., Lesche, M., Hammer, J., et al. (2021). A switch in pdgfrb+ cell derived ECM composition prevents inhibitory scarring and promotes axon regeneration in the zebrafish spinal cord. Dev. Cell *56*, 509 524.e9.

van der Vaart, M., Svoboda, O., Weijts, B.G., Espín Palazón, R., Sapp, V., Pietri, T., Bagnat, M., Muotri, A.R., and Traver, D. (2017). Mecp2 regulates tnfa during zebrafish embryonic development and acute inflammation. Dis. Model. Mech. *10*, 1439 1451.

Wan, J., Ramachandran, R., and Goldman, D. (2012). HB EGF is necessary and sufficient for Muller glia dedifferentiation and retina regeneration. Dev. Cell *22*, 334 347.

Wang, Z., He, X., and Fan, X. (2018). Postnatal administration of memantine rescues TNF alpha induced decreased hippocampal precursor proliferation. Neurosci. Lett. *662*, 173 180.

Wehner, D., Cizelsky, W., Vasudevaro, M.D., Ozhan, G., Haase, C., Kagermeier Schenk, B., Röder, A., Dorsky, R.I., Moro, E., Argenton, F., et al. (2014). Wnt/beta catenin signaling defines organizing centers that orchestrate growth and differentiation of the regenerating zebrafish caudal fin. Cell Rep *6*, 467 481.

Wehner, D., Jahn, C., and Weidinger, G. (2015). Use of the TetON system to study molecular mechanisms of zebrafish regeneration. J Vis Exp *25*, e52756.

Wehner, D., Tsarouchas, T.M., Michael, A., Haase, C., Weidinger, G., Reimer, M.M., Becker, T., and Becker, C.G. (2017). Wnt signaling controls pro regen erative Collagen XII in functional spinal cord regeneration in zebrafish. Nat. Commun. *8*, 126.

Wentzel, A.S., Petit, J., van Veen, W.G., Fink, I.R., Scheer, M.H., Piazzon, M.C., Forlenza, M., Spaink, H.P., and Wiegertjes, G.F. (2020). Transcriptome sequencing supports a conservation of macrophage polarization in fish. Sci. Rep. *10*, 13470.

Westerfield, M. (2000). The Zebrafish Book: A Guide for the Laboratory Use of Zebrafish (Danio rerio), Fourth Edition (University of Oregon Press).

Wolf, F.W., Sarma, V., Seldin, M., Drake, S., Suchard, S.J., Shao, H., O'Shea, K.S., and Dixit, V.M. (1994). B94, a primary response gene inducible by tumor necrosis factor alpha, is expressed in developing hematopoietic tissues and the sperm acrosome. J. Biol. Chem. *269*, 3633 3640.

Yamaguchi, M., Tonou Fujimori, N., Komori, A., Maeda, R., Nojima, Y., Li, H., Okamoto, H., and Masai, I. (2005). Histone deacetylase 1 regulates retinal neu rogenesis in zebrafish by suppressing Wnt and Notch signaling pathways. Development *132*, 3027 3043.

Yamanishi, E., Yoon, K., Alberi, L., Gaiano, N., and Mizutani, K. (2015). NF κB signaling regulates the generation of intermediate progenitors in the devel oping neocortex. Genes Cells *20*, 706 719.

Ye, N., Ding, Y., Wild, C., Shen, Q., and Zhou, J. (2014). Small molecule inhib itors targeting activator protein 1 (AP 1). J. Med. Chem. *57*, 6930 6948.

Yeo, S.Y., Kim, M., Kim, H.S., Huh, T.L., and Chitnis, A.B. (2007). Fluorescent protein expression driven by her4 regulatory elements reveals the spatiotem poral pattern of Notch signaling in the nervous system of zebrafish embryos. Dev. Biol. *301*, 555 567.

Yoshida, M., Horinouchi, S., and Beppu, T. (1995). Trichostatin A and trapoxin: novel chemical probes for the role of histone acetylation in chromatin structure and function. BioEssays *17*, 423 430.

Zhang, Y., Liu, J., Yao, S., Li, F., Xin, L., Lai, M., Bracchi Ricard, V., Xu, H., Yen, W., Meng, W., et al. (2012). Nuclear factor kappa B signaling initiates early dif ferentiation of neural stem cells. Stem Cells *30*, 510 524.

STAR★METHODS

KEY RESOURCES TABLE

REAGENT or RESOURCE	SOURCE	IDENTIFIER
Antibodies		
Mouse anti HuC/HuD (16A11)	ThermoFisher Scientific	Cat# A 21271; RRID:AB 221448
Chicken anti GFP	Abcam	Cat# ab13970; RRID:AB 300798
Mouse anti Tnf	AnaSpec	Cat AS 55383
anti Digoxigenin AP, Fab fragments	Roche	Cat# 11093274910
Rabbit anti histone H4 (acetyl K5+K8+K12+K16)	Abcam	Cat# ab177790; RRID:AB 2732882
Mouse anti alpha tubulin	DSHB	Cat# 12G10; RRID:AB 1157911
IRDye 800CW Goat anti Mouse IgG (H + L) Highly Cross Adsorbed	Li Cor	Cat# 925 32210; RRID:AB 2687825
IRDye 800LT Goat anti Rabbit IgG (H + L) Highly Cross Adsorbed	Li Cor	Cat# 926 32211; RRID:AB 621843
Alexa Fluor ® 488 AffiniPure Donkey Anti Chicken IgY (IgG) (H+L)	Jackson ImmunoResearch	Cat# 703 545 155; RRID:AB 2340375
Alexa Fluor® 594 AffiniPure Donkey Anti Mouse IgG (H+L) (Minimally cross reactive to Rat, pre adsorbed)	Jackson ImmunoResearch	Cat# 715 585 151; RRID:AB 2340855
Chemicals, peptides, and recombinant proteins		
Cas9 protein	BioLabs	Cat# M0386M
Fast Green FCF dye	Sigma	Cat# 2353 45 9
SygRNA tracer	Sigma	Cat#TRACRRNA05N
Dexamethasone	Sigma	Cat# D1756
Lipopolysaccharides from *Escherichia coli* O55:B5	Sigma	Cat# L2880
Pomalidomide	Cayman Chemicals	Cat# 19877
Mocetinostat	Cayman Chemicals	Cat# 18287
TSA	Sigma	Cat# T8552
Recombinant zebrafish Tnf	Kingfisher Biotech	Cat# RP1318Z
Recombinant human TNF	Biolegend	N/A
AP 1 inhibitor SR 11302	Tocris	Cat# 2476
Collagenase	Sigma	Cat# C9891
Critical commercial assays		
BioMix™ Red	Bioline	Cat# Bio 25006
RNeasy Mini Kit	Qiagen	Cat# 74106
iScript cDNA Synthesis Kit	Bio Rad	Cat# 170 8891
SsoAdvanced Universal SYBR Green Supermix	Bio Rad	Cat# 1725271
Click It EdU Imaging Kit	Invitrogen	Cat# C1008
Deposited data		
scRNAseq of mpeg1.1+ cells from lesioned and unlesioned zebrafish larvae spinal cord	ArrayExpress	Accession code: E MTAB 10379
scRNAseq of her4.3+ cells from lesioned and unlesioned zebrafish larvae spinal cord	ArrayExpress	Accession code: E MTAB 10390
Experimental models: Organisms/strains		
WIK wild type strain of zebrafish	European Zebrafish Resource Center (EZRC)	https://zfin.org/action/genotype/view/ZDB GENO 010531 2
Tg (*mnx1:GFP*)	Flanagan Steet et al., 2005	N/A

(*Continued on next page*)

Continued		
REAGENT or RESOURCE	SOURCE	IDENTIFIER
Tg (*olig2*:EGFP)	Shin et al., 2003	N/A
Tg (*olig2*:DsRed2)	Kucenas et al., 2008	N/A
Tg (*mpeg1.1*:EGFP)^{gl22}	Ellett et al., 2011	N/A
Tg (*mpx*:GFP)^{uwm1}	Renshaw et al., 2006	N/A
Tg (*her4.3*:EGFP^{y83})	Yeo et al., 2007	N/A
her4.3:irtTAM2 (3F) p2a AmCyan^{ulm6}	Wehner et al., 2014	N/A
tnfa mutant	Keatinge et al., 2021	N/A
her4.3:TetA;*TetRE*:YFP dnhdac1	This paper	N/A
Oligonucleotides		
control gRNA: 5' CCTCTTACCTCAGTTACAATTTAT 3'	This paper	N/A
gRNA targeting sequence zf *tnfa*: 5' CCCGATGATGGCATTTATTTTGT 3'	Tsarouchas et al., 2018	N/A
gRNA targeting sequence zf *tnfrsf1a* (exon 4): 5' ATAGTTTGCTTGTTCCAGG 3'	This paper	N/A
gRNA targeting sequence zf *tnfrsf1a* (exon 5): 5' AGGGTGAAGACTCCCTGGAA 3'	This paper	N/A
RFLP analysis for *tnfrsf1a* (exon 4) Forward: 5' CAGGAATGCAGTGCAGAAAA 3'	This paper	N/A
RFLP analysis for *tnfrsf1a* (exon 4) Reverse: 3' TGACAATCCAGTGCTATTTTGG 5'	This paper	N/A
RFLP analysis for *tnfrsf1a* (exon 5) Forward: 5' AACATGTGGAGGGTTGGTGT 3'	This paper	N/A
RFLP analysis for *tnfrsf1a* (exon 5) Reverse: 3' CGAGAGCATTCCCATCCTAA 5'	This paper	N/A
Primers for *dnhdac1* mutagenesis and for detecting *hdac1, tnfa, tnfrsf1a and b actin* mRNA, see Method Details	This paper	N/A
Recombinant DNA		
Tet Responder vector	Wehner et al., 2015	N/A
Vector coding for Tol2 transposase	Wehner et al., 2015	N/A
Software and Algorithms		
ImageJ	Schneider et al., 2012	https://imagej.nih.gov/ij/
GraphPad Prism 8.1.2	GraphPad Software Company	https://www.graphpad.com/scientific software/prism/
ZenBlue2.3 software, Zeiss	Carl Zeiss Company	https://www.zeiss.com/microscopy
Odyssey Fc Imaging system and Image Studio Lite (v. 5.2)	Li Cor Corporate Company	https://www.licor.com/bio/image studio lite/
G*Power 3.1	Faul et al., 2009	https://gpower.software.informer.com/3.1/
LightCycler® 96 Instrument Software Version 1.1.1 (Roche)	Roche Life Science Company	https://lifescience.roche.com/en gb/brands/realtime pcr overview.html#software
Cellranger pipeline v3.0.2	10X Genomics	https://support.10xgenomics.com/single cell gene expression/software/downloads/latest
R 1.2.5042	R core team	https://www.R project.org/
Seurat v3.1.5	Stuart et al., 2019	https://satijalab.org/seurat/articles/install.html

RESOURCES AVAILABILITY

Lead contact

Further information and request for resources should be directed to and will be fulfilled by the Lead Contact, Dr. Thomas Becker (thomas.becker@ed.ac.uk).

Materials availability

Unique reagents generated in this study are available from the lead contact upon request.

Data and code availability

The single cell RNA sequencing datasets generated by this study have been deposited on ArrayExpress. The Accession number for the *mpeg1*$^{+}$ dataset is ArrayExpress: E-MTAB-10379 and the Accession number for the *her4.3*$^{+}$ dataset is ArrayExpress: E-MTAB-10390.

EXPERIMENTAL MODEL AND SUBJECT DETAILS

Source of zebrafish used in this study are reported below and in the key resources table.

Animals

All zebrafish lines were kept and raised under standard conditions (Westerfield, 2000) and all experiments were approved by the British Home Office (project license no.: 70/8805). For experimental analyses, we used up to 5 day-old larvae of either sex of the following available zebrafish lines: wild type (*wik*); *Tg (mnx1:GFP* ^{ml2}*)*, abbreviated as *mnx1:*GFP (Flanagan-Steet et al., 2005); *Tg* (*olig2*:EGFP), abbreviated as *olig2*:GFP (Shin et al., 2003); *Tg (olig2:DsRed2)*, abbreviated as *olig2*:DsRed (Kucenas et al., 2008); Tg (*mpeg1.1*:EGFP)^{gl22}, abbreviated as *mpeg1*:GFP (Ellett et al., 2011), Tg (*mpx*:GFP)^{uwm1}, abbreviated as *mpx*:GFP (Renshaw et al., 2006); Tg (*her4.3*:EGFP^{y83}) (formerly known as *her4.1*:EGFP (Yeo et al., 2007)), abbreviated as *her4.3*:GFP; *her4.3*:irtTAM2 (3F)-p2a-AmCyan^{ulm6}, abbreviated as *her4.3*:TetA (Wehner et al., 2014); *tnfa* mutant (Keatinge et al., 2021).

METHOD DETAILS

Spinal cord injuries

Zebrafish larvae at 3 dpf were anaesthetised in PBS containing 0.02 % aminobenzoic-acid-ethyl methyl-ester (MS222, Sigma), as previously described (Wehner et al., 2017). Larvae were transferred to an agarose-coated petri dish. Following removal of excess water, the larvae were placed in a lateral position, and the tip of a sharp 30.5 G syringe needle was used to inflict a stab injury or a dorsal incision on the dorsal part of the trunk to transect the spinal cord at the level of the 15th myotome. After injuries, the larvae were returned into fresh water or into the appropriate solution depending on the experimental procedure.

Generation of TetRE:YFP-dnhdac1 line:

To generate the dominant-negative form of *hdac1* (*dnhdac1*), the histidine in position 142 was exchanged to alanine by site-direct mutagenesis (overlap-extension method). *hdac1* was amplified and cloned from zebrafish cDNA. This template was used to generate *dnhdac1* using the following mutagenic primers to change the nucleotide bases in positions 525 and 526 (XM_005159592) from CA to GC (marked in red) paired with primers with added recognition sites for restriction enzymes (Pair 1: forward: 5'-TTATTTACGCGTC CACCATGGTGAGCAAGGGCGAGGA-3'; reverse: 5'-GCCTCTGATTTCTTAGCAGCATGTAGACCTCCTGCCC-3'; Pair 2: forward: 5'-GGGCAGGAGGTCTACATGCTGCTAAGAAATCAGAGGC-3'; reverse: 5'- TTTATTAGATCTAAAAAACCTCCCACACCTCCCCCT GAACCTC-3'). The two resulting fragments were fused and cloned into the Tet-responder vector (Wehner et al., 2015) down-stream of a YFP coding sequence. Plasmid DNA (50 ng/μl) along with Tol2 transposase mRNA (25 ng/μl) was injected into single cell stage embryos. Once adult, injected fish were screened for founders by breeding with the *her4.3*:TetA Tet-activator line. Founders were visually selected for signal intensity and selectivity.

gRNA injections

The gRNAs were injected into the yolk at the one-cell stage of development. The injection mix was used the same day as prepared. The mix consisted of 1 μl Cas9 protein (BioLabs, M0369M), 1 μl Fast Green FCF dye (Sigma, 2353-45-9), 1 μl 250 ng/μl SygRNA-tracer (Sigma), 1 μl gRNA and 1 μl nuclease-free water. When two gRNAs were co-injected, the nuclease-free water was substituted with the second gRNA. For every experiment two injection mixtures were made, one with the gRNA of interest and one with a control gRNA (5'-CCTCTTACCTCAGTTACAATTTAT-3'). *tnfa* was targeted with a gRNA (5'-CCCGATGATGGCATTTATTTTGT-3') as before (Tsarouchas et al., 2018). *tnfrsf1a* was targeted by co-injection of gRNAs for exons 4 (5'- ATAGTTTGCTTGTTCCAGG -3') and 5 (5'- AGGGTGAAGACTCCCTGGAA -3').

RFLP analysis of gRNA efficiency

To test efficacy of gRNAs targeting *tnfrsf1a* we used Forward primer: 5'-CAGGAATGCAGTGCAGAAAA-3' and Reverse primer: 3'-TGACAATCCAGTGCTATTTTGG-5' for exon 4 and Forward primer: 5'-AACATGTGGAGGGTTGGTGT-3' and Reverse primer: 3'-CGAGAGCATTCCCATCCTAA-5' for exon 5 to span recognition sites for restriction enzymes BstNI and BslI, respectively. Genomic DNA was extracted from individual embryos at 1 dpf by heating the whole embryo with 100 μl of 50 mM NaOH at 95°C for 10 min. PCR products were generated using BioMix™ Red (Bioline, Bio-25006) and were subsequently incubated with 2 μl of the respective restriction enzyme solution (BioLabs) for 1.5 h at the specified temperature, followed by separation on a 2 % agarose gel (100 V for 40 min) and visualisation on a trans-illuminator.

Drug treatment of whole larvae

Dexamethasone (Sigma, Gillingham, UK) was dissolved in DMSO to a stock concentration of 5 mM. The working concentration was 10 μM prepared by dilution from stock solution in fish water. Lipopolysaccharides from *Escherichia coli* O55:B5 (LPS, Sigma) were dissolved in PBS to a stock concentration of 1 mg/ml. The working dilution was 50 μg/ml. Pomalidomide (Cayman Chemicals, Michigan, USA) was diluted in DMSO at a stock concentration of 10 mg/ml. For the treatments, 6.9 μl of the stock where diluted in 1.5 ml of fish water. Mocetinostat (Cayman Chemicals, Ann Arbor, MI, USA) was used at a concentration of 1 μM; TSA (Sigma) was used at 200 nM. Larvae were pre-treated for 2 h before the injury and were incubated for 24 and 48 hpl. Larvae were collected from the breeding tanks and were randomly divided into Petri dishes at a density of maximally 30 larvae per dish, but no formal randomization method was used. For most drug treatments, larvae were incubated with the drug from 3 dpf until 5 dpf, if not indicated differently.

Ex vivo incubations

Per experiment, 150-200 4-day-old *her4.3*:GFP transgenic larvae per condition were incubated in 0.05 % trypsin (preheated to 37°C) on a shaker for 7 min. Samples were put on ice and centrifuged in a chilled (6°C) table top centrifuge at 250 rpm for 7 min. The supernatant was replaced with ice cold PBS, and samples were centrifuged again at the same settings. Tissue fragments were re-suspended in 1 mL PBS (room temperature from here on) and dissociated using a 40 μm mesh filter. Cells were centrifuged at 250 RCF for 7 min, the supernatant was removed, and cells were resuspended in 500 μL of serum-free Iscove's Modified Dulbecco's Medium (IMDM). ERG progenitors were purified by FACS and incubated with various inhibitors and recombinant proteins in IMDM at room temperature for 4 h. At the end of the incubation period, RNA was isolated for qRT-PCR. For incubation, the following inhibitors and proteins were used: recombinant zebrafish Tnf (20 ng/mL, Kingfisher Biotech), recombinant human TNF (20 ng/mL, Biolegend), and the AP-1 inhibitor SR 11302 (1 μM, Tocris, Cat. No. 2476), compared to DMSO vehicle controls.

Immunohistochemistry

All incubations were performed at room temperature unless stated otherwise. Whole-mounts: At the time point of interest, larvae were fixed in 4 % PFA-PBS containing 1 % DMSO at 4 °C overnight. After washes in PBS, larvae were washed in PBTx. After permeabilization by incubation in PBS containing 2 mg/ml Collagenase (Sigma) for 25 min, larvae were washed 3 x in PBTx. Then 50 nM Glycine in PBTx was added for 10 minutes followed by two washes in PSTx. Larvae were then incubated in blocking buffer for 2 h and incubated with primary antibody diluted in blocking buffer at 4°C overnight. On the following day, larvae were washed 3 x in PBTx, followed by incubation with secondary antibody diluted in blocking buffer at 4°C overnight. The next day, larvae were washed three times in PBTx and once in PBS for 15 min each, before mounting in 70 % glycerol. We used the following primary antibodies: mouse anti-HuC/HuD (abbreviated as HuC; 1:100; InVitrogen); chicken anti-GFP (1.300; Abcam Cambridge, USA); mouse anti-Tnf (1:2000, DSHB, Iowa, USA). Appropriate secondary antibodies were bought from Jackson ImmunoResearch (1:300).

In situ hybridisation

In situ hybridization on whole-mount larvae with digoxygenin (DIG)-labelled antisense probes was performed as previously described (Tsata et al., 2021). Larvae were fixed in 4 % paraformaldehyde (PFA; Thermo-Fisher Scientific) in PBS and treated with Proteinase K (Invitrogen) followed by re-fixation for 15 min in 4 % PFA in PBS. DIG-labelled antisense probes were allowed to hybridize overnight at 65°C. This protocol allows efficient probe penetration in whole-mount preparations of 5-day-old larvae (Wehner et al., 2017). Colour reaction was performed after incubation with anti-DIG antibody conjugated to alkaline phosphatase (Sigma-Aldrich) using NBT/BCIP substrate (Roche). Staining reaction was terminated by washing samples in PBT (0.1% Tween-20 in PBS). For NBT/BCIP-stained samples, background staining was cleared by incubating samples in 100% ethanol.

In situ hybridization on agarose sections with DIG-labelled antisense probes was performed as described (Wehner et al., 2017). Larvae were fixed in 4 % paraformaldehyde in PBS (PFA), embedded in 4 % agarose in PBS and sectioned at 50-100 μm using a vibrating blade microtome (Leica). Sections were treated with Proteinase K (Invitrogen) followed by re-fixation in 4 % PFA in PBS. A DIG-labelled antisense probe against *hdac1* was allowed to hybridize overnight at 65 °C. The antisense probe was synthesized from the full-length *hdac1* coding sequence used to generate the *TetRE*:YFP-*dnhdac1* construct. Color reaction was performed after incubation with anti-DIG antibody conjugated to alkaline phosphatase (Sigma-Aldrich) using SIGMAFAST Fast Red (Sigma-Aldrich). Where required, samples were co-labelled with chicken anti-GFP antibody (Abcam, ab13970). Sections were stained for DAPI (Thermo Scientific) to visualize nuclei, followed by two washes in PBS and mounted in 75 % Glycerol in PBS.

For adult in situ hybridization, 50 μm vibratome floating sections were permeabilised with Proteinase K (10 μg / ml) for 9 minutes at room temperature, as described (Reimer et al., 2009). Sections were washed with 2 mg / ml glycine in PBS-Tween (0.1 %), followed by a 20 min re-fixation in 4 % PFA in PBS. Probes were hybridised at 65 °C overnight, extensively washed in SSC buffer and incubated in anti-DIG antibody (1:10000) at 4 °C overnight. After extensive washes in PBST, colorimetric development was allowed to take place for up to 4 hours at room temperature, followed by washes. Sections were either mounted on glass slides for visualisation or processed for immunohistochemical detection of GFP in some transgenic animals.

FACS isolation

Per experiment and sample, 150-200 larvae were collected and the trunk containing the lesion site dissected (similar portion for unlesioned control) on ice for qRT-PCR. Supernatant was removed and replaced with 0.05 % trypsin (pre-heated to 37 °C). After

3-5 minutes tissue was dis-aggregated by pipetting and digestion was blocked by adding 10 % fetal bovine serum. Cell suspensions were pressed through a 40 μm filter, centrifuged at 250 RCF for 7 min and the supernatant replaced by 500 μl of PBS $^{+}$ 5 % fetal bovine serum. Cells were FACS sorted at 4 °C and kept on ice for qRT-PCR.

qRT-PCR

Real-time PCR was performed using a Roche Light Cycler 96 (annealing temperature of 58 °C) with SsoAdvancedTM Universal SYBR® Green Supermix (Bio-Rad, 172-5271). Relative mRNA levels were determined using the Roche Light Cycler 96 SW1 software. Samples were run in duplicate. We used the following primers: *hdac1* forward 5'-TGTCCGAGTACAGCAAGCAG, reverse 5'-TGATGTAGACCTCCTGCCCA-3'; *tnfa* forward 5'-TCACGCTCCATAAGACCCAG-3', reverse 5'-GATGTGCAAAGACACCTGGC -3'; *tnfrsf1a* forward 5-ACTCATGGC GATCCAGCATT-3', reverse 5'-AAGGAGGAGCAGAGCGTTAC-3'; *b-actin* forward 5'- CACG AGAGATCTTCACTCCCC-3', reverse 5'-TCCCATGCCAACCATCACTC-3'.

Western blot

Approximately 500 double-transgenic fish (*her4.3*:TetA*;TetR*E:YFP-*dnhdac1*) were induced at 3 dpf with 485 nM Doxycycline hyclate (Sigma, D9891). Uninduced fish were used as control. 48 h post-induction, fish were treated with trypsin-EDTA (0.05 % ready-made solution; Thermo Scientific) to obtain a single cell suspension for FACS sorting, using AmCyan fluorescence (encoded by the Tetactivator construct and therefore present in both induced and uninduced larvae). After FACS sorting, $1x10^6$ YFP-positive and $1x10^6$ YFP-negative cells were collected in cold Dulbecco's PBS. Cells were spun at 1000 rpm for 5 min. The pellet was lysed in 200 μl RIPA buffer supplemented with cOmplete EDTA-free protease inhibitors (Roche) for 10 min/ 4 °C. After sonication (10 sec), the lysate was centrifuged at 14.000 rpm/10 min/4 °C. The clear supernatant was boiled at 95 °C with Laemmli buffer supplemented with beta-mercaptoethanol. Equal amounts of sample (YFP- and YFP^{+}) were resolved in a 12 % SDS-PAGE gel and proteins transferred to a 0.2 μm nitrocellulose membrane (BioRad). The protein detection was performed with primary antibodies against acetyl-histone H4 (1:1000, rabbit monoclonal, Abcam, ab177790) and alpha tubulin (1:5000, mouse monoclonal, DSHB, 12G10), and secondary antibodies IRDye 800CW goat anti-mouse (1:10000, Li-Cor) and IRDye 800CW goat anti-rabbit (1:10000, Li-Cor). Membrane was scanned using the Odyssey Fc imaging system (Li-Cor).

scRNAseq

Following cell dissociation and FACS sorting (described above), samples were processed on the 10X Chromium platform using 10X Single Cell 3' v3 chemistry following the manufacturer's guidelines (10X Genomics, Pleasanton, USA). For each cell type, the two conditions (unlesioned and lesioned) were prepared in tandem and processed together for GEM generation, reverse transcription, cDNA amplification and library construction following manufacturer's instructions.

The libraries were sequenced on a Novaseq 6000 using a S2 flowcell. The data was first processed using the 10x Cellranger pipeline (version 3.0.2) and mapped to the zebrafish genome GRCz10.The above procedures were carried out as a service by Edinburgh Genomics (Edinburgh, UK). The resulting matrices were subject to quality control, normalisation and analysis in Seurat version 3 (Stuart et al., 2019) package for R, version 1.2.5042. Cells were selected to continue with down-stream analysis based on feature count and mitochondrial gene percentage. For the her4.3 sample, only cells which had more than 200 features and fewer than 4500 features expressed were retained. Additionally, only cells which had less than 5 % of their reads from mitochondrial genes were kept. Based on these criteria, 3680 of the 5588 cells which were sequenced were used for further analysis (66 %). Genes which were found in fewer than 3 cells were filtered out.

For the *mpeg1*:GFP sample, only cells which had more than 200 features and fewer than 6000 features expressed were retained. Additionally, only cells which had less than 20% of their reads from mitochondrial genes were kept. Genes which were found in fewer than 3 cells were filtered out. Based on these criteria, 8346 of the 9245 cells which were sequenced were used for further analysis (90%).

Following this, data was normalised using 'LogNormalize' function with scale factor 10000, then the top 2000 highly variable genes were selected and scaled to unit variance and zero mean with 'Scale Data'. Principal Component Analysis was then performed on these highly variable genes. RunTSNE and FindNeighbours were run based on the first 20 principal components and unsupervised clustering was performed with FindClusters (resolution = 0.5 for the her4.3 sample, resolution = 0.3 for the mpeg1 sample). Differential expression analysis between the two conditions was performed using Seurat's FindMarkers function using a Wilcoxon rank-sum test.

Cell counting in whole-mounted larvae

A volume of interest was defined centered on the lesion site from confocal images. The dimensions were: width = 200 - 300 μm, height = 75 μm (above the notochord), depth = 50 μm. Images were analysed using the Imaris (Bitplane, Belfast, UK) or ImageJ (http://imagej.nih.gov/ij) software. The number of cells was quantified manually in 3D view, blinded to the experimental condition on at least three independent clutches of larvae (Tsarouchas et al., 2018).

To count the number of *mpeg*:GFP^{+} cells close to the spinal progenitor zone in lesioned larvae, two boxes were drawn of 70 x 40 micrometer each, each centring on the lesioned end of the *olig2*:GFP^{+} progenitor zone. *mpeg*:GFP^{+} cells were counted within 40 optical sections (of 1 micrometer thickness) of the centre of the *olig2:*DsRed^{+} zone.

QUANTIFICATION AND STATISTICAL ANALYSIS

Power analysis using G*Power (Faul et al., 2009) was used to calculate statistical power (aim > 0.8) for cell counting experiments and determine the group sizes accordingly. All quantitative data were tested for normality and analysed with parametric and non-parametric tests as appropriate. The statistical analysis was performed using IBM SPSS Statistics 23.0 and GraphPad Prism 8. Shapiro-Wilk's W-test was used in order to assess the normality of the data. Kruskal-Wallis test followed by Dunn's multiple comparisons, One-way ANOVA followed by Bonferroni multiple comparisons test, two-way ANOVA, followed by Bonferroni multiple comparisons, T-test, Mann–Whitney U test or Fisher's exact test were used, as indicated in the figure legends. *$P < 0.05$, **$P < 0.01$, ***$P < 0.001$, n.s. indicates no significance. Error bars indicate the standard error of the mean (SEM). Definitions of analytical units (n) are given in the figure legends. The figures were prepared with Adobe Photoshop CC and Adobe Illustrator CC. Graphs were generated using GraphPad Prism 8.